VANESSA SOFIA LOPES RODRIGUES

UNDERSTANDING P-GLYCOPROTEIN MEDIATED MULTIDRUG RESISTANCE IN CANCER: NEW POTENTIAL TARGETS, BIOMARKERS AND MOLECULAR INHIBITORS

Tese de Candidatura ao grau de Doutor em Patologia e Genética Molecular submetida ao Instituto de Ciências Biomédicas Abel Salazar da Universidade do Porto.

Orientadora – Prof. Doutora Maria Helena da Silva de Vasconcelos Meehan

Categoria – Professora Auxiliar

Afiliação – Faculdade de Farmácia da Universidade do Porto, i3S - Instituto de Investigação e Inovação em Saúde e IPATIMUP – Instituto de Patologia e Imunologia Molecular da Universidade do Porto.

Coorientadora – Doutora Raquel Maria Torres Lima

Categoria – Bolseira de Pós-Doutoramento

Afiliação – i3S - Instituto de Investigação e Inovação em Saúde, IPATIMUP - Instituto de Patologia e Imunologia Molecular da Universidade do Porto e Faculdade de Medicina da Universidade do Porto.

Coorientadora – Prof. Doutora Maria Emília da Silva Pereira de Sousa

Categoria – Professora Auxiliar

Afiliação – Faculdade de Farmácia da Universidade do Porto e CIIMAR/CIMAR – Centro Interdisciplinar de Investigação Marinha e Ambiental da Universidade do Porto.

UNDERSTANDING P-GLYCOPROTEIN MEDIATED MULTIDRUG RESISTANCE IN CANCER: NEW POTENTIAL TARGETS, BIOMARKERS AND MOLECULAR INHIBITORS

Vanessa Lopes-Rodrigues

The candidate performed the experimental work with a doctoral fellowship (SFRH/BD/87646/2012) supported by the "Fundação para a Ciência e a Tecnologia".

The research described in this thesis was conducted at:

i3S, Instituto de Investigação e Inovação em Saúde da Universidade do Porto IPATIMUP and Instituto de Patologia e Imunologia Molecular da Universidade do Porto (Cancer Drug Resistance Group), Porto, Portugal

AUTHORS DECLARATION

Under the terms of the "nº 2, alinea a, do Art.º 31º do Decreto-lei nº 230/2009", is hereby declared that the author afforded a major contribution to the conceptual design and technical execution of the work, interpretation of the results and manuscript preparation of the published articles included in this dissertation.

Under the terms of the "nº 2, alinea a, do Art.º 31º do Decreto-lei nº 230/2009" is hereby declared that the following original publications were prepared in the scope of this dissertation.

Scientific Publications

Articles in international peer-reviewed journals

Review articles

Vanessa Lopes-Rodrigues, Emília Sousa, M. Helena Vasconcelos. "Curcumin as a modulator of P-glycoprotein in cancer: challenges and perspectives" (2016). *Submitted for publication (in Pharmaceuticals).*

Vanessa Lopes-Rodrigues, Hugo Seca, Diana Sousa, Emília Sousa, Raquel T. Lima, M. Helena Vasconcelos. "The network of P-glycoprotein and microRNA interactions" (2014). *Int J Cancer*. 15;1 35(2):253-63.

Research articles

Vanessa Lopes-Rodrigues, Alessio Di Luca , Justyna Mleczko, Paula Meleady, Diana Cabrera, Sebastiaan van Liemp, Michael Henry, Milica Pesic, Raquel T. Lima, Robert O'Connor, J. M. Falcon-Perez, M. Helena Vasconcelos. Identification of the metabolic alterations associated with the multidrug resistant phenotype in cancer and their intercellular transfer mediated by extracellular vesicles. *Submitted for publication (in Scientific Reports).*

Vanessa Lopes-Rodrigues*, Ana Oliveira ***,** Marta Correia-da-Silva, Madalena Pinto, Raquel T. Lima, Emília Sousa, M. Helena Vasconcelos. **"**A novel curcumin derivative which

inhibits P-glycoprotein, arrests cell cycle and induces apoptosis in multidrug resistant cells" (2016). *Accepted for publication pending revisions (in Bioorganic Medicinal Chemistry)*

Vanessa Lopes-Rodrigues, Alessio Di Luca, Diana Sousa, Hugo Seca, Paula Meleady, Michael Henry, Raquel T. Lima, Robert O'Connor, M. Helena Vasconcelos. "Multidrug resistant tumour cells shed more microvesicle-like EVs and less exosomes than their drug-sensitive counterpart cells" (2016). Biochim Biophys Acta. 1860: 618-627.

Vanessa Lopes-Rodrigues, Alessio Di Luca, Diana Sousa, Hugo Seca, Paula Meleady, Michael Henry, Raquel T. Lima, Robert O'Connor, M. Helena Vasconcelos. "Data supporting the shedding of larger extracellular vesicles by multidrug resistant tumour cells" (2016). *Data in Brief*. 6(C): 1023-1027.

***** The authors have equally contributed to the work

Letter to the Editor

Vanessa Lopes-Rodrigues, Cristina P. R. Xavier, Diana Sousa, Hugo Osório, Raquel T. Lima, M. Helena Vasconcelos. "ALIX protein analysis: storage temperature may impair results". *Manuscript in preparation*.

Abstracts published in international periodicals with referees

Vanessa Lopes-Rodrigues, Alessio Di Luca, Diana Sousa, Hugo Seca, Paula Meleady, Michael Henry, Raquel T. Lima, Robert O'Connor, M. Helena Vasconcelos. "P-gp Overexpressing MDR cells shed larger extracellular vesicles than their drug-sensitive counterparts" (2015). *Cancer Res* 75; 4433.

Patents

Co-inventor of a submitted proposal for a Portuguese Patent: "Tamanho e perfil proteico de vesículas extracelulares como marcadores de multirresistência às terapêuticas anti-neoplásicas"; National patent - related process nr: 107841. Under evaluation.

AGRADECIMENTOS/ACKNOWLEDGMENTS

O meu primeiro agradecimento é dirigido à minha orientadora Prof. Doutora Helena Vasconcelos. Em primeiro lugar, muito obrigada pela oportunidade que me deu. Obrigada pelo apoio e incentivo, pelos conhecimentos partilhados e pela supervisão e orientação de todo o trabalho. Agradeço-lhe ainda por ter contribuído para o meu crescimento como investigadora.

À Raquel Lima, minha co-orientadora, o meu muito obrigada por tudo o que me ensinaste, obrigada por teres estado sempre presente e disponível para todas as minhas dúvidas (as existenciais e as mais comuns). Obrigada por toda a orientação que sempre me deste.

À Prof. Doutora Emília Sousa agradeço todo o seu apoio como co-orientadora. Muito obrigada pela objetividade e pela ajuda imediata que sempre me prestou. Obrigada pela sua colaboração.

To JuanMa and Robert O'Connor that gave me the opportunity to work in their labs during my PhD. Thank you for always being there when I needed.

To all the co-authors of the publications, I would like to express my gratitude for their important contribution, for their suggestions and commitment which greatly improved this thesis work. A special thanks to Prof. Milica Pesic for having kindly provided the lung cancer cell lines used in this study.

O meu agradecimento sincero à Professora Fátima Gartner por toda a disponibilidade e amabilidade com que me ajudou a resolver toda a espécie de problemas que foram surgindo durante esta tese.

Ao Professor Sobrinho Simões na qualidade de diretor do IPATIMUP (durante a maior parte do meu doutoramento) agradeço o ter-me permitido realizar este trabalho no seu instituto.

I would like to thank Alessio for helping me with the proteomic studies during my stay in Dublin. Thank you also for the long conversations that ended up always in Portuguese and Italian food, for the lunches and the walks on the park searching for new blossoming flowers.

Justyna, thank you so much for helping me with our "good" friend seahorse. Most off all thank you for your friendship, for the early mornings shared at the lab and the (second) breakfasts with chocolate waffles that wormer my heart during the intense work days.

Quero deixar um agradecimento especial à Ana por ter sintetizado os nossos "bons amigos" derivados da curcumina e pela simpatia e disponibilidade para comigo.

A todos os CDRs passados e presentes o meu muito obrigada, foram vocês que tornaram todo este caminho bem mais fácil. Ao Hugo Seca, o meu primeiro “chefe” no IPATIMUP, obrigada por me ensinares a fazer sempre tudo da forma “perfeita” e principalmente muito obrigada pela tua amizade. À Catarina e à Daniela, o meu muito obrigada por todos os momentos partilhados e pela vossa amizade. Obrigada por tudo o que me transmitiram ao longo dos anos. À minha transmontana preferida, Filipinha, o meu obrigada por tudo! Pela amizade, pelos momentos partilhados e pelo teu carinho. As viagens de carro sem ti nunca mais serão as mesmas. Raquel, mais do que co-orientadora foste uma verdadeira amiga. Agradeço-te toda a amizade e carinho, todos os conselhos e toda a força que sempre me transmitiste ao longo destes anos. Obrigada por me mostrares o que é ser cientista. Diana, em primeiro lugar muito obrigada por toda a ajuda que me deste, tiveste sempre “tempo” para mim. Mesmo nas alturas mais difíceis, trabalhar contigo era um alento e tornava tudo muito mais suportável. Muito obrigada pela tua amizade e pelo carinho que me deste ao longo destes anos. Tiveste sempre uma palavra de apoio e encorajamento necessários para esta jornada.

A todos os Ipatimupianos que partilharam comigo almoços, lanches, conversas e desabafos, o meu muito obrigada. Foi um prazer partilhar o dia a dia com vocês.

À minha família e amigos o meu sincero obrigada, foram um apoio precioso.

Aos meus mais que tudo peludos e de 4 patas o meu agradecimento especial. Laika, Adão e Sofia o vosso amor e lealdade foram essenciais.

Nuno, és (o único) igualzinho a mim, partilhamos código genético e amor, e por isso o meu muito obrigada! Saber que tenho um “mini me” que gosta tanto de mim como eu gosto dele ajudou-me imenso ao longo destes anos.

Aos meus pais, um agradecimento mais do que especial, eterno. A vocês agradeço tudo o que sou. Obrigada pelo que fizeram por mim, por todo o apoio e segurança que sempre me proporcionaram. Se não fossem vocês (e por vocês) não teria sido possível. Obrigada pelo vosso amor incondicional e por estarem sempre presentes na minha vida.

O último agradecimento é para ti, Marcelo. Não existem palavras suficientes para te agradecer. Estiveste sempre ao meu lado nos bons e nos maus momentos, sempre a apoiar-me e nunca a julgar-me. Acima de tudo, obrigada pelo teu amor! Tu és o verdadeiro “co-autor” da minha vida.

O meu obrigada a todos vocês!

ABSTRACT

Cancer multidrug resistance (MDR) is a major cause of therapeutic failure. MDR is mainly due to the overexpression of drug efflux pumps, such as P-glycoprotein (P-gp). Nevertheless, there are no P-gp inhibitors being used in the current clinical practice, due to toxicity problems, drug interactions or pharmacokinetic issues. Curcumin is a secondary metabolite isolated from the turmeric of *Curcuma longa* L. which has been associated with several biological activities, particularly P-gp modulatory activity. However, curcumin shows extensive metabolism and instability, which has justified the recent and intensive search for analogs of curcumin that maintain the P-gp modulatory activity but have enhanced stability.

Besides overexpression of drug efflux pumps, other molecular mechanisms are involved in the MDR phenotype, including metabolic alterations. Indeed, some recent studies showed that it is possible to revert the MDR phenotype by inhibition of glycolysis with specific modulators.

Extracellular vesicles (EVs) are a group of vesicles, that include exosomes and microvesicles, released by all cells. Since they carry a specific cargo (such as proteins and microRNAs) and are present in several body fluids (such as blood), they can be easily collected from cancer patients and could become the source of biomarkers of cancer diagnosis, prognosis or drug resistance. Additionally, several studies have highlighted the relevance of extracellular vesicles (EVs) in metabolism since it was shown that metabolic alterations could affect the shedding and cargo of EVs released by cells.

This thesis aimed to: 1) identify new targets for overcoming P-gp mediated MDR in cancer, 2) identify potential biomarkers of MDR in EVs released by cancer cells and 3) find novel molecules to overcome MDR, by identifying curcumin derivatives with improved P-gp inhibitory effect.

In order to achieve this, two pairs of MDR and drug-sensitive counterpart cell lines were used (from chronic myeloid leukaemia and non-small cell lung cancer), in which the MDR phenotype was mainly due to overexpression of P-gp. Proteins from the cells and their EVs (which were properly characterized by size with Dynamic Light Scattering and Transmission Electron Microscopy and by molecular markers with Western Blot and Flow cytometry) were investigated by proteomics and data was confirmed by Western blot analysis. The metabolic profile was accessed in the cells before and after treatments with specific inhibitors and following incubation with EVs released from the MDR cells.

We have shown that MDR (P-gp overexpressing) cells have a different metabolic profile from the drug-sensitive counterpart cells, exhibiting: (i) a decrease in the pentose phosphate pathway and in the oxidative phosphorylation rate; (ii) an increase in the

glycolysis rate and in the methylation index; (iii) alterations in the glutathione metabolism and in the methionine/S-adenosylmethionine pathway.

Moreover, our results showed that in both cancer cell models, the EVs isolated from MDR cells were bigger, when compared to the EVs released from the drug-sensitive counterpart cells. In addition, CHMP4, CD63, TSG101, Syntenin-1 and Clathrin LCB proteins (previously known to be involved in the biogenesis of exosomes) were less present in the EVs shed by MDR cells. On the other hand, P-gp was only present in the EVs shed by the MDR cell lines. Together, this data indicated that MDR tumour cells secrete more microvesicles, whereas drug-sensitive tumour cells secrete more exosomes. Remarkably, these EVs, from MDR cells, were capable of causing a metabolic switch in the drug-sensitive cancer cells, towards a MDR phenotype.

Finally, in this study, the antitumor and P-gp modulatory activities of a small library of new curcumin derivatives were also tested. For that, the compounds were analysed in the two MDR tumour cell lines (with P-gp overexpression) and their drug-sensitive counterparts. From the series of synthesized curcumin derivatives, a newly synthesized derivative (1,7-*bis*(3-methoxy-4-(prop-2-yn-1-yloxy)phenyl)hepta-1,6-diene-3,5-dione) presenting more potent antitumor and anti-P-gp activities than curcumin itself was identified. In addition, this compound arrested cell cycle at the G2/M phase and induced cell death by apoptosis, in the MDR chronic myeloid leukaemia cell line.

Overall, the work presented in this thesis contributes to the growing knowledge on metabolic alterations in MDR cells and the role of a specific population of EVs in the intercellular transfer of MDR. The specific metabolic alterations identified in this study may be further developed as targets for overcoming MDR. Also, the specific size and protein signature that we have identified in the EVs shed by the MDR cells may have diagnostic significance in cancer, as a source of biomarkers to identify P-gp mediated MDR phenotype. Furthermore, this work also shows the potential of synthetizing new curcumin derivatives to improve curcumin stability and characterized the promising dual activity (antitumor and anti-P-gp) of a novel curcumin derivative.

Keywords: Cancer Multidrug Resistance; P-glycoprotein; Metabolism; Glycolysis; Oxidative Phosphorylation; Extracellular Vesicles; Curcumin.

RESUMO

A resistência a múltiplos fármacos (RMF) é uma das maiores causas de falha terapêutica no tratamento do cancro. A RMF é devida sobretudo à sobre-expressão de bombas de efluxo de fármacos, tais como a glicoproteína P (P-gp). Contudo, na atual prática clinica ainda não são usados inibidores da P-gp, devido a problemas de toxicidade, de interação de fármacos ou problemas farmacocinéticos. A curcumina é um metabolito secundário isolado da *Curcuma longa L*, que tem sido associada a várias atividades biológicas, em particular à atividade moduladora da P-gp. Contudo, a curcumina apresenta um extenso metabolismo e instabilidade, justificando uma procura recente e intensiva de análogos da curcumina que mantenham a atividade moduladora da P-gp mas que apresentem maior estabilidade.

Para além da sobre-expressão de bombas de efluxo, existem outros mecanismos moleculares envolvidos no fenótipo de RMF, tais como alterações metabólicas. De facto, alguns estudos recentes mostraram que é possível reverter o fenótipo de RMF por inibição da glicólise com moduladores específicos.

As vesículas extracelulares (VEs) são um grupo de vesículas libertadas por todas as células e que incluem os exosomas e as microvesiculas. Uma vez que as VEs transportam uma carga específica (tal como proteínas e microRNAs) e estão presentes em vários fluidos corporais (tais como o sangue), podem ser facilmente obtidas de doentes com cancro e poderão eventualmente vir a ser uma fonte de biomarcadores de diagnóstico, prognóstico ou resistência tumoral. Para além disso, vários estudos têm chamado à atenção para a relevância das VEs no metabolismo, uma vez que foi demonstrado que alterações de metabolismo poderiam afetar a libertação e a carga das VEs libertadas pelas células.

Esta tese teve como objetivos: 1) identificar novos alvos para superar a RMF mediada pela P-gp em cancro, 2) identificar potenciais biomarcadores de RMF em VEs libertadas por células tumorais e 3) encontrar novas moléculas que permitam superar a RMF, identificando novos derivados da curcumina com um aumento do efeito inibidor da P-gp.

Para atingir esses objetivos, foram utilizados dois pares de linhas celulares com RMF e as homólogas sensíveis a fármacos (de leucemia mieloide crónica e de cancro do pulmão de células não pequenas), nos quais o fenótipo de RMF era devido sobretudo à sobre-expressão da P-gp As proteínas das células e das respetivas VEs (que foram devidamente caracterizadas segundo o seu tamanho usando Difração de Luz Dinâmica e Microscopia Eletrónica de Transmissão e pela presença de marcadores moleculares com Western blot e citometria de fluxo) foram analisadas por proteómica e os resultados foram confirmados

por Western blot. O perfil metabólico das células foi analisado antes e depois destas serem tratadas com inibidores específicos e após incubação com as VEs libertadas pelas células com fenótipo de RMF.

Mostrámos que as células com RMF (com sobre-expressão da P-gp) apresentam um perfil metabólico diferente do observado nas células homólogas sensíveis a fármacos, mostrando: (i) uma diminuição na via das pentoses fosfato e na fosforilação oxidativa; (ii) um aumento da taxa glicolítica e do índice de metilação; (iii) alterações no metabolismo da glutationa e na via da metionina/S-adenosilmetionina.

Para além disso, os nossos resultados mostraram que em ambos os modelos tumorais, as VEs libertadas pelas células com RMF eram maiores, quando comparadas com as VEs libertadas pelas células homólogas sensíveis a fármacos. Adicionalmente, as proteínas CHMP4, CD63, TSG101, Syntenin-1 e Clathrin LCB (conhecidas por estarem envolvidas na biogénese dos exosomas) estavam presentes em menor quantidade nas VEs libertadas pelas células com RMF. Por outro lado, a P-gp estava presente apenas nas VEs libertadas pelas células com RMF. Em conjunto, estes resultados mostraram que as células cancerígenas com RMF libertam mais microvesiculas, enquanto que as células cancerígenas sensíveis a fármacos libertam mais exosomas. Notavelmente, as VEs libertadas pelas células com RMF foram capazes de causar alterações metabólicas nas células sensíveis a fármacos, no sentido do fenótipo de RMF.

Por último, neste estudo, a atividade anti-tumoral e anti-P-gp de uma pequena livraria de novos derivados da curcumina foram também testadas. Para isso, os compostos foram analisados nas duas linhas celulares tumorais com RMF (com sobre-expressão da P-gp) e nas células homólogas sensíveis a fármacos. De entre os vários novos derivados da curcumina sintetizados, um deles [o 1,7-*bis*(3-methoxy-4-(prop-2-yn-1-yloxy)phenyl)hepta-1,6-diene-3,5-dione] mostrou ter maior atividade anti-tumoral e anti-P-gp do que a própria curcumina. Adicionalmente, este composto parou o ciclo celular na fase G2/M e induziu morte celular por apoptose nas células de leucemia mieloide crónica com RMF.

De um modo geral, o trabalho apresentado nesta tese contribui para o aumento de conhecimento na área das alterações metabólicas nas células com RMF e no papel de uma população específica de VEs na transferência intercelular de RMF. As alterações metabólicas específicas identificadas neste estudo podem ser futuramente desenvolvidas como alvos para ultrapassar a RMF em cancro. Adicionalmente, o tamanho e assinatura proteica específicos que identificamos nas VEs libertadas pelas células com RMF podem vir a ter significado diagnóstico no cancro, como fonte de biomarcadores para identificação do fenótipo de RMF mediada pela P-gp. Para além disso, este trabalho também mostrou o potencial de sintetizar novos derivados da curcumina com o objetivo de melhorar a sua

estabilidade e caracterizou a promissora atividade dupla (anti-tumoral e anti-P-gp) de um novo derivado da curcumina.

Palavras-chave: Resistência cancerígena a múltiplos fármacos; Glicoproteína P; Metabolismo; Glicólise; Fosforilação oxidativa; Vesículas extracelulares; Curcumina.

TABLE OF CONTENTS

INDEX OF FIGURES

INDEX OF TABLES

ABBREVIATIONS

6PGD: 6-Phosphogluconate dehydrogenase

A

ABC: ATP-binding cassette
ABCG: Breast cancer resistant protein
ADP: Adenosine diphosphate
ASCT2: ASC amino-acid transporter 2
ATP: Adenosine triphosphate

C

CSC: Cancer stem cell
CHMP4: Charged multivesicular body protein 4
CO_2: Carbon dioxide

D

DNA: Deoxyribonucleic acid

E

EV: Extracellular vesicle
ESCR: Endosomal sorting complexes required for transport

F

F6P: Fructose-6-phosphate
F1,6BP: Fructose-1,6-biphosphate
FAD: Flavin adenine dinucleotide
$FADH_2$: Hydroquinone FAD

G

GST: Glutathione-S.transferase
GCS: Glutamylcysteine synthetase
GSSG: Oxidized glutathione
G6PD: Glucose-6-phosphate
G6P: Glucose-6-phosphate
GSH: Reduced glutathione

H

H_2O: Water
HIF-1: Hypoxia-induced factor-1

L

lncRNAs: Long non-coding RNA
LC/MS: Liquid chromatography/ mass spectrometry

M

MDR: Multidrug resistance
MDR-1: Multidrug resistance protein-1
MRP-1: Multidrug resistance associated protein-1
miR: microRNA
mRNA: messenger ribonucleic acid
MTA: Methionine-S adenosyltransferase
MTase: Methyltransferases
mTHF: Methyltetrahydrofolate

N

NAD: Nicotinamide adenine dinucleotide
NADH: Reduced NAD
NADP: Nicotinamide adenine dinucleotide phosphate
NADPH: Reduced NADP

O

OXPHOS: Oxidative phosphorylation

P

P-gp: P-glycoprotein
PPP: Pentose phosphate pathway
Dehydrogenase

R

RNA: Ribonucleic acid
RNAi: RNA interference
ROS: Reactive oxygen species
R5P: Ribose 5-phosphate

S

SAMe: S-adenosylmethionine
SAH: S-adenosylhomocysteine

T

TSG10: Tumour susceptibility gene 101
THF: Tetrahydrofolate

CHAPTER I – INTRODUCTION

Part I – Literature Review

1. Multidrug resistance in cancer

The use of chemotherapeutic agents is one of the most common and effective approaches to treat cancer [1]. However, although conventional chemotherapeutic agents affect the growth of rapidly dividing cancer cells, they also affect normal cells, causing devastating secondary effects [2]. New advances in cancer therapy have been focused in targeted therapies (aiming at molecular targets or pathways which are specific or overexpressed in cancer), since they seem to be more effective and less harmful than conventional chemotherapy [3]. Nevertheless, the inefficacy of all of these agents (either conventional or targeted therapies) is frequent and commonly associated with the resistance of cancer cells to anticancer drugs [4].

In some cases of drug resistance, cancer cells may exhibit cross-resistance against multiple unrelated drugs which are structurally and/or functionally different, a phenomenon named multidrug resistance (MDR) [5,6]. MDR may be classified as: i) intrinsic MDR, which occurs naturally, before any drug treatment; or ii) acquired MDR, caused by drug selective pressure and developed during or after the course of treatment, or upon recurrence of the disease [5,6].

Several studies have shown that, for some tumours, treatment failure may be attributed to the presence of cancer stem cells (CSCs), which are extremely resistant to different therapeutic approaches [7]. Indeed, CSCs may differentiate into different types of cells according to a specific condition or environment (i.e. each new population of cells originated from CSCs has the capacity to either remain a CSC or change to other types of more specialized cells with a defined function) and therefore they are extremely challenging from the point of view of cancer therapy [8].

Drug resistance in general, and MDR in particular, is a current clinical problem hard to overcome, particularly due to the great degree of genetic and phenotypic heterogeneity of tumours [9-11]. During treatment, the main cell populations are normally destroyed by the drugs but the more resistant cells, which are smaller cell populations (and which may be CSCs), survive and remain quiescent. Occasionally, the selective pressure (e.g. caused by drug treatment) may cause these quiescent cells to suffer genetic alterations (such as mutations or chromosomal translocations) which allow them to acquire advantageous characteristics, becoming able to proliferate and establish another clone of tumour cells, which is then resistant to the first line of treatment [12].

1.1. MDR mechanisms – an overview

There are several mechanisms involved in intrinsic or acquired MDR (Table 1). Usually, two or more of these mechanisms act simultaneously in each cancer type, thus making it very difficult to overcome MDR [13].

Table 1 – Examples of cellular mechanisms involved in MDR in cancer.

MDR mechanism	Examples		References
	Cellular alterations	Cancer model	
ATP-dependent drug efflux	Overexpression of ABC transporters (e.g. P-gp)	Several cancers	[14]
Increase in drug detoxification	Overexpression of glutathione S-transferases	Primary ovarian cancer and osteosarcoma	[15,16]
Increase in DNA damage repair	Decreased expression of MLH1	Breast cancer	[17]
Cell cycle arrest deregulation	Mutations in p53	Breast cancer and ovarian carcinoma	[18,19]
Deregulation of apoptosis	Overexpression of anti-apoptotic proteins (e.g. Bcl-2)	Breast cancer and Non-Hodgkin's Lymphoma	[20,21]
Alterations in the expression of some microRNAs	Overexpression of microRNA-21	Neuroblastoma	[22]
Metabolic alterations	Increased glycolysis	Breast cancer	[23]

ATP-dependent drug efflux

Drug-efflux, usually resulting from an increased efflux of the cytotoxic drugs by cell-membrane transporters, is the most widely studied MDR mechanism [24]. This mechanism causes a decrease in the intracellular concentrations of anticancer drugs to levels below the therapeutic concentrations, therefore allowing cells to survive treatment[14]. The most common mechanism involves the ATP-binding cassette (ABC) membrane transporters [24]. ABC transporters are usually expressed in several tissues and play a natural role in extruding xenobiotics from the body [14]. To date, 49 ABC transporters have been identified in the humans, which have been divided into seven different categories according to their sequence and structural homology (**ABC**A to **ABC**G) [14]. Among them, the most extensively studied ABC transporters are ABCB1/MDR1 (which codes for P-glycoprotein, P-gp), ABCC1/MRP1 (which codes for multidrug resistance associated protein-1) and ABCG2/BCRP (which codes for breast cancer resistant protein) [25]. The role of the ABC transporter P-gp will be described further in this thesis, in section 1.2. “The particular role of P-glycoprotein in MDR”.

Increase in drug detoxification

An increase in drug detoxification is another significant mechanism of MDR. The effect of cytotoxic drugs that enter the cells is reduced by specific drug-metabolizing enzymes which may be overexpressed in cancer cells, such as cytochrome P4503A, glutathione-S-transferases (GST) and aldehyde dehydrogenases-related phase II enzymes [26]. For example, GST is responsible for the inactivation of some chemotherapeutic drugs, such as carboplatin and cisplatin, by conjugating them with glutathione. These conjugates are then substrates for some ABC-transporters (e.g. MRP1) which cause their efflux from the cell [27].

Increase in DNA damage repair

The ability of cancer cells to recover from DNA damage caused by chemotherapeutic drugs can determine tumour resistance [28]. The DNA damage repair is a complex process involving several important genes which mainly participate in some functionally combined pathways: homologous recombination, non-homologous and joining recombination, nucleotide excision repair, base excision repair and mismatch repair [29].

Many chemotherapeutic drugs (such as platinum drugs, topoisomerase inhibitors and alkylating agents) induce cell death via DNA damage induction [28]. In fact, usually cells undergo apoptosis following an incomplete DNA repair[28]. However, in some cases, cells are capable of overcoming the DNA damage and continue to proliferate, giving rise to cells

with a more resistant phenotype (e.g. the MDR phenotype). Currently, an approach used to overcome the alterations in the DNA repair machinery is the inhibition by specific agents of the DNA damage repair system of malignant cells [30].

Cell cycle arrest deregulation

The fundamental processes of progression through the cell cycle involve the complex interaction of several families of proteins (such as oncogenes and tumour suppressor genes) in a systematic and coordinated manner [31]. Specifically, p53, a tumour suppressor gene that is responsible for the cell cycle arrest [32], determines the destiny of the cells with damaged DNA *i.e*., determines if the cell arrests its cell cycle to allow DNA repair and cell survival, or if the damaged cell enters apoptosis. By doing this, the production of a "daughter" cell with damaged DNA is prevented [32]. However, p53 is often mutated in cancer and the lack of a functional p53 may cause the cell cycle to continue even with the damaged DNA, which may cause a MDR phenotype [33-35].

Deregulation of apoptosis

Some chemotherapeutic agents induce apoptosis and necrosis of the tumour cells [35]. However, alterations in apoptosis have been described as a major cause of MDR [35,36]. This is normally caused by deregulations (usually overexpression) of some anti-apoptotic genes [37,38]. Currently, targeting and activating some apoptosis-inducing proteins in tumour cells has proven to be useful, by conferring a higher sensitivity to drugs and survival rate for some cancer patients [30].

Alterations in the expression of some microRNAs

Some studies have linked alterations in microRNAs expression with the MDR development [39]. There are several factors involved in the deregulation of microRNAs in cancer [40]. This deregulation could potentially lead to defective microRNAs biogenesis pathways, epigenetic modifications (such as methylation of the CpG islands) and deregulation of gene expression [41], all of which may be associated with both increased sensitivity or resistance to anticancer drugs [30]. This dual function (specifically related to the P-gp expression) will be described further in this thesis, in section 1.2.: "The particular role of P-glycoprotein in MDR".

Metabolic alterations

The link between tumour metabolism and MDR is highly complex. It depends on multiple parameters, such as oxygen and nutrient availability or the specific drugs that are being used. Several studies have been published relating MDR to alterations in cellular

metabolism: i) upregulation of hypoxia-induced factor 1 (HIF-1) was associated with chemoresistance [42]; ii) leukaemia models with higher glycolytic rates showed resistance to glucocorticoids [43]; iii) modulation of cellular metabolic pathways contributed to acquired resistance in multiple myeloma cells [44]; iv) glycolytic pyruvate was capable of regulating P-gp expression in multicellular tumour spheroids [45]; and v) hypoxia induced MDR and glycolysis in a orthotopic MDR tumour model in nude mice [46].

The identification of all the metabolic alterations may facilitate overcoming the MDR problem and developing novel therapeutics for cancer. This will be further described in this thesis, in section 1.3: “Metabolic Alterations in MDR”.

1.2. The particular role of P-glycoprotein in MDR

P-glycoprotein was the first discovered member of the ABC transporters, when in 1976 Juliano and Ling characterized a 170 kDa glycoprotein overexpressed in colchicine resistant cell lines that was able to modify drug permeability on those cells [47]. Since then, overexpression of P-gp has been shown to contribute to the MDR phenotype of many cancer cells. As previously referred, this overexpression results in increased cellular drug efflux, causing lower intracellular drug concentration and reducing drugs' efficacy. [24]. Although being mainly described as a transmembranar protein, P-gp is also found in other cellular organelles such as cytoplasmic membrane [48], endoplasmic reticulum [49], nucleus [50] and endosomes [51]. This suggests that P-gp may have other cellular functions that could contribute to drug resistance [39].

P-gp expression may be regulated by several microRNAs, which may contribute to the drug resistant phenotype. In the following section, it is presented a review paper titled: "*The Network of P-glycoprotein and microRNAs interactions"* [39], in which the web of interactions between P-gp and microRNAS is described, following an initial description of the importance of P-gp in MDR.

1.2.1. REVIEW ARTICLE: The network of P-glycoprotein and microRNAs interactions

Vanessa Lopes-Rodrigues, Hugo Seca, Diana Sousa, Emília Sousa, Raquel T. Lima, M. Helena Vasconcelos

Published in International Journal of Cancer: 135, 253–263 (2014)

IJC
International Journal of Cancer

The network of P-glycoprotein and microRNAs interactions

Vanessa Lopes-Rodrigues[1,2,3], Hugo Seca[1,4], Diana Sousa[1,2], Emília Sousa[2,5], Raquel T. Lima[1,2] and M. Helena Vasconcelos[1,4]

[1] Cancer Drug Resistance Group, Institute of Molecular Pathology and Immunology of the University of Porto, IPATIMUP, Porto, Portugal
[2] Center of Medicinal Chemistry of the University of Porto, CEQUIMED-UP, Porto, Portugal
[3] Institute of Biomedical Sciences Abel Salazar, University of Porto, ICBAS-UP, Porto, Portugal
[4] Department of Biological Sciences, Laboratory of Microbiology, Faculty of Pharmacy, University of Porto, Porto, Portugal
[5] Department of Chemical Sciences, Laboratory of Organic and Pharmaceutical Chemistry, Faculty of Pharmacy, University of Porto, Porto, Portugal

Mini Review

Overexpression of P-glycoprotein (P-gp) contributes to the multidrug resistance (MDR) phenotype found in many cancer cells. P-gp has been identified as a promising molecular target, although attempts to find successful therapies to counteract its function as a drug efflux pump have largely failed to date. Apart from its role in drug efflux, P-gp may have other cellular functions such as being involved in apoptosis, and is found in various locations in the cell. Its expression is highly regulated, namely by microRNAs (miRNAs or miRs). In addition, P-gp may regulate the expression of miRs in the cell. Furthermore, both P-gp and miRs may be found in microvesicles or exosomes and may be transported to neighboring, drug-sensitive cells. Here, we review this current issue together with recent evidence of this network of interactions between P-gp and miRs.

P-glycoprotein is Responsible for Drug Resistance in Various Cancers

Overexpression of P-glycoprotein (P-gp) represents one of the main mechanisms, which contribute to the multidrug resistance (MDR) phenotype. Drug resistance associated with high P-gp expression levels may have two main causes, according to the tumor cell type: (a) high basal P-gp levels in the tumor tissue or, (b) induction of P-gp expression after chemotherapy treatment.[1]

P-gp is usually found in the colon, liver, kidney and adrenal gland, where it has a secretory function.[2] Therefore, as expected, high levels of P-gp have been found in cancers arising from these tissues. On the other hand, haematological malignancies such as leukemias, lymphomas and multiple myelomas are characterized by low P-gp expression levels at diagnosis but increased levels after drug treatment and relapse.[1,2]

Indeed, the relevance of P-gp in hematological malignancies has been reported by several authors over the last 20 years.[3–17] Although some discrepancies exist in the published results, they predominantly report the same conclusion: P-gp levels are often increased following chemotherapy treatment. Published data reports evidence for the relevance of P-gp expression for the prognosis of acute myeloid leukemia (AML) and acute lymphoblastic leukemia (ALL) in an age-dependent manner[18] and reveals the induction of P-gp expression during repeated exposure to cytostatic drugs,[19,20] which results in an increase in drug resistance of these haematological malignancies.

In addition to hematological malignancies, many other tumor types such as colon and renal cancers express high levels of P-gp (Table 1). Expression of P-gp has also been related to the pathological grading of colorectal carcinoma, being higher in well differentiated tumors and lower in poorly differentiated ones.[21,22] The mechanisms underlying drug resistance caused by high P-gp levels in colorectal cancer have been unravelled. In fact, the contribution of cyclooxygenase (COX2) to P-gp mediated drug resistance, via phosphorylation of c-Jun, has been described.[23] Moreover, the activation role of some p53 mutants on P-gp promoter has been reported[24,25] as well as the identification of P-gp as a target of transactivation by the β-catenin complex/T cell factor 4, which is thought to be the basis of tumorigenesis in colorectal cancer[26] (Fig. 1—panel *a*).

P-gp expression has also been associated with renal cell carcinoma (RCC), one of the most intrinsically chemoresistant tumor types.[27] Indeed, *MDR-1* transcripts or P-gp protein have been identified in the majority of RCC samples.[28–30] Studies from the National Cancer Institute also support this evidence, reporting high P-gp mRNA levels in several renal

Key words: P-glycoprotein, microRNAs, drug resistance, cancer, microvesicles, exosomes

Abbreviations: ABC: ATP-binding cassette; ALL: acute lymphoblastic leukemia; AML: acute myeloid leukemia; COX: cyclooxygenase; ER: endoplasmic reticulum; MDR: multidrug resistance; miRNA: microRNAs; NBD: nucleotide-binding domain; RCC: renal cell carcinoma; TMD: transmembrane domain

Grant sponsor: PhD grant from FCT (to V.L.R. and H.S.); **Grant numbers:** SFRH/BD/87646/2012 and SFRH/BD/47428/2008; **Grant sponsor:** post-doc grant from FCT (to R.T.L.); **Grant number:** SFRH/BPD/68787/2010; **Grant sponsor:** CEQUIMED-UP; **Grant number:** PEst-OE/SAU/UI4040/2011
DOI: 10.1002/ijc.28500
History: Received 10 Apr 2013; Accepted 13 Sep 2013; Online 1 Oct 2013

Correspondence to: M. Helena Vasconcelos, IPATIMUP, Institute of Molecular Pathology and Immunology of the University of Porto, Rua Dr. Roberto Frias s/n, 4200-465 Porto, Portugal, Tel.: 351-22-5570700, Fax: 351-22-5570799, E-mail: hvasconcelos@ipatimup.pt

Table 1. Increased levels of P-gp in several tumors were found to be associated with cancer drug resistance

Tumour Type	Featured findings	References
AML (Acute Myeloid Leukemia)	• Approximately 50% of patients had leukemic blasts that expressed P-gp, with a slightly greater rate of expression and at higher levels in elderly patients. • Patients with refractory and/or relapsed AML frequently expressed more P-gp than *de novo* patients.	4–8
ALL (Acute Lymphoblastic Leukemia)	• P-gp is observed in 38% of cases of ALL. • Even though some authors did not find significant association between P-gp and prognosis of ALL, others found a correlation between P-gp and poor drug response. • Expression of P-gp in adult ALL patients was higher than in children.	10–14
NHL (Non-Hodgking's Lymphoma)	• In NHL, P-gp expression increased from 2-49% in untreated patients to 64% in post-treated patients.	3
Multiple Myeloma (MM)	• 10-30% of MM patients expressed *MDR-1* gene at diagnosis compared to 50-80% of patients with relapsed or resistant disease. • In some studies P-gp expression was described as an independent predictor of poor clinical outcome.	167–169
Colorectal Cancer	• In adenomatous polyps from patients with familial adenomatous polyposis syndrome, P-gp expression was significantly increased and correlated with β-catenin, a protein involved in the tumourigenesis of colorectal cancer. • P-gp expression related with pathological grading of colorectal carcinoma, (being higher in well differentiated tumours and lower in poorly differentiated ones). • siRNAs targeting MDR-1 in cells suppressed P-gp expression, reverting multidrug resistance in colon cancer cells.	21–24,26
Renal Cancer	• P-gp transcripts or protein identified in normal renal proximal tubules and in the majority of renal cell carcinoma samples indicated that this efflux pump is implicated in both intrinsic and acquired resistance.	27–33
Liver Cancer	• Overexpression of P-gp (but not MRP1) mainly contributes to the MDR of SMMC-7721/ADM cells. • The upregulation of P-gp and BCRP (but not of MRP1 and LRP) were involved in the MDR of HepG2/ADM cells. • Overexpression of P-gp associated with the MDR phenotype of a taxol resistant cell line, QGY-TR50.	170–172
Small and Non-small Cell Lung Cancer (SCLC and NSCLC, respectively)	• Stronger evidence of an association of P-gp expression with outcome in SCLC than in NSCLC; however, some studies reported a significant correlation between tumour P-gp detection and response to paclitaxel/platinum and cisplatin/ ifosfamide/ vinblatine/ radiation in NSCLC. • In chemo-naive NSCLC patients, P-gp transcripts/ protein were identified in 11-32% of surgical specimens, but increased in 61% of tumours that had been treated with chemotherapy.	173–175
Ovarian Cancer	• A meta-analysis showed that, among other potential biomarkers, P-gp is not yet useful as a predictor of prognosis; however, high P-gp expression is associated with poor overall survival as well as with poor progression-free survival in epithelial ovarian cancer. • In cisplatin-resistant ovarian cancer cell line, P-gp can be upregulated as a generalised stress response rather than as a specific response to a substrate.	176–178
Breast Cancer	• Increased activity of P-gp in breast carcinomas was demonstrated using a substrate recognized by this efflux pump. • A meta-analysis indicated that P-gp expression in breast tumours associated with poor response to chemotherapy (patients with tumours expressing P-gp were three times more likely to fail responding to chemotherapy).	179,180
Glioblastoma	• The uptake of erlotinib has proven ineffective in clinical trials due to the actions of P-gp in conjunction with BCRP1. • Elevated glycolysis in tumour spheroids of glioblastoma cells was correlated to increased P-gp expression.	181–183

tumor cell lines[31,32] as well as increased P-gp transcripts associated with *in vitro* resistance of cell lines or primary cultures to paclitaxel and doxorubicin.[33,34]

P-gp was also found to be downregulated during differentiation of pluripotent stem cells.[35] Most interestingly, P-gp levels have been also related to apoptosis. For example, it has been shown that P-gp may confer drug resistance to caspase-mediated apoptosis.[36,37] In addition, ceramide (an inducer of apoptosis) increased glucosylceramide synthase, which in turn induced *MDR-1* overexpression (via β-catenin mediated *MDR-1*

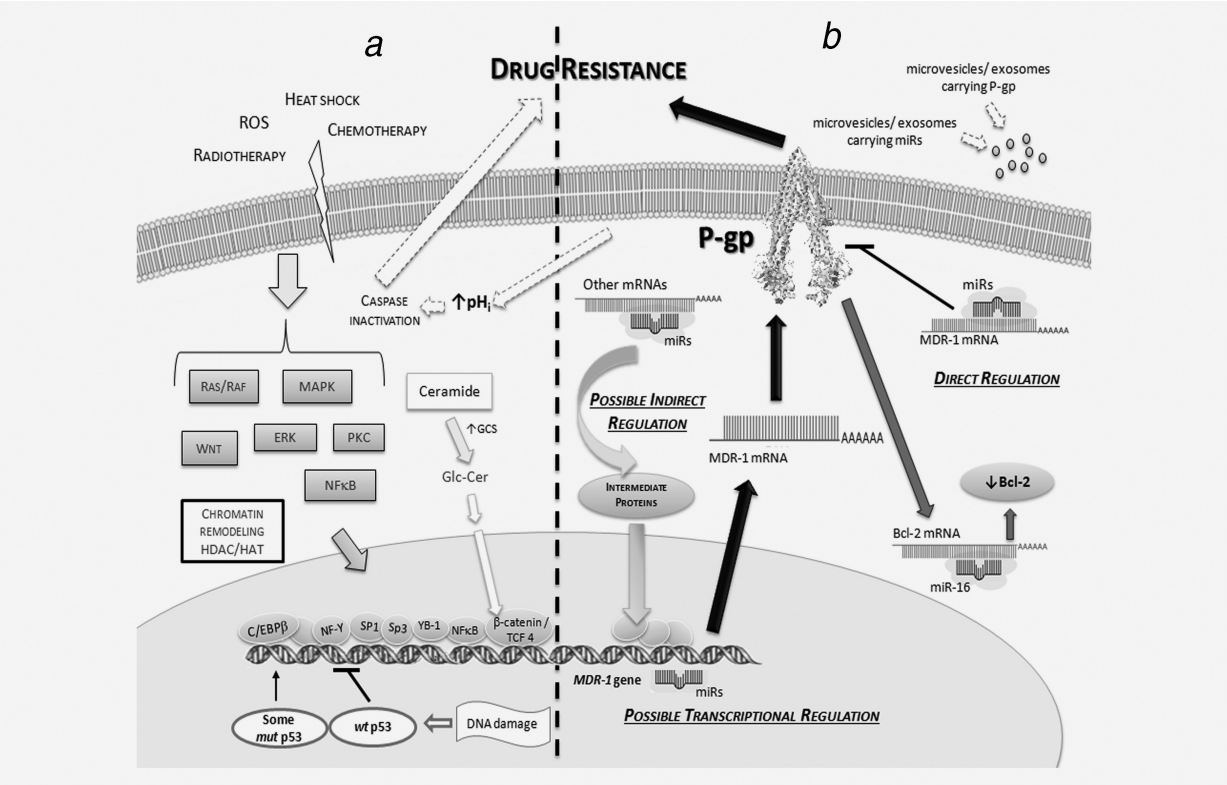

Figure 1. Complex interaction between P-gp, miRs and other cellular proteins to reinforce MDR. (*a*) Different stimuli (such as chemotherapy) may induce different signaling pathways which regulate the expression of proteins involved in *MDR-1* gene transcription and drug resistance. The effect of P-gp on the intracellular pH levels has been suggested to affect apoptosis and drug resistance. (*b*) MDR-1 mRNA levels may be regulated by miRs (directly, indirectly or at the transcriptional level), which will regulate P-gp protein levels and drug resistance. In addition, P-gp may regulate the expression of one miR, which regulates apoptosis and drug resistance. Both P-gp and miRs may be transported to other cells by microvesicles or exosomes. GCS: Glucosylceramide synthase; Glc-Cer: Glucosylceramide; HAT: Histone Acetyltransferases; HDAC: Histone Deacetylase Inhibitors.

promoter activation) and increased P-glycoprotein efflux, regulating cancer drug resistance.[38] Moreover, the overexpression of P-gp is frequently accompanied by an increase in intracellular pH; since apoptosis is often preceded by intracellular acidification, it is possible that increased pH (promoted by P-gp overexpression) could render cells relatively resistant to multiple forms of caspase-dependent cell-death stimuli.[39] All of these processes are relevant to cancer development/therapy (Fig. 1—Panel *a*).

Downregulation of P-gp Levels and Activity as Therapeutic Approaches

P-gp silencing studies have shown promising results in cell lines. For example, some of us have found that downregulation of P-gp caused an increase in drug sensitivity of a resistant chronic myelogenous leukemia cell line (overexpressing P-gp).[40,41] In addition, stable transfection of siRNAs for P-gp was shown to reverse the P-gp dependent MDR of colon cancer cells[42] and short hairpin RNA-mediated P-gp silencing was shown to enhance the sensitivity of ovarian cancer cells to paclitaxel.[43]

These studies, together with the high levels of P-gp observed in cancer patients, illustrate the relevance of this drug efflux pump in the drug resistance phenotype of cancer cells. Consequently, some authors agree that the overexpression of P-gp in itself is a poor prognosis factor. Nevertheless, an idea which has gained ground recently, describes the P-gp associated MDR phenotype as a result of a complex network of signalling pathways and drug resistant proteins.[2,44]

To achieve a more effective chemotherapy, strategies to silence P-gp or develop P-gp inhibitors to block/decrease its activity have been used. To date, four generations of P-gp inhibitors have been described, many of them having reached clinical trials.[45–47] Nevertheless, clinical trials with such inhibitors/modulators have not yet obtained satisfactory results, due to high toxicity of the compounds and poor patient selection criteria.[48] Indeed, P-gp has to date not been successfully translated in therapeutics.

P-gp Synthesis, Cellular Localization, Expression and Function

P-gp is the best characterized efflux pump mediating MDR. It is a 170 kDa membrane protein, member of the ATP-binding cassette (ABC) superfamily of transporters,[49] which acts to prevent the absorption of orally ingested or airborne toxins, xenobiotics or drugs.[50]

P-gp is encoded by the human *MDR-1* gene located at chromosome 7, being synthesized in the endoplasmic reticulum (ER)

as a glycosylated intermediate. It contains 1,280 amino acids arranged in two halves, each encompassing a transmembrane domain (TMD) which spans the membrane and two intracellular nucleotide-binding domains (NBD).[51] The glycosyl moiety in the first extracellular loop of P-gp appears to have a role in the trafficking or stability of P-gp to the cell surface, although it does not seem to be essential for drug transport[52] (Fig. 1—Panel *b*). Although there is still no X-ray data on human P-gp, the structures of mouse[53] and *Caenorhabditis elegans*[54] P-gp were recently obtained at 3.8 and 3.4 Å resolution, respectively. The obtained P-gp 3-D structures highlighted the importance of membrane partitioning when a drug accesses the transporter in the membrane.[54] Apo P-gp structures have an inverted "V" shape inward-facing conformation for drug entry, whereas they have an outward-facing conformation for releasing the substrate to the extracellular medium[53] (Fig. 1—Panel *b*).

P-gp is mainly localized in the plasma membrane. Since the depth of the cellular membrane is about 4 nm, half the P-gp is included in the phospholipid bilayer of the membrane.[55] P-gp is also found at intracellular membranes,[2,56,57] and is frequently observed in the nucleus[58–60] while also being described in the ER,[61] Golgi apparatus,[62,63] endosomes[64] and lysosomes[65] (organelles which are involved in its intracellular trafficking).[57] The presence of P-gp has also been described in mitochondria, where it may be involved in the protection of mitochondrial DNA.[66] Furthermore, protection of the nucleus from drugs has also been suggested as a role for mitochondrial P-gp in MDR cells.[67] However, studies using P-gp-EGFP fusion protein or wild-type P-gp showed no co-localization with a mitochondrial marker.[57,64,68] P-gp may also be present in intracellular vesicles actively contributing to drug sequestration and removal from cells.[66,69]

Several studies have suggested that intracellular P-gp also contributes to drug resistance.[58,70] Indeed, studies using leukemic cell lines and AML patient samples have shown that the levels of total P-gp (protein or mRNA) correlated better with drug efflux than those of surface P-gp protein.[69] Furthermore, a strong association between intracellular P-gp and intrinsic resistance was observed in a human colon carcinoma clone, which did not express P-gp on the plasma membrane.[70] Nevertheless, other studies claim that intracellular P-gp does not seem to have a (major) role in drug resistance.[61,64]

Therefore, it is important to better understand how P-gp is regulated, which seems to be a complex and highly controlled process.[2] Indeed, several signalling pathways and transcription factors have been described as being involved in the regulation of P-gp expression, such as Wnt/β-catenin, Ras/Raf, MAPK/ERK, p53, NF-κB and PKC.[71–77] Moreover, several extracellular stimuli such as heat shock,[78] UV radiation,[79] reactive oxygen species[80,81] and cytotoxic drugs[82,83] induce P-gp expression (Fig. 1—Panel *a*).

Although occurring predominantly at the transcriptional level,[71] regulatory mechanisms of P-gp expression may also be present post-transcriptionally. In fact, in addition to alterations in gene transcription and gene amplification,[84] P-gp expression has also been associated with (*i*) alternative promoter usage,[85] (*ii*) DNA methylation and histone acetylation,[86–88] (*iii*) alterations in *MDR-1* mRNA stability[89,90] and (*iv*) P-gp turnover and intracellular trafficking.[90] More recently, microRNAs (miRNAs or miRs) have emerged in the literature as regulators of the expression of proteins related to drug resistance, including P-gp.[73]

microRNAs as Regulators of P-gp Gene Expression

miRs are a class of single-stranded ncRNAs (non-coding RNAs) ranging from 19 to 25 nucleotides in length and having significant roles in gene regulation. The mRNA-miR pairing occurs mostly through the binding of the miR to the target mRNA 3'-UTR; however, binding to the coding region or to the 5'UTR may also occur.[91] Association of miRs with mRNAs leads to post-transcriptional suppression of the targeted mRNA expression: full complementarity between miR and mRNA leads to mRNA cleavage while partial complementarity leads to translational repression.[92–94] One miR may target several mRNAs. On the other hand, one mRNA may "enclose" several binding sites for the same miR or may have binding sites for different miRs.[95,96] Indeed, different miRs can target the same mRNA for a cooperative regulation, demonstrating how complex the regulation of miRs is.[97–99]

In addition to their canonical function, miRs can also function as positive regulators of gene expression,[100–102] through binding to other regions of the mRNA such as protein-coding exons[103] or to the 5'UTR region.[91,104] It has been suggested that miRs may also bind to the promoter region of genes.[104–106]

miR-mediated regulation allows the expression of a multitude of different mRNAs involved in multiple key cellular processes to be controlled.[107–111] Therefore, miRs biogenesis and their relative abundance must also be tightly regulated,[112,113] especially in what concerns their transcription, processing and cellular localization levels.[114–116] Indeed, transcription factors, enhancers and chromatin modifications may alter miR expression levels, either positively or negatively.[117,118] Ultimately, miRs "control" the cellular phenotype in processes such as development[119] and differentiation.[120] Moreover, their aberrant expression is often associated with a wide variety of diseases, from diabetes[121] to cardiovascular disease[122] and several cancers.[123–127]

Some studies have been published linking the altered expression of some miRs, in different cancer types, to alterations in *MDR-1*/P-gp expression and consequently with the MDR phenotype. Therefore, this section describes the miRs which have already been reported as *MDR-1*/P-gp regulators (Fig. 1—Panel *b*). This regulation may occur post-transcriptionally through the binding of miRs to the 3'-UTR of *MDR-1* (direct regulation) or by miRs targeting and affecting other factors, which modulate P-gp expression (indirect regulation). In addition, regulation may possibly also occur at the transcriptional level, by interaction of miRs with the *MDR*-1 promoter (direct hybridization) or by triplex structure formation (double-stranded DNA/RNA).[128] Figure 2 outlines a schematic representation of the miRs that interact with P-gp.

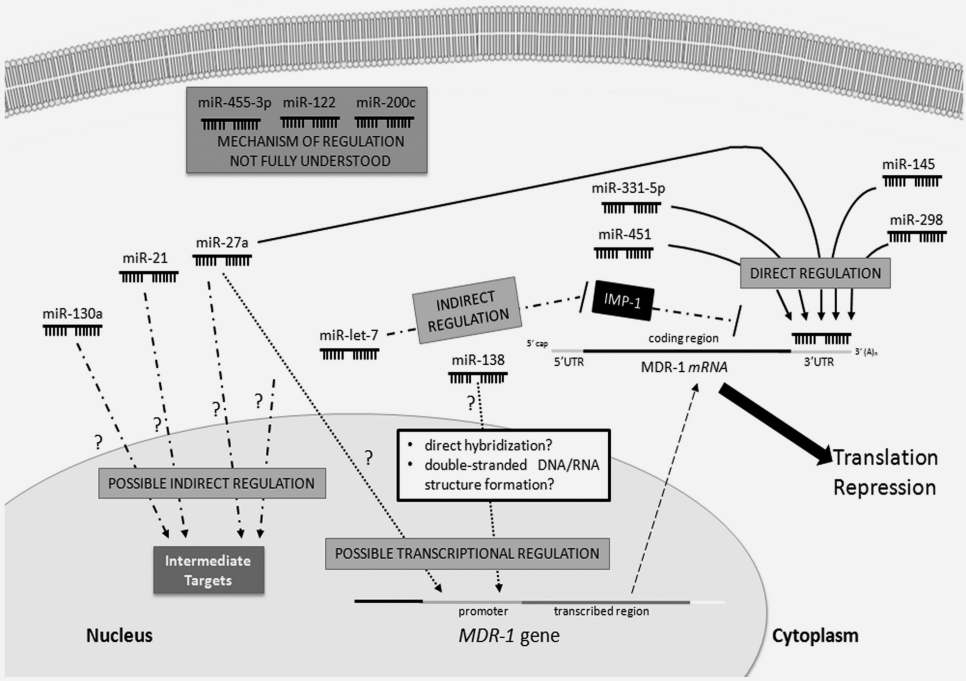

Figure 2. Different mechanisms by which miRs regulate P-gp expression. The regulation of P-gp by miRs may occur post-transcriptionally by: (*i*) direct binding of miRs to the 3'-UTR of *MDR-1* mRNA (direct regulation) or, (*ii*) miRs targeting other mRNAs and therefore altering the levels of other proteins, which modulate P-gp expression (indirect regulation). In addition, regulation may possibly also occur at the transcriptional level, through interaction of miRs with the *MDR*-1 promoter. Often, miRs regulate P-gp levels by mechanisms not yet fully understood. Question marks (?) indicate that the intermediate target is unknown. Solid arrows: direct regulation; Dashed dot arrows: (possible) indirect regulation; Round dot arrows: possible transcriptional regulation.

miRs acting at the post-transcriptional level - direct regulation

Several miRs have been described as direct regulators of P-gp, by direct interaction with the 3'-UTR of the *MDR-1* mRNA region (Fig. 2 and Table 2). In this direct regulation, an inverse correlation between the expression levels of some miRs and P-gp mRNA levels has been observed.[128]

miR-451 was found to regulate P-gp expression through a unique binding site within the *MDR-1* 3'-UTR. By increasing the cellular levels of miR-451, in a doxorubicin-resistant breast cancer cell line (MCF-7/DOX), a decrease in *MDR-1* expression and more importantly, an increase in cellular sensitivity to doxorubicin were observed.[129]

Direct regulation of *MDR-1* has also been described for miR-331-5p (with the description of a putative miR-331-5p binding site) in resistant K562/DOX leukemia cells.[130] In this study, an inverse correlation between *MDR-1* expression and miR-331-5p levels was shown. Furthermore, miR-331-5p overexpression was shown to increase the sensitivity of resistant K562/DOX cells to doxorubicin, through the inhibition of *MDR-1* gene expression.[130]

Impaired processing of miR-298 (due to low expression of Dicer enzyme) has been associated with the modulation of P-gp expression.[131] One study reported that miR-298 directly binds to the *MDR-1* 3′-UTR and that miR-298 downregulation increased P-gp expression and induced resistance to doxorubicin in breast cancer cells (MDA-MB-231).[131]

In addition, miR-145 negatively regulates P-gp expression and function through the repression of *MDR-1* mRNA. Overexpression of miR-145 in a human embryonic kidney cancer cell line decreased *MDR-1* mRNA levels.[132] Interestingly, downregulation of miR-145 in a human colon carcinoma cell line (Caco-2) also increased P-gp expression and P-gp mediated activity, but not *MDR-1* mRNA level, suggesting that in this cell line miR-145 might regulate P-gp through translational repression of *MDR-1* mRNA.[132]

Finally, miR-27a was reported to directly regulate *MDR-1* in a chronic myeloid leukemia cell line (K562).[130] miR-27a expression was shown to inversely correlate with *MDR-1* expression and to increase cell sensitivity to doxorubicin.[130]

miRs acting at the post-transcriptional level—possible indirect regulation

Several miRs have been described as "indirect regulators" of P-gp, by targeting other mRNAs, which code for intermediate proteins or transcription factors involved in *MDR-1* gene activation[128] (Fig. 2 and Table 2).

miR-451, which was mentioned above as a direct regulator, has also been described as an indirect regulator of *MDR-1*/P-gp expression in ovarian and cervical cancer cells.

Table 2. Reported miRs that regulate P-gp in different cancer cells

	Post-Transcriptional regulation						
	Direct	Possibly Indirect regulation	Possibly Transcriptional regulation	Not fully understood regulation	Human Tumour Cells	Performed assays	References
miR-451	x				Breast adenocarcinoma	Luciferase assays	129
		x			Ovarian and cervical cancer	Transfection of miR mimics and antimiR	73
miR-331-5p	x				Chronic myeloid leukaemia	Transfection of miR mimics Luciferase assays	130
miR-298	x				Metastatic breast cancer	Luciferase assays	131
miR-145	x				Embryonic kidney and Colon cancer	Luciferase assays Transfection of miR mimics Rodhamine 123 assay	132
miR-27a	x				Chronic myeloid leukaemia	Luciferase assays Transfection of miR mimics	130
		x			Ovarian and cervical cancer	Transfection of miR mimics and antimiR	73
			x		Esophageal squamous cell carcinoma and Gastric cancer	Transfection of antimiR luciferase assays	106,144
miR-21		x			Breast adenocarcinoma	Transfection of antimiR	141
miR-130a		x			Ovarian cancer	Transfection of antimiR	142
miR-let-7		x			Ovarian cancer	Transfection of siRNA Rodhamine 123 assay	143
miR-138			x		Promyelocytic leukaemia	Luciferase assays Transfection of miR mimics	105
miR-200c				x	Breast adenocarcinoma	Transfection of miR mimcs	145
miR-122				x	Hepatocellular carcinoma	Transfection of miR mimcs	147
miR-455-3p				x	Acute lymphoblastic leukaemia	Microarray analysis Microvesicles transfer	148

Indeed, miR-451 expression was found increased in MDR cells and its inhibition resulted in decreased expression of both P-gp and *MDR-1* mRNA. Therefore, in these cases, the effect of miR-451 in *MDR-1* may be indirect, although the precise mechanisms require further investigation.[73]

Similarly, miR-27a has also been described as being both a direct and indirect regulator of P-gp. In ovarian and cervical cancer cell lines (A2780 and KB-3-1), *MDR-1* mRNA expression was shown to be positively regulated by miR-27a, favoring its role as a possible indirect regulator.[73]

miR-21 is an accepted oncomiR.[133,134] Its expression has been shown to be involved in cellular proliferation,[135,136] apoptosis[135] and autophagy.[137] In addition, its expression is associated with chemoresistance in a variety of cancer cells.[138–140] Interestingly, miR-21 has also been described to indirectly regulate *MDR-1* expression.[141] A novel hyaluronan (HA)-CD44-mediated PKC signalling mechanism which regulates a stem cell marker (Nanog) has been associated with miR-21 production. Indeed, the presence of hyaluronan increased miR-21 levels (via Nanog phosphorylation) leading to a reduction in the levels of the tumor suppressor protein PDCD4 (programmed cell death 4). These two events contributed to an increase in the translation rate of diverse transcripts, including *MDR-1,* in breast cancer cells (MCF-7). In addition, the downregulation of miR-21 significantly attenuated the HA-CD44 activated expression of P-gp.[141]

A recent study carried out in an ovarian cancer cell line (SKOV3)[142] indicated that miR-130a might be associated with *MDR-1*/P-gp mediated drug resistance. By decreasing miR-130 expression, an indirect inhibition of *MDR-1* mRNA and P-gp expression were observed and resistance of these cells to cisplatin, which is an inducer of P-gp expression, was reverted.

Finally, it has been shown that miR-let-7 may indirectly regulate *MDR-1* in ovarian cancer cells. This seems to occur through the downregulation of *IMP-1*, a RNA binding protein, causing destabilization of the *MDR-1* mRNA and therefore downregulation of P-gp expression (Fig. 2).[143] These findings were further substantiated by analysing samples from ovarian cancer patients, where a correlation between downregulation of miR-let-7 and upregulation of both IMP-1 and P-gp proteins was found.[143]

miRs acting at the transcriptional level

In addition to the previously described miRs acting at post-transcriptional level, speculation has arisen regarding the involvement of two miRs with *MDR-1* regulation at the

transcriptional level, implying that these miRs might regulate *MDR-1* by interfering with the gene promoter region[128] (Fig. 2 and Table 2).

In this context, the association between P-gp expression and miR-138 in promyelocytic leukemia cells (HL-60) has been reported. In these cells, upregulation of miR-138 could reverse the MDR phenotype by downregulation of P-gp levels. A luciferase reporter assay permitted the regulatory effects of miR-138 on the *MDR-1* promoter to be analysed, suggesting that the regulation of P-gp through miR-138 might occur at the transcriptional level.[105]

Interestingly, miR-27a (already referred above to be both a direct and possibly indirect regulator) has also been claimed to be a transcriptional regulator of P-gp in esophageal squamous cell carcinoma and gastric cancer cells (ECA-109, TE-13 and MKN45).[106,144] These studies indicated that downregulation of miR-27a might reverse drug resistance and decrease the expression of P-gp.[106,144] In addition, when trying to elucidate the regulatory effects of miR-27a on the promoter activity of *MDR-1*, results suggested that miR-27a might be a modulator of the *MDR-1* promoter.[106]

miRs regulating P-gp through mechanisms of regulation not fully understood

Other miRNAs have been described to associate with *MDR-1* expression, although their mechanisms of action remain unknown (Fig. 2 and Table 2).

miR-200c expression seems to be associated, at least in part, with *MDR-1*/P-gp expression. The upregulation of miR-200c in breast cancer cells (MCF-7), resulted in reduced expression of *MDR-1* mRNA and P-gp, providing evidence for the role of miR-200c in drug resistance, through a mechanism of regulation not yet understood.[145] miR-200c has also been associated with chemotherapy response in patients. Indeed, in breast cancer patients who had received neoadjuvant chemotherapy, it was observed that miR-200c was downregulated in non-responder patients when compared to responders.[145]

miR-122 is a liver specific miR, which is downregulated in hepatocellular carcinoma human patients and animal models.[146] Overexpression of miR-122 in hepatocellular carcinoma cells caused a decrease in the expression of MDR related genes, including *MDR-1*.[147]

miR-455-3p has been related to P-gp levels in human ALL cell lines by mechanisms not fully understood, as will be referred in "P-gp and the microRNAs Involved in its Regulation May Be Present in Microvesicles and Exosomes, and May Be Transferred Between Cells" below.[148]

P-gp Regulates microRNAs Involved in Drug Resistance

To date, only one study has reported the regulation of miRs by P-gp.[149] A possible association between P-gp and radiation sensitivity has been found. Curiously, this study observed overexpression of P-gp, high miR-16 levels and radiation sensitivity in a MDR hepatocellular carcinoma cell line, when compared to its parental counterpart (HepG2). In addition, the transfection of a parental cell line with an *MDR-1* vector induced high levels of miR-16. The authors suggested that P-gp upregulated miR-16, which in turn downregulated Bcl-2 (Fig. 1—Panel *b*), leading to enhanced radiation-induced apoptosis.[149] However, the pathways linking P-gp to miR-16 remain to be fully identified. Nonetheless, this evidence supports a novel role for P-gp in miR regulation, reinforcing the diversity of P-gp functions in cancer cells.

P-gp and the MicroRNAs Involved in its Regulation May Be Present in Microvesicles and Exosomes, and May Be Transferred Between Cells

Increasing interest in microvesicles and exosomes as mediators of intercellular communication has recently emerged amongst the scientific community, due to their ability to transfer intracellular content from donor to recipient cells.[150] Indeed, the concept of non-genetic acquisition of functional P-gp in MDR has previously been described[151] and this could be mediated by microvesicles (50–1000 nm in diameter) or exosomes (40–120 nm)[152] which, once secreted from cells by mechanisms not yet fully understood, could provide vehicles for the intercellular transfer of P-gp from MDR donor to drug-sensitive recipient cells.[153,154]

miRs have also been shown to be included into microvesicles and exosomes and to be capable to targeting neighboring cells,[155–157] entering the blood stream and reaching distant cells.[158,159] Indeed, very recently, microvesicles and exosomes from resistant leukemia and breast cancer cells were shown to incorporate and transfer both P-gp protein and transcripts, together with miRs, to drug-sensitive recipient cells. This transfer resulted in the acquisition, by the recipient cells, of the drug resistant characteristics of the donor cells.[153,160,161] In a recent study, the authors analysed the molecular basis for the acquired traits, looking for some miRs which had previously been reported[73,106,129,130,144] (and described above) as enhancers of P-gp expression in drug resistant cancer cells (miR-27a and miR-451). They demonstrated that the transfer of transcripts and miRs through microvesicles plays an important role in conferring MDR by "retemplating" recipient cells in order to reflect the donor cell (P-gp overexpressed) phenotype.[160]

Other recent work also demonstrated that some miRs that are shed from microvesicles play an important role in MDR.[148] The authors observed that one of the significantly expressed and shed miRs, miR-455-3p, is possibly related to P-gp levels. In this study, results from microarray analysis showed that miR-455-3p was less expressed in a P-gp overexpressing resistant leukemia cell line, when compared with the parental sensitive cell line. Moreover, following the transfer of microvesicles from the resistant to the sensitive cell lines, it was observed that the sensitive cells acquired lower miR-455-3p and higher P-gp levels.[148] The mechanisms involved in the regulation of P-gp by this miR are not understood

(as previously mentioned in "miRs regulating P-gp through mechanisms of regulation not fully understood" section).

More recently, the same research group demonstrated that microvesicles from a resistant human breast adenocarcinoma cell line could transfer a stable MDR trait *in vivo* (in a murine tumor xenograft model). They observed that, following a single injected dose of microvesicles, P-gp was transferred with those microvesicles, co-localized within the xenografted tumor and remained stable for at least 2 weeks. These authors also reported that the transfer of P-gp via microvesicles (*in vitro*) is "cell type selective," depending on the donor cells. Indeed, microvesicles from a resistant leukemia cell line, transferred P-gp to both malignant (sensitive leukemia cell line) and non-malignant cells (human osteoblasts). Nonetheless, microvesicles from resistant breast cancer cell line only transferred P-gp to malignant cells (sensitive breast adenocarcinoma cell line). The authors observed that this could be due to the involvement of a cytoskeletal protein (Ezrin) which is selectively present only in some of the donor cells studied (breast cancer cell line model).[162]

In addition, it is known that miRs involved in P-gp regulation could also be transferred via cell-to-cell contact and drive chemoresistance. Indeed, miR-21 was shed via contact-dependent intercellular transfer, mediated by a transmembrane channel (*SIDT1*—systemic RNA interference defective family of channels).[163]

Future Perspectives

Targeting the transfer of P-gp, and-or miRs that regulate/are regulated by P-gp, to neighboring cells may be an approach to overcome some cases of drug resistance. A possible approach to avoid the transfer of P-gp via microvesicles/exosomes would be the use of small molecules or siRNAs to reduce the amount of P-gp in the donor cells, thus reducing the amount of P-gp that would be transferred in such vesicles. Molecules that reduce P-gp protein levels have been described, such as curcumin[164,165] or bortezomib,[166] and theoretically they should reduce the amount of P-gp transferred from drug resistant to drug-sensitive cells. Alternatively, silencing P-gp gene expression should also reduce the transfer of P-gp from drug resistant to drug-sensitive cells. Our group is currently studying these hypotheses.

In addition, extracellular vesicles themselves constitute a novel class of therapeutic targets to overcome drug resistance.[152] Four strategies should be capable of reducing extracellular vesicle trafficking, namely: (*i*) inhibition of their formation; (*ii*) inhibition of their release; (*iii*) inhibition of their uptake by other cells and (*iv*) blockage of their specific components.[152] The approach of reducing extracellular vesicle trafficking could theoretically reduce the transfer of both P-gp and miRs from drug resistant to drug-sensitive cells.

Acknowledgements

IPATIMUP is an Associate Laboratory of the Portuguese Ministry of Science, Technology and Higher Education and is partially supported by FCT.

References

1. Sharom FJ. ABC multidrug transporters: structure, function and role in chemoresistance. *Pharmacogenomics* 2008;9:105–27.
2. Eckford PD, Sharom FJ. ABC efflux pump-based resistance to chemotherapy drugs. *Chem Rev* 2009;109:2989–3011.
3. Sonneveld P. Multidrug resistance in haematological malignancies. *J Int Med* 2000;247: 521–34.
4. Leith C. Multidrug resistance in leukemia. *Curr Opin Hematol* 1998;5:287–91.
5. Musto P, Melillo L, Lombardi G, et al. High risk of early resistant relapse or leukaemic patients with presence of multidrug resistance associated P-glycoprotein positive cells in complete remission. *Br J Haematol* 1991;77:50–3.
6. Marie JP, Zittoun R, Sikic BI. Multidrug resistance (mdr1) gene expression in adult acute leukemias: correlations with treatment outcome and in vitro drug sensitivity. *Blood* 1991;78:586–92.
7. Pirker R, Wallner J, Geissler K, et al. MDR1 gene expression and treatment outcome in acute myeloid leukemia. *J Natl Cancer Inst* 1991;83: 708–12.
8. Zhou DC, Marie JP, Suberville AM, et al. Relevance of mdr1 gene expression in acute myeloid leukemia and comparison of different diagnostic methods. *Leukemia* 1992;6:879–85.
9. Goasguen JE, Dossot JM, Fardel O, et al. Expression of the multidrug resistance-associated P-glycoprotein (P-170) in 59 cases of de novo acute lymphoblastic leukemia: prognostic implications. *Blood* 1993;81:2394–8.
10. Kuwazuru Y, Hanada S, Furukawa T, et al. Expression of P-glycoprotein in adult T-cell leukemia cells. *Blood* 1990;76:2065–71.
11. Wuchter C, Leonid K, Ruppert V, et al. Clinical significance of P-glycoprotein expression and function for response to induction chemotherapy, relapse rate and overall survival in acute leukemia. *Haematologica* 2000;85:711–21.
12. Kanerva J, Tiirikainen MI, Makipernaa A, et al. Initial P-glycoprotein expression in childhood acute lymphoblastic leukemia: no evidence of prognostic impact in follow-up. *Pediatr Hematol Oncol* 2001;18:27–36.
13. den Boer ML, Pieters R, Kazemier KM, et al. Relationship between major vault protein/lung resistance protein, multidrug resistance-associated protein, P-glycoprotein expression, and drug resistance in childhood leukemia. *Blood* 1998;91:2092–8.
14. Olson DP, Taylor BJ, La M, et al. The prognostic significance of P-glycoprotein, multidrug resistance-related protein 1 and lung resistance protein in pediatric acute lymphoblastic leukemia: a retrospective study of 295 newly diagnosed patients by the Children's Oncology Group. *Leuk Lymph* 2005;46: 681–91.
15. Casale F, D'Angelo V, Addeo R, et al. P-glycoprotein 170 expression and function as an adverse independent prognostic factor in childhood acute lymphoblastic leukemia. *Oncol Rep* 2004;12:1201–7.
16. De Moerloose B, Swerts K, Benoit Y, et al. The combined analysis of P-glycoprotein expression and activity predicts outcome in childhood acute lymphoblastic leukemia. *Pediatr Hematol Oncol* 2003;20:381–91.
17. Plasschaert SL, Vellenga E, de Bont ES, et al. High functional P-glycoprotein activity is more often present in T-cell acute lymphoblastic leukaemic cells in adults than in children. *Leuk Lymph* 2003;44:85–95.
18. Shaffer BC, Gillet JP, Patel C, et al. Drug resistance: still a daunting challenge to the successful treatment of AML. *Drug Resist Updat* 2012;15:62–9.
19. Thorgeirsson SS, Huber BE, Sorrell S, et al. Expression of the multidrug-resistant gene in hepatocarcinogenesis and regenerating rat liver. *Science* 1987;236:1120–2.
20. Kohno K, Sato S, Takano H, et al. The direct activation of human multidrug resistance gene (MDR1) by anticancer agents. *Biochem Biophys Res Commun* 1989;165:1415–21.
21. Maillefert JF, Maynadie M, Tebib JG, et al. Expression of the multidrug resistance glycoprotein 170 in the peripheral blood lymphocytes of rheumatoid arthritis patients. The percentage of lymphocytes expressing glycoprotein 170 is increased in patients treated with prednisolone. *Br J Rheumatol* 1996;35: 430–5.
22. Ho GT, Moodie FM, Satsangi J. Multidrug resistance 1 gene (P-glycoprotein 170): an important determinant in gastrointestinal disease? *Gut* 2003;52:759–66.

23. Sui H, Zhou S, Wang Y, et al. COX-2 contributes to P-glycoprotein-mediated multidrug resistance via phosphorylation of c-Jun at Ser63/73 in colorectal cancer. *Carcinogenesis* 2011;32:667–75.
24. Bush JA, Li G. Regulation of the Mdr1 isoforms in a p53-deficient mouse model. *Carcinogenesis* 2002;23:1603–7.
25. Sampath J, Sun D, Kidd VJ, et al. Mutant p53 cooperates with ETS and selectively up-regulates human MDR1 not MRP1. *J Biol Chem* 2001; 276:39359–67.
26. Yamada T, Takaoka AS, Naishiro Y, et al. Transactivation of the multidrug resistance 1 gene by T-cell factor 4/beta-catenin complex in early colorectal carcinogenesis. *Cancer Res* 2000; 60:4761–6.
27. Baird RD, Kaye SB. Drug resistance reversal—are we getting closer? *Eur J Cancer* 2003;39: 2450–61.
28. Naito S, Sakamoto N, Kotoh S, et al. Expression of P-glycoprotein and multidrug resistance in renal cell carcinoma. *Eur Urol* 1993;24:156–60.
29. Kakehi Y, Kanamaru H, Yoshida O, et al. Measurement of multidrug-resistance messenger RNA in urogenital cancers; elevated expression in renal cell carcinoma is associated with intrinsic drug resistance. *J Urol* 1988;139: 862–5.
30. Kim WJ, Kakehi Y, Kinoshita H, et al. Expression patterns of multidrug-resistance (MDR1), multidrug resistance-associated protein (MRP),glutathione-S-transferase-pi (GST-pi) and DNA topoisomerase II (Topo II) genes in renal cell carcinomas and normal kidney. *J Urol* 1996; 156:506–11.
31. Wu L, Smythe AM, Stinson SF, et al. Multidrug-resistant phenotype of disease-oriented panels of human tumor cell lines used for anticancer drug screening. *Cancer Res* 1992;52:3029–34.
32. Alvarez M, Paull K, Monks A, et al. Generation of a drug resistance profile by quantitation of mdr-1/P-glycoprotein in the cell lines of the National Cancer Institute Anticancer Drug Screen. *J Clin Invest* 1995;95:2205–14.
33. Reinecke P, Schmitz M, Schneider EM, et al. Multidrug resistance phenotype and paclitaxel (Taxol) sensitivity in human renal carcinoma cell lines of different histologic types. *Cancer Invest* 2000;18:614–25.
34. Kanamaru H, Kakehi Y, Yoshida O, et al. MDR1 RNA levels in human renal cell carcinomas: correlation with grade and prediction of reversal of doxorubicin resistance by quinidine in tumor explants. *J Natl Cancer Inst* 1989;81: 844–9.
35. Chaudhary PM, Roninson IB. Expression and activity of P-glycoprotein, a multidrug efflux pump, in human hematopoietic stem cells. *Cell* 1991;66:85–94.
36. Smyth MJ, Krasovskis E, Sutton VR, et al. The drug efflux protein, P-glycoprotein, additionally protects drug-resistant tumor cells from multiple forms of caspase-dependent apoptosis. *Proc Natl Acad Sci U S A* 1998;95:7024–9.
37. Ruefli AA, Tainton KM, Darcy PK, et al. P-glycoprotein inhibits caspase-8 activation but not formation of the death inducing signal complex (disc) following Fas ligation. *Cell Death Differ* 2002;9:1266–72.
38. Liu YY, Gupta V, Patwardhan GA, et al. Glucosylceramide synthase upregulates MDR1 expression in the regulation of cancer drug resistance through cSrc and beta-catenin signaling. *Mol Cancer* 2010;9:145.
39. Johnstone RW, Ruefli AA, Smyth MJ. Multiple physiological functions for multidrug transporter P-glycoprotein? *Trend Biochem Sci* 2000;25:1–6.
40. Seca H, Lima RT, Guimaraes JE, et al. Simultaneous targeting of P-gp and XIAP with siRNAs increases sensitivity of P-gp overexpressing CML cells to imatinib. *Hematology* 2011;16:100–8.
41. Lima RT, Guimaraes JE, Vasconcelos, MH. Overcoming K562Dox resistance to STI571 (Gleevec) by downregulation of P-gp expression using siRNAs. *Cancer Ther* 2007;5:67–76.
42. Xia Z, Zhang L, Chen Q, et al. Stable reversal of multidrug resistance in colon cancer cells by RNA interference targeting the MDR1 gene. *Mol Med Rep* 2009;2:579–84.
43. Xu H, Hong FZ, Li S, et al. Short hairpin RNA-mediated MDR1 gene silencing increases apoptosis of human ovarian cancer cell line A2780/Taxol. *Chin J Cancer Res* 2012;24:138–42.
44. Sharom FJ. The P-glycoprotein multidrug transporter. *Essays Biochem* 2011;50:161–78.
45. Palmeira A, Sousa E, Vasconcelos MH, et al. Three decades of P-gp inhibitors: skimming through several generations and scaffolds. *Curr Med Chem* 2012;19:1946–2025.
46. Palmeira A, Vasconcelos MH, Paiva A, et al. Dual inhibitors of P-glycoprotein and tumor cell growth: (re)discovering thioxanthones. *Biochem Pharmacol* 2012;83:57–68.
47. Palmeira A, Sousa E, Vasconcelos MH, et al. Structure and ligand-based design of P-glycoprotein inhibitors: a historical perspective. *Curr Pharm Design* 2012;18:4197–214.
48. Eichhorn T, Efferth T. P-glycoprotein and its inhibition in tumors by phytochemicals derived from Chinese herbs. *J Ethnopharmacol* 2012;141: 557–70.
49. Gottesman MM, Pastan I. Biochemistry of multidrug resistance mediated by the multidrug transporter. *Ann Rev Biochem* 1993;62:385–427.
50. Szakacs G, Paterson JK, Ludwig JA, et al. Targeting multidrug resistance in cancer. *Nat Rev Drug Discov* 2006;5:219–34.
51. Gros P, Croop J, Housman D. Mammalian multidrug resistance gene: complete cDNA sequence indicates strong homology to bacterial transport proteins. *Cell* 1986;47:371–80.
52. Schinkel AH, Kemp S, Dolle M, et al. N-glycosylation and deletion mutants of the human MDR1 P-glycoprotein. *J Biol Chem* 1993;268: 7474–81.
53. Aller SG, Yu J, Ward A, et al. Structure of P-glycoprotein reveals a molecular basis for poly-specific drug binding. *Science* 2009;323:1718–22.
54. Jin MS, Oldham ML, Zhang Q, et al. Crystal structure of the multidrug transporter P-glycoprotein from Caenorhabditis elegans. *Nature* 2012;490:566–9.
55. Omote H, Al-Shawi MK. Interaction of transported drugs with the lipid bilayer and P-glycoprotein through a solvation exchange mechanism. *Biophys J* 2006;90:4046–59.
56. Willingham MC, Richert ND, Cornwell MM, et al. Immunocytochemical localization of P170 at the plasma membrane of multidrug-resistant human cells. *J Histochem Cytochem* 1987;35: 1451–6.
57. Fu D, Arias IM. Intracellular trafficking of P-glycoprotein. *Int J Biochem Cell Biol* 2012;44: 461–4.
58. Calcabrini A, Meschini S, Stringaro A, et al. Detection of P-glycoprotein in the nuclear envelope of multidrug resistant cells. *Histochem J* 2000;32:599–606.
59. Molinari A, Calcabrini A, Meschini S, et al. Subcellular detection and localization of the drug transporter P-glycoprotein in cultured tumor cells. *Curr Protein Pept Sci* 2002;3:653–70.
60. Baldini N, Scotlandi K, Serra M, et al. Nuclear immunolocalization of P-glycoprotein in multidrug-resistant cell lines showing similar mechanisms of doxorubicin distribution. *Eur J Cell Biol* 1995;68:226–39.
61. Fu D, Bebawy M, Kable EP, et al. Dynamic and intracellular trafficking of P-glycoprotein-EGFP fusion protein: implications in multidrug resistance in cancer. *Int J Cancer* 2004;109:174–81.
62. Molinari A, Calcabrini A, Meschini S, et al. Detection of P-glycoprotein in the Golgi apparatus of drug-untreated human melanoma cells. *Int J Cancer* 1998;75:885–93.
63. Molinari A, Cianfriglia M, Meschini S, et al. P-glycoprotein expression in the Golgi apparatus of multidrug-resistant cells. *Int J Cancer* 1994; 59:789–95.
64. Fu D, Roufogalis BD. Actin disruption inhibits endosomal traffic of P-glycoprotein-EGFP and resistance to daunorubicin accumulation. American journal of physiology. *Cell Physiol* 2007;292: C1543–52.
65. Rajagopal A, Simon SM. Subcellular localization and activity of multidrug resistance proteins. *Mol Biol Cell* 2003;14:3389–99.
66. Solazzo M, Fantappie O, Lasagna N, et al. P-gp localization in mitochondria and its functional characterization in multiple drug-resistant cell lines. *Exp Cell Res* 2006;312:4070–8.
67. Munteanu E, Verdier M, Grandjean-Forestier F, et al. Mitochondrial localization and activity of P-glycoprotein in doxorubicin-resistant K562 cells. *Biochem Pharmacol* 2006;71:1162–74.
68. Paterson JK, Gottesman MM. P-Glycoprotein is not present in mitochondrial membranes. *Exp Cell Res* 2007;313:3100–5.
69. Ferrao P, Sincock P, Cole S, et al. Intracellular P-gp contributes to functional drug efflux and resistance in acute myeloid leukaemia. *Leuk Res* 2001;25:395–405.
70. Meschini S, Calcabrini A, Monti E, et al. Intracellular P-glycoprotein expression is associated with the intrinsic multidrug resistance phenotype in human colon adenocarcinoma cells. *Int J Cancer* 2000;87:615–28.
71. Sun J, Yeung CA, Co NN, et al. Clitocine reversal of P-glycoprotein associated multi-drug resistance through down-regulation of transcription factor NF-kappaB in R-HepG2 cell line. *PloS One* 2012;7:e40720.
72. Shtil AA, Azare J. Redundancy of biological regulation as the basis of emergence of multidrug resistance. *Int Rev Cytol* 2005;246:1–29.
73. Zhu H, Wu H, Liu X, et al. Role of MicroRNA miR-27a and miR-451 in the regulation of MDR1/P-glycoprotein expression in human cancer cells. *Biochem Pharmacol* 2008; 76:582–8.
74. Correa S, Binato R, Du Rocher B, et al. Wnt/beta-catenin pathway regulates ABCB1 transcription in chronic myeloid leukemia. *BMC Cancer* 2012;12:303.
75. Sukhai M, Piquette-Miller M. Regulation of the multidrug resistance genes by stress signals. *J Pharm Pharm Sci* 2000;3:268–80.

76. Shen H, Xu W, Luo W, et al. Upregulation of mdr1 gene is related to activation of the MAPK/ERK signal transduction pathway and YB-1 nuclear translocation in B-cell lymphoma. *Exp Hematol* 2011;39:558–69.
77. Thottassery JV, Zambetti GP, Arimori K, et al. p53-dependent regulation of MDR1 gene expression causes selective resistance to chemotherapeutic agents. *Proc Natl Acad Sci U S A* 1997;94:11037–42.
78. Vilaboa NE, Galan A, Troyano A, et al. Regulation of multidrug resistance 1 (MDR1)/P-glycoprotein gene expression and activity by heat-shock transcription factor 1 (HSF1). *J Biol Chem* 2000;275:24970–6.
79. Hu Z, Jin S, Scotto KW. Transcriptional activation of the MDR1 gene by UV irradiation. Role of NF-Y and Sp1. *J Biol Chem* 2000;275:2979–85.
80. Ziemann C, Burkle A, Kahl GF, et al. Reactive oxygen species participate in mdr1b mRNA and P-glycoprotein overexpression in primary rat hepatocyte cultures. *Carcinogenesis* 1999;20:407–14.
81. Yeh SY, Pan HJ, Lin CC, et al. Hyperglycemia induced down-regulation of renal P-glycoprotein expression. *Eur J Pharmacol* 2012; 690:42–50.
82. Schondorf T, Kurbacher CM, Gohring UJ, et al. Induction of MDR1-gene expression by antineoplastic agents in ovarian cancer cell lines. *Anticancer Res* 2002;22:2199–203.
83. Baker EK, Johnstone RW, Zalcberg JR, et al. Epigenetic changes to the MDR1 locus in response to chemotherapeutic drugs. *Oncogene* 2005;24:8061–75.
84. Riordan JR, Deuchars K, Kartner N, et al. Amplification of P-glycoprotein genes in multidrug-resistant mammalian cell lines. *Nature* 1985;316:817–9.
85. Gomez-Martinez A, Garcia-Morales P, Carrato A, et al. Post-transcriptional regulation of P-glycoprotein expression in cancer cell lines. *Mol Cancer Res* 2007;5:641–53.
86. Kusaba H, Nakayama M, Harada T, et al. Association of 5′ CpG demethylation and altered chromatin structure in the promoter region with transcriptional activation of the multidrug resistance 1 gene in human cancer cells. *Eur J Biochem* 1999;262:924–32.
87. Scotto KW, Egan DA. Transcriptional regulation of MDR genes. *Cytotechnology* 1998;27:257–69.
88. Jin S, Scotto KW. Transcriptional regulation of the MDR1 gene by histone acetyltransferase and deacetylase is mediated by NF-Y. *Mol Cell Biol* 1998;18:4377–84.
89. Lee CH, Bradley G, Ling V. Overexpression of the class II P-glycoprotein gene in primary rat hepatocyte culture: evidence for increased mRNA stability. *Cell Growth Differ* 1995;6:347–54.
90. Yague E, Armesilla AL, Harrison G, et al. P-glycoprotein (MDR1) expression in leukemic cells is regulated at two distinct steps, mRNA stabilization and translational initiation. *J Biol Chem* 2003;278:10344–52.
91. Orom UA, Nielsen FC, Lund AH. MicroRNA-10a binds the 5′UTR of ribosomal protein mRNAs and enhances their translation. *Mol Cell* 2008;30:460–71.
92. Filipowicz W, Bhattacharyya SN, Sonenberg N. Mechanisms of post-transcriptional regulation by microRNAs: are the answers in sight? *Nat Rev Genet* 2008;9:102–14.
93. Valencia-Sanchez MA, Liu J, Hannon GJ, Parker R. Control of translation and mRNA degradation by miRNAs and siRNAs. *Gene Dev* 2006; 20:515–24.
94. Liu J. Control of protein synthesis and mRNA degradation by microRNAs. *Curr Opin Cell Biol* 2008;20:214–21.
95. Brodersen P, Voinnet O. Revisiting the principles of microRNA target recognition and mode of action. *Nat Rev Mol Cell Biol* 2009;10: 141–8.
96. John B, Enright AJ, Aravin A, et al. Human MicroRNA targets. *PLoS Biol* 2004;2:e363.
97. Berezikov E. Evolution of microRNA diversity and regulation in animals. *Nat Rev Genet* 2011; 12:846–60.
98. He L, Hannon GJ. MicroRNAs: small RNAs with a big role in gene regulation. *Nat Rev Genet* 2004;5:522–31.
99. Winter J, Jung S, Keller S, et al. Many roads to maturity: microRNA biogenesis pathways and their regulation. *Nat Cell Biol* 2009;11: 228–34.
100. Place RF, Li LC, Pookot D, et al. MicroRNA-373 induces expression of genes with complementary promoter sequences. *Proc Natl Acad Sci U S A* 2008;105:1608–13.
101. Dong J, Zhao YP, Zhou L, et al. Bcl-2 upregulation induced by miR-21 via a direct interaction is associated with apoptosis and chemoresistance in MIA PaCa-2 pancreatic cancer cells. *Arch Med Res* 2011;42:8–14.
102. Vasudevan S, Tong Y, Steitz JA. Switching from repression to activation: microRNAs can up-regulate translation. *Science* 2007;318:1931–4.
103. Rigoutsos I. New tricks for animal microRNAS: targeting of amino acid coding regions at conserved and nonconserved sites. *Cancer Res* 2009; 69:3245–8.
104. Piriyapongsa J, Bootchai C, Ngamphiw C, et al. microPIR: an integrated database of microRNA target sites within human promoter sequences. *PloS One* 2012;7:e33888.
105. Zhao X, Yang L, Hu J, et al. miR-138 might reverse multidrug resistance of leukemia cells. *Leuk Res* 2010;34:1078–82.
106. Zhang H, Li M, Han Y, et al. Down-regulation of miR-27a might reverse multidrug resistance of esophageal squamous cell carcinoma. *Dig Dis Sci* 2010;55:2545–51.
107. Fu LL, Wen X, Bao JK, et al. MicroRNA-modulated autophagic signaling networks in cancer. *Int J Biochem Cell Biol* 2012;44:733–6.
108. Lima RT, Busacca S, Almeida GM, et al. MicroRNA regulation of core apoptosis pathways in cancer. *Eur J Cancer* 2011;47:163–74.
109. Bueno MJ, Malumbres M. MicroRNAs and the cell cycle. *Biochim Biophys Acta* 2011;1812:592–601.
110. Bueno MJ, Perez de Castro I, Malumbres M. Control of cell proliferation pathways by microRNAs. *Cell Cycle* 2008;7:3143–8.
111. Li MA, He L. microRNAs as novel regulators of stem cell pluripotency and somatic cell reprogramming. *BioEssays* 2012;34:670–80.
112. Bethune J, Artus-Revel CG, Filipowicz W. Kinetic analysis reveals successive steps leading to miRNA-mediated silencing in mammalian cells. *EMBO Rep* 2012;13:716–23.
113. Huntzinger E, Izaurralde E. Gene silencing by microRNAs: contributions of translational repression and mRNA decay. *Nat Rev Genet* 2011;12:99–110.
114. Slezak-Prochazka I, Durmus S, Kroesen BJ, et al. MicroRNAs, macrocontrol: regulation of miRNA processing. *RNA* 2010;16:1087–95.
115. Davis-Dusenbery BN, Hata A. Mechanisms of control of microRNA biogenesis. *J Biochem* 2010;148:381–92.
116. Melo SA, Moutinho C, Ropero S, et al. A genetic defect in exportin-5 traps precursor microRNAs in the nucleus of cancer cells. *Cancer Cell* 2010;18:303–15.
117. Ozsolak F, Poling LL, Wang Z, et al. Chromatin structure analyses identify miRNA promoters. *Genes Dev* 2008;22:3172–83.
118. Wang J, Lu M, Qiu C, et al. TransmiR: a transcription factor-microRNA regulation database. *Nucleic Acids Res* 2010;38:D119–22.
119. Amiel J, de Pontual L, Henrion-Caude A. miRNA, development and disease. *Adv Genet* 2012;80:1–36.
120. Hinton A, Hunter S, Reyes G, et al. From pluripotency to islets: miRNAs as critical regulators of human cellular differentiation. *Adv Genet* 2012;79:1–34.
121. Natarajan R, Putta S, Kato M. MicroRNAs and diabetic complications. *J Cardiovasc Transl Res* 2012;5:413–22.
122. van Rooij E, Olson EN. MicroRNA therapeutics for cardiovascular disease: opportunities and obstacles. *Nat Rev Drug Discov* 2012; 11:860–72.
123. Liu H. MicroRNAs in breast cancer initiation and progression. *Cell Mol Life Sci* 2012;69:3587–99.
124. Singh PK, Brand RE, Mehla K. MicroRNAs in pancreatic cancer metabolism. *Nat Rev Gastroenterol Hepatol* 2012;9:334–44.
125. Schetter AJ, Okayama H, Harris CC. The role of microRNAs in colorectal cancer. *Cancer J* 2012; 18:244–52.
126. Seca H, Almeida GM, Guimaraes JE, et al. miR signatures and the role of miRs in acute myeloid leukaemia. *Eur J Cancer* 2010;46:1520–7.
127. Borralho PM, Simoes AE, Gomes SE, et al. miR-143 overexpression impairs growth of human colon carcinoma xenografts in mice with induction of apoptosis and inhibition of proliferation. *PloS One* 2011;6:e23787.
128. Toscano-Garibay JD, Aquino-Jarquin G. Regulation exerted by miRNAs in the promoter and UTR sequences: MDR1/P-gp expression as a particular case. *DNA Cell Biol* 2012;31:1358–64.
129. Kovalchuk O, Filkowski J, Meservy J, et al. Involvement of microRNA-451 in resistance of the MCF-7 breast cancer cells to chemotherapeutic drug doxorubicin. *Mol Cancer Ther* 2008; 7:2152–9.
130. Feng DD, Zhang H, Zhang P, et al. Down-regulated miR-331-5p and miR-27a are associated with chemotherapy resistance and relapse in leukaemia. *J Cell Mol Med* 2011;15:2164–75.
131. Bao L, Hazari S, Mehra S, et al. Increased expression of P-glycoprotein and doxorubicin chemoresistance of metastatic breast cancer is regulated by miR-298. *Am J Pathol* 2012;180: 2490–503.
132. Ikemura K, Yamamoto M, Miyazaki S, et al. MicroRNA-145 post-transcriptionally regulates the expression and function of P-glycoprotein in intestinal epithelial cells. *Mol Pharmacol* 2013; 83:399–405.
133. Pan X, Wang ZX, Wang R. MicroRNA-21: a novel therapeutic target in human cancer. *Cancer Biol Ther* 2010;10:1224–32.

134. Schramedei K, Morbt N, Pfeifer G, et al. MicroRNA-21 targets tumor suppressor genes ANP32A and SMARCA4. *Oncogene* 2011;30: 2975–85.
135. Si ML, Zhu S, Wu H, et al. miR-21-mediated tumor growth. *Oncogene* 2007;26:2799–803.
136. Roldo C, Missiaglia E, Hagan JP, et al. MicroRNA expression abnormalities in pancreatic endocrine and acinar tumors are associated with distinctive pathologic features and clinical behavior. *J Clin Oncol* 2006;24:4677–84.
137. Seca H LR, Lopes-Rodrigues V, Guimarães JE, et al. Targeting miR-21 induces autophagy and chemosensitivity of leukemia cells. *Curr Drug Targets* 2013;14:1135–43.
138. Gong C, Yao Y, Wang Y, et al. Up-regulation of miR-21 mediates resistance to trastuzumab therapy for breast cancer. *J Biol Chem* 2011;286: 19127–37.
139. Valeri N, Gasparini P, Braconi C, et al. MicroRNA-21 induces resistance to 5-fluorouracil by down-regulating human DNA MutS homolog 2 (hMSH2). *Proc Natl Acad Sci U S A* 2010;107: 21098–103.
140. Shi L, Chen J, Yang J, et al. MiR-21 protected human glioblastoma U87MG cells from chemotherapeutic drug temozolomide induced apoptosis by decreasing Bax/Bcl-2 ratio and caspase-3 activity. *Brain Res* 2010;1352:255–64.
141. Bourguignon LY, Spevak CC, Wong G, et al. Hyaluronan-CD44 interaction with protein kinase C(epsilon) promotes oncogenic signaling by the stem cell marker Nanog and the Production of microRNA-21, leading to down-regulation of the tumor suppressor protein PDCD4, anti-apoptosis, and chemotherapy resistance in breast tumor cells. *J Biol Chem* 2009;284:26533–46.
142. Yang L, Li N, Wang H, et al. Altered microRNA expression in cisplatin-resistant ovarian cancer cells and upregulation of miR-130a associated with MDR1/P-glycoprotein-mediated drug resistance. *Oncol Rep* 2012;28:592–600.
143. Boyerinas B, Park SM, Murmann AE, et al. Let-7 modulates acquired resistance of ovarian cancer to Taxanes via IMP-1-mediated stabilization of multidrug resistance 1. *Int J Cancer* 2012;130: 1787–97.
144. Zhao X, Yang L, Hu J. Down-regulation of miR-27a might inhibit proliferation and drug resistance of gastric cancer cells. *J Exp Clin Cancer Res* 2011;30:55.
145. Chen J, Tian W, Cai H, et al. Down-regulation of microRNA-200c is associated with drug resistance in human breast cancer. *Med Oncol* 2012;29:2527–34.
146. Kutay H, Bai S, Datta J, et al. Downregulation of miR-122 in the rodent and human hepatocellular carcinomas. *J Cell Biochem* 2006;99:671–8.
147. Xu Y, Xia F, Ma L, et al. MicroRNA-122 sensitizes HCC cancer cells to adriamycin and vincristine through modulating expression of MDR and inducing cell cycle arrest. *Cancer Lett* 2011; 310:160–9.
148. Jaiswal R, Luk F, Gong J, et al. Microparticle conferred microRNA profiles—implications in the transfer and dominance of cancer traits. *Mol Cancer* 2012;11:37.
149. Tsang TY, Tang WY, Chan JY, et al. P-glycoprotein enhances radiation-induced apoptotic cell death through the regulation of miR-16 and Bcl-2 expressions in hepatocellular carcinoma cells. *Apoptosis* 2011;16:524–35.
150. Lee TH, D'Asti E, Magnus N, et al. Microvesicles as mediators of intercellular communication in cancer—the emerging science of cellular 'debris'. *Semin Immunopathol* 2011;33:455–67.
151. Levchenko A, Mehta BM, Niu X, et al. Intercellular transfer of P-glycoprotein mediates acquired multidrug resistance in tumor cells. *Proc Natl Acad Sci U S A* 2005;102:1933–8.
152. Lee Y, El Andaloussi S, Wood MJ. Exosomes and microvesicles: extracellular vesicles for genetic information transfer and gene therapy. *Hum Mol Genet* 2012;21:R125–34.
153. Bebawy M, Combes V, Lee E, et al. Membrane microparticles mediate transfer of P-glycoprotein to drug sensitive cancer cells. *Leukemia* 2009;23:1643–9.
154. Gong J, Jaiswal R, Mathys JM, et al. Microparticles and their emerging role in cancer multidrug resistance. *Cancer Treat Rev* 2012;38:226–34.
155. Valadi H, Ekstrom K, Bossios A, et al. Exosome-mediated transfer of mRNAs and microRNAs is a novel mechanism of genetic exchange between cells. *Nat Cell Biol* 2007;9:654–9.
156. Yang M, Chen J, Su F, et al. Microvesicles secreted by macrophages shuttle invasion-potentiating microRNAs into breast cancer cells. *Mol Cancer* 2011;10:117.
157. Umezu T, Ohyashiki K, Kuroda M, et al. Leukemia cell to endothelial cell communication via exosomal miRNAs. *Oncogene* 2013;32:2747–55.
158. Ogawa R, Tanaka C, Sato M, et al. Adipocyte-derived microvesicles contain RNA that is transported into macrophages and might be secreted into blood circulation. *Biochem Biophys Res Commun* 2010;398:723–9.
159. Zhang Y, Liu D, Chen X, et al. Secreted monocytic miR-150 enhances targeted endothelial cell migration. *Mol Cell* 2010;39:133–44.
160. Jaiswal R, Gong J, Sambasivam S, et al. Microparticle-associated nucleic acids mediate trait dominance in cancer. *FASEB J* 2012;26:420–9.
161. Pasquier J, Galas L, Boulange-Lecomte C, et al. Different modalities of intercellular membrane exchanges mediate cell-to-cell p-glycoprotein transfers in MCF-7 breast cancer cells. *J Biol Chem* 2012;287:7374–87.
162. Jaiswal R, Luk F, Dalla PV, et al. Breast cancer-derived microparticles display tissue selectivity in the transfer of resistance proteins to cells. *PloS One* 2013;8:e61515.
163. Elhassan MO, Christie J, Duxbury MS. Homo sapiens systemic RNA interference-defective-1 transmembrane family member 1 (SIDT1) protein mediates contact-dependent small RNA transfer and microRNA-21-driven chemoresistance. *J Biol Chem* 2012;287:5267–77.
164. Anuchapreeda S, Leechanachai P, Smith MM, et al. Modulation of P-glycoprotein expression and function by curcumin in multidrug-resistant human KB cells. *Biochem Pharmacol* 2002;64: 573–82.
165. Chearwae W, Anuchapreeda S, Nandigama K, et al. Biochemical mechanism of modulation of human P-glycoprotein (ABCB1) by curcumin I, II, and III purified from Turmeric powder. *Biochem Pharmacol* 2004;68:2043–52.
166. O'Connor R, Ooi MG, Meiller J, et al. The interaction of bortezomib with multidrug transporters: implications for therapeutic applications in advanced multiple myeloma and other neoplasias. *Cancer Chemother Pharmacol* 2013;71: 1357–68.
167. Tucci M, Quatraro C, Dammacco F, Silvestris F. Role of active drug transporters in refractory multiple myeloma. *Curr Top Med Chem* 2009;9:218–24.
168. Dalton WS. Mechanisms of drug resistance in hematologic malignancies. *Semin Hematol* 1997; 34:3–8.
169. Pilarski LM, Mant MJ, Belch AR. Drug resistance in multiple myeloma: novel therapeutic targets within the malignant clone. *Leuk Lymph* 1999;32:199–210.
170. Yan F, Wang XM, Liu ZC, et al. JNK1, JNK2, and JNK3 are involved in P-glycoprotein-mediated multidrug resistance of hepatocellular carcinoma cells. *Hepatobiliary Pancreat Dis Int* 2010;9:287–95.
171. Sun Z, Zhao Z, Li G, et al. Relevance of two genes in the multidrug resistance of hepatocellular carcinoma: in vivo and clinical studies. *Tumori* 2010;96:90–6.
172. Zhou Y, Ling XL, Li SW, et al. Establishment of a human hepatoma multidrug resistant cell line in vitro. *World J Gastroenterol* 2010;16:2291–7.
173. Stewart DJ. Tumor and host factors that may limit efficacy of chemotherapy in non-small cell and small cell lung cancer. *Crit Rev Oncol Hematol* 2010;75:173–234.
174. Jemal A, Siegel R, Ward E, et al. Cancer statistics, 2009. *CA Cancer J Clin* 2009;59:225–49.
175. Stewart DJ, Tomiak E, Shamji FM, et al. Phase II study of alternating chemotherapy regimens for advanced non-small cell lung cancer. *Lung Cancer* 2004;44:241–9.
176. Richert ND, Aldwin L, Nitecki D, et al. Stability and covalent modification of P-glycoprotein in multidrug-resistant KB cells. *Biochemistry* 1988; 27:7607–13.
177. Stordal B, Hamon M, McEneaney V, et al. Resistance to paclitaxel in a cisplatin-resistant ovarian cancer cell line is mediated by P-glycoprotein. *PLoS One* 2012;7:e40717.
178. Xu L, Cai J, Yang Q, et al. Prognostic significance of several biomarkers in epithelial ovarian cancer: a meta-analysis of published studies. *J Cancer Res Clin Oncol* 2013;139:1257–77.
179. Trock BJ, Leonessa F, Clarke R. Multidrug resistance in breast cancer: a meta-analysis of MDR1/gp170 expression and its possible functional significance. *J Natl Cancer Inst* 1997;89: 917–31.
180. Gottesman MM, Fojo T, Bates SE. Multidrug resistance in cancer: role of ATP-dependent transporters. *Nat Rev Cancer* 2002; 2:48–58.
181. de Vries NA, Buckle T, Zhao J, et al. Restricted brain penetration of the tyrosine kinase inhibitor erlotinib due to the drug transporters P-gp and BCRP. *Invest New Drugs* 2012;30:443–9.
182. Wartenberg M, Richter M, Datchev A, et al. Glycolytic pyruvate regulates P-Glycoprotein expression in multicellular tumor spheroids via modulation of the intracellular redox state. *J Cell Biochem* 2010;109: 434–46.
183. Haar CP, Hebbar P, Wallace GCt, et al. Drug resistance in glioblastoma: a mini review. *Neurochem Res* 2012;37:1192–200.

1.2.2. Inhibitors of P-gp synthesis and function

Decreasing P-gp expression and/or function (*i.e*., drug efflux) with P-gp inhibitors would result in an increased bioavailability of the drugs that are normally effluxed by P-gp. To date, four generations of P-gp inhibitors have been described, with many of their representatives having reached clinical trials [52]. However, none of these compounds has been successful, due to undesirable side effects as well as low effectiveness (drug interactions or pharmacokinetic issues) [54,55]. Therefore, it is essential to identify novel inhibitors of P-gp activity or expression [53].

Some of the most effective cancer drugs to date are derived from natural products. Indeed, natural products and their synthetic derivatives comprise more than half of the anticancer drug candidates developed in the last decades [54]. Curcumin, a secondary metabolite isolated from the turmeric of *Curcuma longa L*., has been associated with a beneficial P-gp inhibitory effect (both in terms of function and expression inhibition). However, the poor availability and extensive metabolism of the curcumin molecule have enhanced the search for more efficient and stable novel synthetized analogs of curcumin [54].

The following review, titled: “Curcumin as a modulator of P-glycoprotein in cancer: challenges and perspectives”, summarizes and compares the effects of curcumin and curcumin analogs on P-glycoprotein function and expression.

1.2.2.1. REVIEW ARTICLE: Curcumin as a modulator of P-glycoprotein in cancer: challenges and perspectives

Vanessa Lopes-Rodrigues, Emília Sousa and M. Helena Vasconcelos

Submitted for publication (in Pharmaceuticals)

Review

Curcumin as a modulator of P-glycoprotein in cancer: challenges and perspectives

Vanessa Lopes-Rodrigues [1,2,3], Emília Sousa [4,5], M. Helena Vasconcelos [1,2,6,*]

[1] i3S - Instituto de Investigação e Inovação em Saúde, Universidade do Porto, Portugal;

[2] Cancer Drug Resistance Group, IPATIMUP - Institute of Molecular Pathology and Immunology of the University of Porto, IPATIMUP, 4200-465 Porto, Portugal;

[3] ICBAS-UP - Institute of Biomedical Sciences Abel Salazar, University of Porto, ICBAS-UP, 4099-003 Porto, Portugal;

[4] Laboratory of Organic and Pharmaceutical Chemistry, Department of Chemical Sciences, Faculty of Pharmacy, University of Porto, Rua Jorge Viterbo Ferreira, 228, 4050-313 Porto, Portugal;

[5] CIIMAR/CIMAR - Interdisciplinary Centre of Marine and Environmental Research, University of Porto, Portugal;

[6] Laboratory of Microbiology, Department of Biological Sciences, FFUP - Faculty of Pharmacy, University of Porto, 4050-313 Porto, Portugal.

***** corresponding author: M. Helena Vasconcelos, i3S, Instituto de Investigação e Inovação em Saúde, Universidade do Porto, Rua Alfredo Allen 208, 4200-135 Porto, Portugal; Tel.: +351 220 408 800; Fax: +351 225570799; E-mail: hvasconcelos@ipatimup.pt

Academic Editor: name

Received: date; Accepted: date; Published: date

Abstract: Multidrug resistance (MDR) presents a serious challenge to the efficiency of cancer treatment and may be associated with the overexpression of drug efflux pumps. P-glycoprotein (P-gp) is a drug efflux pump often found overexpressed in cases of acquired MDR. Nevertheless, there are no P-gp inhibitors being used in the current clinical practice, due to toxicity problems, drug interactions or pharmacokinetic issues. Therefore, it is important to identify novel inhibitors of P-gp activity or expression. Curcumin is a secondary metabolite isolated from the turmeric of *Curcuma longa* L. which has been associated with several biological activities, particularly P-gp modulatory activity (by inhibiting both P-gp function and expression). However, curcumin shows extensive metabolism and instability, which has justified the recent and intensive search for analogs of curcumin that maintain the P-gp modulatory activity but have enhanced stability. This review summarizes and compares the effects of curcumin and several curcumin analogs on P-glycoprotein function and expression, emphasizing the potential of these molecules

for the possible development of safe and effective inhibitors of P-gp to overcome MDR in human cancer.

Keywords: P-glycoprotein, multidrug resistance; curcumin; curcumin analogs

PACS: J0101

1. P-glycoprotein as a major cause of cancer multidrug resistance

Cancer cells may have inherent or may develop resistance to antitumor drugs. In some cases, cells are cross-resistant to several unrelated (structurally and mechanistically different) drugs, a phenomenon known as multidrug resistance (MDR) [1,2].

Overexpression of P-glycoprotein (P-gp) is one of the main mechanisms involved in the development of MDR [1,2]. P-gp (encoded by the *MDR1* gene, also referred to as ABCB1) is a drug-efflux pump from the ATP-binding cassette (ABC) transporters family, which efficiently removes cytotoxic drugs from the intracellular environment through an ATP dependent mechanism [3]. This glycoprotein is composed of two highly hydrophobic integral membrane domains and two hydrophilic nucleotide binding domains (Figure 1) [4].

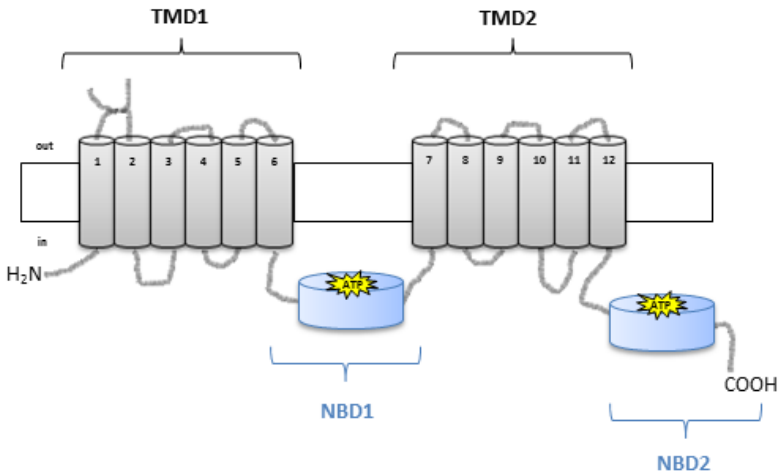

Figure 1. Schematic representation of P-gp structure with two halves, each with a transmembrane domain (TMD1 and TMD2) and a nucleotide-binding domain (NBD1 and NBD2) (adapted from [5]).

The TMDs, composed of six membrane α-helices (TM1-TM6 and TM7-TM12), contain the drug binding sites and define the translocation pathway across the membrane; the two cytoplasmic NBDs couple the energy associated with ATP binding and hydrolysis, which is necessary for drug transport [6].

Different studies have shown that by inhibiting P-gp it is possible to counteract some cases of MDR in cancer [7]. There are many known MDR modulators belonging to several chemical classes, including calcium channel blockers, indole alkaloids, cyclosporine's and calmodulin inhibitors [8]. However, the described modulators presented toxicity problems associated with the need for the use of very high doses in order to produce the required results [9]. To minimize these risks, new analogs of these compounds are being tested and developed with the goal of finding potent MDR modulators with less toxicity problems [10].

Some of the most effective cancer treatments to date are derived from natural products, such as taxol [11]. Indeed, natural products and their synthetic derivatives comprise more than half of the approved anticancer drug candidates developed in the last decades [12]. Research on natural dietary phytochemicals from foods, herbs, and dietary supplements is increasing due to the low toxicity expected.

The search for P-gp inhibitors has uncovered several natural compounds with this activity such as flavonoids, quercetin, morin, catechins, capsaicin, and curcumin [13-15]. In this review, studies on the effects of curcumin and curcumin analogs on P-gp expression and activity are summarized, with the aim of highlighting the potential of these molecules for the possible development of safe and effective inhibitors of P-gp to overcome MDR in human cancer.

2. Curcumin as a natural product that inhibits P-gp

Curcumin (Figure 2) is a phytochemical obtained from the dried rhizomes of *Curcuma longa* L. (turmeric), which has been used over the last centuries as a food additive, in cosmetics and as a form of traditional herbal medicine [16]. It has a wide range of pharmacological activities and presents low levels of toxicity.

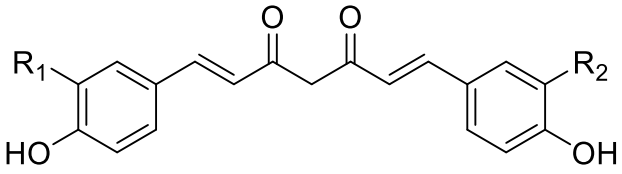

Curcumin $R_1, R_2 = OCH_3$
Demethoxycurcumin $R_1 = OCH_3, R_2 = H$
Bisdemethoxycurcumin $R_1, R_2 = H$

Figure 2. Main curcuminoids isolated from turmeric of *Curcuma longa* L..

Several studies have demonstrated a beneficial effect for curcumin in Alzheimer disease [17] and also in cases of high cholesterol by inhibiting the intestinal absorption of cholesterol and consequently reducing its blood levels [18]. Curcumin was also described as an anti-HIV [19] and antibacterial agent [20]. Additionally, curcumin presents strong antioxidant, anti-inflammatory, and antiangiogenic properties and was also described as having wound healing and anticancer effects [16,21].

Curcumin inhibits the growth of a wide variety of tumour cells, including gastric cancer [22] colon carcinoma [23] and breast cancer cells [24]. Curcumin was described as inhibiting the phosphorylation of AKT and AKT-related gene products, thereby presenting antitumor effects [25]. In addition, curcumin has been shown to downregulate the AKT kinase signaling, inhibiting proliferation and inducing apoptosis in T-cell leukaemia cell lines [26]. Interestingly, curcumin has been also described to be capable of suppressing P-gp expression and function and therefore reversing the MDR phenotype [27-29].

2.1. Curcumin as modulator of P-glycoprotein function

Curcumin was described as having a role in reversing MDR through the modulation of P-gp. Specifically, curcumin has been described as an inhibitor of the function of P-gp in several *in vitro and in vivo* models [21,30].

Several studies unraveled that the role of curcumin in the modulation of MDR occurred through its interaction with P-gp. In 2002, Anuchapreeda and collaborators [31] demonstrated that curcumin reduced P-gp mediated drug-efflux in MDR cervical carcinoma cells, in a dose dependent manner. The authors also performed biochemical studies which have shown the direct interaction between P-gp and curcumin [31]. Two years later, the same group [32] purified the three major curcuminoids from the previous used curcumin mixture [31] (curcumin, demethoxycurcumin and bisdemethoxycurcumin, Figure 2) and analyzed the effect of the three curcuminoids on the modulation of P-gp function, in the same MDR human cervical carcinoma cell line [32]. The authors suggested that these three curcuminoids are not substrates of P-gp, since they presented similar IC50 values for cytotoxicity between the MDR and the drug-sensitive cell lines used in the study [32]. In addition, they observed that curcumin was the most effective MDR modulator among the three curcuminoids, and could possibly be used in combination with conventional chemotherapy to reverse MDR in cancer [32].

Curcumin was also demonstrated to reverse MDR in a different model, a gastric carcinoma MDR cell line, possibly through a decrease in P-gp function which was observed in the treated cells [33]. In addition, two different MDR human cancer cell models (cervical and breast carcinoma MDR cell lines) that were treated with the three major curcuminoids

(Figure 2), presented inhibition of P-gp function, which significantly increased the intracellular accumulation of rhodamine in a dose dependent manner [34]. Also, the interaction of one of curcumin metabolites, tetrahydrocurcumin, with the P-gp molecule was clearly indicated by an ATPase assay and by photo affinity labeling of P-gp [34].

The above mentioned studies were performed in order to study the capacity of curcumin to revert MDR. However, curcumin was also shown to have an effect in preventing the induction of MDR [35]. This was observed in a chronic myeloid leukaemia cell line that was pre-treated with curcumin before being exposed for 24 hours to doxorubicin with the purpose of selecting for more resistant cell line (with overexpression of P-gp). These cells, presented an increase in the intracellular rh123 accumulation levels, and an increase in the sensitivity towards doxorubicin (almost comparable to cells that were not exposed to doxorubicin), whereas the cells that were not pretreated with curcumin (but exposed to doxorubicin) presented a decrease in the intracellular rh123 accumulation levels and became more resistant to doxorubicin [35].

2.2. Curcumin as modulator of P-glycoprotein expression

Curcumin has been described not only to inhibit the function of P-gp but also the expression of P-gp, at the protein and at the mRNA level. This role of curcumin, as inhibitor of the expression of P-gp, was originally described in 2002 [31], in a work in which it was shown that treatment of MDR cervical carcinoma cells caused a decrease in the protein and in the mRNA levels of P-gp [31]. The same authors have latter on isolated the three more important natural curcuminoids from turmeric (Figure 2, curcumin, demethoxycurcumin and bisdemethoxycurcumin), and compared them for their ability to modulate P-gp expression in the same model (a MDR human cervical carcinoma cell line) [36]. They have demonstrated that bisdemethoxycurcumin was the most active of the curcuminoids present in turmeric, regarding the inhibition of the P-gp expression. In addition, treatment of the MDR cells with curcumin increased their sensitivity to vinblastine, which was consistent with a decrease in P-gp expression [36].

The effect of curcumin in P-gp expression was also demonstrated in other MDR cancer cell models, such as in a human MDR gastric cancer cell line [33], a human MDR colon cancer cell line [37] and a mouse MDR leukaemia cell line [28], in which it was described that the inhibitory effect of curcumin in the expression of P-gp ultimately lead to MDR modulation and cellular sensitization to common drugs. From a mechanistic point of view, it was proposed that curcumin can contribute to counteract the MDR phenotype, probably by suppression of P-gp expression via inhibition of the PI3K/Akt/NF-kB signaling pathway [28].

The role of curcumin in preventing MDR by decreasing P-gp expression in a chronic myeloid leukaemia model was also shown [35]. In addition, it was found that all the three curcuminoids (curcumin, demethoxycurcumin and bisdemethoxycurcumin, Figure 2) were capable of preventing MDR induced by doxorubicin in that model (chronic myeloid leukaemia). However, the preventive effect of each curcuminoid was different, with demethoxycurcumin being the most active of the curcuminoids for prevention of *MDR1* mRNA and P-gp overexpression [38].

Finally, it was demonstrated that both the chemotherapeutic and chemosensitizing effects of curcuminoids (by downregulation of P-gp expression) in colon cancer cells were mediated through modulation of a microRNA (miR-27a-ZBTB10-Sp-axis) [39].

Although these works have demonstrated that curcumin is an effective inhibitor of P-gp expression *in vitro*, animal experimentation was further required to determine if curcumin had potential as an effective and safe chemosensitizer. Curcumin was shown to have capacity to inhibit the expression of P-gp in xenografts of human colon cancer cells in mice. Indeed, curcumin treatment significantly reduced the expression of the MDR1 gene and of P-gp protein in the xenografts of mice, when compared to the control group [37]. These results suggested that curcumin could partially reverse the MDR phenotype. Additionally, curcumin inhibited xenograft growth [37]. The P-gp inhibitory activity of curcumin was also demonstrated in an *in vivo* model of colon cancer, by a novel method, the *in situ* cancerous colonic single pass perfusion method in rats [29].

3. Strategies for overcoming limitations of curcumin

The previously mentioned studies suggested that curcumin could become a promising lead compound for overcoming MDR in cancer. However, this compound is very unstable and has low bioavailability *in vivo* [21]. Indeed, curcumin is highly hydrophobic, which prevent its absorption across the gut, therefore having a rapid metabolism and a limited tissue distribution [40] In summary, the instability of the molecule and its poor pharmacokinetics profile are major drawbacks for its possible clinical use. This became evident in a Phase I clinical trial, during which very high oral doses of curcumin (8-12 g/daily) resulted in peak plasma concentrations in the nanomolar range only [41,42]. Therefore, two strategies have been employed in order to overcome this problem: the incorporation of curcumin into pharmaceutical formulations to improve its delivery and the design and synthesis of analogues of curcumin aiming to obtain better stability and bioavailability.

3.1. Improving the intracellular delivery of curcumin

It has been reported that a more pronounced downregulation of P-gp expression was observed when curcumin was delivered in nanoemulsion formulations (heterogeneous mixtures of oil in water, where the oil droplets have a nanometer size, which allow the solubilization of hydrophobic compounds such as curcumin) when compared to curcumin alone [43]. Furthermore, it was shown that chitosan–PBCA nanoparticles decreased the expression levels of P-gp in the MDR cells when compared to control curcumin alone [44]. Finally, a preparation of mixed micelles (polymeric micelles and surfactant micelles) loaded with curcumin caused a significant improvement in the cytotoxic activity and in the oral bioavailability, when compared to curcumin alone [45]. These improved effects could be attributed to the solubilization of the hydrophobic curcumin into the micelle core, together with the P-gp inhibitory effect of curcumin.

3. 2 Curcumin derivatives and analogs as inhibitors of P-gp

Over the past few years, several curcumin derivatives/analogs have been synthesized with the objective of obtaining molecules more stable and bioavailable than curcumin, while not losing their biological activity (Table 1).

Table 1 – Reported curcumin derivatives/analogs with P-gp modulatory effect

Compounds	MDR cancer model	Inhibitors of P-gp function	Inhibitors of P-gp expression	REF
Unsymmetrical curcumin mimics with various amide moieties	MDR cervical adenocarcinoma	X		[46]
Heterocyclic cyclohexanone monocarbonyl analogs of curcumin	Human embryonic kidney cells and canine kidney cells transfected with wild-type P-gp	X		[47]
Chloro and asymmetrical series of synthetic curcumin derivatives	MDR acute lymphoblastic leukaemia	X		[48]
Diketone and cyclohexanone curcumin analogs	MDR chronic myeloid leukaemia	X	X	[49]

3.2.1. Curcumin derivatives and analogs as modulators of P-glycoprotein function

Several authors have attempted to understand the MDR modulatory effect of curcumin and the disadvantages that curcumin presents in terms of pharmacokinetics profile, from a chemical perspective. They have attempted to synthesize better compounds, i.e. maintaining the MDR modulatory effect while improving the stability and availability of curcumin.

For instance, twelve unsymmetrical curcuminoids with various amide groups were synthesized and tested for MDR reversal activity. Three of the compounds presented a potent MDR reversal activity by inhibiting the drug efflux function of P-gp, while the others

were only moderately potent [46]. This work also showed, from the preliminary structure-activity study, that only half of the curcumin symmetrical structure is a promising lead structure for a MDR reversal agent [46].

Moreover, monocarbonyl analogs of curcumin have been described to be more stable than curcumin, since they do not have the unstable β-diketone moiety of curcumin [50]. Indeed, 23 heterocyclic cyclohexanone monocarbonyl analogs of curcumin were synthesized and investigated for their inhibitory effects against the P-gp function (using flow cytometry and resistance reversal assays) [47]. Many of these compounds inhibited P-gp function, most of them being more potent than curcumin itself. Moreover, some of these analogs showed potent anticancer activity [47], which raised the possibility of using them as antitumor dual agents (similarly to the above described curcumin effect).

Additionally, the cytotoxic and P-gp inhibitory activity of 19 chloro and asymmetrical series of synthetic curcumin derivatives was studied in a MDR acute lymphoblastic leukaemia model [48]. Some of the compounds caused a significant increase in doxorubicin uptake rates (an effect that was better than that of verapamil), indicating a remarkable inhibition of P-gp function (since doxorubicin is a P-gp substrate) [48].

Finally, five diketone and four cyclohexanone curcumin analogs were synthesized and studied regarding the intracellular accumulation of P-gp substrates (such as rhodamine 123 and doxorubicin), in order to evaluate their effect as inhibitors of P-gp function. Two of these compounds (1,7-bis-(3,4-dimethoxy-phenyl)- hepta-1,6-diene-3,5-dione and 2,6-bis-(3,4-dimethoxy-benzylidene)-cyclo- hexanone) caused a strong inhibitory effect of P-gp function [49], which suggests that these analogs may be strong MDR modulators.

3.2.2 Curcumin derivatives and analogs as modulators of P-glycoprotein expression

From the above mentioned published studies only one study investigated the inhibitory activity of the analogs in terms of P-gp expression [49]. From the studied diketone and four cyclohexanone curcumin analogs mentioned above (section 3.2.1), three of them showed a strong effect as inhibitors of P-gp expression. Interestingly, one of the analogs (2,6-bis-(3,4-dimethoxy-benzylidene)-cyclo- hexanone) caused simultaneous inhibition of the expression and of the function of P-gp [49]. This compound might be a very good candidate for an MDR modulator, since it has dual inhibitory effects (on both P-gp function and expression), increased the sensitivity of the MDR cells to paclitaxel and also has better stability than curcumin itself.

4. Future perspectives

It is believed that the level of P-gp in the cell lines is much higher than that in human tissues [51], which means that lower concentrations of P-gp modulators should be effective inhibitors of P-gp *in vivo,* when compared to *in vitro* studies. Therefore, even though curcumin and derivatives are considered to be non-toxic, a low therapeutic dose could be favorable in future *in vivo* studies.

Future studies should also consider the synergistic effects of curcumin with other compounds, on P-gp transporter function and expression. Combinatorial studies with several natural compounds or with conventional anticancer drugs could be carried out in order to identify potential synergistic or additive effects.

Acknowledgments: The work of the author's laboratories is funded by: project NORTE-01-0145-FEDER-000029, supported by Norte Portugal Regional Programme (NORTE 2020), under the PORTUGAL 2020 Partnership Agreement, through the European Regional Development Fund (ERDF); INNOVMAR - Innovation and Sustainability in the Management and Exploitation of Marine Resources, reference NORTE-01-0145-FEDER-000035, Research Line NOVELMAR; FEDER - Fundo Europeu de Desenvolvimento Regional funds through the COMPETE 2020 - Operacional Programme for Competitiveness and Internationalisation (POCI), Portugal 2020, and by Portuguese funds through FCT - Fundação para a Ciência e a Tecnologia/ Ministério da Ciência, Tecnologia e Inovação in the framework of the project "Institute for Research and Innovation in Health Sciences" (POCI-01-0145-FEDER-007274). The authors thank the Portuguese Foundation for Science and Technology (FCT) for the PhD grant of VLR (SFRH/BD/87646/2012).

Conflicts of Interest: The authors declare no conflict of interest.

References

1. Gottesman, M.M.; Fojo, T.; Bates, S.E. Multidrug resistance in cancer: Role of atp-dependent transporters. *Nature reviews. Cancer* **2002**, *2*, 48-58.

2. Lopes-Rodrigues, V.; Seca, H.; Sousa, D.; Sousa, E.; Lima, R.T.; Vasconcelos, M.H. The network of p-glycoprotein and microrna interactions. *International journal of cancer. Journal international du cancer* **2014**, *135*, 253-263.

3. Eckford, P.D.; Sharom, F.J. Abc efflux pump-based resistance to chemotherapy drugs. *Chem Rev* **2009**, *109*, 2989-3011.

4. Krishna, R.; Mayer, L.D. Modulation of p-glycoprotein (pgp) mediated multidrug resistance (mdr) using chemosensitizers: Recent advances in the design of selective mdr modulators. *Curr Med Chem Anticancer Agents* **2001**, *1*, 163-174.

5. Srinivas, E.; Murthy, J.N.; Rao, A.R.; Sastry, G.N. Recent advances in molecular modeling and medicinal chemistry aspects of phospho-glycoprotein. *Current drug metabolism* **2006**, *7*, 205-217.

6. Stenham, D.R.; Campbell, J.D.; Sansom, M.S.; Higgins, C.F.; Kerr, I.D.; Linton, K.J. An atomic detail model for the human atp binding cassette transporter p-glycoprotein derived from disulfide cross-linking and homology modeling. *FASEB journal : official publication of the Federation of American Societies for Experimental Biology* **2003**, *17*, 2287-2289.

7. Palmeira, A.; Vasconcelos, M.H.; Paiva, A.; Fernandes, M.X.; Pinto, M.; Sousa, E. Dual inhibitors of p-glycoprotein and tumour cell growth: (re)discovering thioxanthones. *Biochemical pharmacology* **2012**, *83*, 57-68.

8. Palmeira, A.; Sousa, E.; Vasconcelos, M.H.; Pinto, M.; Fernandes, M.X. Structure and ligand-based design of p-glycoprotein inhibitors: A historical perspective. *Current pharmaceutical design* **2012**, *18*, 4197-4214.

9. Krishna, R.; Mayer, L.D. Multidrug resistance (mdr) in cancer. Mechanisms, reversal using modulators of mdr and the role of mdr modulators in influencing the pharmacokinetics of anticancer drugs. *European journal of pharmaceutical sciences : official journal of the European Federation for Pharmaceutical Sciences* **2000**, *11*, 265-283.

10. Liscovitch, M.; Lavie, Y. Cancer multidrug resistance: A review of recent drug discovery research. *IDrugs* **2002**, *5*, 349-355.

11. Colegate, S.M.a.M., R.J. *Bioactive natural products: Detection, isolation and structural determination.* 2 nd edition ed.; CRC Press: Boca Raton, 2008.

12. Newman, D.J.; Cragg, G.M. Natural products as sources of new drugs over the last 25 years. *J Nat Prod* **2007**, *70*, 461-477.

13. Conseil, G.; Baubichon-Cortay, H.; Dayan, G.; Jault, J.M.; Barron, D.; Di Pietro, A. Flavonoids: A class of modulators with bifunctional interactions at vicinal atp- and steroid-binding sites on mouse p-glycoprotein. *Proceedings of the National Academy of Sciences of the United States of America* **1998**, *95*, 9831-9836.

14. Zhang, S.; Morris, M.E. Effects of the flavonoids biochanin a, morin, phloretin, and silymarin on p-glycoprotein-mediated transport. *J Pharmacol Exp Ther* **2003**, *304*, 1258-1267.

15. Nabekura, T.; Kamiyama, S.; Kitagawa, S. Effects of dietary chemopreventive phytochemicals on p-glycoprotein function. *Biochem Biophys Res Commun* **2005**, *327*, 866-870.

16. Sharma, R.A.; Gescher, A.J.; Steward, W.P. Curcumin: The story so far. *Eur J Cancer* **2005**, *41*, 1955-1968.

17. Chen, S.Y.; Chen, Y.; Li, Y.P.; Chen, S.H.; Tan, J.H.; Ou, T.M.; Gu, L.Q.; Huang, Z.S. Design, synthesis, and biological evaluation of curcumin analogues as multifunctional agents for the treatment of alzheimer's disease. *Bioorg Med Chem* **2011**, *19*, 5596-5604.

18. Shishodia, S.; Sethi, G.; Aggarwal, B.B. Curcumin: Getting back to the roots. *Ann N Y Acad Sci* **2005**, *1056*, 206-217.

19. Mazumder, A.; Raghavan, K.; Weinstein, J.; Kohn, K.W.; Pommier, Y. Inhibition of human immunodeficiency virus type-1 integrase by curcumin. *Biochemical pharmacology* **1995**, *49*, 1165-1170.

20. Rai, D.; Singh, J.K.; Roy, N.; Panda, D. Curcumin inhibits ftsz assembly: An attractive mechanism for its antibacterial activity. *Biochem J* **2008**, *410*, 147-155.

21. Anand, P.; Thomas, S.G.; Kunnumakkara, A.B.; Sundaram, C.; Harikumar, K.B.; Sung, B.; Tharakan, S.T.; Misra, K.; Priyadarsini, I.K.; Rajasekharan, K.N., *et al.* Biological activities of curcumin and its analogues (congeners) made by man and mother nature. *Biochemical pharmacology* **2008**, *76*, 1590-1611.

22. Yu, L.L.; Wu, J.G.; Dai, N.; Yu, H.G.; Si, J.M. Curcumin reverses chemoresistance of human gastric cancer cells by downregulating the nf-kappab transcription factor. *Oncol Rep* **2011**, *26*, 1197-1203.

23. Wichitnithad, W.; Nimmannit, U.; Wacharasindhu, S.; Rojsitthisak, P. Synthesis, characterization and biological evaluation of succinate prodrugs of curcuminoids for colon cancer treatment. *Molecules* **2011**, *16*, 1888-1900.

24. Yodkeeree, S.; Ampasavate, C.; Sung, B.; Aggarwal, B.B.; Limtrakul, P. Demethoxycurcumin suppresses migration and invasion of mda-mb-231 human breast cancer cell line. *Eur J Pharmacol* **2010**, *627*, 8-15.

25. Wang, H.; Geng, Q.R.; Wang, L.; Lu, Y. Curcumin potentiates antitumor activity of l-asparaginase via inhibition of the akt signaling pathway in acute lymphoblastic leukaemia. *Leuk Lymphoma* **2012**, *53*, 1376-1382.

26. Hussain, A.R.; Al-Rasheed, M.; Manogaran, P.S.; Al-Hussein, K.A.; Platanias, L.C.; Al Kuraya, K.; Uddin, S. Curcumin induces apoptosis via inhibition of pi3'-kinase/akt pathway in acute t cell leukaemias. *Apoptosis : an international journal on programmed cell death* **2006**, *11*, 245-254.

27. Anuchapreeda, S.; Thanarattanakorn, P.; Sittipreechacharn, S.; Tima, S.; Chanarat, P.; Limtrakul, P. Inhibitory effect of curcumin on mdr1 gene expression in patient leukemic cells. *Arch Pharm Res* **2006**, *29*, 866-873.

28. Choi, B.H.; Kim, C.G.; Lim, Y.; Shin, S.Y.; Lee, Y.H. Curcumin down-regulates the multidrug-resistance mdr1b gene by inhibiting the pi3k/akt/nf kappa b pathway. *Cancer letters* **2008**, *259*, 111-118.

29. Neerati, P.; Sudhakar, Y.A.; Kanwar, J.R. Curcumin regulates colon cancer by inhibiting p-glycoprotein in in-situ cancerous colon perfusion rat model. *J Cancer Sci Ther* **2013**, *5*, 313-319.

30. Oliveira, A.S.; Sousa, E.; Vasconcelos, M.H.; Pinto, M. Curcumin: A natural lead for potential new drug candidates. *Current medicinal chemistry* **2015**, *22*, 4196-4232.

31. Anuchapreeda, S.; Leechanachai, P.; Smith, M.M.; Ambudkar, S.V.; Limtrakul, P.N. Modulation of p-glycoprotein expression and function by curcumin in multidrug-resistant human kb cells. *Biochemical pharmacology* **2002**, *64*, 573-582.

32. Chearwae, W.; Anuchapreeda, S.; Nandigama, K.; Ambudkar, S.V.; Limtrakul, P. Biochemical mechanism of modulation of human p-glycoprotein (abcb1) by curcumin i, ii, and iii purified from turmeric powder. *Biochemical pharmacology* **2004**, *68*, 2043-2052.

33. Tang, X.Q.; Bi, H.; Feng, J.Q.; Cao, J.G. Effect of curcumin on multidrug resistance in resistant human gastric carcinoma cell line sgc7901/vcr. *Acta Pharmacol Sin* **2005**, *26*, 1009-1016.

34. Limtrakul, P.; Chearwae, W.; Shukla, S.; Phisalphong, C.; Ambudkar, S.V. Modulation of function of three abc drug transporters, p-glycoprotein (abcb1), mitoxantrone resistance protein (abcg2) and multidrug resistance protein 1 (abcc1) by tetrahydrocurcumin, a major metabolite of curcumin. *Mol Cell Biochem* **2007**, *296*, 85-95.

35. Xu, D.; Tian, W.; Shen, H. Curcumin prevents induced drug resistance: A novel function? *Chin J Cancer Res* **2011**, *23*, 218-223.

36. Limtrakul, P.; Anuchapreeda, S.; Buddhasukh, D. Modulation of human multidrug-resistance mdr-1 gene by natural curcuminoids. *BMC Cancer* **2004**, *4*, 13.

37. Lu, W.D.; Qin, Y.; Yang, C.; Li, L.; Fu, Z.X. Effect of curcumin on human colon cancer multidrug resistance in vitro and in vivo. *Clinics (Sao Paulo)* **2013**, *68*, 694-701.

38. Xu, D.; Tian, W.; Shen, H. P-gp upregulation may be blocked by natural curcuminoids, a novel class of chemoresistance-preventing agent. *Mol Med Rep* **2013**, *7*, 115-121.

39. Noratto, G.D.; Jutooru, I.; Safe, S.; Angel-Morales, G.; Mertens-Talcott, S.U. The drug resistance suppression induced by curcuminoids in colon cancer sw-480 cells is mediated by reactive oxygen species-induced disruption of the microrna-27a-zbtb10-sp axis. *Mol Nutr Food Res* **2013**, *57*, 1638-1648.

40. Anand, P.; Kunnumakkara, A.B.; Newman, R.A.; Aggarwal, B.B. Bioavailability of curcumin: Problems and promises. *Molecular pharmaceutics* **2007**, *4*, 807-818.

41. Cheng, A.L.; Hsu, C.H.; Lin, J.K.; Hsu, M.M.; Ho, Y.F.; Shen, T.S.; Ko, J.Y.; Lin, J.T.; Lin, B.R.; Ming-Shiang, W.*, et al.* Phase i clinical trial of curcumin, a chemopreventive agent, in patients with high-risk or pre-malignant lesions. *Anticancer Res* **2001**, *21*, 2895-2900.

42. Vareed, S.K.; Kakarala, M.; Ruffin, M.T.; Crowell, J.A.; Normolle, D.P.; Djuric, Z.; Brenner, D.E. Pharmacokinetics of curcumin conjugate metabolites in healthy human subjects. *Cancer Epidemiol Biomarkers Prev* **2008**, *17*, 1411-1417.

43. Ganta, S.; Amiji, M. Coadministration of paclitaxel and curcumin in nanoemulsion formulations to overcome multidrug resistance in tumour cells. *Molecular pharmaceutics* **2009**, *6*, 928-939.

44. Duan, J.; Mansour, H.M.; Zhang, Y.; Deng, X.; Chen, Y.; Wang, J.; Pan, Y.; Zhao, J. Reversion of multidrug resistance by co-encapsulation of doxorubicin and curcumin in chitosan/poly(butyl cyanoacrylate) nanoparticles. *International journal of pharmaceutics* **2012**, *426*, 193-201.

45. Patil, S.; Choudhary, B.; Rathore, A.; Roy, K.; Mahadik, K. Enhanced oral bioavailability and anticancer activity of novel curcumin loaded mixed micelles in human lung cancer cells. *Phytomedicine* **2015**, *22*, 1103-1111.

46. Um, Y.; Cho, S.; Woo, H.B.; Kim, Y.K.; Kim, H.; Ham, J.; Kim, S.N.; Ahn, C.M.; Lee, S. Synthesis of curcumin mimics with multidrug resistance reversal activities. *Bioorg Med Chem* **2008**, *16*, 3608-3615.

47. Revalde, J.L.; Li, Y.; Hawkins, B.C.; Rosengren, R.J.; Paxton, J.W. Heterocyclic cyclohexanone monocarbonyl analogs of curcumin can inhibit the activity of atp-binding cassette transporters in cancer multidrug resistance. *Biochemical pharmacology* **2015**, *93*, 305-317.

48. Ooko, E.; Alsalim, T.; Saeed, B.; Saeed, M.E.; Kadioglu, O.; Abbo, H.S.; Titinchi, S.J.; Efferth, T. Modulation of p-glycoprotein activity by novel synthetic curcumin derivatives in sensitive and multidrug-resistant t-cell acute lymphoblastic leukaemia cell lines. *Toxicol Appl Pharmacol* **2016**, *305*, 216-233.

49. Mapoung, S.; Pitchakarn, P.; Yodkeeree, S.; Ovatlarnporn, C.; Sakorn, N.; Limtrakul, P. Chemosensitizing effects of synthetic curcumin analogs on human multi-drug resistance leukemic cells. *Chem Biol Interact* **2016**, *244*, 140-148.

50. Liang, G.; Shao, L.; Wang, Y.; Zhao, C.; Chu, Y.; Xiao, J.; Zhao, Y.; Li, X.; Yang, S. Exploration and synthesis of curcumin analogues with improved structural stability both in vitro and in vivo as cytotoxic agents. *Bioorg Med Chem* **2009**, *17*, 2623-2631.

51. Ambudkar, S.V.; Dey, S.; Hrycyna, C.A.; Ramachandra, M.; Pastan, I.; Gottesman, M.M. Biochemical, cellular, and pharmacological aspects of the multidrug transporter. *Annu Rev Pharmacol Toxicol* **1999**, *39*, 361-398.

1.3. Metabolic Alterations in MDR

Metabolism is involved, directly or indirectly, in essentially everything a cell does. In fact, it is through metabolism that cells produce energy and the required precursor metabolites needed to fuel all cellular processes. The cellular metabolic network is coordinated by interacting genes and proteins, consisting of several metabolic pathways where enzymatic reactions connect metabolites in a related process [55]. All the players and specific reactions are controlled by a complex regulatory structure, mostly composed by proteins and signalling molecules, which confer dynamism and strength to the cell [56]. These metabolic properties are regulated through several checkpoints in normal cells [55]. However, in cancer cells, many of these regulatory networks are deregulated in order to adapt the tumour cell's metabolism to their uncontrolled growth, proliferation and survival [57]. Also, it is possible that some metabolic alterations may be required for malignant transformation [56]. Indeed, alterations in cellular metabolism are considered a hallmark of cancer, being as widespread in cancer cells as many of the other cancer-associated traits [36].

Normal cells need to be stimulated by growth factors in order to take up nutrients from the environment [61]. This allows preventing uncontrolled proliferation. On the other hand, cancer cells acquire several mutations and other alterations, which functionally alter signaling pathways, overcoming the dependence on growth factors to take up nutrients. Some of these pathways may activate the uptake and metabolism of nutrients, promoting cell survival and fuel to cell growth [58,59].

Cancer cells require multiple alterations to the normal metabolism of all major classes of macromolecules (carbohydrates, proteins, lipids and nucleic acids), in order to support their basic needs for cell division. These cells require high maintenance of energy by rapid generation of ATP, maintenance of balanced redox status and increased biosynthetic capacity [56]. Since MDR cancer cells are highly proliferative and require high energy supply [24], it has been suggested that the pharmacological modulation of metabolic processes in MDR cancer cells could contribute to overcoming this phenotype and improve the efficiency of cancer chemotherapy [60,61]. Some pathways (such as the pentose phosphate pathway, the glutathione metabolism, the methionine/S-adenosylmethionine pathway, glycolysis and oxidative phosphorylation, which are going to be described below), could be altered and somehow implicated in the MDR phenotype.

1.3.1. The Warburg effect

Otto Warburg observed, back in 1924, that cancer cells metabolize glucose in a distinct manner when compared to cells in normal tissues [62,63]. Warburg discovered that cancer cells (unlike normal cells) produce high amounts of lactate from glucose, even when in the presence of enough oxygen to support mitochondrial oxidative phosphorylation (OXPHOS). This phenomenon was named "The Warburg's effect" [62,63].

The Warburg's effect remains not fully understood, partly because it is difficult to understand why do proliferating cells suffer a metabolic switch to a less efficient metabolism in terms of ATP production (since the metabolism of glucose to lactate generates only 2 ATPs per molecule of glucose, whereas OXPHOS generates up to 36 ATPs) [64]. However, the inefficient ATP production is not a problem to proliferating mammalian cancer cells since they are exposed to a continued supply of glucose and other nutrients from the blood. In fact, there is evidence that ATP may never be limiting in these cells (using aerobic glycolysis), since they exhibit high ratios of ATP/ADP [59,65]. Also, it was discovered that glycolysis leads to faster ATP production. Indeed, the rate of ATP production may be up to 100 times faster in glycolysis than in OXPHOS [66], so the increased rate of ATP production resulting from glycolysis confers a selective growth advantage to cancer cells [67,68]. In addition, glycolysis is much "safer" to cancer cells than OXPHOS, because OXPHOS produces reactive oxygen species (ROS) which can be very damaging to the delicate balance of ROS maintained in an abnormal cancer cell (a high ROS content in cancer cells renders them more susceptible to cell death induced by oxidative stress) [69].

Another possible explanation for the metabolic switch is that cancer cells have additional metabolic requirements besides ATP production, to meet their biosynthetic needs. Such metabolic requirements are fulfilled with aerobic glycolysis (rather than with OXPHOS) through the production of glycolytic intermediates [70], which are then integrated into various metabolic pathways to generate *de novo* nucleotides, lipids, amino acids, and NADPH [68,71,72].

The factors that trigger the metabolic switch from OXPHOS to aerobic glycolysis in cancer cells are beginning to be elucidated. The first proposed trigger was tumour hypoxia [67]. However, cancer cells seem to use a glycolytic metabolism even before being exposed to hypoxic conditions [73,74]. Indeed, recent evidence suggests that tumour hypoxia is important for cancer cells, but it may be a late-occurring event and not a major contributor to the metabolic switch towards aerobic glycolysis [70,74,75] As an alternative hypothesis, the triggers to the metabolic switch could be oncogenic pathways, which initiate cell-independent nutrient uptake and proliferative metabolic program [70].

The Warburg effect is also evident in the MDR tumour cells [16]. Indeed, it was observed that some MDR tumours have an increase in glycolysis and a decrease in OXPHOS comparing to drug-sensitive cancer cells [45]. Also, these metabolic alterations are associated with an increase in P-gp expression, which may indicate that both occurrences may be closely related [45]. More recently, it was shown that a metabolic switch conforming to the Warburg effect, was associated with melphalan resistance in multiple myeloma cells [44]. These metabolic changes could be relevant to the MDR phenotype due to the high demand for rapid ATP production by MDR cells. Indeed, cells expressing MDR transporters (such as P-gp), require ATP as the energy source to perform drug efflux [76].

1.3.1.1. Glycolysis

Glycolysis represents one of the first bio-energetic mechanisms to appear during the eukaryotic phylogeny [77]. It is a critical catabolic process of the glucose, using one molecule of glucose to produce two molecules of pyruvate, giving rise to two ATP molecules and two reduced nicotinamide adenine dinucleotide (NADH) molecules (Figure 1) [77].

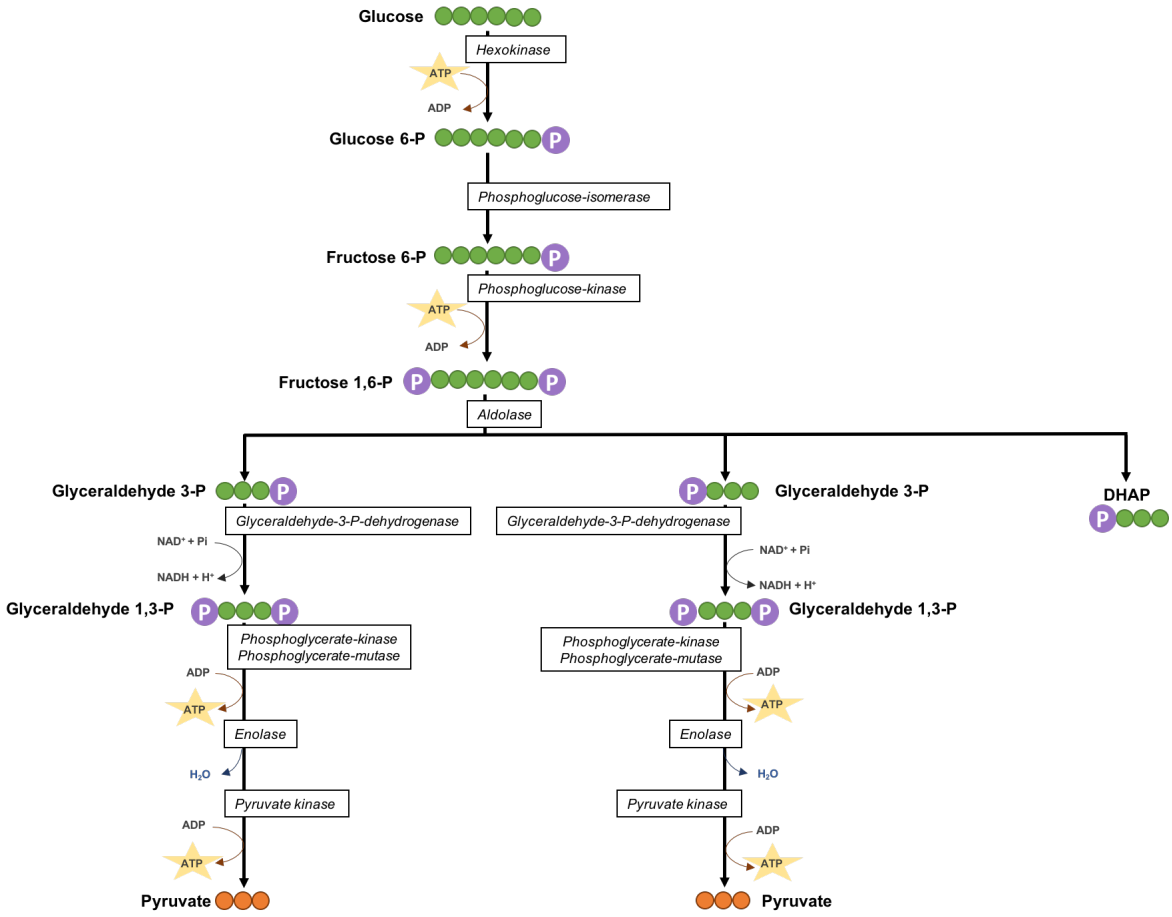

Figure 1 – Glycolysis pathway. The pathway of glycolysis initiates with the phosphorylation of glucose to glucose-6-phosphate (G6P). G6P is then converted to fructose-6-phosphate (F6P) that is further phosphorylated to form fructose-1,6- biphosphate (F1,6BP). Two molecules of ATP are consumed during these two steps of phosphorylation. F1,6BP is then used in order to produce glyceraldehyde 3-P (and dihydroxiacetone-phosphate which is isomerized to glyceraldehyde 3-P), which is then oxidized and phosphorylated to form glyceraldehyde 1,3-P. Glyceraldehyde 1,3-P is converted to 3-phosphoglycerate producing a molecule of ATP *via* substrate-level phosphorylation. 3-Phosphoglycerate is then isomerized to 2-phosphoglycerate, which is dehydrated to produce phosphoenolpyruvate. Phosphoenolpyruvate is subsequently converted to pyruvate with the production of another molecule of ATP. Two molecules of glyceraldehyde 3-phosphate are oxidized to two pyruvates, and four molecules of ATP are produced *via* two steps of substrate-level phosphorylation. The net yield is two molecules of ATP per molecule of glucose oxidized [77].

In normal cells, the fate of pyruvate largely depends on the cellular supply of oxygen. In the absence (or low levels) of oxygen, pyruvate may be transformed into lactate *via* the anaerobic glycolysis pathway. On the other hand, in the presence of oxygen, pyruvate may be oxidized to CO_2 and H_2O through the oxidative phosphorylation (OXPHOS) pathway, resulting in the production of larger amounts of ATP [78]. As already referred, cancer cells have abnormal glucose metabolism, characterized by aerobic glycolysis. Thus, most cancer cells produce large amounts of lactic acid independently of the availability of oxygen [70].

The energy dependence of the MDR transport suggests that MDR cells, when developing the resistance phenotype, probably suffer some alterations in the cell's energy supply. Indeed, it has been suggested that a MDR human breast carcinoma cell line presented an increase in the glycolysis rate related to an increased in the energy-dependent drug detoxification [79]. In addition, some MDR-reversing drugs, such as verapamil, increased the lactate production in P-gp overexpressing tumour cells [80]. Therefore, given the fact that ABC transporters (such as P-gp) are ATPase dependent, glycolysis modulation may eventually contribute to sensitize cancer cells to chemotherapy treatment. Indeed, recent studies have shown that the inhibition of glycolysis sensitizes MDR cells to common chemotherapeutic drugs [45,23,81]. They showed that the inhibition of glycolysis with energetic modulators, such as 2-deoxy-D-glucose and iodoacetate, reverted the MDR phenotype. Moreover, glycolysis inhibition in MDR cells caused downregulation of P-gp expression [23,45] and function [23], showing a direct relationship between glycolysis and P-gp expression in MDR cells and the potential of glycolysis inhibitors to overcome P-gp mediated drug resistance.

1.3.1.2. Oxidative Phosphorylation (OXPHOS)

OXPHOS generates more ATP per metabolite than the glycolytic pathway [82]. Indeed, together with the citric acid cycle, produces a total of four molecules of ATP, ten molecules of NADH, and two molecules of $FADH_2$. Then, electrons from NADH and $FADH_2$ are transferred to molecular oxygen, coupled to the formation of an additional 32 to 34 ATP molecules by oxidative phosphorylation. Electron transport and oxidative phosphorylation are performed by several protein complexes in the inner mitochondrial membrane, serving as the major source of cellular energy (Figure 2).

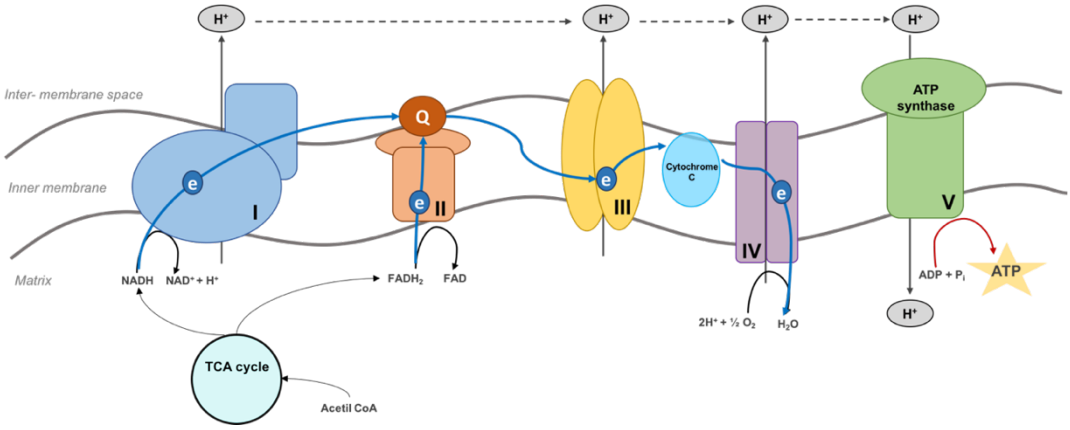

Figure 2 – Electron transport and oxidative phosphorylation. During oxidative phosphorylation, electrons derived from NADH or $FADH_2$ are combined with O_2, and the energy released from these oxidation/reduction reactions is used to drive the synthesis of ATP from ADP. The transfer of electrons from NADH and FADH2 to O_2 is an energy-yielding reaction. This energy must be produced gradually, by the transport of electrons through a series of carriers, which constitute the electron transport chain. These carriers are organized into four complexes and transporters, ubiquinone and cytochrome C. A fifth protein complex serves to couple the energy-yielding reactions of electron transport to ATP synthesis [77]. I – complex I; II – complex II; III – complex III; IV – complex IV; V – complex V; Q- ubiquinone.

Although the majority of the scientific reports showed a role for glycolysis in MDR, surprisingly, recent studies also showed a fundamental role for OXPHOS in cancer and particularly in MDR. Indeed, it was recently shown that melanoma cells are critically dependent on oxidative phosphorylation (OXPHOS) rather than on glycolysis [83,84]. Furthermore, that respiratory function is essential for the tumourigenic and metastatic potential of breast cancer and melanoma cells [85,86]. In addition, it was observed that the most aggressive ovarian cancer cell lines showed a marked dependence on glutamine rather than on glucose [87], and that CSCs from epithelial ovarian cancer patients privilege OXPHOS and resist glucose deprivation [88]. These studies suggest that glycolysis is not the main pathway sustaining tumour growth in these systems.

Particularly, regarding the role of OXPHOS in the MDR phenotype, it was recently shown that cisplatin-resistant cells from ovarian cancer have an increase in the oxidative metabolism, when compared with their sensitive counterparts. In fact, when using pharmacological inhibitors of mitochondrial OXPHOS (such as metformin and oligomycin) the cisplatin resistance was reverted [89]. Also, in a different study, using transcriptomics data of liver metastases from chemotherapy treated and chemo-naive colon cancer patients, it was observed that upon chemotherapy treatment, cancer cells shift their metabolism from glycolysis towards OXPHOS [90]. Finally, a 3-D cell model of breast cancer cells formed a discrete cell sub-population with elevated MDR transport capacity and with a specific metabolic phenotype (mixed glycolytic/oxidative energy sustenance) [91].

1.3.2. The Pentose Phosphate Pathway (PPP)

The pentose phosphate pathway (PPP) was first described in 1926 as being important for cellular metabolism (when the introduction of new antimalarial drugs led to the first medical description of a drug-induced hemolytic anemia correlated with an intrinsic defect of red blood cells metabolism) [92]. The PPP is now known to be not only a shunt pathway in the metabolism of hexose monophosphate, but also a critical pathway in cell redox balance and proliferative fate.

PPP has been conserved throughout evolution, given its important role as a supplier of nucleic acid precursors and reducing equivalents [93]. The percentage of glucose metabolized by the PPP varies in a tissue-dependent manner. In cells, the basal rate of PPP varies depending on the amount of $NADP^+$ and other cell conditions (such as proliferative activity and exposure to oxidizing agents), modifying the $NADP^+$/NADPH ratio [94] (Figure 3).

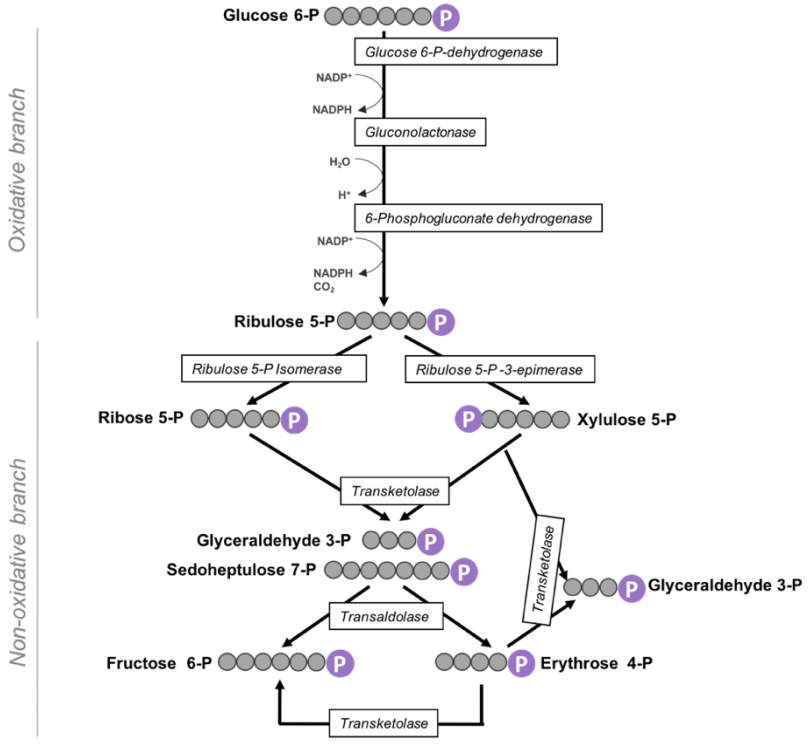

Figure 3 – Pentose phosphate pathway. PPP is normally divided in two branches, an oxidative and a non-oxidative branch. The activity of the oxidative branch is usually higher than the activity of the non-oxidative one [95]. To begin, in the oxidative branch, glucose-6-phosphate (G6P) is oxidized into 6-phosphogluconolactone by glucose-6-phosphate dehydrogenase (G6PD), producing NADPH. The last resulting metabolite, ribulose 5-phosphate can be then converted into ribose 5-phosphate (R5P) and used for the synthesis of nucleotides. Then, in the non-oxidative branch of PPP, the reaction produces F6P and glyceraldehyde 3-phosphate, which can be either metabolized in the glycolytic pathway or reintroduced into the PPP.

Alterations in the PPP activity are frequent during the development or progression of cancer, since PPP provides two substrates that are necessary for the dividing cells (ribose 5-phosphate and NADPH) and also helps protecting cells from ROS damage [96]. Being important for cellular transformation, it can be used as a therapeutic target. In addition to its role in cellular proliferation, experimental observations suggested that PPP may be involved in the promotion of invasion, angiogenesis and resistance to therapy [96].

Therefore, an efficient PPP is required for tumour growth [72]. Indeed, several studies have detected higher G6PD activity in tumour tissues when compared to normal tissues [97]. For example, the non-oxidative branch of PPP has been suggested to be an important source of ribose 5-phosphate synthesis in tumour cells [98-100].

PPP activity also plays a role in cellular escape from apoptosis. In fact, an apoptosis-resistant clone of human promyelocytic HL-60 cells presented higher PPP activity than sensitive cells, having increased levels of NADPH [101]. Moreover, the up-regulation of the PPP is normally associated with invasive and metastatic tumours. Actually, some studies have proposed that the activation of the non-oxidative branch of the PPP can be considered a hallmark of metastatic tumours [98,102].

Additionally, since PPP is important for the control of the cellular redox balance (which is a critical aspect of chemotherapy success), a new and important therapeutic option consists in targeting PPP with selective and specific modulators. This approach may create new therapeutic anticancer options [96].

In terms of therapeutics, high levels of NADPH and GSH together with an active PPP were found to have a role in MDR [103,104]. In some studies, it was observed that the oxidative branch of the PPP is much more active in MDR cells than in their drug-sensitive counterparts. For example, the activity of PPP is two-fold higher in the resistant P388 murine lymphocytic leukaemia cells, as a consequence of a 40% higher activity of the two NADPH-producing dehydrogenases G6PD and 6PGD [105]. Also, a MDR human T-lymphoblastoid model showed higher levels of GSH and G6PD activity than the sensitive counterpart [59]. Recently, it was described that the overexpression of G6PD induces doxorubicin resistance in cells, which could sugest that the activation of PPP may contribute for an acquired MDR phenotype [106]. Furthermore drug-resistant cells are more sensitive to G6PD inhibition than their sensitive counterpart cells [107]. Therefore, it may be hypothesized that the detoxification mechanism for which PPP is responsible could be contributing to maintain the MDR phenotype.

However, it was also described that drug resistant cells may have similar or lower levels of G6PD and PPP than the drug sensitive counterparts [108-111]. Actually, for some chemotherapeutic drugs, a lower activity of G6PD could be in theory beneficial. The cells with low G6PD-mediated synthesis of NADPH may have advantage because, during

anthracycline-induced oxidative stress, the NADPH produced by G6PD could be used by cytochrome P450 reductase, thus triggering the conversion of doxorubicin and mitoxantrone to their toxic metabolites [112,113]. In general, since MDR relies on different mechanisms, the activation or inactivation of the PPP may have opposite effects, depending on the drug used, the tumour type and the molecular mechanism of MDR predominant in the model.

1.3.3. The Glutathione (GSH) Metabolism

Glutathione (GSH) is one of the most important antioxidants in the cell and has an important role in cell physiology, both in a normal state (e.g. in cell proliferation, apoptosis, immune response) and in disease (e.g. cancer, liver diseases, Parkinson disease) [114]. GSH modulates the cellular response to redox changes, detoxifies drug metabolites, regulates gene expression and apoptosis and is involved in the transmembrane transport of organic solutes [115]. Alterations in the GSH cellular pool may contribute to the accumulation of ROS produced by the cells, by generating an imbalance between oxidative and antioxidant molecules [116] (Figure 4). GSH metabolism may occur in all cell types, with the liver being the major producer and exporter of GSH [117].

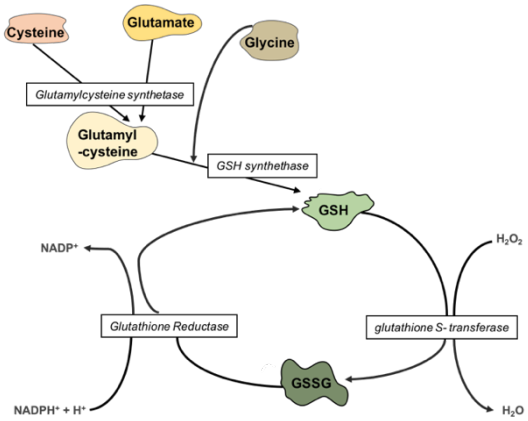

Figure 4 – Glutathione metabolism. The synthesis of GSH from glutamate, cysteine, and glycine is catalyzed sequentially by two cytosolic enzymes, the glutamylcysteine synthetase (GCS) and the GSH synthetase. GSH – Reduced glutathione; GSSG – Oxidized Glutathione.

One of the mechanisms involved in MDR cellular acquisition by cancer cells involves the overexpression of enzymes responsible for the detoxification of the cell, which could inhibit the cytotoxic effect of antitumor drugs. In fact, several drugs which are currently used in the clinic (e.g. alkylating agents) are known substrates of glutathione S- transferases (GSTs) [118]. In addition, a close association between high levels of GSH and GSTs and the development of MDR in cancer cells has already been demonstrated [119]. Moreover, an

association between P-gp and high level activity of the GST enzyme was reported in an abundant number of MDR cell lines [120]. So, the therapeutic use of GST inhibitors may become an important way to counteract the MDR phenotype, as it has been already demonstrated by treating MDR cells with several GST inhibitors (e.g. ethacrynic acid and TLK199), sensitizing MDR cells to chemotherapy [121].

Another important role for GSH in MDR is its contribution for the transport activities (transport of several compounds after being associated with GSH) of some drug efflux pumps from the MRP family. In fact, drug resistance in MRP1-overexpressing cells was partially reversed when using an inhibitor of the GSH synthesis [122].

1.3.4. Methionine/ S-adenosylmethionine (SAMe) pathway

The methionine pathway is found in all types of organisms. Methionine has four major functions, being [123]: i) required for protein synthesis; ii) a precursor of glutathione [124]; iii) required for the formation of polyamines; and iv) a major source of methyl groups for methylation of DNA and other molecules [125].

In particular, methionine plays a fundamental role in transmethylation reactions, being required for S-adenosylmethionine (SAMe) synthesis [126,127]. SAMe is the predominant biological methyl group donor by methyltransferases, and plays a key role in hundreds of biochemical and physiological reactions [128]. Cellular transmethylation reactions use the active methyl group of SAMe (Figure 5).

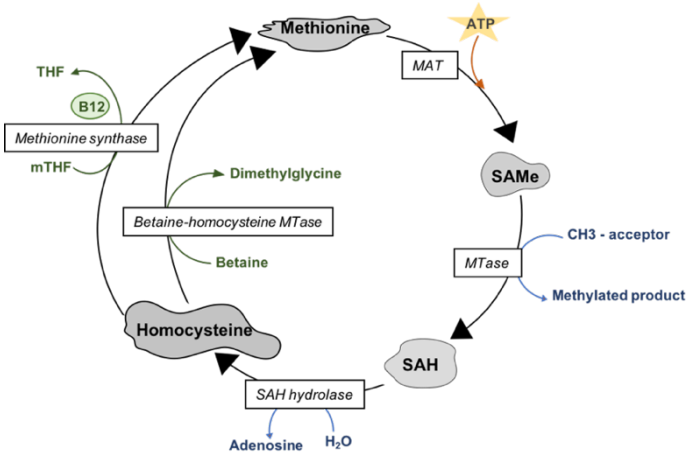

Figure 5 – Methionine metabolism. SAMe donates its methyl group and the resulting product is S-adenosylhomocysteine (SAH). Both produced metabolites in the methylation SAMe-dependent reaction, MTA and S-adenosylhomocysteine, are recycled back to methionine via homocysteine in the methionine cycle [129]. MAT – methionine-S adenosyltransferase; SAMe - S-adenosylmethionine; MTase – methyltransferases; SAH - S-adenosylhomocysteine; THF – tetrahydrofolate; mTHF – 5-methyltetrahydrofolate.

Since the metabolic cycling of methionine is a key pathway for many methylation reactions, alterations in the methionine pathway are implicated in several diseases including cancer [130]. The interface between epigenetics and metabolism is a new possibility for the discovery of new cancer therapeutic targets [131]. Many tumour cells have an absolute need for methionine, whereas normal cells are relatively resistant to exogenous methionine restriction. In fact, it was described that an increase in the methylation index could be associated with the onset of hepatocellular carcinoma [132]. Therefore, inhibitors of the methionine cycle in cancer cells could result in novel and efficient anticancer therapies [131,133].

Furthermore, cancer resistance to general chemotherapeutics and their ability to evade apoptosis are related to the high activity of the methionine cycle in these cells (which permits the methylation of specific genes and activation of multiple survival pathways) [130,134,135]. In fact, when using a methylation inhibitor in a MDR acute lymphoblastic leukaemia cell line, it was possible to revert drug resistance [136]. Moreover, treatment of MDR hepatocellular carcinoma cells with cobalamin (a methylation inhibitor) downregulated P-gp expression due to the increase in the production of SAMe and phosphatidylcholine [137]. These results indicate that the development of resistance could also be methylation-dependent.

1.4. Intercellular transfer of MDR by extracellular vesicles (EVs)

An extracellular vesicle secretion pathway was first described in the early 1980s, when cells from different organisms were found capable of releasing EVs into the extracellular environment. During the past few years, EVs have been isolated from several body fluids such as blood, urine, saliva, amniotic fluid, breast milk, bile, semen, ascites and cerebrospinal fluid [138,139,140]. The origin of these vesicles is diverse and they have been named differently according to their biogenesis, cargo and size.

In the majority of the studies on the biochemical composition of EVs, a bulk of mixed populations of vesicles (obtained by ultracentrifugation) is analyzed. As a consequence, the correct composition and molecular markers of each type of EV is currently unknown [140]. Due to the diversity in the EVs secreted by cells and since the nomenclature is still being debated [141], the scientific experts in EVs are alerting to the need of describing the detailed methodology used in their isolation.

Nonetheless, it is accepted that there are three main classes of EVs:

A) Exosomes

The term exosome was first proposed in 1987 to define EVs with endosomal origin [142]. Exosomes are derived from the endosomal pathway and have sizes ranging from 30 to 100 nm [143]. Exosomes are formed by their release from late endosomal compartments to the plasma membrane, through the fusion of multivesicular bodies. The key step in exosome biogenesis is the reorganization of endosomal membrane proteins (CD9 and CD63) into microdomains. Next, endosomal sorting complexes required for transport (ESCRTs) are recruited to the site of budding. ESCRT-I and -II drive endosomal membrane budding via Alix, that simultaneously binds to TSG101 (component of the ESCRT-I) and CHMP4 (component of ESCRT-III) [143,144].

Their exosomal membrane is enriched in phosphatidylserine (because of its origin) and several markers have been described such as tetraspanins, ESCRT components, TSG110, Alix and Flotilin [144]. ALIX is one of the best well known molecular markers of exosomes; however, several recent Western blot studies have shown different bands for this protein, which could lead to misleading interpretations of data [145-147].

B) Microvesicles

Microvesicles are larger vesicles, with sizes ranging from 50 to 2000 nm, generated by budding from the plasma membrane [143]. They were first characterized as products of activated blood platelets and erythrocytes [148]. The microvesicle membrane is more similar

to the parental cell membrane than the exosomal membrane and presents different specific markers (e.g. integrins, selectins and CD40 ligand) [144].

An usually accepted hypothesis for the microvesicles biogenesis consists in induction of microvesicles formation by translocation of phosphatidylserine to the outer-membrane leaflet through the activity of flippases, leading to a typical plasma membrane curvature [149]. Most of the proteins involved in this process (e.g. ARF6 and PLD2) are different from the ones involved in exosome biogenesis.

C) Apoptotic bodies

Apoptotic bodies are generated through budding of the apoptotic cells plasma membrane and have sizes ranging from 500 to 2000 nm [143]. They have extensive amounts of phosphatidylserine and their content is mostly nuclear fractions and cell organelles [144].

The EVs cargo is not a reflection of the donor cell composition but the result of a regulated sorting mechanism [150]. The nature (and abundance) of the EVs cargo depends on the type and physiological or pathological condition of the donor cell and the specific biogenesis pathway that leads to the formation of each type of EVs [151]. All the cargo proteins and RNAs which have been described in EVs, are included in public databases such as *Vesiclepedia* and *Evpedia* [152,153]. The EVs cargo is highly heterogeneous since they can contain proteins (from the plasma membrane, the endocytic pathway or the cytosol), nucleic acids (fragments of DNA, mRNAs and microRNAs) and lipids (cholesterol, diglycerides, sphingolipids, phospholipids and glycerophospholipids) [154].

After their formation, EVs are released into the extracellular environment by several mechanisms. Several molecules are involved in this process, such as: i) ceramide (that accumulates in the membrane of the EVs) [155], ii) Ca^{2+} -dependent scramblase (that allows the exchange of phospholipids between the two leaflets to increase membrane curvature, in order to facilitate the release of the EVs) [156], iii) annexin-2 [156], iv) chromosome segregation 1-like protein [157] and v) hyaluronan synthase [158].

After being released, EVs are capable of transferring their cargo to other cells by different approaches. While some release their contents into the extracellular space after breaking down [159], others, which maintain their structure for longer periods, are capable of circulating in several fluids (such as blood and lymph) and reach a target cell [160]. Furthermore, after their release, EVs do not randomly interact with recipient cells, often presenting preference for certain target cells [161]. Upon contact, EVs roll over the plasma membrane, followed by the binding of specific membrane proteins (from the syncytin-1 family) to their cell receptors (ASCT2). The membrane binding is then converted rapidly into

fusion (in a similar way to what happens with retroviruses). Specifically, proteins from the EVs membranes are structurally rearranged and their hydrophobic sequences are inserted into the target cell plasma membrane, which suffers lipid and protein reorganization [162,163]. Interestingly, the interaction between EVs and target cells occurs not only by membrane fusion, but also by an active process, a specific type of endocytosis [164]. Once inside the recipient cell, EVs fit within clathrin vesicles and might fuse with the endosome membrane and discharge their contents into the cytoplasm. Alternatively, they may be retained within the endosome lumen or may be targeted to lysosomes for degradation [164].

EVs are important multifunctional signaling complexes for the control of fundamental cellular and biological functions, by participating in the maintenance of normal physiology [165], such as stem cell maintenance [166], tissue repair [167], immune surveillance [168] and blood coagulation [169]. Such a wide-range of cellular and biological functions indicates that EVs may have an important role in disease [165]. One of the best understood roles for EVs in disease is in cancer, which has been studied over the past 17 years. EVs are secreted by most type of cancer cells including leukaemia, melanoma, ovarian, lung, prostate, breast and colorectal cancer. The specific functions of EVs in cancer include participation in the following processes: proliferation, extracellular matrix remodeling, invasion, migration, angiogenesis and the metastatic cascade. Also, EVs from tumour cells can also mediate drug resistance and immunosuppression [170-172].

Recently, several studies have identified EVs as important mediators of the dissemination of cancer drug resistance traits [173-176], by two main mechanisms. The first mechanism consists in the sequestration of drugs by the EVs, making them unavailable to the target cancer cells [177]. The second mechanism consists in the intercellular transfer of MDR mediators, by EVs, from MDR (donor) cells to drug-sensitive (recipient) cells (Figure 6). Following this transfer, drug-sensitive recipient cells may acquire a more resistant phenotype, similar to the one of the MDR donor cells. Indeed, several players associated with MDR in cancer may be transferred by EVs, being considered responsible for the transfer of a MDR phenotype. Some of the described components of the EVs cargo which are known to be responsible for the intercellular transfer of a MDR phenotype are drug-efflux pumps (such as P-gp), microRNAs and lncRNAs (Figure 6) [178].

The transfer of P-gp (in a MDR context) was first shown in a neuroblastoma model, in which the drug-sensitive cells acquired functional P-gp after co-culture of these cells with the MDR counterpart cells (with overexpression of P-gp) [179]. By acquiring functional P-gp, the drug-sensitive cells became resistant, and the resistant phenotype persisted for 4 months [179]. Having these results into account, Bebawy and colleagues [180] demonstrated for the first time, by flow cytometry, that functional P-gp may be transferred by EVs. These authors showed that EVs transfer P-gp from resistant to drug-sensitive human acute

lymphoblastic leukaemia cells. A subsequent study described the role of EVs in transferring P-gp, which was associated with docetaxel-resistance, in prostate cancer cells [180]. The importance of P-gp transfer by EVs was also confirmed in breast cancer cells [172] and ovarian cancer cells [181]. Interestingly, besides showing the P-gp transfer between docetaxel-resistant breast cancer cells and their drug-sensitive counterparts, the authors also showed an increase in the P-gp levels of the recipient cells which was proportional to the amount of EVs co-cultured with those cells [172]. The transfer of P-gp was also confirmed *in vivo* [173,179]. For example, Lechvenko and co-workers used a neuroblastoma xenograft mouse model of drug-sensitive cells, drug-resistant cells and a mixture of the two populations to show P-gp transfer *in vivo* [179]. Interestingly, they showed that the transfer of P-gp *in vivo* was more effective than *in vitro* [179], which could indicate higher efficiency of P-gp transfer by EVs in a more physiological environment.

In summary, P-gp carried by EVs plays a prominent role in the intercellular transfer of MDR, by providing the receiving cells with means to efflux chemotherapeutic drugs.

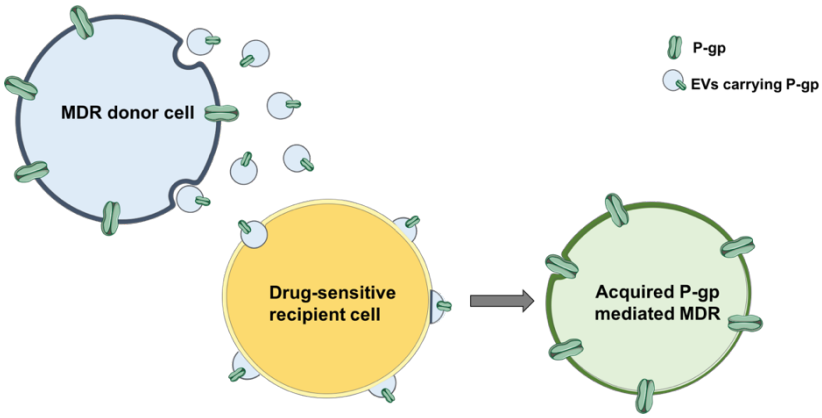

Figure 6 – Intercellular transfer of P-gp mediated MDR by extracellular vesicles (EVs) in cancer.

Several studies have associated metabolic alterations with the shedding and cargo of extracellular vesicles (EVs) [182,183,184]. Following these results, a set of evidence supporting a role for EVs in drug metabolism was provided by several proteomic studies, which have revealed the presence of different xenobiotic metabolizing enzymes on EVs. For example, in a recent study, proteomic analysis allowed the identification of several proteins related to drug metabolism in the cargo of EVs [185].

Recently, other studies have highlighted the relevance of EVs in drug metabolism since it was shown that an increase of lactate production [182] may be associated with the release of EVs, and that EVs are responsible for the transfer of metabolic alterations such as the inhibition of glutamine metabolism [183] and alterations in the glucose metabolism [184].

Part II – Rationale and Aims

Multidrug resistance (MDR) presents a serious challenge to the efficacy of cancer treatment. As previously mentioned, MDR is a complex phenomenon involving several independent or interconnected mechanisms, with overexpression of drug efflux pumps such as P-glycoprotein (P-gp) playing a significant role [39]. In addition, it has been documented that the release of extracellular vesicles (EVs) by MDR cells allows the transfer of their cargo (shed by the releasing/donor cells) to recipient drug-sensitive cells. This EVs-mediated process appears to be relevant for the transfer of the MDR phenotype from MDR to drug-sensitive cells [180,186,187]. Moreover, since EVs contain a tissue-disease-type signature, consisting of a cargo of proteins and nucleic acids selectively packaged into the EVs membrane structure that protects the luminal contents from protease degradation [188], EVs could function as excellent molecular targets and biomarkers, namely of MDR.

To date, there are no clinically-available drugs to counteract the MDR phenotype caused by P-gp [189], which justifies the demand for identifying novel molecular targets and novel molecules to counteract P-gp mediated MDR. In addition, there is no minimally-invasive means to diagnose MDR using non-tumour biological samples [189], which justifies the need for identifying novel biomarkers of P-gp mediated MDR.

Thus the aims of the present work were to:

1. **<u>Identify new targets for overcoming P-gp mediated MDR in cancer</u>**

   To address this main objective, two lines of research were followed:

   1.1. Identify metabolic alterations associated with the P-gp mediated MDR phenotype

   To address this issue, two pairs of MDR and their drug-sensitive counterpart cell lines, from two different cancer models (chronic myeloid leukaemia and non-small cell lung cancer) were analyzed by proteomics, using label-free liquid chromatography - mass spectrometry quantitative profiling. The obtained results were further validated by different assays (such as Western blot or analysis of GSH and ROS levels). Furthermore, all these cell lines were metabolically profiled using the *Seahorse* technology.

1.2. Verify if the identified metabolic alterations are transferred by EVs from MDR cells to drug-sensitive cells

In order to address this question, the drug-sensitive cancer cell lines were profiled using the *Seahorse* technology, to analyze possible alterations in the glycolytic pathway, following co-culture with EVs shed by MDR cells.

2. Identify potential biomarkers of MDR in EVs released by cancer cells

In order to study the relevance of EVs as possible biomarkers of MDR, the cell lines and their respective EVs were profiled according to their size and specific protein content.

3. Find novel molecules to overcome MDR, by identifying curcumin derivatives with improved P-gp inhibitory effect

New curcumin derivatives were synthesized by our collaborators (from FFUP/CIIMAR) and their biological activity was studied, in terms of antitumor activity and anti-P-gp activity. Further identification of compounds with dual activity (antitumor and anti-P-gp) was also carried out.

CHAPTER II – RESULTS AND DISCUSSION

1. RESEARCH ARTICLE

Identification of the metabolic alterations associated with the multidrug resistant phenotype in cancer and their intercellular transfer mediated by extracellular vesicles

Vanessa Lopes-Rodrigues, Alessio Di Luca, Justyna Mleczko, Paula Meleady, Michael Henry, Milica Pesic, Diana Cabrera, Sebastiaan van Liempd, Raquel T. Lima, Robert O'Connor, Juan M. Falcon-Perez, M. Helena Vasconcelos

Submitted for publication (in Scientific Reports)

Identification of the metabolic alterations associated with the multidrug resistant phenotype in cancer and their intercellular transfer mediated by extracellular vesicles

Vanessa Lopes-Rodrigues[1,2,3], Alessio Di Luca[4], Justyna Mleczko[5], Paula Meleady[4], Michael Henry[4], Milica Pesic[6], Diana Cabrera[5], Sebastiaan van Liempd[5,] Raquel T. Lima[1,2,7], Robert O'Connor[4], Juan M. Falcon-Perez[5,8], M. Helena Vasconcelos[1,2,9*]

[1] i3S - Instituto de Investigação e Inovação em Saúde, Universidade do Porto, Portugal

[2] Cancer Drug Resistance Group, IPATIMUP - Institute of Molecular Pathology and Immunology of the University of Porto, 4200-465 Porto, Portugal;

[3] ICBAS-UP - Institute of Biomedical Sciences Abel Salazar, University of Porto, 4099-003 Porto, Portugal;

[4]NICB - National Institute for Cellular Biotechnology, Dublin City University, Dublin 9, Ireland

[5]Exosomes Laboratory & Metabolomics platform, CIC bioGUNE, CIBERehd, Derio, Spain

[6]Institute for Biological Research "Sinisa Stankovic", University of Belgrade, Despota Stefana 142, 11060 Belgrade, Serbia

[7] Department of Pathology - FMUP - Faculty of Medicine of the University of Porto, Porto, Portugal, Alameda Prof. Hernâni Monteiro, 4200-319 Porto, Portugal

[8]IKERBASQUE, Basque Foundation for Science, 48011 Bilbao, Spain

[9]Department of Biological Sciences, FFUP - Faculty of Pharmacy, University of Porto, 4050-313 Porto, Portugal;

*Corresponding author: M. Helena Vasconcelos, IPATIMUP, Institute of Molecular Pathology and Immunology of the University of Porto, Rua Alfredo Allen, 208 4200-135 Porto, Portugal; Tel.: 351-22-0408800; Fax: 351-22-5570799; E-mail: hvasconcelos@ipatimup.pt.

Abstract

Multidrug resistance (MDR) is a serious obstacle to efficient cancer treatment. Overexpression of P-glycoprotein (P-gp) plays a significant role in MDR. Recent studies proved that targeting cellular metabolism could sensitize MDR cells. In addition, metabolic alterations could affect the extracellular vesicles (EVs) cargo and release. This study aimed to: i) identify metabolic alterations in P-gp overexpressing cells that could be involved in the development of MDR and, ii) identify a potential role for the EVs in the acquisition of the MDR. Two different pairs of MDR and their drug-sensitive counterpart cancer cell lines were used. Our results showed that MDR (P-gp overexpressing) cells have a different metabolic profile from their drug-sensitive counterparts, demonstrating decreases in the pentose phosphate pathway and oxidative phosphorylation rate; increases in glutathione metabolism and glycolysis; and alterations in the methionine/S-adenosylmethionine pathway. Remarkably, EVs from MDR cells were capable of stimulating a metabolic switch in the drug-sensitive cancer cells, towards a MDR phenotype. In conclusion, obtained results contribute to the growing knowledge about metabolic alterations in MDR cells and the role of EVs in the intercellular transfer of MDR. The specific metabolic alterations identified in this study may be further developed as targets for overcoming MDR.

Keywords: Multidrug Resistance; P-glycoprotein; Metabolism; Glycolysis; OXPHOS; Extracellular Vesicles

Introduction

The development of multidrug resistance (MDR) in cancer is a serious impediment to treatment success. MDR is defined as a phenotype of the cells resistant to multiple structurally and functionally different drugs. Such resistance is multifactorial and may be due to various mechanisms [1,2]. There are several important mechanisms involved in MDR whose identification has generated valuable information on how to circumvent MDR and improve chemotherapy treatment.

One of the most important known mechanism is the overexpression of ATP-binding cassette (ABC) transporters, commonly known as drug efflux pumps, such as P-glycoprotein (P-gp) [2], which is frequently overexpressed in cancer [3]. P-gp transports drug-substrates across the cell membrane, thus decreasing their intracellular concentrations to sub-lethal [4].

Several studies pointed to a relation between MDR and alterations in cellular metabolism: i) upregulation of hypoxia-induced factor 1 (HIF-1) was shown to be associated with chemoresistance [5]; ii) leukaemia models with higher glycolytic rates were resistant to glucocorticoids [6]; iii) modulation of cellular metabolic pathways was demonstrated to contribute to acquired resistance in multiple myeloma cells [7]; iv) glycolytic pyruvate was capable of regulating P-gp expression in multicellular tumour spheroids [8]; and v) hypoxia was shown to induceMDR and glycolysis in an orthotopic MDR tumour model in nude mice [9]. Ultimatelly, these studies may contribute to understanding how MDR could be circumvented by application of specific metabolic modulators and inhibitors. Therefore, it is important to identify metabolic alterations in MDR cancer cells, which could lead to the identification of new metabolic molecular targets to circumvent MDR in cancer.

The formation of Extracellular vesicles (EVs) and their release have been implicated in pathological processes such as cancer [10-12] and shown to be relevant for the intercellular transfer of a drug-resistant phenotype [12-14]. Indeed, drug-sensitive cancer cells can become drug-resistant following intracellular incorporation of EVs shed by drug-resistant cancer cells [13-16]. We have previously shown that the EVs population shed by MDR cells is different from the one shed by drug-sensitive counterpart cells, thus suggesting that MDR cells produce more microvesicles and less exosomes than their drug-sensitive counterpart cells [17]. In addition, several studies have stated that metabolic alterations in cancer cells could induce alterations in the EVs' cargo and its release [18-20]. So far, it is unclear if these metabolic alterations are caused by or could be responsible for the MDR phenotype.

Here we provide evidence that MDR cancer cell lines (overexpressing P-gp) acquired a different metabolic profile from their drug-sensitive counterpart cells and that the

EVs released by MDR cells caused a metabolic switch towards the MDR phenotype in the recipient cells.

Results

Protein profiling and bioinformatics analysis of MDR and drug-sensitive counterpart cell lines identified differentially expressed proteins (DEPs)

For protein profiling, each of the four biological replicates of each condition was run by LC–MS. The data was transferred to *Progenesis QI* for proteomics to compare drug-sensitive cancer cells (K562 and NCI-H460) with their MDR counterparts (K562Dox and NCI-H460/R). Individual comparisons were carried out for each pair of cell lines: K562 *versus* K562Dox and NCI-H460 *versus* NCI-H460/R. Following Progenesis LC–MS analysis, peptide features with ANOVA<0.05 and 1+, 2+ and 3+ charge states were subjected to MASCOT database searching. The MASCOT mgf files were then resubmitted to the Progenesis software to yield a list of identified proteins. These lists were further interrogated to exclude proteins with less than 2 peptides matched, a fold change <1.5 and not statistically significant.

A total of 91 significant ($p < 0.05$) differentially expressed proteins (DEPs) were identified when comparing the K562 *vs.* K562Dox cells and 67 significant DEPs ($p < 0.05$) were identified when comparing the NCI-H460 *vs.* NCI-H460/R cells. A full list of the DEPs identified for each cell line is available in the Supplementary Information (Tables S1 and S2).

Gene Ontology (GO) bioinformatics analysis indicated that the greatest difference between MDR cells and their drug-sensitive counterparts occurred in metabolic processes

Using the *Database for Annotation, Visualization and Integrated Discovery (DAVID)* network analysis tool, the molecular functions/localizations of the DEPs data sets were analyzed according to GO functional annotations and categories. GO analysis of cellular components, molecular functions and biological processes were performed on the 91 DEPs (K562 *vs.* K562Dox) and 67 DEPs (NCI-H460 *vs.* NCI-H460/R) identified with the *Progenesis* software. Pie diagrams represent the GO analysis of the identified DEPs (Fig. 1). The GO analysis revealed that most of the DEPs (for both cancer cell models) have cytoplasmic origin (42% in K562 *vs.* K562Dox and 44% in NCI-H460 *vs.* NCI-H460/R), cytoskeleton origin (17% for both models) and membrane localization (6% in K562 *vs.*

K562Dox and 5% in NCI-H460 *vs.* NCI-H460/R) (Fig.1A). The functional classification of these proteins from both cancer cell models implied that they are mostly involved in catalytic activities, structure molecule activities and protein binding activities (Fig.1B). Noteworthy, analysis of the biological processes indicated that the greatest difference between the MDR cells and their drug-sensitive counterparts occurred in metabolic processes (50% in K562 *vs.* K562Dox and 63% in NCI-H460 *vs.* NCI-H460/R) (Fig.1C). The remaining different biological processes were associated with transport, development processes and cell organization and biogenesis.

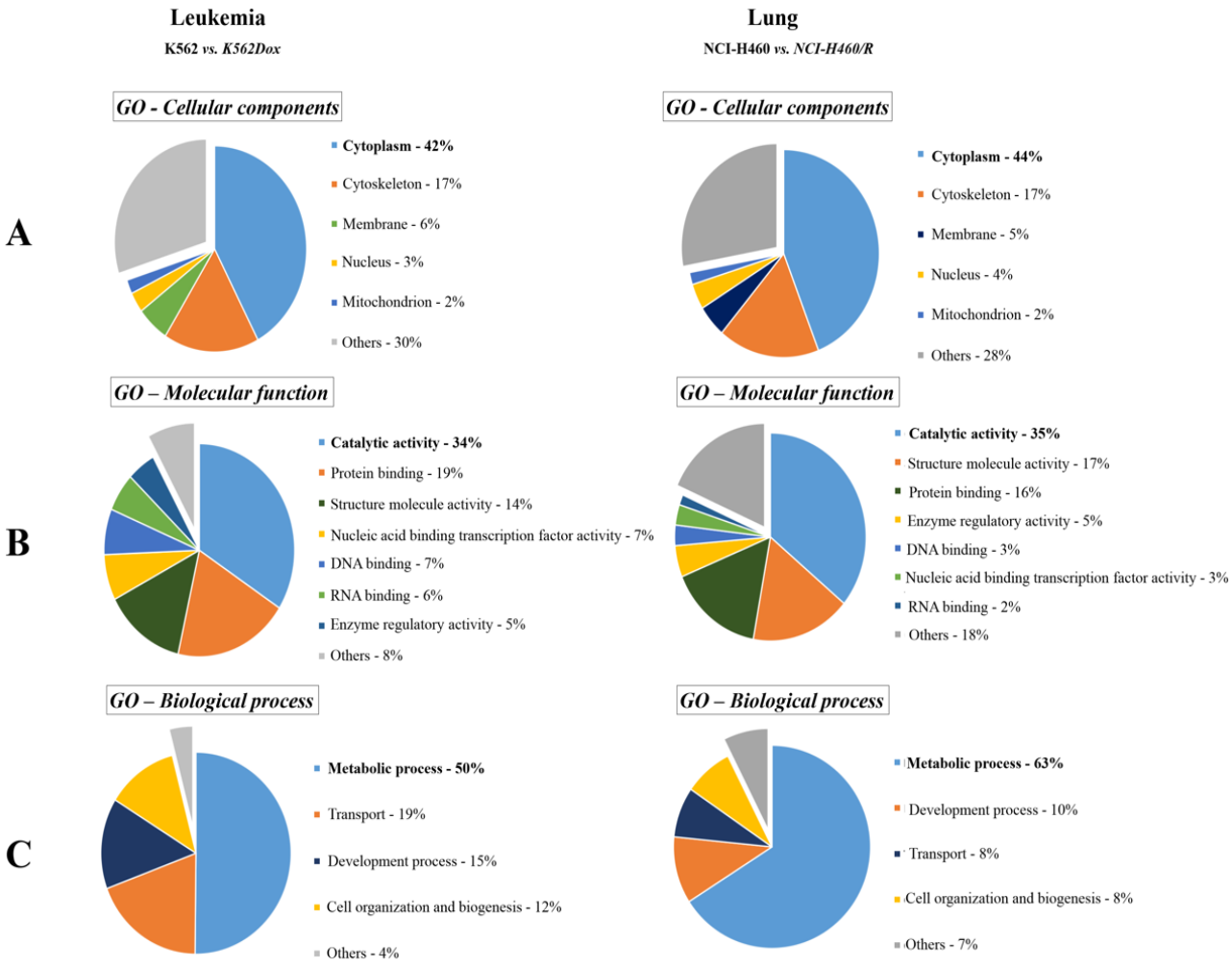

Figure 1 – GO analysis of all the differentially expressed proteins (DEPs) identified with the *Progenesis QI* software in both pairs of counterpart drug-sensitive and MDR cancer cell lines: K562 *versus* K562Dox and NCI-H460 *versus* NCI-H460/R. A) GO - Cellular component analysis of the identified proteins; B) GO - Molecular functional analysis of the identified proteins; and C) GO - Biological process analysis of the identified proteins.

KEGG pathway enrichment analysis indicated that the most significant active pathways enriched in the MDR cells were involved in metabolic processes

Following the identification of the DEPs, the most significant active pathways were analysed using KEGG pathway enrichment analysis. Results indicated that the most significantly active pathways enriched in the MDR cells were those involved in metabolic processes. The glutathione metabolism (GSH), pentose phosphate pathway (PPP) and glycolysis were found to be the most enriched pathways identified in both cancer cell models (Table 1). In the chronic myeloid leukaemia model (K562Dox) the following 4 DEPs were found to be involved in the GSH metabolism pathway (G6PD, PRDX2, IDH1 and 6PGD), 3 DEPs in the PPP pathway (G6PD, ALDOC and 6PGD) and 2 DEPs in the glycolysis pathway (ALDOC and PKM2). In the non-small cell lung cancer model the following 5 DEPs were found to be involved in the GSH metabolism pathway (G6PD, PRDX2, IDH1, MGST1 and 6PGD), 4 DEPs in the PPP pathway (G6PD, TALDO1, TKT and 6PGD) and 1 DEP involved in the glycolysis pathway (ALDH3A1) (Table 1).

Table 1 | Metabolic pathways found enriched with DEPs in MDR cells

	Term	Count [a]	ANOVA (P)	Genes Symbol
K562 *vs.* K562Dox	Glutathione metabolism	4	0.0086	G6PD, PRDX2, IDH1, 6PGD
	Pentose phosphate pathway	3	0.0025	G6PD, ALDOC, 6PGD
	Glycolysis	2	0.01	ALDOC, PKM2
NCI-H460 *vs.* NCI-H460/R	Glutathione metabolism	5	0.00064	G6PD, 6PGD. IDH1, MGST1, PRDX2
	Pentose phosphate pathway	4	0.00099	G6PD, 6PGD, TKT, TALDO1
	Glycolysis	1	nd	ALDH3A1

Results were analyzed with DAVID software for KEGG pathway enrichment
[a] Number of proteins involved in each pathway
nd – no data

Other DEPs involved in MDR and metabolic processes were identified by bioinformatics analysis

In addition to the DEPs referred above (Table 1) other DEPs also involved in metabolic process and MDR were analyzed in terms of normalized abundance between MDR and drug-sensitive counterpart cells (for both cancer cell models) (Table 2).

The DEP with the highest fold change was P-gp, which was upregulated in both MDR cells with a fold change of 18.8 for K562Dox *vs.* K562 and 64.5 for NCI-H460/R *vs.* NCI-H460. In terms of metabolic processes, most of the DEPs involved in the

PPP pathway were downregulated in the two MDR models (ALDOC, G6PD, 6PGD and TKT) and only TALDO1 was upregulated in the NCI-H460/R cells (Table 2). Regarding GSH metabolism, the enzymes responsible for the $NADP^+$ reduction to NADPH (G6PD, 6PGD and IDH1) were downregulated in the MDR cells but MGST1 was upregulated in NCI-H460/R cells. Regarding glycolysis, ALDOC was downregulated in MDR cells but the enzyme responsible for the pyruvate production (PKM2) was upregulated. Additionally, DEPs involved in the TCA cycle were also identified (ACLY and ACO2). ACLY was upregulated whereas ACO2 was downregulated in the MDR cancer cell models (Table 2).

Interestingly HIOU1 and NDRG1 (both involved in cellular response to hypoxia) and MTHFD1 (an enzyme involved in the methionine pathway) were upregulated in the MDR cells (Table 2).

Table 2 | DEPs involved in MDR and metabolic processes

		UniProt accession no.	Protein description	Gene Symbol	Peptides	Mascot Score	ANOVA (P)	Fold Change [a]
K562 *vs.* K562Dox	***Increased in MDR cells***	P08183	P-glycoprotein	MDR1	6	404.08	1.24e-009	18.80
		Q9Y4L1	Hypoxia up-regulated protein 1	HYOU1	4	282.01	3.19e-005	2.05
		Q92597	Protein NDRG1	NDRG1	2	118.12	4.32e-006	1.84
		P53396	ATP-citrate synthase	ACLY	5	289.70	7.19e-006	1.84
		P14618	Pyruvate kinase	PKM2	10	706,77	4,25E-03	1.52
		P11586	C-1-tetrahydrofolate synthase	MTHFD1	2	97,89	9,83E-04	1.51
	Decreased in MDR cells	P09972	Fructose-bisphosphate aldolase C	ALDOC	7	550.98	0.01	0.66
		P52209	6-phosphogluconate dehydrogenase	6PGD	2	111,38	2,84E-03	0.65
		O75874	Isocitrate dehydrogenase	IDH1	3	218,56	2,63E-05	0.65
		P32119	Peroxiredoxin-2	PRDX2	5	372.45	1.35e-003	0.60
		P11413	Glucose-6-phosphate 1-dehydrogenase	G6PD	4	250.70	7.79e-007	0.39
NCI-H460 vs. NCI-H460/R	***Increased in MDR cells***	P08183	Multidrug resistance protein 1	MDR1	2	175.04	9.14E-06	64.52
		P10620	Microsomal glutathione S-transferase 1	MGST1	2	105,19	1.33e-004	1.80
		P37837	Transaldolase	TALDO1	2	116.98	4.64e-004	1.53
	Decreased in MDR cells	O75874	Isocitrate dehydrogenase	IDH1	4	327.28	7.79E-05	0.66
		Q99798	Aconitate hydratase, mitochondrial	ACO2	2	132,35	2.38e-003	0.63
		P29401	Transketolase	TKT	8	489.12	7.25e-005	0.60
		P52209	6-phosphogluconate dehydrogenase	6PGD	7	570.89	3.89E-06	0.54
		P32119	Peroxiredoxin-2	PRDX2	2	133.35	0.02	0.52
		P11413	Glucose-6-phosphate 1-dehydrogenase	G6PD	13	1012.1	1.22E-06	0.41
		P30838	Aldehyde dehydrogenase	ALDH3A1	6	352,67	1.74e-005	0.40

[a]MDR cells/ Drug-sensitive cells

Results obtained by quantitative label-free proteomic approach were validated by Western blot

The expression of P-gp, G6PD, 6PGD and IDH1 were further validated by Western blot. We focused the validation on DEPs involved in MDR, glutathione metabolism and pentose phosphate pathway. Consistent with the results obtained with the proteomic analysis, P-gp was found upregulated while G6PD, 6PGD and IDH1 were downregulated in the MDR cells (K562Dox and NCI-H460/R) when compared with their drug-sensitive counterpart cells (K562 and NCI-H460) (Fig.2).

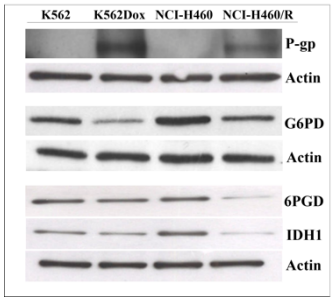

Figure 2 – Validation by Western blot analysis of some DEPs initially identified by quantitative proteomics. Representative blots were chosen from three independent experiments. Actin was used as a loading control.

MDR cells presented higher levels of reduced glutathione (GSH) and lower levels of reactive oxygen species (ROS)

Since most of the proteins that had been identified as DEPs in MDR cells were related to metabolic processes such as GSH metabolism and PPP, the GSH (one of the main detoxification agents in the cell) and ROS levels were analyzed in both tumour models.

MDR cells (K562Dox and NCI-H460/R) presented significantly higher levels of GSH when compared to their drug-sensitive counterpart cells (K562 and NCI-H460) (Fig. 3A, B). In agreement with this higher capacity provided by the higher levels of GSH to respond to oxidative stress, MDR cells presented lower levels of ROS when compared to their drug-sensitive counterpart cells (Fig. 3 C, D).

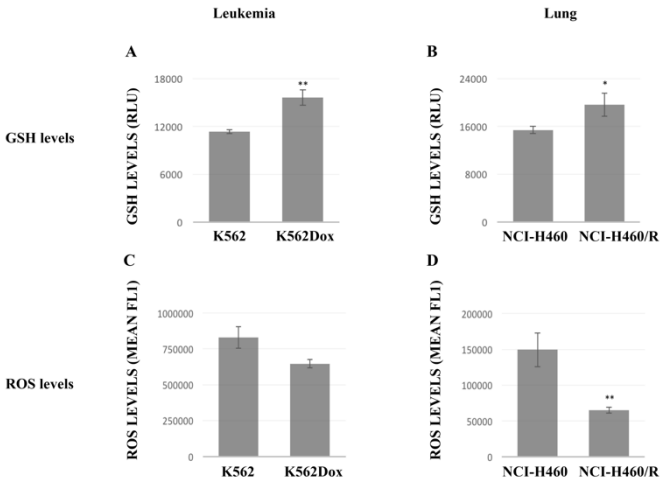

Figure 3 – Comparison of GSH and ROS levels between drug-sensitive and MDR cancer cell lines. A) GSH levels in K562 and K562Dox cells. **B)** GSH levels in NCI-H460 and NCI-H460/R cells. GSH levels are represented as Relative Luminescence Units (RLU). **C)** ROS levels in K562 and K562Dox cells. **D)** ROS levels in NCI-H460 and NCI-H460/R cells. The ROS levels are represented as mean fluorescence. Staurosporine was used as a positive control. Results are the mean ± SEM of 3 independent experiments. * $p \leq 0.05$ and ** $p \leq 0.01$.

Changes in methionine/S-adenosylmethionine pathway were identified in the MDR cancer cells

As we found GSH significantly increased in MDR cells, we were also interested in studying the metabolic pathways involved in the biosynthesis of GSH. The main cellular pathway that generates precursor for the synthesis of GSH corresponds to the methionine/S-adenosylmethionine (SAMe) pathway. By UPLC-MS metabolomics [21] we have quantified metabolites belonging to this pathway in the MDR and their drug-sensitive counterpart cells (Table 3 and Table S3). Methionine was upregulated in both MDR cancer cells. On the contrary, S-adenosylhomocysteine (SAH) and spermidine were downregulated in both MDR cancer cell lines (K562Dox and NCI-H460/R) (Table 3). In addition, no alterations in S-adenosylmethionine (SAMe) were found in both cancer cell models (Table 3). Some other metabolites were found altered (such as 5´-deoxy-5´-methylthioadenosine (MTA, dcSAMe, Betaine, Choline and Serine) but in different manners between the two cancer models.

Furthermore, the methylation index (SAMe/SAH), which represents the methylation capacity of the cells, was higher in MDR cells. In the chronic myeloid leukaemia model, K562 cells had a methylation index of 6.97, whereas the methylation index for K562Dox cells was 12.05. In the non-small cell lung cancer model, NCI-H460 cells had a methylation index of 2.43 whereas the methylation index for NCI-H460/R cells was 9.79.

Table 3 | Semi-quantitative analysis of metabolites of the methionine/ SAMe pathway in two pairs of MDR and their drug-sensitive counterpart cell lines

	Metabolite description	Fold change [a]	ANOVA (P)
K562 *vs.* K562Dox	Methionine	1.54	2,25E-05
	5´-deoxy-5´-methylthioadenosine (MTA)	1.44	8,37E-04
	S-adenosylhomocysteine (SAH)	0.57	7,67E-06
	S-adenosylmethionine (SAMe)	0.99	8,49E-01
	Spermidine	0.85	3,68E-03
	Betaine	1.02	4,79E-01
	Choline	0.63	3,48E-06
	Decarboxylated S-adenosyl methionine (dc-SAMe)	1.42	4,72E-05
	Serine	0.50	0
	Threonine	0.99	8,59E-01
NCI-H460 vs. NCI-H460/R	Methionine	1.91	3,55E-05
	5´-deoxy-5´-methylthioadenosine (MTA)	1.13	1,44E-01
	S-adenosylhomocysteine (SAH)	0.25	2,42E-05
	S-adenosylmethionine (SAMe)	0.99	7,85E-01
	Spermidine	0.81	1,33E-02
	Betaine	1.71	2,78E-04
	Choline	5.94	2,54E-07
	Decarboxylated S-adenosyl methionine (dc-SAMe)	0.50	1,79E-04
	Serine	1.04	1,78E-01
	Threonine	0.99	8,15E-01

[a] MDR cells / drug-sensitive cells

MDR cells (NCI-H460/R) showed an increase in the non-glycolytic acidification, glycolysis, glycolytic capacity and glycolytic reserve

In order to gain new insights into the metabolic phenotype of MDR cells, the extracellular acidification rate (ECAR), which reflects the rate of glycolysis, and the oxygen consumption rate (OCR), which reflects the rate of oxidative phosphorylation (OXPHOS), were measured in both MDR and sensitive cancer cell cells. Measurements were performed

in both, basal cellular state and after treatments with compounds capable of modulating glycolysis and OXPHOS.

To analyze the glycolytic function, a glycolysis stress test was performed. The ECAR was measured in cells treated sequentially with: their glucose-free assay media as a control (Fig. 4A, blue line A); then with glucose to allow the cells to enter into glycolysis (Fig. 4A, blue line B); next with olygomycin (an ATP coupler) in order to inhibit ATP synthesis by blocking the proton channel and shifting the energy production to glycolysis (Fig. 4A, blue line C); and finally with 2-deoxyglucose (2-DG) which is a glucose analog that inhibits glycolysis through competitive binding to glucose hexokinase (Fig. 4A, blue line D). The resulting data allowed calculating the following parameters: Non-glycolytic acidification (= last rate measurement prior to glucose injection); Glycolysis (= maximum rate measurement before oligomycin injection – last rate measurement before glucose injection); Glycolytic capacity (= maximum rate measurement after oligomycin injection – last rate measurement before glucose injection); Glycolytic reserve (= glycolytic capacity – glycolysis).

In terms of glycolytic function, the MDR cells (NCI-H460/R) showed a statistically significant increase in the non-glycolytic acidification, glycolysis, glycolytic capacity and glycolytic reserve, when compared to their drug-sensitive counterpart cells (NCI-H460) (Fig.4 A).

To analyse the mitochondrial respiration, a mitochondrial stress test was performed. The OCR was measured during cells' treatment with: corresponding assay media (Fig. 4B, blue line A); then with olygomycin (Fig. 4B, blue line B); next with FCCP [electron transporter chain accelerator] that is an uncoupling agent which disrupts ATP synthesis leading to the collapse of the mitochondrial membrane potential and causing rapid consumption of energy and oxygen without the generation of ATP (Fig. 4B, blue line C); and finally with rotenone (complex I inhibitor) which shuts down mitochondrial respiration by preventing the transfer of electrons from complex I to coenzyme Q (Fig. 4B, blue line D). These modulators allowed to calculate the following parameters: Non-mitochondrial respiration (= minimum rate measurement after rotenone injection); Basal respiration (= last rate measurement before first injection - non-mitochondrial respiration rate); Maximal respiration (= maximum rate measurement after FCCP injection – non-mitochondrial respiration); Proton leak (= minimum rate measurement after olygomycin injection – non-mitochondrial respiration); ATP production (= last rate measurement before olygomycin injection – minimum rate measurement after olygomycin injection); Spare capacity (= maximal respiration – basal respiration).

Regarding the mitochondrial respiration, the MDR cells showed a statistically significant decrease in the non-mitochondrial respiration, basal respiration, maximal respiration, proton leak, ATP production and spare capacity (Fig.4 B).

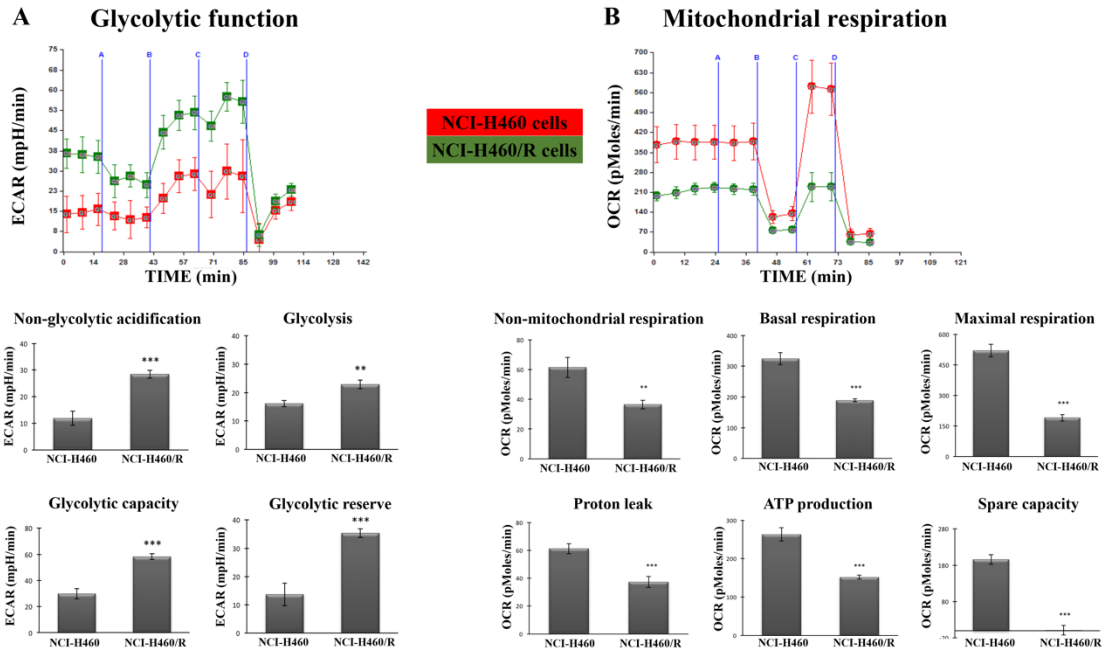

Figure 4 –Global metabolic differences between the NCI-H460 and NCI-H460/R counterpart cell lines. Cells were metabolically profiled using *Seahorse XF-24 Analyser*. **A –** Representative results of a glycolysis stress test, which measures extracellular acidification rate (ECAR) following addition of glucose-free media (blue line A), glucose (blue line B), oligomycin (blue line C) and 2-deoxyglucose (blue line D). **B -** Representative results of a mitochondrial stress test, measuring the oxygen consumption rate (OCR) in glucose-containing media, following sequential addition of media (blue line A), oligomycin (blue line B), FCCP (blue line C) and rotenone (blue line D). Results are the mean ±SEM from three independent experiments, with four to eight replicates per experiment. *$p \leq 0.05$; **$p \leq 0.01$; ***$p \leq 0.001$ of NCI- H460 *vs.* NCI-H460/R cells.

PPP inhibitor changed the metabolic phenotype of NCI-H460 cells towards the phenotype of their MDR counterparts (NCI-H460/R)

As aforementioned, sensitive cells possess more rate limiting enzymes of the PPP than their corresponding MDR cells (Tables 1 and 2 and Fig. 2). In addition, they showed a decrease in glycolytic parameters (Fig.4 A) and an increase in mitochondrial respiration (Fig. 4 B). In order to confirm that the PPP is involved in the MDR phenotype, NCI-H460 cells (drug-sensitive) were treated with a sub-lethal concentration of dichloroacetate (DCA, a PPP inhibitor) and consequent alterations in glycolysis and OXPHOS were observed. After DCA treatment, the drug-sensitive cells acquired a metabolic phenotype similar to the one observed in the MDR cells, presenting an increase in glycolysis, glycolytic capacity and glycolytic reserve, and a decrease in their basal respiration, maximal respiration and ATP production by OXPHOS (Fig. 5). The MDR cells (NCI-H460/R) treated with DCA showed no changes in glycolytic function and mitochondrial respiration (data not shown).

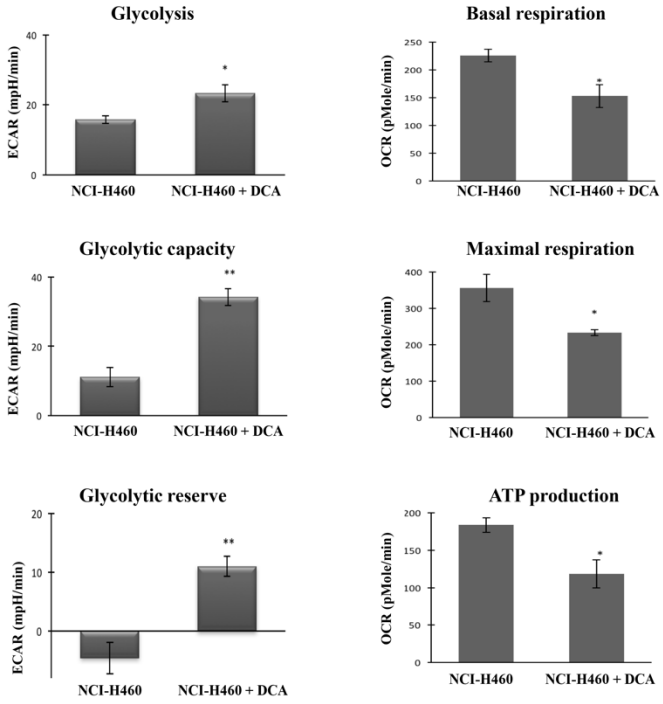

Figure 5 – Alterations in NCI-H460 cell metabolism after treatment with a PPP inhibitor. NCI-H460 cells were treated with 5 mM DCA for 24 h and subsequently metabolically profiled, using the *Seahorse XF-24 Analyser*. Data represent mean ± SEM from three independent experiments, with four replicates per experiment. *$p \leq 0.05$; **$p \leq 0.01$; NCI-H460 *vs.* NCI-H460+DCA. ECAR - extracellular acidification rate; OCR - oxygen consumption rate.

P-gp inhibitor changed the metabolic phenotype of MDR cells (NCI-H460/R) towards the phenotype of their corresponding sensitive cells (NCI-H460)

In order to confirm the possible influence of P-gp in the observed metabolic alterations of the MDR cells, the NCI-H460/R were treated with a sub-lethal concentration of a well-known P-gp inhibitor, verapamil, and the levels of glycolysis and OXPHOS were analyzed. After treatment with verapamil, the MDR cells acquired a metabolic phenotype more similar to the one observed in sensitive cells, presenting a decrease in glycolysis, glycolytic capacity, glycolytic reserve and non-glycolytic acidification, and an increase in their basal respiration (Fig. 6).

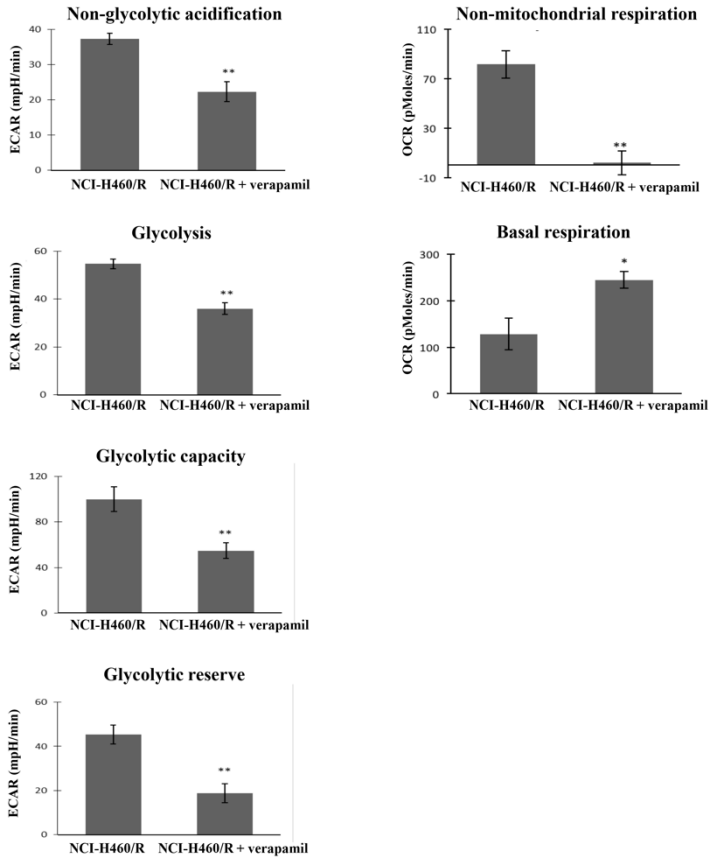

Figure 6 – Alterations in the NCI-H460/R cellular metabolism after treatment with a P-gp inhibitor. NCI-H460/R cells were treated with 2 μM verapamil for 15 h and subsequently metabolically profiled using the *Seahorse XF-24 Analyser* for measuring alterations in glycolysis, glycolytic capacity, glycolytic reserve, non-glycolytic acidification, basal respiration, maximal respiration and non-mitochondrial respiration. Data represent three independent experiments, with four replicates per experiment. *$p \leq 0.05$; **$p \leq 0.01$; NCI-H460/R *vs.* NCI-H460/R+verapamil. ECAR - extracellular acidification rate; OCR - oxygen consumption rate.

EVs from MDR cells were able to transfer their metabolic phenotype to the sensitive cells

Next, we wanted to verify if MDR phenotype could be transferred to the drug-sensitive cells via EVs shed by the MDR cells. Therefore, drug-sensitive cells (NCI-H460) were treated with EVs isolated from the counterpart pairs of non-small cell lung cancer cells (NCI-H460 and NCI-H460/R) and chronic myeloid leukaemia cells (K562 and K562Dox) (Fig. S1). After 15 h incubation, the drug-sensitive cells treated with the EVs shed by MDR cells (NCI-H460/R - Fig. 7A and K562Dox - Fig. 7B) acquired a metabolic phenotype more similar to the MDR cellular phenotype, *i.e.*, an increase in glycolysis and in glycolytic capacity.

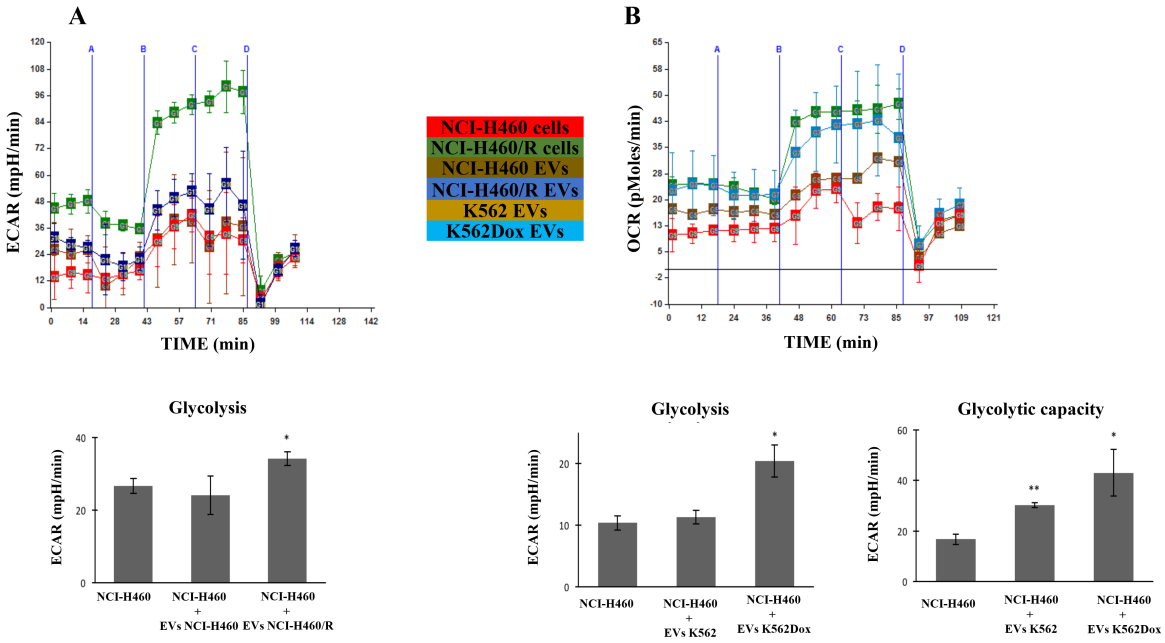

Figure 7 – Alterations observed in NCI-H460 cellular metabolism after treatment with EVs shed by MDR cells. NCI-H460 cells were treated with 18 x 10^8 EVs for 15 h and subsequently metabolically profiled using *Seahorse XF-24 Analyser*. The results of glycolysis stress test are shown as ECAR measurements after addition of glucose-free media (blue line A), glucose (blue line B), oligomycin (blue line C) and 2-deoxyglucose (blue line D). **A)** NCI-H460 cells were treated with their own EVs and with EVs isolated from NCI-H460/R cells. **B)** NCI-H460 cells were treated with EVs isolated from the pair chronic myeloid leukaemia counterpart cells, K562 and K562Dox. Data represents the results from two independent experiments, with four replicates each. A two-tailed $*p \leq 0.05$; $**p \leq 0.01$; $***p \leq 0.001$ NCI-H460 *vs.* NCI-H460+EVs NCI-H460; NCI-H460 *vs.* NCI-H460+EVs NCI-H460/R; NCI.H460 *vs.* NCI-H460+EVs K562; NCI-H460 *vs.* NCI-H460+EVs K562Dox.

Discussion

Multidrug resistance (MDR) is a major problem in cancer treatment responsible for chemotherapy failure [4]. MDR cancer cells usually have multiple mechanisms of resistance [14]. One of the most frequent MDR mechanism is the overexpression of ABC transporters, such as P-gp [2]. Recent findings pointed that altered metabolic pathways help cancer cells to proliferate, adapt their metabolism to nutrient limited conditions, and importantly develop drug resistant phenotypes [22]. Therefore, targeting cellular metabolism could chemosensitize MDR cells [9,23,24]. Understanding the metabolic adaptations of MDR cancer cells is important for the identification of new approaches to counteract this phenotype.

In the present study, we have identified a complex network of metabolic alterations associated with the MDR phenotype that could lead to the identification of more efficient therapeutic MDR circumvention strategies. In addition, we have shown that EVs released

by MDR cells are capable of stimulating a metabolic alteration (towards a MDR phenotype) in recipient drug-sensitive cancer cells.

We confirmed that comparative proteomic approach is a powerful tool to investigate MDR mechanisms in cancer cells. MDR and their corresponding drug-sensitive cell lines from two distinct models (chronic myeloid leukaemia and non-small cell lung cancer) were subjected to a label-free LC-MS quantitative proteomics. The obtained data allowed a comparison between the proteome from MDR cells and the one obtained from their drug-sensitive counterparts. In terms of biological processes, most of the identified DEPs (differentially expressed proteins between drug-sensitive and MDR cells) were involved in metabolic processes and the most active pathways enriched were those involved in cellular metabolism (GSH, PPP and Glycolysis). Therefore, we showed that the two MDR cell models acquired a similar metabolic profile but significantly distinct from the metabolic profile observed in their corresponding drug-sensitive cells.

Interestingly, most of the DEPs involved in the PPP (including the rate limiting enzyme, G6PD) were downregulated in the MDR cells. PPP is a pivotal biosynthetic pathway branched to glycolysis and one of the main antioxidant cellular defense systems [25]. PPP has a central role as a source of nucleic acid precursors and provides reducing power and ribose phosphate to the cell [26]. Changes in the PPP activity can affect response to anticancer drugs, however the specific role of PPP in MDR phenotype is still unclear. Other authors implied that PPP is more active in MDR tumours [27,28]. Moreover, evidence suggested that elevated levels of NADPH and GSH, together with an active PPP, play an important role in MDR [29,30]. Our results together with other recent studies [31,32] contradict the above mentioned reports, showing that PPP enzymes are downregulated in MDR cells. These results are controversial since one of the roles of PPP is to provide reducing power to the GSH metabolism and high levels of GSH in tumours have been linked to the development of MDR [33]. In addition, we found increased GSH levels in both MDR models, as previously published by other authors [34,35]. Moreover, since GSH is a detoxification agent [36], the levels of ROS in the MDR cells were decreased. In all, our results suggest that MDR cells are capable of maintaining high GSH levels even when PPP is downregulated. Therefore, we assumed that MDR cells upregulated another source of GSH.

The methionine cycle is a key pathway for many methylation reactions (methylation of DNA, histones and non-histone proteins, such as transcription factors) and could be the source of cysteine residues necessary for GSH synthesis [37]. Growing evidence links aberrant regulation of methylation to tumourigenesis [38]. The epigenetic mechanisms underlying drug resistance have not been fully elucidated, although some studies have suggested the contribution of an altered chromatin state to drug resistance [39]. Our results showed considerable differences between MDR and their drug-sensitive cells, in the

amount of several metabolites of the methionine/SAMe pathway. Methionine levels were significantly increased in the MDR cells, which could lead to the GSH increase observed in those cells. In addition, the methylation capacity of the cells was increased in both MDR models and this could be attributed to the metabolic alterations in MDR cells during development of their resistant phenotype. In agreement with our results, other authors have described that treatment with a methylation inhibitor reversed drug resistance indicating that the development of some cases of drug resistance could be methylation-dependent [40]. Also, MTA, dcSAMe, betaine, choline and serine are altered in MDR cells, although not in a similar manner. These differentially altered metabolites indicate that among these two MDR models there are also metabolic differences, which enhance the idea of the complex metabolism associated to MDR.

The energy dependence of drug transport in MDR cells suggests that during development of MDR, cells undergo alterations in the energy utilization pathways. The main cell energy carrier, ATP, is produced in two metabolic pathways: glycolysis and/or oxidative phosphorylation (OXPHOS) of metabolic fuels [22]. One of the fundamental hallmarks of cancer cells is the shift in the balance between these two energy-production pathways, in favor to glycolysis, known as the Warburg effect [41,42,43]. For this reason, glycolysis inhibition has attracted significant interest as a possible way to sensitize cancer cells to chemotherapy. Indeed, several studies in different cancer models have demonstrated an efficient suppression of MDR by glycolytic inhibitors [8,23,24,44,45]. Moreover, during the course of this work another study has suggested the possibility of an accelerated process of glycolysis in MDR cells to increase their energy supply [46]. To our knowledge, a comparison between MDR and drug-sensitive cells in terms of metabolic energy supply, using different modulators of glycolysis and OXPHOS, has never been performed. The results presented herein showed a statistically significant increase in glycolysis and in the glycolytic capacity of the MDR cells (NCI-H460/R), together with a decrease in the mitochondrial basal respiration and in the maximal capacity of the cells to perform OXPHOS compared to the drug-sensitive counterparts (NCI-H460). Therefore, our findings indicate that MDR cells, when acquiring the resistant phenotype, enhance their switch in the cellular energy supply pathways from OXPHOS to glycolysis. This altered metabolic activity in MDR cells could be crucial for: i) supporting uncontrolled proliferation, since glycolysis provides the intermediates necessary for biosynthetic pathways; ii) allowing the use of the most abundant extracellular nutrient (glucose) to produce abundant ATP. Even though the yield of ATP per glucose consumed is low, if the glycolytic flux is high enough, the percentage of cellular ATP produced by glycolysis can exceed the one produced by OXPHOS [47,48]. Therefore, this metabolic phenotype could be beneficial for MDR cells at both levels of bioenergetics and biosynthesis.

Although MDR cells perform less OXPHOS, the application of different OXPHOS modulators (oligomycin, FCCP and rotenone) affected more the drug-sensitive than their MDR counterpart cells. The OCR levels in the MDR cells have been less affected than the OCR levels in drug-sensitive cells. This suggests that MDR cells are more capable of sustaining the acquired metabolic phenotype in order to maintain the higher energy demand. In accordance, it was reported that the relationship between drug resistance and glycolysis may partially be due to the radical scavenging potential of the glycolytic intermediates, and the link between them and the cellular redox status [49].

Furthermore, the increase in glycolysis could be responsible for the decrease in the PPP observed in the MDR cells. Since some of the glycolysis and PPP intermediates are the same, it is possible that MDR cells are directing these intermediates mostly to glycolysis, in order to sustain the energy for the requested biosynthetic pathways. In fact, we demonstrated that when the PPP pathway was inhibited (with DCA [50]), drug-sensitive cells (NCI-H460) acquired a metabolic phenotype similar to that observed in MDR cells by increasing glycolysis and decreasing OXPHOS. These results support the hypothesis that there is a competition between glycolysis and PPP activity in the MDR phenotype.

Additionally, in multicellular tumour spheroids and in doxorubicin-resistant human breast adenocarcinoma cells, the inhibition of glycolysis raised intracellular ROS, downregulated P-gp and reverted the MDR phenotype [8,23]. In agreement with these data, our work showed that treatment of MDR cells (NCI-H460/R) with a P-gp inhibitor (verapamil) switched their metabolic phenotype to that characteristic of sensitive cells (decrease in glycolysis and an increase in OXPHOS).

Several studies have associated metabolic alterations with the shedding and cargo of EVs in different types of cells (such as increase lactate production [18], inhibition of glutamine metabolism [19] and the presence of several enzymes involved in glucose and glutamine metabolism [20]). The importance of EVs in the transfer of the MDR phenotype has been recently described [13,14,51]. Therefore, the acquisition by MDR cells of a different metabolic phenotype, could be responsible for the differences in: (i) the type of EVs population released by MDR cells; (ii) their cargo and (iii) the capacity to transfer phenotypes to receiving cells. In fact, we have recently shown that MDR cells shed a different population of EVs (more microvesicle-like EVs and less exosomes) when compared to the EVs shed by the drug-sensitive counterpart cells [17,52]. Additionally, our results showed that drug-sensitive cells (NCI-H460) co-incubated with EVs from MDR cells (NCI-H460/R and K562Dox), acquired a metabolic phenotype (increase in glycolysis) similar to the one observed in MDR cells. These results showed that, independently of the origin of the MDR cells (leukaemia or lung cancer), their EVs are capable of inducing such alterations. However, surprisingly, our results showed that the EVs from the sensitive

leukemic cell line were also capable of inducing alterations in the glycolytic capacity of the recipient drug-sensitive cells. The reason for this is unknown, but is possibly due to the exposure of cells to high levels of EVs, therefore not related to MDR. Furthermore, a recent study has described that glutamine metabolism was altered in cancer cells following incubation with large EVs (microvesicles), an effect that was not observed upon incubation with exosomes [20]. This further highlights the importance of verifying the type of EVs released by donor cells, since different EVs may transfer different phenotypes to receiving cells.

Conclusions

In conclusion, P-gp overexpressing MDR cells may employ various protective metabolic strategies to survive (schematically represented in Fig.8). These include (i) alterations in the GSH metabolism, (ii) increasing the methylation index influencing epigenetic regulation, (iii) increasing the rates of glycolysis and (iv) changing the phenotype of the surrounding drug-sensitive cells, by EVs mediated transfer of new features. Our results indicate that the development of MDR is a complex phenomenon that involves several simultaneous metabolic alterations.

We clarified for the first time the complex metabolic network of the various metabolic alterations associated with MDR in cancer cells. In addition, that MDR cancer cells are more capable than drug-sensitive cells of sustaining its specific metabolic profile. Specifically, we showed for the first time that MDR cancer cells, besides increased glycolysis also have increased glycolytic capacity and glycolytic reserve, while their OXPHOS rate is decreased. In addition, our work found differences between MDR and drug-sensitive cells in the amount of several metabolites of the methionine/SAMe pathway which regulates DNA and protein methylation, as well as GSH production. Finally, we demonstrated for the first time the transfer of metabolic information from MDR to drug-sensitive cancer cells through a specific population of EVs.

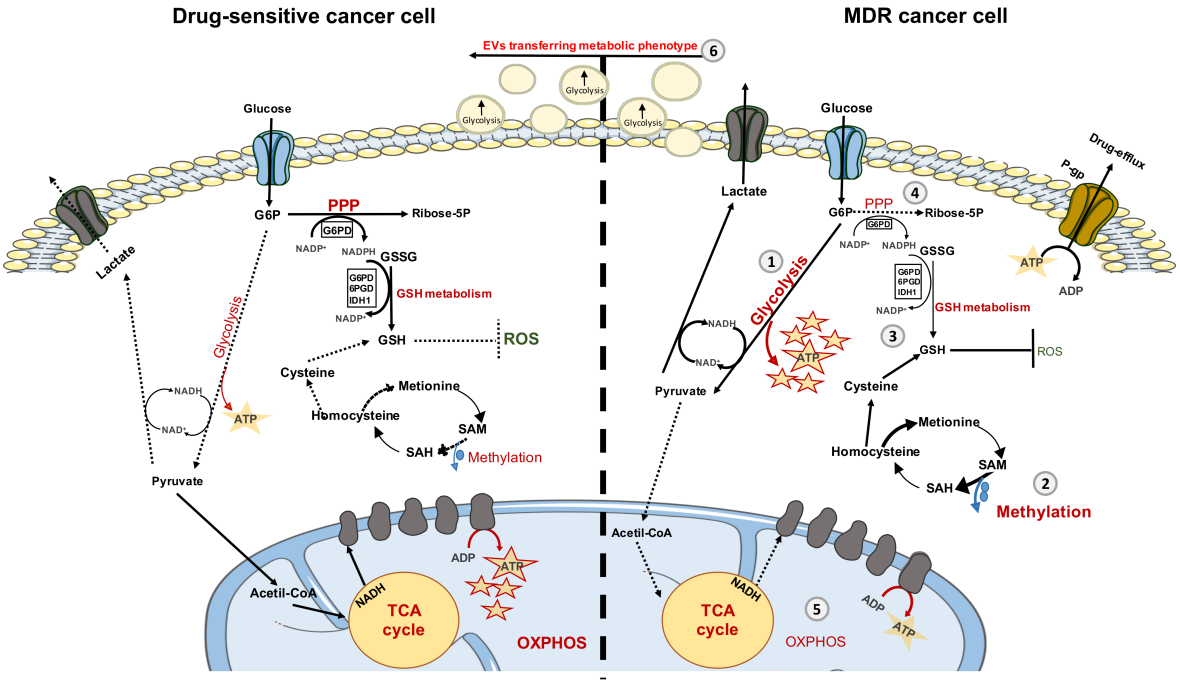

Figure 8 – Schematic representation of the observed metabolic differences between drug-sensitive cells and their counterpart MDR cells. P-gp overexpressing MDR cancer cells have various protective metabolic strategies. These include: increasing rates of glycolysis (1) and methylation capacity (2), alterations in the GSH metabolism (3), decreasing rates of PPP (4) and OXPHOS (5) and finally changing the phenotype of the surrounding drug-sensitive cells by EVs-mediated transfer of new features (6). Filled lines and arrows: increased pathways; Dashed lines and arrows: decreased pathways; Bold and bigger fonts: increased metabolic processes; Smaller fonts: decreased metabolic processes.

Materials and methods

Cell culture

The chronic myeloid leukaemia cell line K562 was from *European Collection of Cell Cultures* (ECACC) and its P-gp overexpressing counterpart cell line K562Dox was a kind gift of Dr. J.P. Marie (Paris, France) [53,54]. The non-small cell lung cancer cell line NCI-H460 and its drug-resistant P-gp overexpressing counterpart cell line NCI-H460/R were a kind gift from Dr. M. Pešić (Belgrade, Serbia) [55,56]. All cell lines were genotyped and routinely monitored for mycoplasma contamination by PCR (VenorGeM® Advance Mycoplasma Detection Kit, Minerva). All cells were routinely grown in RPMI-1640 (with Ultraglutamine I and 25mM HEPES) medium (Lonza), supplemented with 10% fetal bovine serum (FBS, PAA) at 37ºC in a humidified incubator with 5 % CO_2 in air. Cell number and viability were analyzed with trypan blue exclusion assay. All experiments were carried out with exponentially growing cells having over 90% viability.

Sample preparation and mass spectrometry using LC/MS/MS

Pellets from cells (K562, K562Dox, NCI-H460 and NCI-H460/R) were processed and 10 µg of proteins were analyzed by mass spectrometry using LC/MS/MS as previously described [17]. Biological replicates (from 4 independent experiments) were analyzed for each sample type.

Label-Free LC-MS quantitative profiling

Label-free LC–MS analysis was carried out using *Progenesis QI* for proteomics v4.1 software (NonLinear Dynamics, UK), essentially as recommended by the manufacturer (see www.nonlinear.com for further background to alignment, normalization, calculation of peptide abundance, etc.).

This software extracts quantitative information from MS1 data by aligning the data based on the LC retention time of each sample to a reference file (sample run that yielded most peptide ions); this allows for any drift in retention time, giving an adjusted retention time for all runs in the analysis.

Results were filtered, based on statistical analysis. The *Progenesis* peptide quantification algorithm calculates peptide abundance as the sum of the peak areas within its isotope boundaries. Each abundance value is then transformed to a normalized abundance value by applying a global scaling factor. Protein abundance was calculated as the sum of the abundances of all peptide ions, which have been identified as coming from the same protein. Any peptides with an ANOVA score of $p > 0.05$ were eliminated. The MS2 data for the remaining peptides was exported and the resulting MGF file used to search the NewUniProtSwissprot database (updated in January 2014) on the MASCOT server (www.matrixscience.com) for protein identifications. The search parameters used were as follows: 1) species, Homo sapiens; 2) allowed number of missed cleavages, 2; 3) fixed modification, carboxylmethyl; 4) variable modifications, methionine oxidation; 5) peptide mass tolerance ± 20 ppm; 6) MS/MS tolerance ± 0.6 Da; and 7) peptide charge + 1, +2 and +3. Only peptides with ion scores of 40 and above were considered and re-imported back into *Progenesis QI* software for further analysis. Peptide identifications were imported into the *Progenesis* software and assigned to the matching features. Protein scores were based on ANOVA values with a cut off of $p < 0.05$. Differentially expressed proteins (DEPs) between drug-sensitive and MDR cells with ≥2 peptides matched and a ≥ 1.5 fold differences in abundance were considered as significant. Peptide conflicts occur when a peptide is identified as present in more than one protein. These were resolved by assigning the peptide to the protein with the greater number of hits, a greater Mascot score or a lower mass error; when conflicts could not be clearly resolved, the peptide was excluded from the

analysis.

Bioinformatics analysis of the detected DEPs

The two data sets (DEPs from K562 *vs.* K562Dox cells and NCI-H460 *vs.* NCI-H460/R cells) were analyzed using bioinformatics methods. Database for Annotation, Visualization, and Integrated Discovery (DAVID 6.7) was used to identify protein and molecular pathway modifications. UniProt accession numbers were obtained by *Progenesis* software. To understand the high-level functions and utilization of the biological systems from molecular-level information, the *Kyoto Encyclopedia of Genes and Genomes (KEGG)* pathway was used. Distributions in subcellular locations, biological processes and molecular functions were assigned to each protein based on *Gene Ontology (GO)* categories. The significantly ($p < 0.05$) enriched categories are presented.

Analysis of Protein Expression by Western Blot

Cell pellets were lysed in Winman's Buffer (1% NP-40, 0.1 M Tris-HCl pH 8.0, 0.15 M NaCl and 5 mM EDTA) with EDTA-free protease inhibitor cocktail (Roche). Total protein content of cell lysates was quantified with "DC Protein assay kit" (Bio-Rad) and 20 µg of protein were subjected to SDS-PAGE (12% Bis-Tris gel). Following electrophoretic transfer of the proteins into nitrocellulose membranes (GE Healthcare, UK), membranes were then incubated with the following primary antibodies: goat anti-Actin (1:2000; Santa Cruz Biotechnology), mouse anti-P-gp (P7965) (1:2000; Sigma), G6PD (1:200; Santa Cruz Biotechnology), 6PGD (1:200; Santa Cruz Biotechnology) and IDH1 (1:200; Santa Cruz Biotechnology). The following secondary antibodies were then used: anti-mouse IgG-HRP; anti-rabbit IgG-HRP or anti-goat IgG-HRP (all diluted 1:2000; Santa Cruz Biotechnology). Signal was detected using the ECL Western blot Detection Reagents (GE Healthcare, UK), the Amersham Hyperfilm ECL (GE Healthcare, UK), and the Kodak GBX developer and fixer (Sigma, EUA) [57]. The intensity of the bands obtained in each film was further analyzed using the software Quantity One – 1D Analysis (Bio-Rad, USA).

GSH/GSSG-Glo™ assay

To measure GSH levels, the GSH/GSSG-Glo™ Assay (Promega, USA) was used following manufacturer's instructions. Briefly, 5000 cells/well were plated in white 96-opaque well plates. NCI-H460 and NCI-H460/R cells were plated in 100µl of RPMI-1640; K562 and K562Dox cells were plated in 20µl of Hanks Balanced Salt Solution (HBSS). Total glutathione lysis reagent or oxidized glutathione lysis reagent were added to the cells. After incubation at room temperature a luciferin generation reagent was added to all samples and the plates were incubated for 30 min at room temperature. Luminescence was quantified

using a microplate reader (Biotek Instruments Inc. Synergy MX. USA). Positive control (cells treated with 5 μM Staurosporine for 4h) and wells with no cells were also included as controls. GSH levels were calculated as follows: GSH levels=total glutathione levels – oxidized glutathione levels

ROS Detection

2′,7′-dichlorodihydrofluorescein diacetate (H2DCF-DA) analysis by flow cytometry were used to measure ROS concentration in drug-sensitive and MDR cells. K562 and K562Dox cells ($8x10^5$/well) were plated in 6-well plates; NCI-H460 and NCI-H460/R cells ($3x10^5$/well) were plated in 6-well plates at for 24h. Cells were harvested and incubated in adequate medium with 10 μM CM-H2DCFDA for 45 min at 37 ºC in the dark. Cells were subsequently washed twice in PBS and the CM-H2DCFDA fluorescence was analyzed in a BD Accuri flow cytometer (FL1-H channel). A positive control (cells treated with 1 μM Staurosporine for 6h) was also included. Mean fluorescence intensity was calculated after correction for auto-fluorescence.

Semi-quantitative analysis of metabolites of the methionine/S-adenosylmethionine pathway

Total cell pellets (4 independent preparations for each cell line) were lysed in 500 μL of a mixture of ice-cold water/metanol/10 mM acetic acid (49/50/1 v/v/v %) with a tissue homogenizer (Precellys) in 1 x 20 second cycles at 6000 rpm. Subsequently, 400 μL of the homogenate was transferred to a new aliquot and shaken at 1400 rpm for 30 minutes at 4 °C. Next the aliquots were centrifuged for 15 min at 14000 rpm at 4 °C. 75 μL of the supernatant was transferred to a fresh aliquot and placed at -80 °C for 20'. The chilled supernatants were evaporated with a speedvac in approximately 3h. The resulting pellets were resuspended in 100 μL water/acetonitrile (MeCN)/formic acid (40/60/0.1 v/v/v %, resuspension solution).

Concentrations of methionine, MTA, SAMe, SAH, spermidine and spermine were determined with a semi-quantitative method. Calibration curves for these compounds were obtained, by measuring serial dilutions of a pooled standard mixture in resuspension solution. The concentrations for all compounds in the dilutions ranged from 100 μM to 0.025 μM. For the standard mixtures, separate 10 mM stocks of the standards were made. These were then pooled and further diluted in resuspension solution in order to obtain the final concentrations as used for the calibration curve.

Samples were measured with a UPLC system (Acquity, Waters, Manchester) coupled to a Time of Flight mass spectrometer (ToF MS, SYNAPT G2, Waters). A 2.1 x 100 mm, 1.7 μm BEH amide column (Waters), thermostated at 40 °C, was used to separate the

analytes before entering the MS. Solvent A (aqueous phase) consisted of 99.5% water, 0.5% formic acid and 20 mM ammonium formate while solvent B (organic phase) consisted of 29.5% water, 70% MeCN, 0.5% formic acid and 1 mM ammonium formate.

In order to obtain a good separation of the analytes the following gradient was used: from 5% A to 50% A in 2.4 minutes in curved gradient (#8, as defined by Waters), from 50% A to 99.9% A in 0.2 minutes constant at 99.9% A for 1.2 minutes, back to 5% A in 0.2 minutes. The flow rate was 0.250 mL/min and the injection volume was 2 µL. All samples were injected randomly. After every 10 injections a QC sample was injected. All samples were injected in duplicate.

Analytes were measured in enhanced duty cycle (EDC) mode, optimized for the mass of the analyte in question. MTA was measured in scan function 1 (EDC at 298), choline was measured in scan function 2 (EDC at 104), methionine was measured in scan function 3 (EDC at 150), SAH was measured in scan function 8 (EDC at 385), SAMe was measured in scan function 10 (EDC at 399), spermidine was measured in scan function 12 (EDC at 146), spermine was measured in scan function 13 (EDC at 203). The cone voltage was between 20 and 25 depending on the analyte. A 2 ng/mL leucine-enkephalin solution in water/acetonitrile/formic acid (49.9/50/0.1 %v/v/v) was infused at 10 µL/min and used for a lock mass which was measured each 47 seconds for 0.5 seconds. Spectral peaks were automatically corrected for deviations in the lock mass.

Extracted ion traces were obtained for methionine (*m/z* = 150.0589), SAH (*m/z* = 385.1294), SAMe (*m/z* =399.1451), MTA (*m/z* =298.097), spermidine (*m/z* =146.1657) and Spermine (*m/z* =203.2236) in a 20 mDa window and subsequently smoothed (2 points, 2 iterations) and integrated with QuanLynx software (Waters, Manchester).

Extracellular flux assay using Seahorse XF-24 Analyser

ECAR, reflecting the rate of glycolysis, and OCR, reflecting the rate of OXPHOS, were measured using a *Seahorse Bioscience* (Copenhagen, Denmark) XF24 analyzer. Briefly, 2 x 10^4 cells/well for glycolysis stress test and 3 x 10^4 cells/well for mitochondrial stress test were plated in *Seahorse XF24* plates in 200 µl of RPMI-1640 and incubated for 20-24h at 37ºC in a humidified incubator with 5 % CO_2 in air and 1h hour prior to the XF assay in a humidified incubator without CO_2 with the corresponding assay media. In the experiments where the cells were treated with DCA, the treatment was performed for 24h with a concentration of 5mM. The verapamil treatment was performed for 15h with 2µM. NCI-H460/R treated with DCA and NCI-H460 treated with verapamil were used as controls.

Basal OCR measurements were made in DMEM containing 10mM sodium pyruvate (Invitrogen, California, EUA), 10 mM Glucose (Invitrogen, California, EUA) and 10mM

Glutamax (Invitrogen, California, EUA) and Basal ECAR measurements were made in DMEM without any supplementation.

Steady-state (baseline) oxygen consumption rates and extracellular acidification rates were measured. Non-glycolytic acidification, glycolysis, glycolytic capacity and glycolytic reserve were measured, through ECAR, by injecting: glucose, oligomycin and 2-deoxyglucose. Basal respiration, proton leak, spare capacity, maximal respiration, non-mitochondrial respiration and ATP production were measured, through OCR, after the sequential injection of oligomycin, FCCP and rotenone. All measurements were normalized to protein quantity with crystal violet.

Co-culture of NCI-H460 cells with EVs

EVs were isolated from the culture media of drug-sensitive or MDR cells by various centrifugation steps as previously described [17]. EVs pellets were re-suspended in 100 µl of PBS and frozen at - 80 ºC. NCI-H460 cells were treated with 18 x 10^8 EVs (quantified by nanoparticle tracking analysis as in supplementary information) for 15 hours and were subsequently metabolically profiled using *Seahorse XF-24 Analyzer*.

Statistical analysis

All presented data resulted from at least three independent experiments (excluding the EVs treatment which was performed in two independent experiments only). All data was statistically analyzed with the two-tailed unpaired Student's *t*-test. Results were considered statistically significant when $p \leq 0.05$.

Acknowledgments

This article is a result of the project NORTE-01-0145-FEDER-000029, supported by Norte Portugal Regional Programme (NORTE 2020), under the PORTUGAL 2020 Partnership Agreement, through the European Regional Development Fund (ERDF).

This work was partially financed by FEDER - Fundo Europeu de Desenvolvimento Regional funds through the COMPETE 2020 - Operacional Programme for Competitiveness and Internationalisation (POCI), Portugal 2020, and by Portuguese funds through FCT - Fundação para a Ciência e a Tecnologia/ Ministério da Ciência, Tecnologia e Inovação in the framework of the project "Institute for Research and Innovation in Health Sciences" (POCI-01-0145-FEDER-007274). Health Basque Government (2015111149 to JM-F), Ramón Areces Foundation to JM-F, Instituto de Salud Carlos III (PI12/01604 to JM-F), Spanish Ministry of Economy and Competitiveness MINECO (SAF2015-66312 to JM-F) all

of them co-financed by ERDF (FEDER) Funds from the European Commission, “A way of making Europe”.

The authors thank the Portuguese Foundation for Science and Technology (FCT) for the PhD grant of VLR (SFRH/BD/87646/2012) and for the post-doc grant of RTL (SFRH/BPD/68787/2010). The authors also acknowledge the European COST Action for supporting the European Network on Microvesicles and Exosomes in Health and Disease (ME-HaD, BM1202) and funding the short-term mission (ECOST-STSM-BM1202-180216-071544) of VR to CIC bioGUNE.

Author contributions

VLR carried out most of the laboratory work and wrote the manuscript. JM, DC and SVL helped in the metabolism-related experiments and analysis of data. ADL, PM and MH provided expertise in proteomic analysis and helped with the bioinformatics analysis of data. MP provided the lung cancer pair of cell lines, had several critical discussions with MHV and proof-read the manuscript. RTL, ROC and JMFP co-supervised some of the experiments, helped planning those experiments and proof-read the manuscript. ROC and JMFP were responsible for supervising the work that was carried out in Dublin and Bilbao, respectively, and provided necessary reagents and facilities. MHV was the main supervisor of this work and was responsible for most of the funding, conceiving the study, planning and coordinating the work and helping writing the manuscript. All authors agreed with the last version of the manuscript.

Additional Information (including a Competing Financial Interests Statement)

The authors have no conflicts of interest to declare.

Additional information

Supplementary information accompanies this paper.

References

1 Larsen, A. K., Escargueil, A. E. & Skladanowski, A. Resistance mechanisms associated with altered intracellular distribution of anticancer agents. *Pharmacol Ther* **85**, 217-229 (2000).

2 Lopes-Rodrigues, V. *et al.* The network of P-glycoprotein and microRNAs interactions. *International journal of cancer. Journal international du cancer* **135**, 253-263, doi:10.1002/ijc.28500 (2014).

3 Eckford, P. D. & Sharom, F. J. ABC efflux pump-based resistance to chemotherapy drugs. *Chem Rev* **109**, 2989-3011, doi:10.1021/cr9000226 (2009).

4 Gottesman, M. M., Fojo, T. & Bates, S. E. Multidrug resistance in cancer: role of ATP-dependent transporters. *Nature reviews. Cancer* **2**, 48-58, doi:10.1038/nrc706 (2002).

5 Semenza, G. L. HIF-1 mediates metabolic responses to intratumoural hypoxia and oncogenic mutations. *J Clin Invest* **123**, 3664-3671, doi:10.1172/JCI67230 (2013).

6 Koczula, K. M. *et al.* Metabolic plasticity in CLL: adaptation to the hypoxic niche. *Leukaemia : official journal of the Leukaemia Society of America, Leukaemia Research Fund, U.K* **30**, 65-73, doi:10.1038/leu.2015.187 (2016).

7 Zub, K. A. *et al.* Modulation of cell metabolic pathways and oxidative stress signaling contribute to acquired melphalan resistance in multiple myeloma cells. *PloS one* **10**, e0119857, doi:10.1371/journal.pone.0119857 (2015).

8 Wartenberg, M. *et al.* Glycolytic pyruvate regulates P-Glycoprotein expression in multicellular tumour spheroids via modulation of the intracellular redox state. *J Cell Biochem* **109**, 434-446, doi:10.1002/jcb.22422 (2010).

9 Milane, L., Duan, Z. & Amiji, M. Role of hypoxia and glycolysis in the development of multi-drug resistance in human tumour cells and the establishment of an orthotopic multi-drug resistant tumour model in nude mice using hypoxic pre-conditioning. *Cancer Cell Int* **11**, 3, doi:10.1186/1475-2867-11-3 (2011).

10 D'Souza-Schorey, C. & Clancy, J. W. Tumour-derived microvesicles: shedding light on novel microenvironment modulators and prospective cancer biomarkers. *Genes & development* **26**, 1287-1299, doi:10.1101/gad.192351.112 (2012).

11 Kucharzewska, P. & Belting, M. Emerging roles of extracellular vesicles in the adaptive response of tumour cells to microenvironmental stress. *J Extracell Vesicles* **2**, doi:10.3402/jev.v2i0.20304 (2013).

12 Yanez-Mo, M. *et al.* Biological properties of extracellular vesicles and their physiological functions. *Journal of extracellular vesicles* **4**, 27066, doi:10.3402/jev.v4.27066 (2015).

13 Bebawy, M. *et al.* Membrane microparticles mediate transfer of P-glycoprotein to drug sensitive cancer cells. *Leukaemia : official journal of the Leukaemia Society of America, Leukaemia Research Fund, U.K* **23**, 1643-1649, doi:10.1038/leu.2009.76 (2009).

14 Corcoran, C. *et al.* Docetaxel-resistance in prostate cancer: evaluating associated phenotypic changes and potential for resistance transfer via exosomes. *PloS one* **7**, e50999, doi:10.1371/journal.pone.0050999 (2012).

15 Pasquier, J. *et al.* Different modalities of intercellular membrane exchanges mediate cell-to-cell p-glycoprotein transfers in MCF-7 breast cancer cells. *The Journal of biological chemistry* **287**, 7374-7387, doi:10.1074/jbc.M111.312157 (2012).

16 Zhang, F. F. *et al.* Microvesicles mediate transfer of P-glycoprotein to paclitaxel-sensitive A2780 human ovarian cancer cells, conferring paclitaxel-resistance. *Eur J Pharmacol* **738**, 83-90, doi:10.1016/j.ejphar.2014.05.026 (2014).

17 Lopes-Rodrigues, V. *et al.* Multidrug resistant tumour cells shed more microvesicle-like EVs and less exosomes than their drug-sensitive counterpart cells. *Biochimica et biophysica acta* **1860**, 618-627, doi:10.1016/j.bbagen.2015.12.011 (2016).

18 Fruhbeis, C., Helmig, S., Tug, S., Simon, P. & Kramer-Albers, E. M. Physical exercise induces rapid release of small extracellular vesicles into the circulation. *J Extracell Vesicles* **4**, 28239, doi:10.3402/jev.v4.28239 (2015).

19 Santana, S. M., Antonyak, M. A., Cerione, R. A. & Kirby, B. J. Cancerous epithelial cell lines shed extracellular vesicles with a bimodal size distribution that is sensitive to glutamine inhibition. *Phys Biol* **11**, 065001, doi:10.1088/1478-3975/11/6/065001 (2014).

20 Minciacchi, V. R. *et al.* Large oncosomes contain distinct protein cargo and represent a separate functional class of tumour-derived extracellular vesicles. *Oncotarget* **6**, 11327-11341, doi:10.18632/oncotarget.3598 (2015).

21 van Liempd, S., Cabrera, D., Mato, J. M. & Falcon-Perez, J. M. A fast method for the quantitation of key metabolites of the methionine pathway in liver tissue by high-resolution mass spectrometry and hydrophilic interaction ultra-performance liquid chromatography. *Anal Bioanal Chem* **405**, 5301-5310, doi:10.1007/s00216-013-6883-4 (2013).

22 Rahman, M. & Hasan, M. R. Cancer Metabolism and Drug Resistance. *Metabolites* **5**, 571-600, doi:10.3390/metabo5040571 (2015).

23 Ma, S., Jia, R., Li, D. & Shen, B. Targeting Cellular Metabolism Chemosensitizes the Doxorubicin-Resistant Human Breast Adenocarcinoma Cells. *Biomed Res Int* **2015**, 453986, doi:10.1155/2015/453986 (2015).

24 Xu, R. H. *et al.* Inhibition of glycolysis in cancer cells: a novel strategy to overcome drug resistance associated with mitochondrial respiratory defect and hypoxia. *Cancer research* **65**, 613-621 (2005).

25 Kruger, N. J. & von Schaewen, A. The oxidative pentose phosphate pathway: structure and organisation. *Curr Opin Plant Biol* **6**, 236-246 (2003).

26 Eggleston, L. V. & Krebs, H. A. Regulation of the pentose phosphate cycle. *Biochem J* **138**, 425-435 (1974).

27 Polimeni, M. *et al.* Modulation of doxorubicin resistance by the glucose-6-phosphate dehydrogenase activity. *Biochem J* **439**, 141-149, doi:10.1042/BJ20102016 (2011).

28 Chen, Y. *et al.* Multiple myeloma acquires resistance to EGFR inhibitor via induction of pentose phosphate pathway. *Sci Rep* **5**, 9925, doi:10.1038/srep09925 (2015).

29 Estrela, J. M., Ortega, A. & Obrador, E. Glutathione in cancer biology and therapy. *Crit Rev Clin Lab Sci* **43**, 143-181, doi:10.1080/10408360500523878 (2006).

30 Meijerman, I., Beijnen, J. H. & Schellens, J. H. Combined action and regulation of phase II enzymes and multidrug resistance proteins in multidrug resistance in cancer. *Cancer treatment reviews* **34**, 505-520, doi:10.1016/j.ctrv.2008.03.002 (2008).

31 Wang, Z. *et al.* Identification of proteins responsible for adriamycin resistance in breast cancer cells using proteomics analysis. *Sci Rep* **5**, 9301, doi:10.1038/srep09301 (2015).

32 Gehrmann, M. L., Fenselau, C. & Hathout, Y. Highly altered protein expression profile in the adriamycin resistant MCF-7 cell line. *J Proteome Res* **3**, 403-409 (2004).

33 Townsend, D. M. & Tew, K. D. The role of glutathione-S-transferase in anti-cancer drug resistance. *Oncogene* **22**, 7369-7375, doi:10.1038/sj.onc.1206940 (2003).

34 Krzyzanowski, D., Bartosz, G. & Grzelak, A. Collateral sensitivity: ABCG2-overexpressing cells are more vulnerable to oxidative stress. *Free radical biology & medicine* **76**, 47-52, doi:10.1016/j.freeradbiomed.2014.07.020 (2014).

35 Tai, D. J. *et al.* Changes in intracellular redox status influence multidrug resistance in gastric adenocarcinoma cells. *Exp Ther Med* **4**, 291-296, doi:10.3892/etm.2012.591 (2012).

36 Dirven, H. A., van Ommen, B. & van Bladeren, P. J. Glutathione conjugation of alkylating cytostatic drugs with a nitrogen mustard group and the role of glutathione S-transferases. *Chem Res Toxicol* **9**, 351-360, doi:10.1021/tx950066l (1996).

37 Wang, S. T., Chen, H. W., Sheen, L. Y. & Lii, C. K. Methionine and cysteine affect glutathione level, glutathione-related enzyme activities and the expression of

glutathione S-transferase isozymes in rat hepatocytes. *J Nutr* **127**, 2135-2141 (1997).

38 Montenegro, M. F. *et al.* Targeting the epigenetic machinery of cancer cells. *Oncogene* **34**, 135-143, doi:10.1038/onc.2013.605 (2015).

39 Chen, C. C. *et al.* Changes in DNA methylation are associated with the development of drug resistance in cervical cancer cells. *Cancer Cell Int* **15**, 98, doi:10.1186/s12935-015-0248-3 (2015).

40 Onda, K. *et al.* Decitabine, a DNA methyltransferase inhibitor, reduces P-glycoprotein mRNA and protein expressions and increases drug sensitivity in drug-resistant MOLT4 and Jurkat cell lines. *Anticancer Res* **32**, 4439-4444 (2012).

41 Hanahan, D. & Weinberg, R. A. Hallmarks of cancer: the next generation. *Cell* **144**, 646-674, doi:10.1016/j.cell.2011.02.013 (2011).

42 Cairns, R. A., Harris, I. S. & Mak, T. W. Regulation of cancer cell metabolism. *Nature reviews. Cancer* **11**, 85-95, doi:10.1038/nrc2981 (2011).

43 Warburg, O. On respiratory impairment in cancer cells. *Science* **124**, 269-270 (1956).

44 Koshkin, V., Ailles, L. E., Liu, G. & Krylov, S. N. Metabolic Suppression of a Drug-Resistant Subpopulation in Cancer Spheroid Cells. *J Cell Biochem* **117**, 59-65, doi:10.1002/jcb.25247 (2016).

45 Tavares-Valente, D., Baltazar, F., Moreira, R. & Queiros, O. Cancer cell bioenergetics and pH regulation influence breast cancer cell resistance to paclitaxel and doxorubicin. *Journal of bioenergetics and biomembranes* **45**, 467-475, doi:10.1007/s10863-013-9519-7 (2013).

46 Qinghong, S. *et al.* Comparative proteomics analysis of differential proteins in respond to doxorubicin resistance in myelogenous leukaemia cell lines. *Proteome Sci* **13**, 1, doi:10.1186/s12953-014-0057-y (2015).

47 Guppy, M., Greiner, E. & Brand, K. The role of the Crabtree effect and an endogenous fuel in the energy metabolism of resting and proliferating thymocytes. *Eur J Biochem* **212**, 95-99 (1993).

48 Warburg, O. On the origin of cancer cells. *Science* **123**, 309-314 (1956).

49 Sattler, U. G., Walenta, S. & Mueller-Klieser, W. [Lactate and redox status in malignant tumours]. *Anaesthesist* **56**, 466-469, doi:10.1007/s00101-007-1164-2 (2007).

50 De Preter, G. *et al.* Inhibition of the pentose phosphate pathway by dichloroacetate unravels a missing link between aerobic glycolysis and cancer cell proliferation. *Oncotarget* **7**, 2910-2920, doi:10.18632/oncotarget.6272 (2016).

51 Sousa, D., Lima, R. T. & Vasconcelos, M. H. Intercellular Transfer of Cancer Drug Resistance Traits by Extracellular Vesicles. *Trends in molecular medicine* **21**, 595-608, doi:10.1016/j.molmed.2015.08.002 (2015).

52 Lopes-Rodrigues, V. *et al.* Data supporting the shedding of larger extracellular vesicles by multidrug resistant tumour cells. *Data Brief* **6**, 1023-1027, doi:10.1016/j.dib.2016.02.004 (2016).

53 Marie, J. P., Faussat-Suberville, A. M., Zhou, D. & Zittoun, R. Daunorubicin uptake by leukemic cells: correlations with treatment outcome and mdr1 expression. *Leukaemia : official journal of the Leukaemia Society of America, Leukaemia Research Fund, U.K* **7**, 825-831 (1993).

54 Seca, H., Lima, R. T., Guimaraes, J. E. & Helena Vasconcelos, M. Simultaneous targeting of P-gp and XIAP with siRNAs increases sensitivity of P-gp overexpressing CML cells to imatinib. *Hematology* **16**, 100-108, doi:10.1179/102453311X12940641877803 (2011).

55 Pesic, M. *et al.* Induced resistance in the human non small cell lung carcinoma (NCI-H460) cell line in vitro by anticancer drugs. *J Chemother* **18**, 66-73, doi:10.1179/joc.2006.18.1.66 (2006).

56 Podolski-Renic, A. *et al.* Molecular and cytogenetic changes in multi-drug resistant cancer cells and their influence on new compounds testing. *Cancer Chemother Pharmacol* **72**, 683-697, doi:10.1007/s00280-013-2247-1 (2013).

57 Lima, R. T., Martins, L. M., Guimaraes, J. E., Sambade, C. & Vasconcelos, M. H. Chemosensitization effects of XIAP downregulation in K562 leukaemia cells. *Journal of chemotherapy* **18**, 98-102, doi:10.1179/joc.2006.18.1.98 (2006).

Supplementary Information

Identification of the metabolic alterations associated with the multidrug resistant phenotype in cancer and their intercellular transfer mediated by extracellular vesicles

Vanessa Lopes-Rodrigues[1,2,3], Alessio Di Luca[4], Justyna Mleczko[5], Paula Meleady[4], Michael Henry[4], Milica Pesic[6], Diana Cabrera[5], Sebastiaan van Liempd[5,] Raquel T. Lima[1,2,7], Robert O'Connor[4], Juan M. Falcon-Perez[5,8], M. Helena Vasconcelos[1,2,9*]

Supplementary Material and Methods

Nanoparticle Tracking Analysis

A NanoSight LM10 system (Malvern, U.K.) equipped with a fast video capture and particle-tracking software was used to measure the rate of Brownian motion. All settings for the camera were fixed and kept constant for all measurements during the session. For each sample, at least five videos of 30–60 s with more than 200 detected tracks per video, and in at least one dilution, were taken and analyzed using the Nanoparticle Tracking Analysis software to obtain the mean, mode, median vesicle size and an estimation of the particle concentration. Results represent the mean of all videos acquired for a given sample.

Table S1 | Statistically significant DEPs identified with the progenesis software when comparing K562 cells with the K562Dox cells.

Accession	Peptides	Score	ANOVA (P)	Highest mean condition[a]	Description
P02100	12	1151.5	7,85E-10	K562	Hemoglobin subunit epsilon
P08183	6	404.08	1,24E-09	K562Dox	Multidrug resistance protein 1
Q96AE4	3	169.33	6,60E-09	K562	Far upstream element-binding protein 1
P02008	6	671.58	5,46E-08	K562	Hemoglobin subunit zeta
Q5JQC4	2	116.32	7,57E-08	K562	Cancer/testis antigen 47A
P13667	9	637.04	8,40E-08	K562Dox	Protein disulfide-isomerase
P21333	17	1078.45	9,94E-08	K562	Filamin-A
Q96GU1	3	254.71	1,43E-07	K562	P antigen family member 5
P07237	8	477.65	1,48E-07	K562Dox	Protein disulfide-isomerase
Q14315	7	448.29	1,73E-07	K562	Filamin-C
P41252	2	103.29	1,77E-07	K562Dox	Isoleucine--tRNA ligase, cytoplasmic
Q8NBS9	4	220.76	2,75E-07	K562Dox	Thioredoxin domain-containing protein 5
P69905	3	333.21	3,53E-07	K562	Hemoglobin subunit alpha
P08107	10	858.34	5,35E-07	K562	Heat shock 70 kDa protein 1A/1B
P13489	5	395.69	6,32E-07	K562	Ribonuclease inhibitor
Q8WUM4	6	340.95	6,84E-07	K562	Programmed cell death 6-interacting protein
P11413	4	250.7	7,79E-07	K562	Glucose-6-phosphate 1-dehydrogenase
P50402	2	112.04	9,19E-07	K562	Emerin
Q53FZ2	2	130.62	1,28E-06	K562Dox	Acyl-coenzyme A synthetase ACSM3, mitochondrial
Q15758	2	103.85	1,50E-06	K562	Neutral amino acid transporter B(0)
P14625	11	707.02	1,56E-06	K562Dox	Endoplasmin
P14314	6	431.33	1,65E-06	K562Dox	Glucosidase 2 subunit beta
P51659	2	133.11	1,77E-06	K562Dox	Peroxisomal multifunctional enzyme type 2
P11310	2	133.95	1,97E-06	K562	Medium-chain specific acyl-CoA dehydrogenase, mitochondrial
Q15084	6	478.14	2,15E-06	K562Dox	Protein disulfide-isomerase A6
Q9BXL5	3	203.27	2,59E-06	K562	Hemogen
P04350	4	262.01	2,87E-06	K562Dox	Tubulin beta-4A chain
O75369	4	259.91	2,95E-06	K562	Filamin-B
Q9UJZ1	4	319.38	3,22E-06	K562Dox	Stomatin-like protein 2, mitochondrial
Q9Y6G9	2	134.98	3,33E-06	K562Dox	Cytoplasmic dynein 1 light intermediate chain 1
P69892	11	1152.26	3,45E-06	K562	Hemoglobin subunit gamma-2
Q9Y2B0	2	117.53	3,65E-06	K562Dox	Protein canopy homolog 2
P30101	13	860.94	3,88E-06	K562Dox	Protein disulfide-isomerase A3
P50454	7	483.96	3,90E-06	K562Dox	Serpin H1
P11021;O95399	21	1732.04	3,96E-06	K562Dox	78 kDa glucose-regulated protein
Q92597	2	118.12	4,32E-06	K562Dox	Protein NDRG1

P21980	3	167.42	4,51E-06	K562	Protein-glutamine gamma-glutamyltransferase 2
Q02809	2	112.2	4,86E-06	K562Dox	Procollagen-lysine,2-oxoglutarate 5-dioxygenase 1
P40121	4	231.66	5,10E-06	K562Dox	Macrophage-capping protein
P04083	4	342.1	5,57E-06	K562Dox	Annexin A1
P30040	2	96.26	7,00E-06	K562Dox	Endoplasmic reticulum resident protein 29
P53396	5	289.7	7,19E-06	K562Dox	ATP-citrate synthase
O00584	2	209.89	7,98E-06	K562Dox	Ribonuclease T2
Q9BVA1	3	201.5	9,89E-06	K562Dox	Tubulin beta-2B chain
P02794	5	371.7	9,99E-06	K562	Ferritin heavy chain
Q15008	2	105.05	1,12E-05	K562	26S proteasome non-ATPase regulatory subunit 6
P23284	11	645.7	1,36E-05	K562Dox	Peptidyl-prolyl cis-trans isomerase B
P69891	12	1201.47	1,60E-05	K562	Hemoglobin subunit gamma-1
P32322	3	167.48	1,98E-05	K562Dox	Pyrroline-5-carboxylate reductase 1, mitochondrial
Q15942	2	128.16	3,04E-05	K562	Zyxin
P49915	3	168.86	3,09E-05	K562	GMP synthase [glutamine-hydrolyzing]
Q03252	2	139.3	3,19E-05	K562Dox	Lamin-B2
Q9Y4L1	4	282.01	3,19E-05	K562Dox	Hypoxia up-regulated protein 1
P27824	5	349.95	3,35E-05	K562Dox	Calnexin
P13639	10	667.85	3,53E-05	K562Dox	Elongation factor 2
Q13200	3	182.57	4,02E-05	K562	26S proteasome non-ATPase regulatory subunit 2
P49321	10	621.17	4,15E-05	K562	Nuclear autoantigenic sperm protein
P02792	3	153.53	5,15E-05	K562	Ferritin light chain
Q09666	4	241.99	5,80E-05	K562Dox	Neuroblast differentiation-associated protein AHNAK
Q92945	11	679.83	7,93E-05	K562Dox	Far upstream element-binding protein 2
Q15019	2	94.95	8,59E-05	K562	Septin-2
Q16698	2	163.1	1,15E-04	K562Dox	2,4-dienoyl-CoA reductase, mitochondrial
Q7KZF4	2	122.97	1,19E-04	K562	Staphylococcal nuclease domain-containing protein 1
Q969H8	2	128.77	1,31E-04	K562Dox	UPF0556 protein C19orf10
P27797	12	729.75	1,43E-04	K562Dox	Calreticulin
O43175	5	343.55	2,09E-04	K562Dox	D-3-phosphoglycerate dehydrogenase
Q14697	5	375.47	2,22E-04	K562Dox	Neutral alpha-glucosidase AB
P02042	2	138.28	2,63E-04	K562	Hemoglobin subunit delta
Q13162	6	410.59	3,67E-04	K562Dox	Peroxiredoxin-4
Q9Y5M8	2	135.82	3,88E-04	K562Dox	Signal recognition particle receptor subunit beta
O43852	4	262.95	5,64E-04	K562Dox	Calumenin
P51572	2	116.83	5,80E-04	K562Dox	B-cell receptor-associated protein 31
O76070	2	112.31	8,97E-04	K562Dox	Gamma-synuclein
P84095	2	122.1	1,13E-03	K562	Rho-related GTP-binding protein RhoG
P32119	5	372.45	1,35E-03	K562Dox	Peroxiredoxin-2
O43242	2	100.28	1,56E-03	K562	26S proteasome non-ATPase regulatory subunit 3
Q13838	3	145.46	1,72E-03	K562	Spliceosome RNA helicase DDX39B

P17174	2	88.59	2,79E-03	K562	Aspartate aminotransferase, cytoplasmic
P99999	3	230.82	3,20E-03	K562	Cytochrome c
P04792	4	255.67	3,45E-03	K562Dox	Heat shock protein beta-1
Q01581	5	349.64	3,58E-03	K562Dox	Hydroxymethylglutaryl-CoA synthase, cytoplasmic
P49006	3	202.04	3,83E-03	K562	MARCKS-related protein
Q9NSI8	2	92.03	3,95E-03	K562Dox	SAM domain-containing protein SAMSN-1
O95816	2	93.14	1,09E-02	K562	BAG family molecular chaperone regulator 2
Q6FI81	2	100.08	1,11E-02	K562	Anamorsin
Q9BRP8	2	135.58	1,11E-02	K562Dox	Partner of Y14 and mago
P09972	7	550.98	1,29E-02	K562	Fructose-bisphosphate aldolase C
P09429	2	95.34	1,38E-02	K562Dox	High mobility group protein B1
P51571	2	134.15	1,56E-02	K562Dox	Translocon-associated protein subunit delta
Q14103	2	133.1	1,75E-02	K562	Heterogeneous nuclear ribonucleoprotein D0
P30613	2	94.94	2,71E-02	K562	Pyruvate kinase PKLR

[a] Indicates if the protein were upregulated in K562 or K562Dox cells

Table S2 | Statistically significant DEPs identified with the *Progenesis* software when comparing NCI-H460 cells with the NCI-H460/R cells.

Accession	Peptides	Score	ANOVA (P)	Highest mean condition[a]	Description
Q13509	4	224.36	1,76E-09	NCI-H460	Tubulin beta-3 chain
P05120	7	398.27	1,24E-08	NCI-H460/R	Plasminogen activator inhibitor 2
P03956	2	147.55	3,55E-08	NCI-H460/R	Interstitial collagenase
P26447	2	120.38	6,86E-08	NCI-H460	Protein S100-A4
Q9Y2T3	4	294.37	8,20E-08	NCI-H460/R	Guanine deaminase
P14923	3	147.28	9,27E-08	NCI-H460	Junction plakoglobin
Q04828;P51857	12	945.06	1,09E-07	NCI-H460	Aldo-keto reductase family 1 member C1
Q9UHB6	4	263.19	2,31E-07	NCI-H460/R	LIM domain and actin-binding protein 1
P04350	3	189.21	3,27E-07	NCI-H460	Tubulin beta-4A chain
P42330	9	719.08	4,61E-07	NCI-H460	Aldo-keto reductase family 1 member C3
O15067	3	163.69	6,01E-07	NCI-H460	Phosphoribosylformylglycinamidine synthase
O14745	2	115.52	9,36E-07	NCI-H460	Na(+)/H(+) exchange regulatory cofactor NHE-RF1
P29966	5	351.65	1,02E-06	NCI-H460/R	Myristoylated alanine-rich C-kinase substrate
P42704	8	429.18	1,15E-06	NCI-H460	Leucine-rich PPR motif-containing protein, mitochondrial
Q15942	5	289.61	1,20E-06	NCI-H460/R	Zyxin
P11413	13	1012.11	1,22E-06	NCI-H460	Glucose-6-phosphate 1-dehydrogenase
Q96C19	2	139.32	1,34E-06	NCI-H460	EF-hand domain-containing protein D2
P30043	3	158.45	1,42E-06	NCI-H460	Flavin reductase (NADPH)
O95994	6	421.56	2,01E-06	NCI-H460/R	Anterior gradient protein 2 homolog
P18206	9	557.89	2,95E-06	NCI-H460	Vinculin
Q16799	2	118.69	3,10E-06	NCI-H460	Reticulon-1
P52209	7	570.89	3,89E-06	NCI-H460	6-phosphogluconate dehydrogenase, decarboxylating
P17812	3	149.08	3,93E-06	NCI-H460/R	CTP synthase 1
O43795	2	91.81	4,41E-06	NCI-H460/R	Unconventional myosin-Ib
O60271	3	164.13	4,72E-06	NCI-H460/R	C-Jun-amino-terminal kinase-interacting protein 4
P08107;P17066	14	1029.09	5,69E-06	NCI-H460/R	Heat shock 70 kDa protein 1A/1B
O75369	21	1372.59	5,73E-06	NCI-H460	Filamin-B
O95831	3	192.79	6,91E-06	NCI-H460	Apoptosis-inducing factor 1, mitochondrial
P08183	2	175.04	9,14E-06	NCI-H460/R	Multidrug resistance protein 1
Q16643	3	252.38	1,32E-05	NCI-H460/R	Drebrin
P20810	2	130.59	1,43E-05	NCI-H460	Calpastatin
Q96B97	2	153.1	1,48E-05	NCI-H460/R	SH3 domain-containing kinase-binding protein 1
Q92598	4	219.52	1,62E-05	NCI-H460/R	Heat shock protein 105 kDa
Q13501	7	676	1,65E-05	NCI-H460/R	Sequestosome-1
P30838	6	352.67	1,74E-05	NCI-H460	Aldehyde dehydrogenase, dimeric NADP-preferring
P52597	2	142.8	2,35E-05	NCI-H460	Heterogeneous nuclear ribonucleoprotein F

P11717	2	120.61	2,56E-05	NCI-H460	Cation-independent mannose-6-phosphate receptor
P43490	4	203.87	4,30E-05	NCI-H460	Nicotinamide phosphoribosyltransferase
P04181	2	148.51	6,00E-05	NCI-H460	Ornithine aminotransferase, mitochondrial
P29401	8	489.12	7,25E-05	NCI-H460	Transketolase
O75874	4	327.28	7,79E-05	NCI-H460	Isocitrate dehydrogenase [NADP] cytoplasmic
Q70E73	3	151.34	8,46E-05	NCI-H460/R	Ras-associated and pleckstrin homology domains-containing protein 1
P55795	3	183.51	8,62E-05	NCI-H460	Heterogeneous nuclear ribonucleoprotein H2
Q9UBR2	2	95.6	1,18E-04	NCI-H460	Cathepsin Z
Q13557	2	121.31	1,24E-04	NCI-H460/R	Calcium/calmodulin-dependent protein kinase type II subunit delta
P10620	2	105.19	1,33E-04	NCI-H460/R	Microsomal glutathione S-transferase 1
P46821	4	277.49	1,51E-04	NCI-H460	Microtubule-associated protein 1B
P00492	2	135.13	1,92E-04	NCI-H460	Hypoxanthine-guanine phosphoribosyltransferase
Q96HC4	4	285.33	1,99E-04	NCI-H460	PDZ and LIM domain protein 5
Q8TAT6	2	88.72	2,07E-04	NCI-H460/R	Nuclear protein localization protein 4 homolog
Q9Y2B0	2	137.58	2,36E-04	NCI-H460	Protein canopy homolog 2
Q92804	2	156.39	3,07E-04	NCI-H460	TATA-binding protein-associated factor 2N
P12277	3	178.13	3,26E-04	NCI-H460	Creatine kinase B-type
P45880	3	215.06	4,38E-04	NCI-H460	Voltage-dependent anion-selective channel protein 2
P37837	2	116.98	4,64E-04	NCI-H460/R	Transaldolase
P13797;Q14651	3	184.99	4,83E-04	NCI-H460	Plastin-3
P21291	4	320.55	5,15E-04	NCI-H460	Cysteine and glycine-rich protein 1
O43175	5	345.57	7,53E-04	NCI-H460	D-3-phosphoglycerate dehydrogenase
P46940	7	407.01	2,20E-03	NCI-H460/R	Ras GTPase-activating-like protein IQGAP1
Q99798	2	132.35	2,38E-03	NCI-H460	Aconitate hydratase, mitochondrial
Q9ULV4	2	105.68	4,90E-03	NCI-H460/R	Coronin-1C
P78527	2	142.87	9,44E-03	NCI-H460/R	DNA-dependent protein kinase catalytic subunit
P22392	6	298.01	1,02E-02	NCI-H460/R	Nucleoside diphosphate kinase B
P31689	2	100.79	1,81E-02	NCI-H460/R	DnaJ homolog subfamily A member 1
P32119	2	133.35	1,83E-02	NCI-H460	Peroxiredoxin-2
P05141	4	265.29	2,35E-02	NCI-H460	ADP/ATP translocase 2
P31949	3	185.3	2,80E-02	NCI-H460	Protein S100-A11

[a] Indicates if the protein were upregulated in NCI-NCI-H460 or NCI-NCI-H460/R cells

Table S3 | Intensity and Amount of the Metabolites associated with the methionine/ S-adenosylmethionine pathway.

	Metabolite description	drug-sensitive cells	MDR cells
K562 *vs.* K562Dox	Methionine *	246.2 ± 3.0	378.2 ± 3.6
	5´-deoxy-5´-methylthioadenosine (MTA) *	6.8 ± 0.4	9.8 ± 0.3
	S-adenosylhomocysteine (SAH) *	37.5 ± 0.4	21.5 ± 0.5
	S-adenosylmethionine (SAMe) *	261.2 ± 3.8	259.1 ± 8.7
	Spermidine *	1906.8 ± 25.9	1611.9 ± 40.8
	Betaine **	2041.2 ± 27.43	2084 ± 41.96
	Choline **	13255 ± 43.57	8301 ± 113.74
	Decarboxylated S-adenosyl methionine (dc-SAMe) **	520 ± 14.08	738 ± 14.05
	Serine **	4 ± 0.00	2 ± 0.00
	Threonine **	222 ± 3.51	220 ± 8.37
NCIH460 vs. NCI-H460/R	Methionine *	473.5 ± 6.3	905.5 ± 20.4
	5´-deoxy-5´-methylthioadenosine (MTA) *	2.4 ± 0.1	2.7 ± 0.1
	S-adenosylhomocysteine (SAH) *	143.16 ± 5.2	35.1 ± 0.9
	S-adenosylmethionine (SAMe) *	347.3 ± 8.0	343.5 ± 8.2
	Spermidine *	2627.8 ± 39.1	2115.9 ± 94.8
	Betaine **	897 ± 22.89	1531 ± 34.79
	Choline **	650 ± 67.41	3859 ± 71.03
	Decarboxylated S-adenosyl methionine (dc-SAMe) **	44 ± 1.00	22 ± 0.86
	Serine **	10 ± 0.37	11 ± 0.40
	Threonine **	305 ± 7.89	302 ± 8.10

*Amount (pmol) per 1e6 cell

**Intensity (peak *Amount(pmol)per1e6cell **Intensity (peak height)/1e6cell

Figure S1

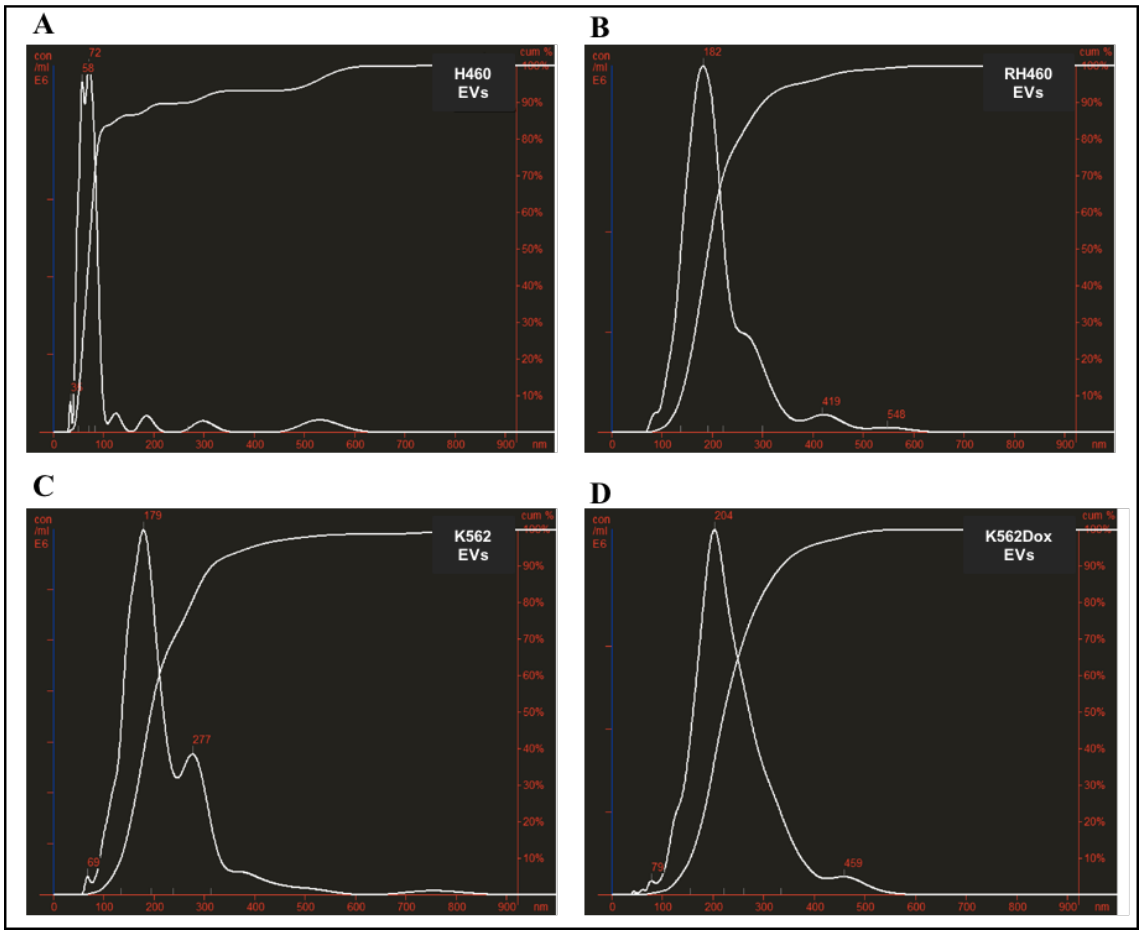

Figure S1 – Analysis of the size distribution of the EVs released from the two pairs of drug-sensitive and MDR counterpart cell lines, obtained with the Nanosight nanoparticle tracking system. **A –** EVs isolated from NCI-H460 cells. **B –** EVs isolated from NCI-H460/R cells. **C –** EVs isolated from K562 cells. **D -** EVs isolated from K562Dox cells.

2. RESEARCH ARTICLE

Multidrug resistant tumour cells shed more microvesicle-like EVs and less exosomes than their drug-sensitive counterpart cells

Vanessa Lopes-Rodrigues, Alessio Di Luca, Diana Sousa, Hugo Seca, Paula Meleady, Michael Henry, Raquel T. Lima, Robert O'Connor, M. Helena Vasconcelos

Published in Biochimica et Biophysica Acta 1860 (2016): 618–627

Biochimica et Biophysica Acta 1860 (2016) 618–627

Contents lists available at ScienceDirect

Biochimica et Biophysica Acta

journal homepage: www.elsevier.com/locate/bbagen

Multidrug resistant tumour cells shed more microvesicle-like EVs and less exosomes than their drug-sensitive counterpart cells

Vanessa Lopes-Rodrigues [a,b,c], Alessio Di Luca [d], Diana Sousa [a,b,e], Hugo Seca [a,b], Paula Meleady [d], Michael Henry [d], Raquel T. Lima [a,b,f], Robert O'Connor [d], M. Helena Vasconcelos [a,b,e,*]

[a] i3S — Instituto de Investigação e Inovação em Saúde, Universidade do Porto, Portugal
[b] Cancer Drug Resistance Group, IPATIMUP — Institute of Molecular Pathology and Immunology of the University of Porto, 4200-465 Porto, Portugal
[c] ICBAS-UP — Institute of Biomedical Sciences Abel Salazar, University of Porto, 4099-003 Porto, Portugal
[d] NICB — National Institute for Cellular Biotechnology, Dublin City University, Dublin 9, Ireland, UK
[e] Department of Biological Sciences, FFUP — Faculty of Pharmacy, University of Porto, 4050-313 Porto, Portugal
[f] Department of Pathology and Oncology, FMUP — Faculty of Medicine of the University of Porto, 4200-319 Porto, Portugal

ARTICLE INFO

Article history:
Received 25 June 2015
Received in revised form 6 November 2015
Accepted 16 December 2015
Available online 17 December 2015

Keywords:
Multidrug resistance
Tumour cells
Extracellular vesicles

ABSTRACT

Background: Multidrug resistance (MDR) is a serious impediment to cancer treatment, with overexpression of drug efflux pumps such as P-glycoprotein (P-gp) playing a significant role. In spite of being a major clinical challenge, to date there is no simple, minimally invasive and clinically validated method for diagnosis of the MDR phenotype using non-tumour biological samples. Recently, P-gp has been found in extracellular vesicles (EVs) shed by MDR cancer cells. This study aimed to compare the EVs shed by MDR cells and their drug-sensitive cellular counterparts, in order to identify biomarkers of MDR.
Methods: Two pairs of MDR and drug-sensitive counterpart tumour cell lines were studied as models. EVs were characterized in terms of size and molecular markers and their protein content was investigated by proteomic analysis and Western blot.
Results: We found that MDR cells produced more microvesicle-like EVs and less exosomes than their drug-sensitive counterpart. EVs from MDR cells contained P-gp and presented a different content of proteins known to be involved in the biogenesis of EVs, particularly in the biogenesis of exosomes.
Conclusions: The determination of the size and of this particular protein content of EVs shed by tumour cells may allow the development of a minimally-invasive simple method of detecting and predicting MDR.
General significance: This work describes for the first time that cancer multidrug resistant cells shed more microvesicle-like EVs and less exosomes than their drug-sensitive counterpart cells, carrying a specific content of proteins involved in EV biogenesis that could be further studied as biomarkers of MDR.

1. Introduction

Multidrug resistance (MDR) presents a serious challenge to the efficacious treatment of cancer. Overexpression of drug efflux pumps can be a significant cause of cancer drug resistance. MDR cells may be present in a tumour at the time of diagnosis (intrinsic resistance) or may arise following drug exposure due to drug-selective pressure (acquired resistance) [1]. Ultimately, MDR cells will survive treatment with drugs which are substrates of such drug-efflux pumps and hence through selection can come to dominate the tumour phenotype. In spite of the important clinical implications of cancer cell MDR, there are currently no clinically-available drugs to counteract the effects of these drug efflux pumps since clinical trials of putative agents have demonstrated poor efficacy. Moreover, there is no minimally-invasive means to diagnose MDR using non-tumour biological samples, which would aid the identification of a patient population that might be likely to be impacted by such inhibitors [2]. Indeed, a biomarker of MDR would aid identification of patients at greater risk of treatment failure. Ideally, any such biomarker would be easily sampled from patient's plasma, for example if it was shed by such MDR-overexpressing tumour cells.

Drug efflux pumps such as P-glycoprotein (P-gp), ABCG2 or MRP1 belong to the ATP-binding cassette (ABC) superfamily of transporters and are responsible for the increased efflux of a variety of structurally unrelated drugs [3]. P-gp is the best studied efflux pump mediating MDR. It is a 170 kDa membrane protein [4] and has been associated with drug resistance in various cancers [1,5]. Several studies, including some carried out by members of our team [6–9], have attempted to develop compounds that act as P-gp inhibitors but, so far, clinical studies have failed to demonstrate an improvement in therapeutic efficacy

* Corresponding author at: IPATIMUP, Institute of Molecular Pathology and Immunology of the University of Porto, Rua Julio Amaral de Carvalho, 45 4200-135 Porto, Portugal.
E-mail address: hvasconcelos@ipatimup.pt (M.H. Vasconcelos).

http://dx.doi.org/10.1016/j.bbagen.2015.12.011
0304-4165/

and there is no clinically approved P-gp inhibitor [6,8,10]. P-gp expression has been found to be regulated by a transient receptor potential channel 5 (TrpC5) protein [11], which is a cation channel with Ca^{2+} permeability involved in vesicular trafficking [12]. Very recently TrpC-5 has been found in the extracellular vesicles (EVs) shed by adriamycin-resistant human breast cancer cells [11]. The authors who identified this characteristic of EVs have suggested that monitoring TRPC-5 containing EVs in circulation could be used to predict drug resistance [13].

EVs are a group of vesicles which include exosomes (with endosomal origin and sizes ranging from 30 to 100 nm), microvesicles (with plasma membrane origin and sizes ranging from 50 to 2000 nm) or even apoptotic bodies (produced by cells undergoing apoptosis and sizes ranging from 50 to 5000 nm) [14]. EVs are released from all cells and are not only relevant for physiological processes (such as immune response) [15] but have also been implicated in pathological processes such as cancer [16–18] [19]. EVs are known to be shed in greater amounts by tumour cells than from normal cells [17] and have been shown to be relevant for the transfer of the drug resistant phenotype. Indeed, tumour drug-sensitive cells have been shown to become drug-resistant following incorporation of EVs shed from tumour drug-resistant cells [20–23]. In addition, EVs were shown to be involved in the intercellular transfer of functional P-gp from MDR donor cells to drug-sensitive recipient cells [20–24].

EVs transport material from the releasing cells (donor cells) such as proteins, miRNAs or even DNA [25] and may be incorporated by neighbouring cells (receiving cells), in a process resembling a paracrine effect, or may circulate in the blood and eventually be incorporated by distant (receiving) cells thereby causing systemic effects [26]. In this way, EVs may have tremendous implications in the field of biomarker discovery [25].

In this work, while studying the relevance of EVs as biomarkers of MDR, we have discovered that the EVs shed by MDR cells were bigger than the ones shed by their drug-sensitive cellular counterparts. Additionally, we have shown that the EVs from MDR cells contain P-gp and have a different content of proteins known to be involved in the biogenesis of EVs, when compared with EVs from drug-sensitive counterpart cells. In summary, our results suggest that MDR cells produce more microvesicles whereas their drug-sensitive counterparts produce more exosomes. To our knowledge, this has never been described. Additionally, we propose that the determination of the size of the EVs and of their content in these specific proteins could be further explored to detect and predict MDR phenotype.

2. Methods

2.1. Cell lines and reagents

The non-small cell lung cancer cell line NCI-H460 (named H460 in the figures for reasons of space convenience) and its drug-resistant P-gp overexpressing counterpart cell line RH460 were a kind gift of Dr. M. Pešić (Belgrade, Serbia) [27,28]. The chronic myeloid leukaemia cell line K562 was from *European Collection of Cell Cultures* (ECACC) and its P-gp overexpressing counterpart cell line K562Dox cells was a kind gift of Dr. J.P. Marie (Paris, France) [5,29]. All cell lines were genotyped. To preserve P-gp expression in the K562Dox cell line, 1 μM doxorubicin was added to the cells every 2 weeks. All experiments with the K562Dox cells were performed 6 days after doxorubicin was added to the cells, in order to maintain the same P-gp expression levels throughout the experiments. All cells were routinely grown in RPMI-1640 (with Ultraglutamine I and 25 mM HEPES) medium (Lonza) supplemented with 10% foetal bovine serum (FBS, PAA) at 37 °C in a humidified incubator with 5% CO_2 in air. Cells were routinely monitored by PCR for possible mycoplasma contamination (VenorGeM® Advance Mycoplasma Detection Kit, Minerva). Cell number and viability were analysed with trypan blue exclusion assay. All experiments were carried out with exponentially growing cells having over 90% viability. For experiments involving EVs, the following antibodies were used for Western blotting: TSG101 (4A10) (1:1000) from Gentex; Clathrin LCB (sc-28277) (1:200), Syntenin-1 (sc-100336) (1:200), Actin (sc-1616) (1:2000), cytochrome *c* (sc-13560) (1:1000), CHMP4B (sc-82556) (1:100), goat anti-rabbit IgG-HRP (Sc-2004) (1:2000), goat anti-mouse IgG-HRP (Sc-2031) (1:2000), donkey anti-goat IgG-HRP (Sc-2020) (1:2000) from Santa Cruz; P-gp (P7965) (1:2000) from Sigma and Hsp70 (EXOAB-Hsp70A-1) (1:500), CD63 (EXOAB-CD63A-1) (1:1000), CD81 (EXOAB-CD81A-1) (1:500) from SBI. The following antibodies were used for flow cytometry: cytochrome *c* (sc-13,560) (1:5), CD63 (sc-5275) (1:5), CD81 (sc-7637) (1:5) from Santa Cruz and rabbit anti-mouse FITC (F 0261) (1:20) from Dako.

2.2. Extracellular vesicle isolation

EVs were collected from equivalent amounts of EV-depleted culture medium (Fig. S3), conditioned by equivalent amounts of cells. EVs were isolated from these culture media by various centrifugation steps at 4 °C: 10 min at 500 *g* to remove cells and 10 min at 2000 *g* to remove debris (centrifuge 5810R, Eppendorf); 30 min at 10,000 *g* to remove larger vesicles and apoptotic bodies (high speed centrifuge AVANTI J-25, Beckman Coulter) and 60 min at 100,000 *g* to pellet the EVs, followed by one wash (in PBS) and another centrifugation at 100,000 *g* for 60 min to remove soluble serum and secreted proteins (Optima XE-100 Ultracentrifuge, Beckman Coulter) [30]. EV pellets were processed according to different protocols as follows.

2.3. Dynamic light scattering

The EV size/diameter was measured by dynamic light scattering (DLS), using a Nano series Malvern Zetasizer Instrument (Prager Instruments). The mean hydrodynamic diameter of exosomes was calculated by fitting a Gaussian function to the measured size distribution. Prior to the DLS measurement, each EV pellet was re-suspended in 100 μL of PBS and added to a cuvette with a 10 mm path length. DLS measurements were conducted at 20 °C, operating at 633 nm and recording the back scattered light at an angle of 173°. The sample temperature was allowed to equilibrate for 7 min before each measurement. The measurement duration was adjusted automatically with three measurements per sample. Results (from 4 independent experiments) were represented as light scattering intensity (percentage) vs. size (nm). Outliers were detected and rejected by calculation of the Dixon's *Q* ratio, using $P = 0.05$.

2.4. Transmission electron microscopy

EVs were re-suspended in PBS, deposited onto Formvar-carbon coated electron microscopy grids and maintained in the dark at room temperature for 2 min to allow the membranes to adsorb. EVs were then stained with 5% uranyl acetate. EVs were visualized in a JEM 1400 transmission electron microscope at an accelerating voltage of 80 kV (Jeol). Digital images were obtained using Orius 1100 W (Gatan). Images of at least 200 EVs (per sample, from 3 independent experiments) were taken and ImageJ software was used to determine particle size. Microsoft's Excel software was used to analyse data and create particle size distribution histograms.

2.5. Western blotting

EVs or the corresponding donor cells were washed in PBS and then re-suspended in Winman's buffer (1% NP-40, 0.1 M Tris–HCl pH 8.0, 0.15 M NaCl, and 5 mM EDTA) with EDTA-free protease inhibitor cocktail (Roche), and quantified using a modified Lowry assay (Bio-Rad). After quantification, proteins (5–8 μg in the case of EVs and 20–40 μg in the case of cells) were separated on a 12% Bis–Tris SDS-PAGE gel loaded and transferred onto a nitrocellulose membrane (GE Healthcare). Membranes were then incubated with the previous mentioned primary antibodies. Signal was detected using the ECL Western blot Detection

Reagents (GE Healthcare), the Amersham Hyperfilm ECL (GE Healthcare), and the Kodak GBX developer and fixer (Sigma) [31]. Proteins were analysed from two or three independent experiments. The intensity of the bands obtained in each film was further analysed using the software Quantity One—1D Analysis (Bio-Rad, USA). The statistical analysis of the Western blots densitometry was carried out using the Student's t-test. Data was analysed with the unpaired test. Differences were considered statistically significant if $P \leq 0.05$ in drug-sensitive versus MDR.

2.6. Flow cytometry

EVs were re-suspended in PBS, loaded into 4-mm-diameter aldehyde/sulphate latex beads (Interfacial Dynamics, Life Technologies) and incubated overnight at 4 °C under agitation. Vesicle-coated beads were further incubated for 30 min with 100 mM glycine to block the remaining binding sites. The bead–EV complexes were washed three times in PBS with 0.5% BSA. The bead–EV complexes were incubated with the primary antibodies previous described (CD63, CD81 and cytochrome *c* — corresponding isotype control) for 30 min at 4 °C, before being washed three times in PBS with 0.5% BSA. The bead–vesicle complexes were then incubated with the secondary antibody (goat anti-mouse FITC, Dako) for 30 min at 4 °C and washed twice in PBS with 0.5% BSA [30]. Samples from the NSCLC model were analysed with a BD Accuri Flow cytometer (BD Biosciences) and samples from the CML model were analysed with the same cytometer or with the FACSCalibur (BD Biosciences) flow cytometer. The flow cytometry data (from three or four independent experiments) was analysed using the FlowJo Software (Tri Star Inc.).

2.7. Sample preparation and mass spectrometry using LC/MS/MS

Pellets from EVs were lysed in lysis buffer (7 M urea, 2 M thiourea, 30 mM Tris, 4% CHAPS). Following a clean-up step of the protein lysates using the "Ready Prep 2-D clean up kit" (Bio-Rad), protein was quantified using the "Quick Start Bradford assay" (Bio-Rad). Protein extracts from EVs (3 μg) were re-suspended in 50 mM ammonium bicarbonate, reduced in 0.5 mM DTT at 56 °C for 20 min, allowed to cool to room temperature and alkylated using 55 mM Idoacetamine for 15 min at room temperature. Proteins were digested with Trypsin Gold (Promega; ratio of 1:19 trypsin:protein) overnight at 37 °C. Samples were then additionally cleaned up using "Pep-clean C18 spin columns" (Thermo Fisher Scientific), spun in a vacuum centrifuge until dried and stored at −20 °C. Before the mass spectrometry analysis, dried peptides were re-suspended in 25 μL of 0.1% formic acid in 2% acetonitrile.

Nano LC–MS/MS analysis was carried out using an Ultimate 3000 nanoLC system (Dionex) coupled to a hybrid linear ion trap/Orbitrap mass spectrometer (LTQ Orbitrap XL; Thermo Fisher Scientific). Five μL of digest was loaded onto a C18 trap column (C18 PepMap, 300 m ID × 5 mm, 5 m particle size, 100 Å pore size; Dionex) and desalted for 3 min using a flow rate of 25 μL/min in 0.1% TFA in 2% ACN. The trap column was then switched online with the analytical column PepMap C18, 75 μm ID × 500 mm, 3 μm particle and 100 Å pore size; (Dionex) and peptides were eluted with the following binary gradients of solvents A and B: 0–25% solvent B in 240 min and 25–50% solvent B in a further 60 min, where solvent A consisted of 2% acetonitrile (ACN) and 0.1% formic acid in water and solvent B consisted of 80% ACN and 0.08% formic acid in water. Column flow rate was set to 350 nL/min. Data was acquired in data-dependent mode and externally calibrated, with Xcalibur software, version 2.0.7 (Thermo Fisher Scientific). Survey scan MS data were acquired in the Orbitrap on the 400–1800 m/z range with the resolution set to a value of 30,000 at 400 m/z. Up to three of the most intense multiply charged ions (1+, 2+ and 3+) per survey scan were CID fragmented in the linear ion trap. Collision energy was normalized to 35%. A dynamic exclusion window was applied within 40 s. Full scan mass spectra were recorded in profile mode and tandem mass spectra in centroid mode. Biological replicates (from 4 independent experiments) were analysed for each sample type.

MS data analysis was carried out using the workflow in Proteome Discoverer software 1.4.0 (Thermo Scientific) for processing LTQ Orbitrap raw file with Sequest HT and Mascot. Database searches were performed using the UniProtKB/SwissProt Human database (SwissProt fasta database was downloaded in January 2014). The search parameters used were as follows: Peptide mass tolerance set to 20 ppm, MS/MS mass tolerance set at 0.6 Da; up to two missed cleavages were allowed, carbamidomethylation set as a fixed modification and methionine oxidation set as a variable modification. The following filters were applied: maximum peptide delta Cn = 0.1; for charge state 1, XCorr > 1.9; for charge state 2, XCorr > 2.2; for charge state 3, XCorr > 3.75; Mascot significance threshold = 0.05; peptide ion scores ≥ 40. Protein identifications were accepted if they passed the above statistical criteria. A protein was considered identified in the EVs when it was recognized at least in one of the four biological replicate samples. The proteins involved in the biogenesis of EVs were identified the in the following number of independent experiments: once in the case of Clathrin LCB, twice in the case of TSG101 and three times in the case of Syntenin-1, CHMP4B and Alix.

3. Results

3.1. Multidrug resistant cells produce larger EVs than their sensitive cellular counterparts

In this work, two different pairs of isogenic cell line models were used, chronic myeloid leukaemia, CML (K562 and its MDR counterpart, overexpressing P-gp — K562Dox) and non-small cell lung cancer, NSCLC (NCI-H460 and its MDR counterpart, overexpressing P-gp — RH460). Cells were genotyped to confirm their origin (data not shown) and confirmation of the MDR phenotype in the K562Dox and RH460 cells (when compared to their drug-sensitive counterparts) was also carried out with two different drugs, doxorubicin and etoposide (Fig. S1). EVs from the two different models were collected by ultracentrifugation and characterized in terms of size and presence of EV markers (Fig. 1). The size of the isolated populations of EVs was analysed by two different approaches: dynamic light scattering (DLS) and transmission electron microscopy (TEM). EVs have been described as including vesicles of different sizes (including exosomes and microvesicles) [14] and indeed the results obtained showed heterogeneous populations of EVs, with size ranging from 10 to 1000 nm by DLS and 10 to 300 nm by TEM (Fig. 1A and B). CD63, CD81 and Hsp70 (markers of EVs) were observed in the populations analysed (EVs from the two pairs of isogenic models) and the absence of cytochrome *c* was confirmed, which excluded possible contamination by cellular debris in the populations analysed (Fig. 1C). P-gp expression was only detected in EVs shed by the MDR cell lines (K562Dox and RH460; Fig. 1C) and not in their sensitive counterparts, in agreement with the fact that this drug-efflux pump is only present in the MDR cell lines (Figs. 1C and S1).

Interestingly, when carefully analysing the populations of EVs in terms of size, a clear difference was observed between the sensitive EVs and their MDR counterparts. Indeed, EVs produced by MDR cells had an average diameter bigger than the diameter of EVs produced by their sensitive counterparts (Fig. 1A and B). This was observed in both cell line models used (CML and NSCLC) and by the two different size characterization methods performed, DLS and TEM. Even though both techniques used to analyse sizes indicated the same trend, i.e. bigger EVs in MDR cells, slight quantitative differences were observed between the two techniques. This is probably due to the fact that unlike TEM, DLS is an indirect method that measures the light scattered by the particles, therefore it is less sensitive in distinguishing single particles from aggregates, when compared to TEM. Indeed, when analysing TEM results for both pairs of cell lines (direct EVs observation) it was verified that EVs from sensitive cells presented a size range between 10 and 80 nm, which was lower than the size range between 40 and 200 nm of the

EVs isolated from the MDR cells. These results showed that MDR cells shed EV populations with a different size (and possibly a different intracellular origin) when compared to their drug- sensitive cellular counterparts. In addition, MDR cells seem to produce more EVs than the sensitive counterpart cell lines, as can be seen by the DLS count rate and protein quantification (Table 1 in [32]).

3.2. Multidrug resistant cells shed EVs with a different signature of proteins known to be involved in the biogenesis of EVs

Given the fact that the EVs isolated from the MDR cells were bigger in size than their drug-sensitive counterparts, the possibility that these vesicles had different intracellular origins and therefore different protein contents was raised. Thus, an extensive proteomic analysis of the content of EVs shed from the pair of chronic myeloid leukaemia cells (K562 and K562Dox) was carried out using LC/MS/MS technology. For the two types of isolated vesicles, a total of 304 proteins were identified. This technique allowed to identify 232 proteins in EVs shed from K562 cells and 207 proteins in EVs shed from K562Dox cells, of which 135 proteins overlapped in the two models of EVs (Table 2 in [32]). A PHANTER analysis was performed, but no major differences were observed between the two types of EVs, in terms of protein clusters involved in biological processes, molecular functions or pathways (Fig. 1 in [32]). Overall, most of the proteins identified in this study were in agreement with proteins previously identified in EVs produced by other cells (according to the ExoCarta exosome database, www.

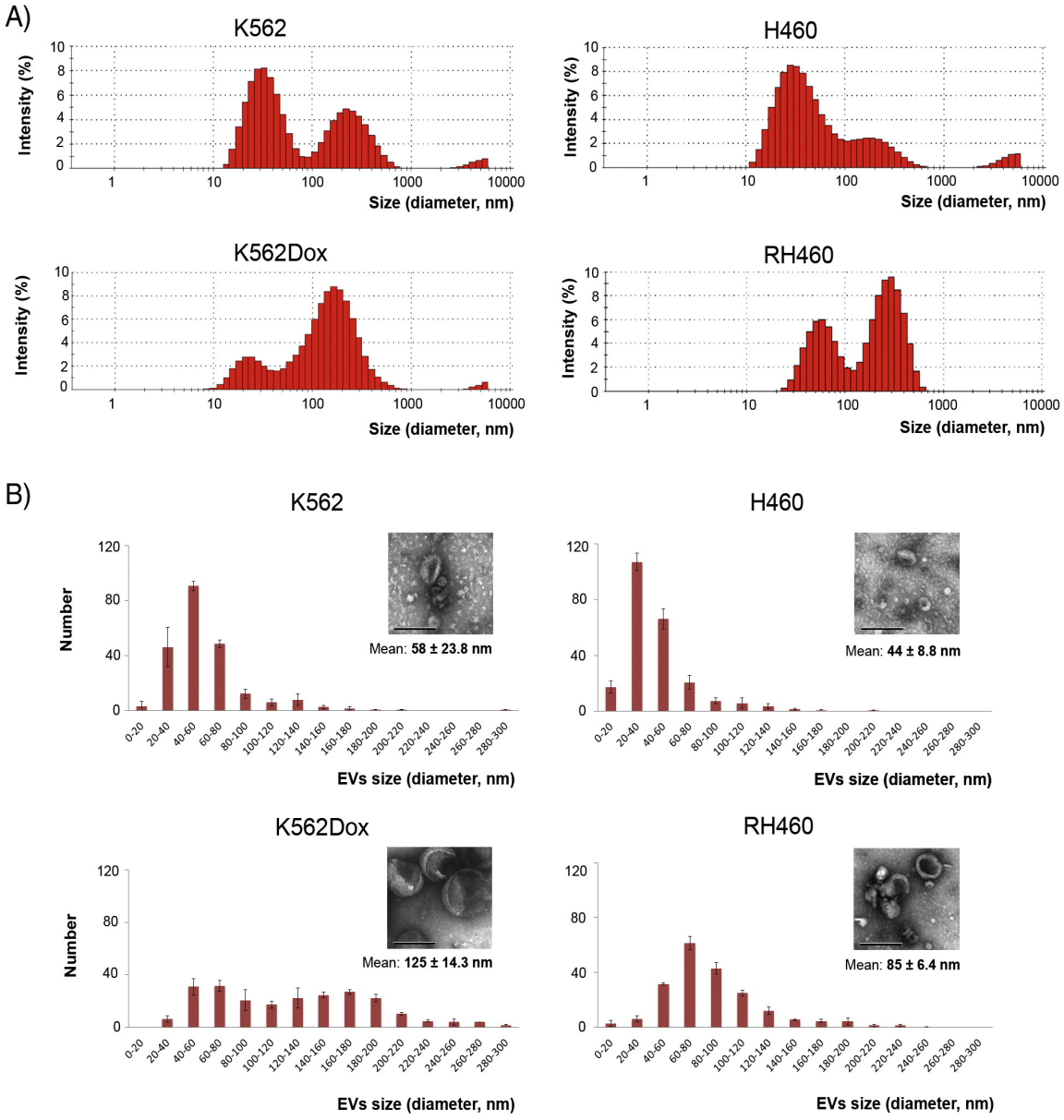

Fig. 1. Multidrug resistant cells (K562Dox and RH460) produce EVs with bigger sizes than their sensitive cellular counterparts (K562 and NCI-H460). A — Size distribution of EVs isolated from K562 and K562Dox cells (left panel) or from NCI-H460 and RH460 cells (right panel) analysed by dynamic light scattering. Results are the mean of 4 independent experiments (biological replicates) and were generated by the Zetasizer software v7.03. B — Size distribution histograms of EVs isolated from: K562 and K562Dox cells (left panel) or from NCI-H460 and RH460 cells (right panel) analysed by transmission electron microscopy. Results are expressed as mean ± SEM from 3 independent experiments (biological replicates) (with representative TEM image), in which at least 200 EVs were analysed. Scale bar = 200 nm. C — Expression of EV markers in cells and EVs isolated from the four cell lines (K562, K562Dox, NCI-H460 and RH460) analysed by Western blot (upper panels). Image refers to crop blots from samples run under the same experimental conditions (Fig. 1 in [32]). Flow cytometry analysis of EV markers on EVs isolated from the four cell lines (lower panels). EVs were coated with beads prior to being incubated with the appropriate antibodies and analysed by flow cytometry. Results are the mean of at least 3 independent experiments (biological replicates).

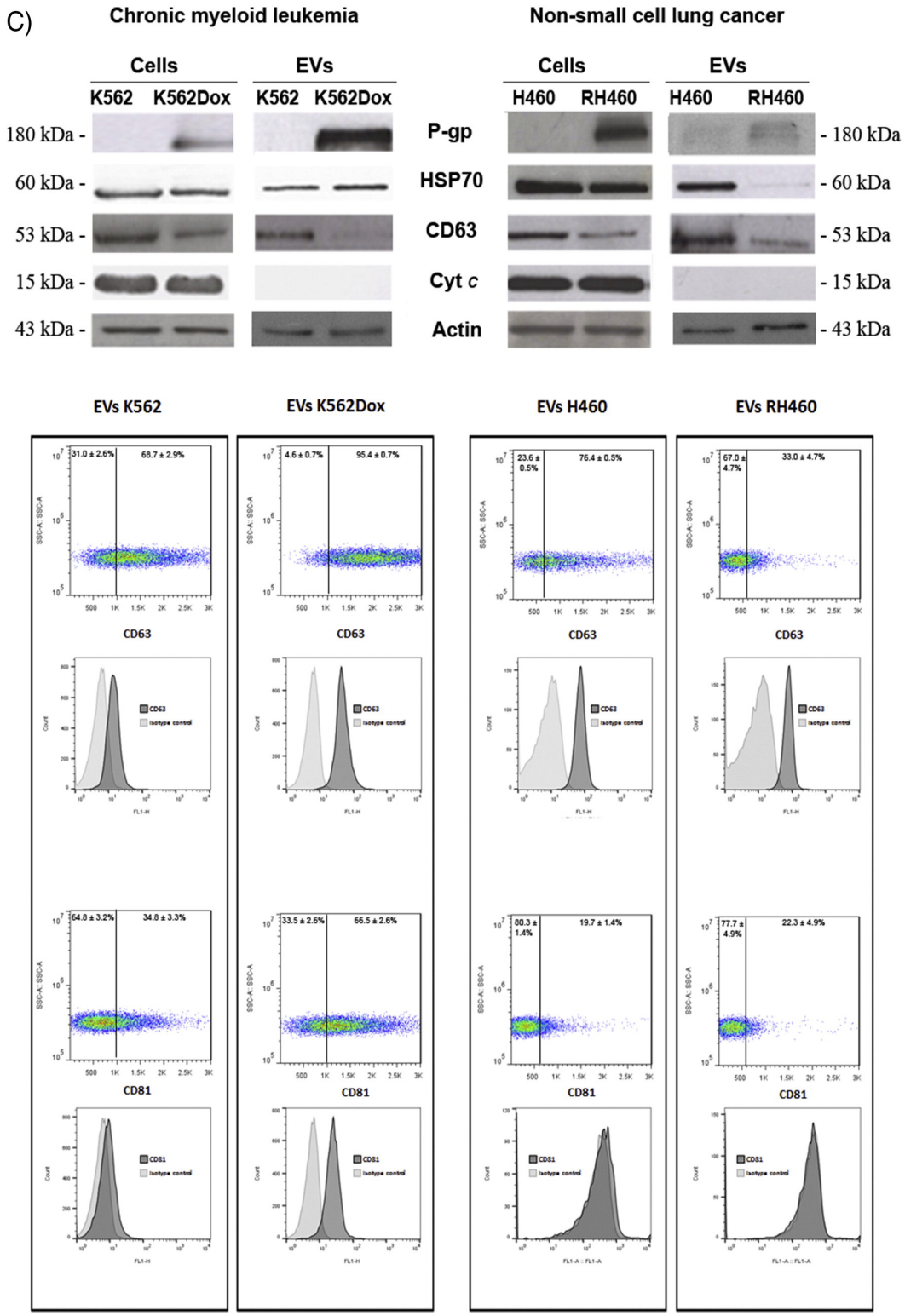

Fig. 1 (*continued*).

exocarta.org). In addition, these results from the detailed protein analysis further supported the fact that EVs were accurately isolated in this study (as had been previously shown with the data presented above, in Fig 1). LC/MS/MS results were then carefully analysed in order to identify proteins previously known to be relevant for the biogenesis of EVs, which could present different patterns of expression in the EVs from the two cell lines. From the 304 proteins identified, 4 of them were described as being involved in the biogenesis of EVs: Alix (Q8WUM4), Clathrin light chain B (P09497), Syntenin-1 (O00560) and TSG101 (Q99816) (Table 1). Alix, Clathrin light chain B and

Table 1
Proteins involved in EV biogenesis identified by mass spectrometry in K562 and K562Dox EV preparations.

Protein name	UniProt accession [a]	Function in EV biogenesis	Mass (kDa) [b]	∑Coverage % by amino acid	∑Unique peptides	K562 EVs	K562Dox EVs
Alix	Q8WUM4	Binds the ESCRT-I with ESCRT-III	96	19.01	12	ND	Detected
CHMP4B	Q9H444	Component of ESCRT-III	24.9	20.09	4	Detected	Detected
Clathrin LCB	P09497	Coats the early endosome membrane	25.2	4.37	1	ND	Detected
Syntenin-1	O00560	Interacts directly with Alix	32.4	7.72	2	Detected	ND
TSG101	Q99816	Component of ESCRT-I	43.9	2.56	1	ND	Detected

ND—not detected.
[a] Accession number in the UniProt database.
[b] Molecular weight of the protein.

TSG101 were only detected in EVs from K562Dox cells, whereas Syntenin-1 was only detected in EVs from K562 cells. In addition, another protein known to be involved in the biogenesis of EVs, CHMP4B (Q9H444), was identified in the EVs shed from both cell lines.

We then sought to validate these proteomic findings using Western blot analysis. These analyses were performed in the EVs from the leukaemia pair of MDR and drug-sensitive cells and also extended to the EVs from the NSCLC pair of MDR and drug-sensitive cells, in order to confirm if there was a "protein signature" common to EVs shed by MDR cells independently of their cellular context (in this case CML vs. NSCLC). In addition to the expression of 4 referred proteins, the levels of CD63 (EV marker), were also analysed (Fig. 2).

Results from the comparison of protein expression between EVs of MDR cells and their drug-sensitive counterparts, by Western blot analysis, showed that TSG101, Syntenin-1, Clathrin light chain B, CHMP4B and CD63 proteins had higher expression in the EVs from the drug-sensitive cells (K562 and NCI-H460) (Fig. 2). These results show that some of the proteins previously described as being involved in the biogenesis of exosomes are less packaged into the EVs shed from MDR cells, when compared to their sensitive counterparts. This suggests that EVs shed by MDR cells not only are larger but have a different type of biogenesis from the EVs shed by drug-sensitive cells.

Furthermore, the expression levels of these proteins were also analysed in the cell lines that gave origin to those EVs (the pairs of MDR and drug-sensitive counterparts from CML and NSCLC), by Western blot (Fig. 3). The results showed no significant differences between the MDR cells and the drug-sensitive counterparts, in both the lung and leukaemia models, contrary to what was previously observed in the EVs, indicating that there is selectively packaging of the previously mentioned proteins into the EVs.

4. Discussion

Since multidrug resistance (MDR) is a major cause of cancer treatment failure [1], biomarkers of MDR are urgently needed to guide better treatment decisions.

In the present study, we demonstrate that MDR cells shed bigger EVs and with a particular protein content. Nevertheless, these proteins were detected with similar expression levels in the pairs of MDR and drug sensitive cell lines, which suggests that there is selective packaging of those proteins into the EVs. Selective packaging of EVs has been previously described in several studies. Valadi and collaborators reported that secretory EVs from mast cells contain not only a distinctive set of proteins but also of mRNAs and microRNAs [33]. Recently, other group also demonstrated a selective packaging of miRNAs in the EVs cargo, upon release from the donor cells [34]. Additionally, they have also shown that EVs selectively incorporate transcripts of the vesiculation machinery (floppase and scramblase) [34]. Our work adds knowledge and impact to the previous studies as we have shown selective packaging of other proteins involved in the biogenesis of EVs themselves, associated with different sizes of EVs. We believe that this finding could be further studied in order to develop a "biomarker of MDR". We do not know if these characteristics (typical size and protein content) are specific of MDR, of P-gp overexpression or of drug resistance in general, since in this study we only used MDR cell models (with P-gp overexpression) and some authors previously noted intensive formation of membrane vesicles in an atypical MDR cell line (without overexpression of P-gp) [35].

Different types of EVs, including exosomes and microvesicles, have different intracellular origin and biogenesis (exosomes having endosomal origin and smaller sizes and microvesicles having a plasma membrane origin and bigger sizes) [14]. Therefore, exosomes and microvesicles probably have different composition and function as well. We found that the drug-sensitive cells produce smaller EVs containing greater amounts of proteins described to be mainly involved in the biogenesis of exosomes, whereas MDR cells produce bigger EVs containing smaller amounts of those proteins. This is true for both the MDR models used in this study (CML and NSCLC), which suggests that a different generalized intercellular origin of the EVs shed from MDR cells or sensitive cells may exist. It is possible that MDR cells produce more microvesicles, whereas drug-sensitive cells produce more exosomes. Indeed, regarding the sizes of the vesicles, the EVs shed from the drug-sensitive cells had a size range between 10 and 80 nm which is closer to the "exosomes size range" (30 to 100 nm [14]). In the EVs isolated from the MDR cells, the sizes oscillated between 40 to 200 nm, closer to the microvesicle size range of 50 to 2000 nm [14]. Moreover, proteins such as TSG101 [36–39], CHMP4 [37], CD63 [14], Syntenin-1 [37] and Clathrin [40], here found to be increased in the drug-sensitive EVs (in the Western blot results) have been described to be mainly involved in the biogenesis of exosomes.

Exosomes are formed within the endosomal network. They are released from late endosomal compartments to the plasma membrane through the fusion of multivesicular bodies. The key step in exosome formation is the reorganization of endosomal membrane proteins (CD9 and CD63) into microdomains. Next, endosomal sorting complexes required for transport (ESCRTs) are recruited to the site of budding. ESCRT-I and -II drive endosomal membrane budding via Alix that simultaneously binds to TSG101 (component of the ESCRT-I) and CHMP4 (component of ESCRT-III) [14,41]. Syntenin-1 has been shown to interact directly with Alix in the exosomes formation [37] and Clathrin is the protein that forms a coat in the EVs membrane, playing a major role in the internalization of EVs [42].

The development of methods to discriminate between microvesicles and exosomes is one of the main goals of the EV field. Unfortunately, there is still a lack of necessary knowledge to distinguish different EV populations according to their size, structure or protein compositions. Some proteins were described as being specifically involved in the biogenesis of microvesicles [43] [14], but recently some of them were also found to be important for the biogenesis of exosomes (such as ARF6 and PLD2 [44]). Nevertheless, a conventionally accepted hypothesis is that the microvesicles formation is induced by translocation of phosphatidylserine to the outer-membrane leaflet through the activity of flippases, leading to the plasma membrane curvature [45]. Our data raise the possibility that P-gp might be involved in this process since it has been previously described to act as a flippase for simple glycosphingolipids [46] and since our results indicate that the MDR cells, which overexpress P-gp, shed bigger EVs (possibly microvesicles) with lower amounts of proteins involved in biogenesis of exosomes. This hypothesis needs to be investigated.

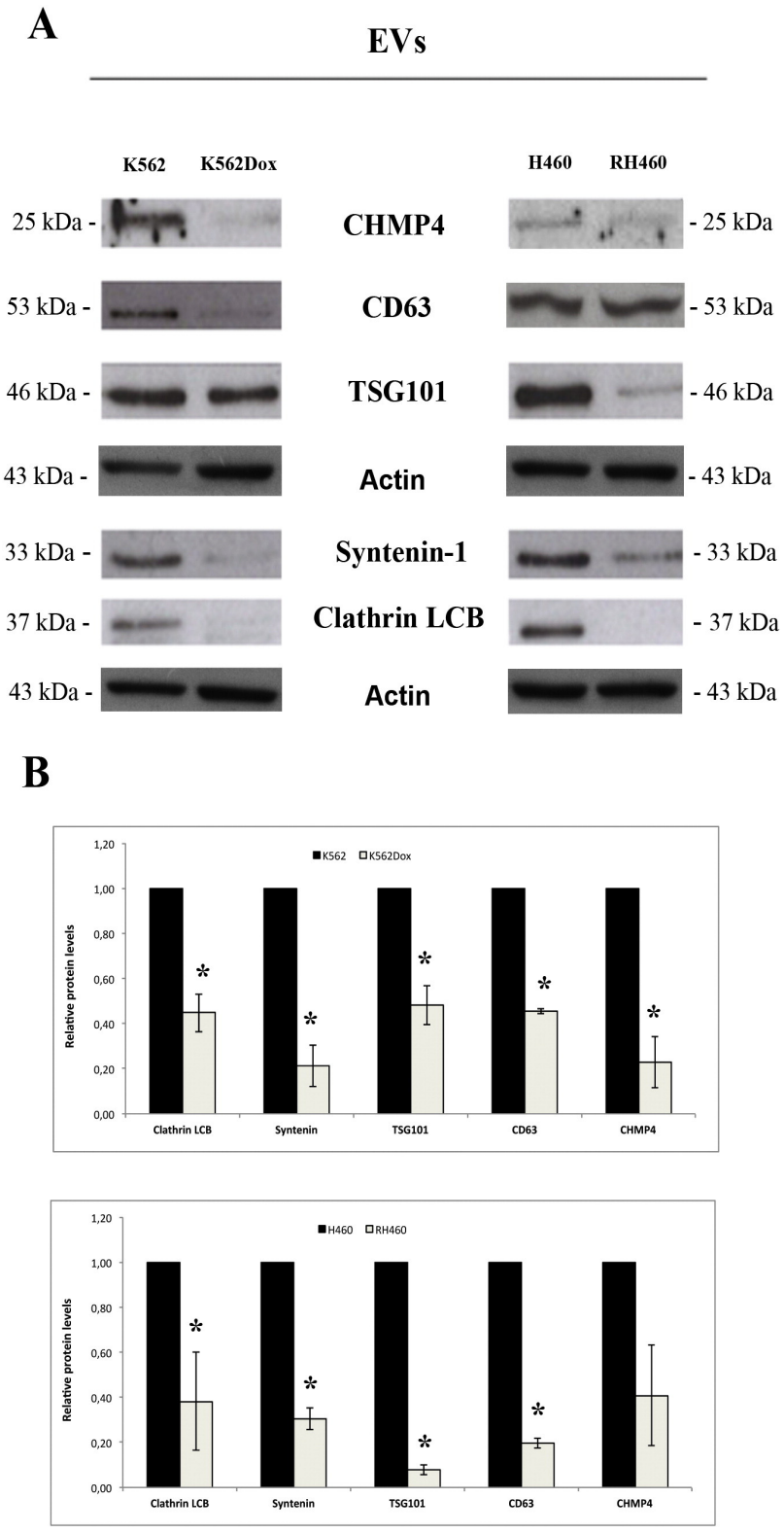

Fig. 2. EVs shed by MDR cells exhibit a different signature of proteins involved in the biogenesis of EVs, when compared to their sensitive counterparts. EV's protein content was analysed by Western blot and the levels of proteins involved in the biogenesis of EVs, together with the levels of CD63 (EVs marker), were compared between the EVs shed by the MDR cells and their sensitive counterparts. Blots are representative of three independent experiments (biological replicates). Image refers to crop blots from samples run under the same experimental conditions (Fig. 1 in [32]). Densitometry analysis was performed and results are represented as a % of relative protein expression (comparing the EVs shed from MDR cells, with the EVs from the drug-sensitive counterpart cells). Intensity of the bands was normalized with a corresponding internal control (actin), as previously published by other authors [52]. Each bar represents the mean ± SE from three independent experiments (biological replicates). * indicates $P \leq 0.05$.

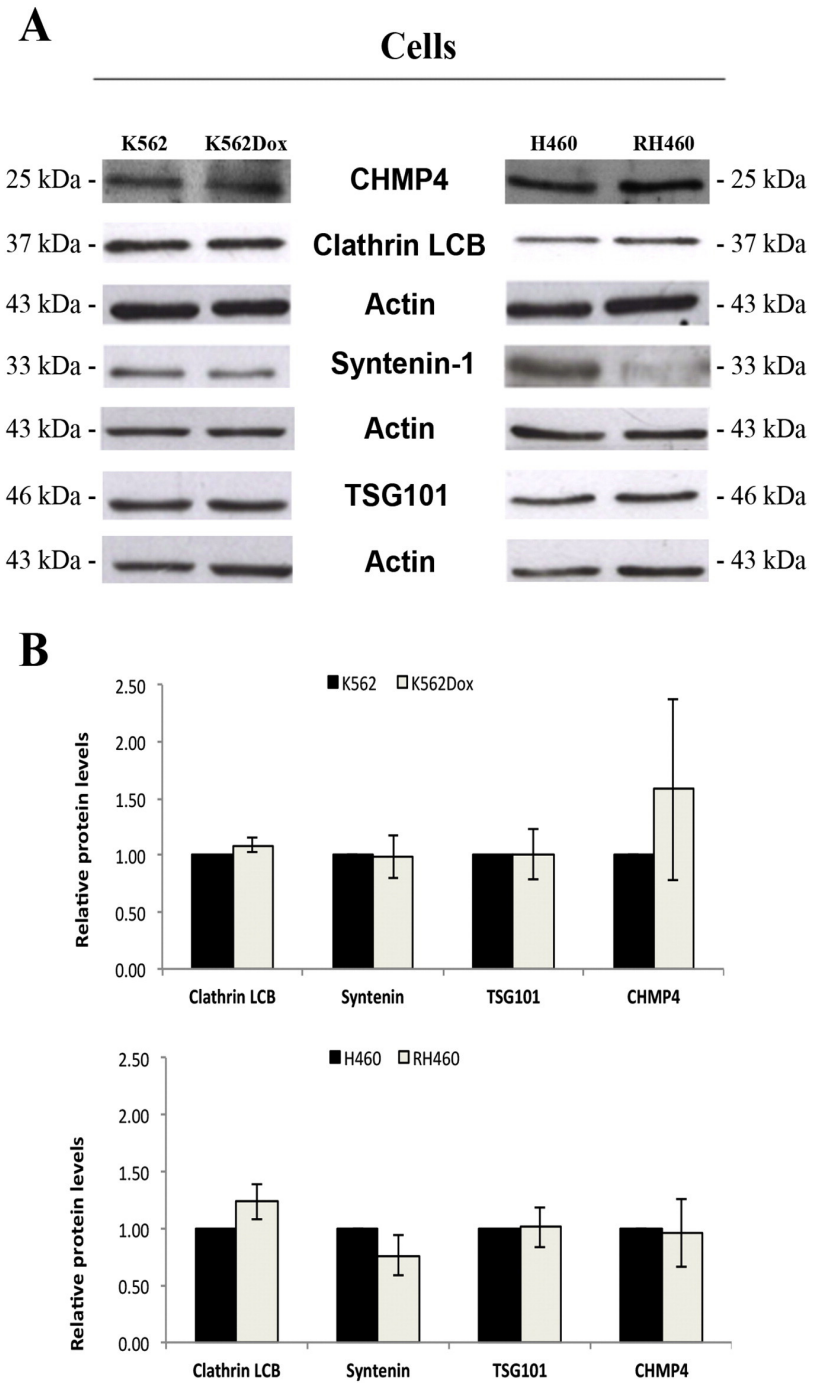

Fig. 3. MDR cells and their sensitive counterparts do not present differences in the expression of most of the proteins involved in the biogenesis of EVs. Cellular protein content was analysed by Western blot and the levels of proteins involved in the biogenesis of EVs were compared between the MDR cells and their sensitive counterparts. Blots are representative of three independent experiments (biological replicates). Image refers to crop blots from samples run under the same experimental conditions. In the densitometry analysis charts, results are presented as % of relative protein expression comparing MDR cells with the drug-sensitive counterpart cells. Intensity of bands was normalized with the corresponding internal control (actin). Each bar represents the mean ± SE from 3 independent experiments (biological replicates). * indicates $P \leq 0.05$.

Another relevant observed difference was that the MDR cells produced more EVs than the sensitive counterpart cell lines. The fact that MDR cells produce more EVs has been previously described in other studies. In 2012, Goler-Baron et al. showed that the inhibition of Akt signalling in a MDR breast cancer cell line resulted in the re-localization of ABCG2 from the EVs to the plasma membrane, which possibly led to a decrease in number and size of EVs [47]. Other work demonstrated that the increased expression of Annexin A3, in platinum-resistant ovarian cancer cells, resulted in the formation of increased numbers of multivesicular bodies (MVBs) in the cytoplasm [48]. Finally, another group demonstrated that the intracellular compartment of exosome assembly (MVB formation) was regulated by the ATP-binding cassette transporter A3 (ABCA3), associated with MDR. They observed a huge exosome release mediated by ABCA3 [49]. According to these reports and our own results, P-gp is possibly involved in the regulation of the EVs release in some way, since it is a common overexpressed protein

between the two models used in the present study (CML and NSCLC). It would be interesting to study if and how P-gp could be regulating the release and content of EVs. It is known that EVs may be isolated in pathological states and that those EVs contain a tissue-disease-type signature where a cargo of proteins and RNA are selectively package. Besides, EVs present a membrane structure that helps to protect the luminal contents from protease degradation and they are a less complex sample when compared to whole bodily fluids. Therefore, they could function as excellent molecular biomarkers to be used for diagnosis and prognosis [50,51], particularly given the fact that EVs can be easily collected from body fluids in a non-invasive approach, making them optimal biomarkers in order to diagnose cancer and even other diseases such as ones caused by microorganisms which shed EVs.

Combining this knowledge with our results, we propose that the specific size and protein content that we have here identified for the EVs shed by the MDR cells may have diagnostic significance in cancer as biomarkers to identify the MDR phenotype. However, the present work was only performed in vitro (in cell lines) and this hypothesis needs in vivo validation in mice and human samples. Therefore, our future work will investigate this hypothesis by monitoring these biomarkers in plasma of nude mice xenografted with human tumours and in plasma of patients with MDR tumours.

Author contributions

VLR carried out most of the laboratory work and wrote the manuscript. DS and HS helped in some experiments and analysis of data. ADL, PM and MH provided expertise in proteomic analysis and helped with the bioinformatic analysis of data. ROC and RTL co-supervised the experiments, helped in the planning of the experiments and proof-read the manuscript. MHV was the main supervisor of this work; planned and coordinated the work and helped in writing the manuscript. All authors agreed with the last version of the manuscript.

Competing financial interest statement

Nothing to declare.

Transparency Document

The Transparency Document associated with this article can be found, in the online version.

Acknowledgements

IPATIMUP integrates the i3S Research Unit, which is partially supported by FCT, the Portuguese Foundation for Science and Technology. This work is funded by FEDER funds through the Operational Programme for Competitiveness Factors—COMPETE and National Funds through the FCT—Foundation for Science and Technology, under the projects "PEst-C/SAU/LA0003/2013"; NORTE-07-0162-FEDER-00018 — "Contributos para o reforço da capacidade do IPATIMUP enquanto actor do sistema regional de inovação" and NORTE-07-0162-FEDER-000067 — "Reforço e consolidação da capacidade infraestrutural do IPATIMUP para o sistema regional de inovação", both supported by Programa Operacional Regional do Norte (ON.2 — O Novo Norte), through FEDER funds under the Quadro de Referência Estratégico Nacional (QREN). The proteomic work was also made possible through funding provided in part from awards from Science Foundation Ireland, Grant code 08/SRC/B1410 and the Irish Cancer Society, grant code CCRC13GAL. The authors thank the Portuguese Foundation for Science and Technology (FCT) for the PhD grants of VLR and DS (SFRH/BD/87646/2012 and SFRH/BD/98054/2013, respectively) and for the post-doc grant of RTL (SFRH/BPD/68787/2010).

Appendix A. Supplementary data

Supplementary data to this article can be found online at http://dx.doi.org/10.1016/j.bbagen.2015.12.011.

References

[1] V. Lopes-Rodrigues, H. Seca, D. Sousa, E. Sousa, R.T. Lima, M.H. Vasconcelos, The network of P-glycoprotein and microRNAs interactions. International Journal of Cancer, J. Int. Cancer 135 (2014) 253–263.
[2] N.S. Wind, I. Holen, Multidrug resistance in breast cancer: from in vitro models to clinical studies, Int. J. Breast Cancer 2011 (2011) 967419.
[3] L. Huang, C. Perrault, J. Coelho-Martins, C. Hu, C. Dulong, M. Varna, J. Liu, J. Jin, C. Soria, L. Cazin, A. Janin, H. Li, et al., Induction of acquired drug resistance in endothelial cells and its involvement in anticancer therapy, J. Hematol. Oncol. 6 (2013) 49.
[4] M.M. Gottesman, I. Pastan, Biochemistry of multidrug resistance mediated by the multidrug transporter, Annu. Rev. Biochem. 62 (1993) 385–427.
[5] H. Seca, R.T. Lima, J.E. Guimaraes, M.H. Helena, Simultaneous targeting of P-gp and XIAP with siRNAs increases sensitivity of P-gp overexpressing CML cells to imatinib, Hematology 16 (2011) 100–108.
[6] A. Palmeira, M.H. Vasconcelos, A. Paiva, M.X. Fernandes, M. Pinto, E. Sousa, Dual inhibitors of P-glycoprotein and tumor cell growth: (re)discovering thioxanthones, Biochem. Pharmacol. 83 (2012) 57–68.
[7] A. Palmeira, E. Sousa, M.H. Vasconcelos, M.M. Pinto, Three decades of P-gp inhibitors: skimming through several generations and scaffolds, Curr. Med. Chem. 19 (2012) 1946–2025.
[8] A. Palmeira, E. Sousa, M.H. Vasconcelos, M. Pinto, M.X. Fernandes, Structure and ligand-based design of P-glycoprotein inhibitors: a historical perspective, Curr. Pharm. Des. 18 (2012) 4197–4214.
[9] A. Palmeira, F. Rodrigues, E. Sousa, M. Pinto, M.H. Vasconcelos, M.X. Fernandes, New uses for old drugs: pharmacophore-based screening for the discovery of P-glycoprotein inhibitors, Chem. Biol. Drug Des. 78 (2011) 57–72.
[10] L. Zinzi, E. Capparelli, M. Cantore, M. Contino, M. Leopoldo, N.A. Colabufo, Small and innovative molecules as new strategy to revert MDR, Front. Oncol. 4 (2014) 2.
[11] X. Ma, Y. Cai, D. He, C. Zou, P. Zhang, C.Y. Lo, Z. Xu, F.L. Chan, S. Yu, Y. Chen, R. Zhu, J. Lei, et al., Transient receptor potential channel TRPC5 is essential for P-glycoprotein induction in drug-resistant cancer cells, Proc. Natl. Acad. Sci. U. S. A. 109 (2012) 16282–16287.
[12] V.J. Bezzerides, I.S. Ramsey, S. Kotecha, A. Greka, D.E. Clapham, Rapid vesicular translocation and insertion of TRP channels, Nat. Cell Biol. 6 (2004) 709–720.
[13] X. Ma, Z. Chen, D. Hua, D. He, L. Wang, P. Zhang, J. Wang, Y. Cai, C. Gao, X. Zhang, F. Zhang, T. Wang, et al., Essential role for TrpC5-containing extracellular vesicles in breast cancer with chemotherapeutic resistance, Proc. Natl. Acad. Sci. U. S. A. 111 (2014) 6389–6394.
[14] J.C. Akers, D. Gonda, R. Kim, B.S. Carter, C.C. Chen, Biogenesis of extracellular vesicles (EV): exosomes, microvesicles, retrovirus-like vesicles, and apoptotic bodies, J. Neuro-Oncol. 113 (2013) 1–11.
[15] Y. Lee, S. El Andaloussi, M.J. Wood, Exosomes and microvesicles: extracellular vesicles for genetic information transfer and gene therapy, Hum. Mol. Genet. 21 (2012) R125–R134.
[16] A.S. Azmi, B. Bao, F.H. Sarkar, Exosomes in cancer development, metastasis, and drug resistance: a comprehensive review, Cancer Metastasis Rev. 32 (2013) 623–642.
[17] C. D'Souza-Schorey, J.W. Clancy, Tumor-derived microvesicles: shedding light on novel microenvironment modulators and prospective cancer biomarkers, Genes Dev. 26 (2012) 1287–1299.
[18] P. Kucharzewska, M. Belting, Emerging roles of extracellular vesicles in the adaptive response of tumour cells to microenvironmental stress, J. Extracell. Vesicles 2 (2013).
[19] M. Yanez-Mo, P.R. Siljander, Z. Andreu, A.B. Zavec, F.E. Borras, E.I. Buzas, K. Buzas, E. Casal, F. Cappello, J. Carvalho, E. Colas, A. Cordeiro-da Silva, et al., Biological properties of extracellular vesicles and their physiological functions, J. Extracell. Vesicles 4 (2015) 27066.
[20] M. Bebawy, V. Combes, E. Lee, R. Jaiswal, J. Gong, A. Bonhoure, G.E. Grau, Membrane microparticles mediate transfer of P-glycoprotein to drug sensitive cancer cells, Leukemia 23 (2009) 1643–1649.
[21] C. Corcoran, S. Rani, K. O'Brien, A. O'Neill, M. Prencipe, R. Sheikh, G. Webb, R. McDermott, W. Watson, J. Crown, L. O'Driscoll, Docetaxel-resistance in prostate cancer: evaluating associated phenotypic changes and potential for resistance transfer via exosomes, PLoS ONE 7 (2012), e50999.
[22] J. Pasquier, L. Galas, C. Boulange-Lecomte, D. Rioult, F. Bultelle, P. Magal, G. Webb, F. Le Foll, Different modalities of intercellular membrane exchanges mediate cell-to-cell p-glycoprotein transfers in MCF-7 breast cancer cells, J. Biol. Chem. 287 (2012) 7374–7387.
[23] F.F. Zhang, Y.F. Zhu, Q.N. Zhao, D.T. Yang, Y.P. Dong, L. Jiang, W.X. Xing, X.Y. Li, H. Xing, M. Shi, Y. Chen, I.C. Bruce, et al., Microvesicles mediate transfer of P-glycoprotein to paclitaxel-sensitive A2780 human ovarian cancer cells, conferring paclitaxel-resistance, Eur. J. Pharmacol. 738 (2014) 83–90.
[24] D. Sousa, R.T. Lima, M.H. Vasconcelos, Intercellular transfer of cancer drug resistance traits by extracellular vesicles, Trends Mol. Med. 21 (2015) 595–608.
[25] S. Principe, A.B. Hui, J. Bruce, A. Sinha, F.F. Liu, T. Kislinger, Tumor-derived exosomes and microvesicles in head and neck cancer: implications for tumor biology and biomarker discovery, Proteomics 13 (2013) 1608–1623.
[26] E.L. Samir, A. IMg, X.O. Breakefield, M.J.A. Wood, Extracellular vesicles: biology and emerging therapeutic opportunities, Nat. Rev. Drug Discov. 12 (2013) 347–357.

[27] M. Pesic, J.Z. Markovic, D. Jankovic, S. Kanazir, I.D. Markovic, L. Rakic, S. Ruzdijic, Induced resistance in the human non small cell lung carcinoma (NCI-H460) cell line in vitro by anticancer drugs, J. Chemother. 18 (2006) 66–73.
[28] A. Podolski-Renic, M. Jadranin, T. Stankovic, J. Bankovic, S. Stojkovic, M. Chiourea, I. Aljancic, V. Vajs, V. Tesevic, S. Ruzdijic, S. Gagos, N. Tanic, et al., Molecular and cytogenetic changes in multi-drug resistant cancer cells and their influence on new compounds testing, Cancer Chemother. Pharmacol. 72 (2013) 683–697.
[29] J.P. Marie, A.M. Faussat-Suberville, D. Zhou, R. Zittoun, Daunorubicin uptake by leukemic cells: correlations with treatment outcome and mdr1 expression, Leukemia 7 (1993) 825–831.
[30] C. Thery, S. Amigorena, G. Raposo, A. Clayton, Isolation and characterization of exosomes from cell culture supernatants and biological fluids, Curr. Protoc. Cell Biol. (2006) (Chapter 3:Unit 3 22).
[31] R.T. Lima, L.M. Martins, J.E. Guimaraes, C. Sambade, M.H. Vasconcelos, Chemosensitization effects of XIAP downregulation in K562 leukemia cells, J. Chemother. 18 (2006) 98–102.
[32] V. Lopes-Rodrigues, A. Di Luca, D. Sousa, H. Seca, P. Meleady, M. Henry, R.T. Lima, R. O'Connor, M. Helena Vasconcelos, Data supporting the shedding of larger extracellular vesicles by multidrug resistant tumour cells, Data Brief (2015).
[33] H. Valadi, K. Ekstrom, A. Bossios, M. Sjostrand, J.J. Lee, J.O. Lotvall, Exosome-mediated transfer of mRNAs and microRNAs is a novel mechanism of genetic exchange between cells, Nat. Cell Biol. 9 (2007) 654–659.
[34] R. Jaiswal, F. Luk, J. Gong, J.M. Mathys, G.E. Grau, M. Bebawy, Microparticle conferred microRNA profiles—implications in the transfer and dominance of cancer traits, Mol. Cancer 11 (2012) 37.
[35] M. Dietel, H. Arps, H. Lage, A. Niendorf, Membrane vesicle formation due to acquired mitoxantrone resistance in human gastric carcinoma cell line EPG85-257, Cancer Res. 50 (1990) 6100–6106.
[36] M. Colombo, C. Moita, G. van Niel, J. Kowal, J. Vigneron, P. Benaroch, N. Manel, L.F. Moita, C. Thery, G. Raposo, Analysis of ESCRT functions in exosome biogenesis, composition and secretion highlights the heterogeneity of extracellular vesicles, J. Cell Sci. 126 (2013) 5553–5565.
[37] M.F. Baietti, Z. Zhang, E. Mortier, A. Melchior, G. Degeest, A. Geeraerts, Y. Ivarsson, F. Depoortere, C. Coomans, E. Vermeiren, P. Zimmermann, G. David, Syndecan-Syntenin-ALIX regulates the biogenesis of exosomes, Nat. Cell Biol. 14 (2012) 677–685.
[38] L. Abrami, L. Brandi, M. Moayeri, M.J. Brown, B.A. Krantz, S.H. Leppla, F.G. van der Goot, Hijacking multivesicular bodies enables long-term and exosome-mediated long-distance action of anthrax toxin, Cell Rep. 5 (2013) 986–996.
[39] K. Trajkovic, C. Hsu, S. Chiantia, L. Rajendran, D. Wenzel, F. Wieland, P. Schwille, B. Brugger, M. Simons, Ceramide triggers budding of exosome vesicles into multivesicular endosomes, Science 319 (2008) 1244–1247.
[40] C. Escrevente, S. Keller, P. Altevogt, J. Costa, Interaction and uptake of exosomes by ovarian cancer cells, BMC Cancer 11 (2011) 108.
[41] G. Raposo, W. Stoorvogel, Extracellular vesicles: exosomes, microvesicles, and friends, J. Cell Biol. 200 (2013) 373–383.
[42] R. Wubbolts, R.S. Leckie, P.T. Veenhuizen, G. Schwarzmann, W. Mobius, J. Hoernschemeyer, J.W. Slot, H.J. Geuze, W. Stoorvogel, Proteomic and biochemical analyses of human B cell-derived exosomes. Potential implications for their function and multivesicular body formation, J. Biol. Chem. 278 (2003) 10963–10972.
[43] V. Muralidharan-Chari, J. Clancy, C. Plou, M. Romao, P. Chavrier, G. Raposo, C. D'Souza-Schorey, ARF6-regulated shedding of tumor cell-derived plasma membrane microvesicles, Curr. Biol. 19 (2009) 1875–1885.
[44] R. Ghossoub, F. Lembo, A. Rubio, C.B. Gaillard, J. Bouchet, N. Vitale, J. Slavik, M. Machala, P. Zimmermann, Syntenin-ALIX exosome biogenesis and budding into multivesicular bodies are controlled by ARF6 and PLD2, Nat. Commun. 5 (2014) 3477.
[45] T.R. Graham, M.M. Kozlov, Interplay of proteins and lipids in generating membrane curvature, Curr. Opin. Cell Biol. 22 (2010) 430–436.
[46] P.D. Eckford, F.J. Sharom, The reconstituted P-glycoprotein multidrug transporter is a flippase for glucosylceramide and other simple glycosphingolipids, Biochem. J. 389 (2005) 517–526.
[47] V. Goler-Baron, I. Sladkevich, Y.G. Assaraf, Inhibition of the PI3K-Akt signaling pathway disrupts ABCG2-rich extracellular vesicles and overcomes multidrug resistance in breast cancer cells, Biochem. Pharmacol. 83 (2012) 1340–1348.
[48] J. Yin, X. Yan, X. Yao, Y. Zhang, Y. Shan, N. Mao, Y. Yang, L. Pan, Secretion of annexin A3 from ovarian cancer cells and its association with platinum resistance in ovarian cancer patients, J. Cell. Mol. Med. 16 (2012) 337–348.
[49] T. Aung, B. Chapuy, D. Vogel, D. Wenzel, M. Oppermann, M. Lahmann, T. Weinhage, K. Menck, T. Hupfeld, R. Koch, L. Trumper, G.G. Wulf, Exosomal evasion of humoral immunotherapy in aggressive B-cell lymphoma modulated by ATP-binding cassette transporter A3, Proc. Natl. Acad. Sci. U. S. A. 108 (2011) 15336–15341.
[50] Y. Yoshioka, N. Kosaka, Y. Konishi, H. Ohta, H. Okamoto, H. Sonoda, R. Nonaka, H. Yamamoto, H. Ishii, M. Mori, K. Furuta, T. Nakajima, et al., Ultra-sensitive liquid biopsy of circulating extracellular vesicles using ExoScreen, Nat. Commun. 5 (2014) 3591.
[51] S. Boukouris, S. Mathivanan, Exosomes in bodily fluids are a highly stable resource of disease biomarkers, Proteomics Clin. Appl. (2015).
[52] R. Jaiswal, F. Luk, P.V. Dalla, G.E. Grau, M. Bebawy, Breast cancer-derived microparticles display tissue selectivity in the transfer of resistance proteins to cells, PLoS ONE 8 (2013), e61515.

Supplementary Information

Multidrug resistant tumour cells shed more microvesicle-like EVs and less exosomes than their drug-sensitive counterpart cells

Vanessa Lopes-Rodrigues, Alessio Di Luca, Diana Sousa, Hugo Seca, Paula Meleady[4], Michael Henry, Raquel T. Lima, Robert O'Connor, M. Helena Vasconcelos

Supplementary Methods

Response of cells to chemotherapeutic drugs

For the analysis of the response of the pair of chronic myeloid leukaemia cells (K562 and K562Dox) to drugs, cells (3 x10^5/ml, plated in 24-well plates) were treated for 48 h with serial dilutions of etoposide (ranging from 50 to 800 nM; Sigma) or doxorubicin (ranging from 7.5 to 120 nM; Sigma). Cell number and viability was then determined with the trypan blue exclusion assay. For the analysis of the response of the pair of non-small cell lung cancer cells (H460 and RH460) to drugs, the sulforhodamine B (SRB) assay was carried out (with cells in 5% FBS supplemented medium). Briefly, cells (5x10^3/well) were plated in 96-well plates and incubated for 24 h. Cells were then treated with serial dilutions of etoposide (ranging from 20 nM to 1.6μM) or doxorubicin (ranging from 15 to 240 nM). Following 48 h, plates were fixed with 10% ice cold trichloroacetic acid, washed with water and stained with SRB. After washing with 1% acetic acid, SRB was solubilized with 10 mM Tris base and absorbance (510 nm) was measured in a microplate reader (Synergy Mx, Biotek Instruments Inc.). In all experiments, the effect of the drug solvent (DMSO) was analysed by treating with the maximum concentration used.

Ponceau-S staining

Proteins isolated from EVs (5 to 8 μg) were separated on a 12% Bis-Tris SDS– PAGE gel and transferred onto a nitrocellulose membrane (GE Healthcare). The molecular weight marker *Precision Plus Protein Standards, Dual color, Catalog #161-0374* from BIO-RAD (3 μl) was also included. For loading control, membranes were stained with a Ponceau-S solution (Sigma).

Supplementary Figure Legend

Figure S1: K562Dox and RH460 are multidrug resistant and overexpress P-glycoprotein. Dose-response curves of K562/K562 Dox cells (**A**) and H460/RH460 cells (**B**) following 48 h treatment with doxorubicin and etoposide (upper panel). P-gp protein expression levels in these pairs of cells lines analysed by Western blot (lower panel).

Figure S2: Ponceau-S staining of the Western Blot membranes with the proteins isolated from the EVs shed by the two pairs of isogenic cell lines, in order to confirm equal loading of the proteins extracted from the EVs. Left panel refers to Figure 2; Middle and right panels refer to Figure 1C.

Figure S3: FBS depleted do not express TSG101, P-gp, Syntenin-1 and Clathrin LCB. FBS depleted and EVs protein content was analysed by Western blot and the levels of proteins involved in the biogenesis of EVs and P-gp expression were compared between the FBS depleted and EVs isolated from K562 and K562Dox cells. Image refers to crop blots from samples run under the same experimental conditions.

Supplementary Figures

Figure S1

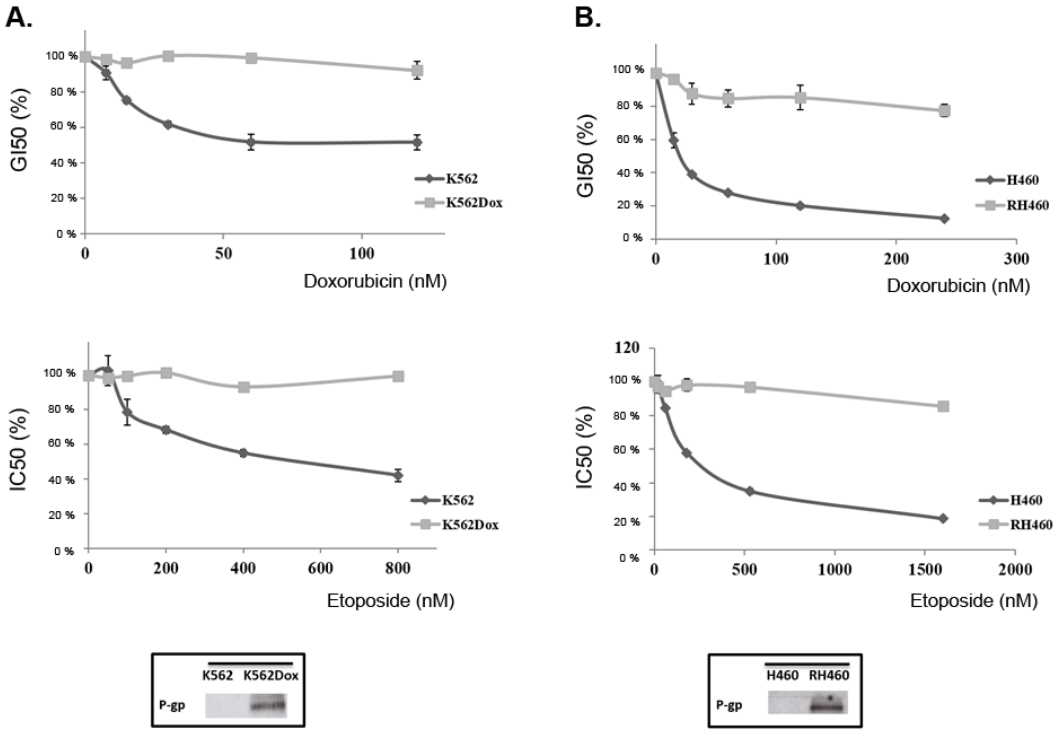

Figure S2

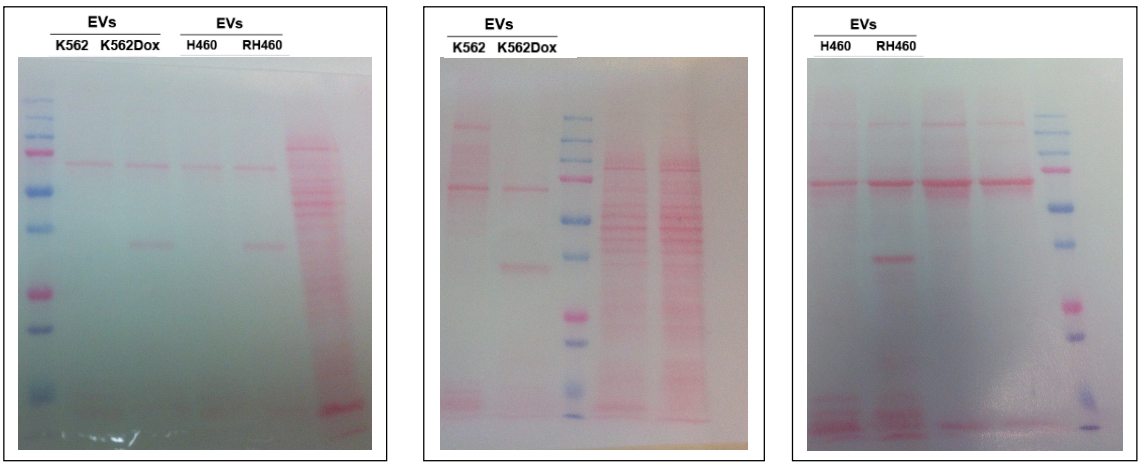

Figure S3

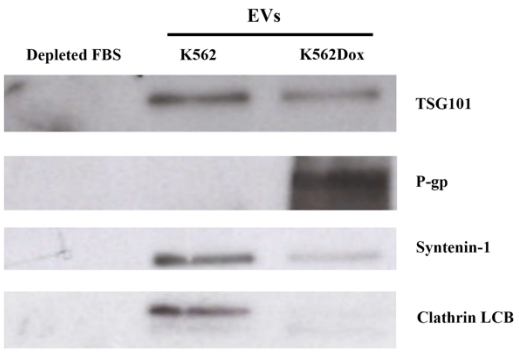

3. DATA ARTICLE

Data supporting the shedding of larger extracellular vesicles by multidrug resistant tumour cells

Vanessa Lopes-Rodrigues, Alessio Di Luca, Diana Sousa, Hugo Seca, Paula Meleady, Michael Henry, Raquel T. Lima, Robert O'Connor, M. Helena Vasconcelos

Published in Data in Brief 6 (2016): 1023-1027

Data in Brief 6 (2016) 1023–1027

Contents lists available at ScienceDirect

Data in Brief

journal homepage: www.elsevier.com/locate/dib

Data Article

Data supporting the shedding of larger extracellular vesicles by multidrug resistant tumour cells

Vanessa Lopes-Rodrigues [a,b,c], Alessio Di Luca [d], Diana Sousa [a,b,e], Hugo Seca [a,b], Paula Meleady [d], Michael Henry [d], Raquel T. Lima [a,b,f], Robert O'Connor [d], M. Helena Vasconcelos [a,b,e,*]

[a] *i3S – Instituto de Investigação e Inovação em Saúde, Universidade do Porto, Portugal*
[b] *Cancer Drug Resistance Group, IPATIMUP – Institute of Molecular Pathology and Immunology of the University of Porto, 4200-465 Porto, Portugal*
[c] *ICBAS-UP – Institute of Biomedical Sciences Abel Salazar, University of Porto, 4099-003 Porto, Portugal*
[d] *NICB – National Institute for Cellular Biotechnology, Dublin City University, Dublin 9, Ireland*
[e] *Department of Biological Sciences, FFUP – Faculty of Pharmacy, University of Porto, 4050-313 Porto, Portugal*
[f] *Department of Pathology and Oncology, FMUP – Faculty of Medicine of the University of Porto, Alameda Prof. Hernâni Monteiro, 4200-319 Porto, Portugal*

ARTICLE INFO

Article history:
Received 23 December 2015
Received in revised form
29 January 2016
Accepted 1 February 2016
Available online 8 February 2016

ABSTRACT

To date, there are no simple and minimally invasive methods to diagnose MDR. Extracellular vesicles (EVs) are shed by all cells, carry a specific cargo from the donor cells and are present in several body fluids, which means that they can potentially be easily collected from cancer patients and become the source of biomarkers to diagnose cancer. This data article contains a full list of the proteins identified in the EVs shed by an isogenic pair of chronic myeloid leukaemia cells (MDR cells and their drug-sensitive counterparts) by LC/MS/MS analysis, together with their GeneOntology analysis. In addition, it also contains data from protein content analysis and Dynamic light scattering count-rate events of the referred EVs as well as of the EVs shed from an isogenic pair of non-small cell lung cancer cells (MDR cells and their drug-sensitive counterparts). The interpretation of the data presented in this article and further

DOI of original article: http://dx.doi.org/10.1016/j.bbagen.2015.12.011
* Corresponding author at: i3S – Instituto de Investigação e Inovação em Saúde, Universidade do Porto, Rua Alfredo Allen 208, 4200-135 Porto, Portugal.
E-mail address: hvasconcelos@ipatimup.pt (M.H. Vasconcelos).

http://dx.doi.org/10.1016/j.dib.2016.02.004

extensive insights can be found in "Multidrug resistant tumour cells shed more microvesicles-like EVs and less exosomes than their drug-sensitive counterpart cells" [1].

Specifications Table

Subject area	Health sciences
More specific subject area	*Cancer Multidrug resistance, Extracellular vesicles*
Type of data	*Tables and figure*
How data was acquired	Optima XE – 100 Ultracentrifuge, Beckman Coulter; Nano series Malvern Zetasizer Instrument (Prager Instruments); Ultimate 3000 nanoLC system (Dionex) coupled to a hybrid linear ion trap/Orbitrap mass spectrometer (LTQ Orbitrap XL; Thermo Fisher Scientific).
Data format	*Analyzed*
Experimental factors	*Multidrug resistance*
Experimental features	*Extracellular vesicles (EVs) isolated from multidrug resistant (MDR) cells (overexpressing P-glycoprotein) and from their drug-sensitive counterpart cells were used to obtain the data.*
Data source location	*– i3S – Instituto de Investigação e Inovação em Saúde, Universidade do Porto, Portugal* *– Cancer Drug Resistance Group, IPATIMUP – Institute of Molecular Pathology and Immunology of the University of Porto, Porto, Portugal* *– NICB – National Institute for Cellular Biotechnology, Dublin City University, Dublin 9, Ireland*
Data accessibility	*Data within this article*

Value of the data

- These data describe the quantification of EVs isolated from MDR cells and from their drug sensitive counterpart cells.
- Data regarding the use of LC–MS/MS analysis to compare EVs isolated from MDR and drug-sensitive counterpart cells.
- EVs isolated from MDR and their drug-sensitive counterpart cells could be valuable for future research on the acquisition of MDR phenotype and improving knowledge in the diagnosis of MDR.

Data

The protein content and DLS count-rate events of EVs isolated from MDR and drug-sensitive cells have been shown (Table 1). In Table 2 a list of proteins identified by mass spectrometry, in EVs isolated from CML cells (*K562 – drug-sensitive* cells and *K562Dox – MDR cells*) have been mentioned. Moreover, Fig. 1 shows Gene Ontology analysis performed in the protein list obtained by LC/MS/MS of

Table 1
Protein content and DLS count-rate events of EVs isolated from MDR and drug-sensitive cells from both models (CML and NSCLC).

	Protein content (μg)	Count Rate (kcps)
K562	9 ± 0.7	167.3 ± 2.28
K562Dox	14 ± 1.5	265.9 ± 7.71
H460	7 ± 2.2	149.5 ± 9.3
RH460	11 ± 2.8	168.4 ± 5.8

EVs were isolated from the two pairs of (MDR and drug-sensitive) cell lines (from CML and NSCLC). Proteins were extracted and quantified. Count rate was determined by DLS. Data refers to protein quantity (μg) and count rates obtained for EVs isolated from the same number of cells. Results refer to $\mu g \pm$ S.E. or to kcps $\pm$ S.E.

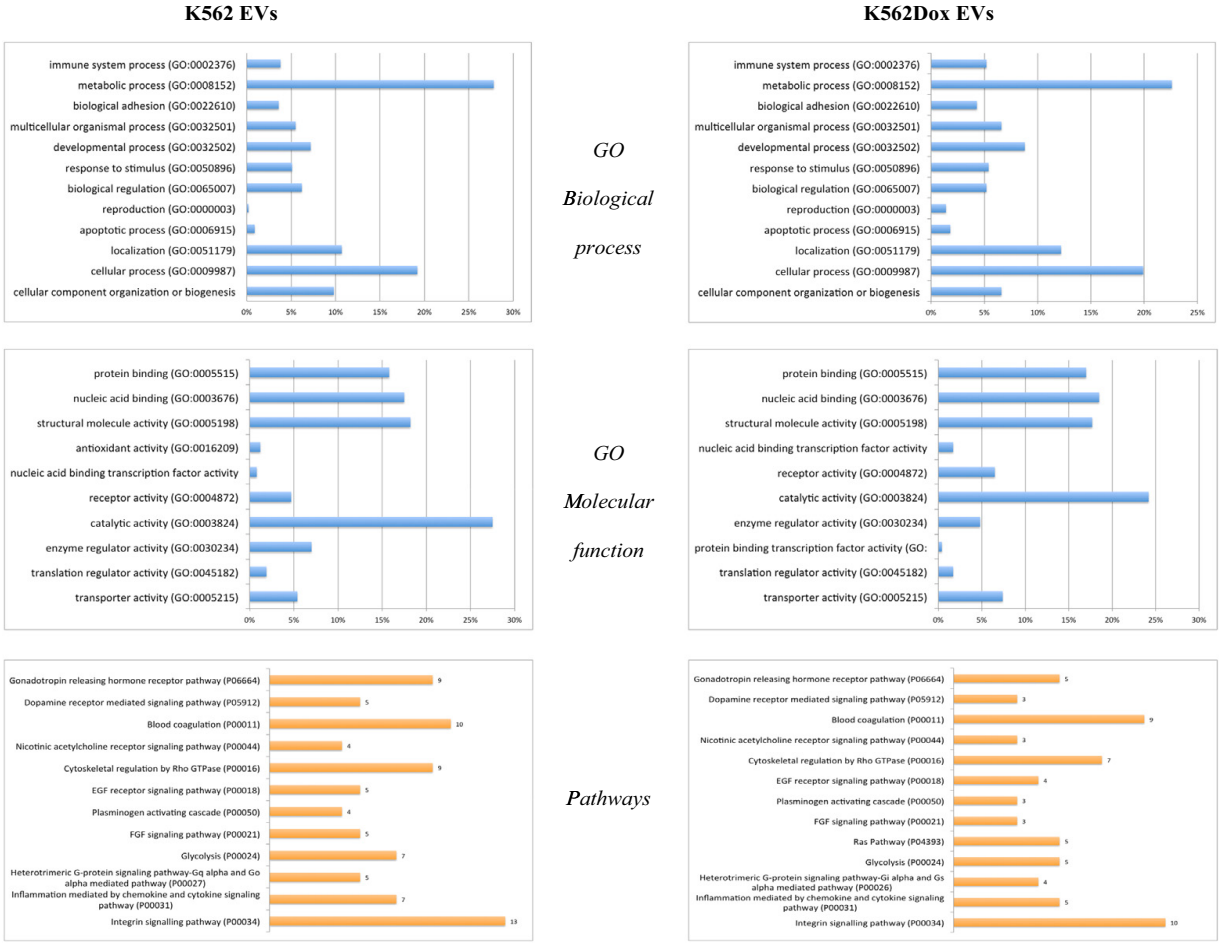

Fig. 1. Gene Ontology analysis based on biological process, molecular function and pathway. The analysis was performed in the protein list obtained by LC/MS/MS analysis in the EVs isolated from K562 and K562Dox cells.

EVs isolated from K562 and K562Dox cells, based on the biological processes, molecular functions and pathways.

1. Experimental design, materials and methods

EVs were isolated from two pairs of isogenic cell lines (MDR and the drug-sensitive counterpart) from two different cancer models, non-small cell lung cancer-NSCLC *(H460 – drug-sensitive cells and*

RH460 – MDR cells) [2,3] and chronic myeloid leukaemia-CML (*K562 – drug-sensitive* cells and *K562Dox – MDR cells*) [4,5]. Cells were used to isolate EVs, for protein quantification (Table 1), Dynamic light scattering (Table 1) and proteomic experiments (Table 2 and Fig. 1).

1.1. Isolation of Extracellular vesicles

EVs were collected from the supernatant of equivalent amounts of cells, cultured in EVs-depleted culture medium. EVs were isolated from these culture media as previously published [6,1] by various centrifugation steps.

1.2. Protein quantification

Protein amount of the isolated EVs was quantified as previous published [1].

1.3. Count rate analysis using dynamic light scattering

EVs count rate was measured by dynamic light scattering (DLS), using a Nano series Malvern Zetasizer Instrument (Prager Instruments) as previously published [1].

1.4. Sample preparation and mass spectrometry

Pellets of EVs were prepared using previously established methods [1]. Nano LC–MS/MS analysis was carried out using an Ultimate 3000 nanoLC system (Dionex) coupled to a hybrid linear ion trap/Orbitrap mass spectrometer (LTQ Orbitrap XL; Thermo Fisher Scientific) [1]. MS data analysis was carried out as previously described [1]. A protein was considered as being identified in the EVs when it was recognized at least in one of the four biological replicate samples.

1.5. PHANTER analysis

Proteins identified in the samples of EVs were analysed using GeneOntology (GO) in the PANTHER database to identify biological processes, molecular functions and pathways (http://www.pantherdb.org/).

Acknowledgements

IPATIMUP integrates the i3S Research Unit, which is partially supported by FCT, the Portuguese Foundation for Science and Technology. This work is funded by FEDER funds through the Operational Programme for Competitiveness Factors-COMPETE and National Funds through the FCT-Foundation for Science and Technology, under the projects “PEst-C/SAU/LA0003/2013” NORTE-07-0162-FEDER-00018 – Contributos para o reforço da capacidade do IPATIMUP enquanto actor do sistema regional de inovação and NORTE-07-0162-FEDER-000067-Reforço e consolidação da capacidade infraestrutural do IPATIMUP para o sistema regional de inovação, both supported by Programa Operacional Regional do Norte (ON.2 – O Novo Norte), through FEDER funds under the Quadro de Referência Estratégico Nacional (QREN). The proteomic work was also made possible through funding provided in part from awards from Science Foundation Ireland, Grant code 08/SRC/B1410 and the Irish Cancer Society, Grant code CCRC13GAL. The authors thank the Portuguese Foundation for Science and Technology (FCT) for the PhD grants of VLR and DS (SFRH/BD/87646/2012 and SFRH/BD/98054/2013, respectively) and for the post-doc grant of RTL (SFRH/BPD/68787/2010).

Appendix A. Supplementary material

Supplementary data associated with this article can be found in the online version at http://dx.doi.org/10.1016/j.dib.2016.02.004.

References

[1] Vanessa Lopes-Rodrigues, Alessio Di Luca, Diana Sousa, Hugo Seca, Paula Meleady, Michael Henry, Raquel T. Lima, Robert O'Connor, M. Helena Vasconcelos, Multidrug resistant tumour cells shed more microvesicles-like EVs and less exosomes than their drug-sensitive counterpart cells, BBA – Gen. Subj. 1860 (3) (2016) 618–627.
[2] M. Pesic, J.Z. Markovic, D. Jankovic, S. Kanazir, I.D. Markovic, L. Rakic, S. Ruzdijic, Induced resistance in the human non small cell lung carcinoma (NCI-H460) cell line in vitro by anticancer drugs, J. Chemother. 18 (2006) 66–73.
[3] A. Podolski-Renic, M. Jadranin, T. Stankovic, J. Bankovic, S. Stojkovic, M. Chiourea, I. Aljancic, V. Vajs, V. Tesevic, S. Ruzdijic, S. Gagos, N. Tanic, et al., Molecular and cytogenetic changes in multi-drug resistant cancer cells and their influence on new compounds testing, Cancer Chemother. Pharmacol. 72 (2013) 683–697.
[4] J.P. Marie, A.M. Faussat-Suberville, D. Zhou, R. Zittoun, Daunorubicin uptake by leukemic cells: correlations with treatment outcome and mdr1 expression, Leukemia 7 (1993) 825–831.
[5] H. Seca, R.T. Lima, J.E. Guimaraes, M. Helena Vasconcelos, Simultaneous targeting of P-gp and XIAP with siRNAs increases sensitivity of P-gp overexpressing CML cells to imatinib, Hematology 16 (2011) 100–108.
[6] C. Thery, S. Amigorena, G. Raposo, A. Clayton, Isolation and characterization of exosomes from cell culture supernatants and biological fluids, Curr. Protoc. Cell Biol./Editor. Board, Juan S. Bonifacino ... [et al.] (2006) 22, Chapter 3:Unit 3.

4. LETTER TO THE EDITOR

ALIX protein analysis: storage temperature may impair results

Vanessa Lopes-Rodrigues, Cristina P. R. Xavier, Diana Sousa, Raquel T. Lima, Hugo Osório, M. Helena Vasconcelos

Manuscript in preparation

LETTER TO THE EDITOR

ALIX protein analysis: storage temperature may impair results

Vanessa Lopes-Rodrigues[1,2,3], Cristina P. R. Xavier[1,2], Diana Sousa[1,2,4], Hugo Osório[1,5,6], Raquel T. Lima[1,2,5], M. Helena Vasconcelos[1,2,4*]

[1] i3S - Instituto de Investigação e Inovação em Saúde, Universidade do Porto, Porto, Portugal

[2] Cancer Drug Resistance Group, IPATIMUP - Institute of Molecular Pathology and Immunology of the University of Porto, 4200-465 Porto, Portugal;

[3]Institute of Biomedical Sciences Abel Salazar, ICBAS-UP – Institute of Biomedical Sciences Abel Salazar of the University of Porto, 4099-003 Porto, Portugal;

[4]Department of Biological Sciences, FFUP - Faculty of Pharmacy of the University of Porto, 4050-313 Porto, Portugal

[5]Department of Oncology, FMUP – Faculty of Medicine of the University of Porto, 4200-319 Porto, Portugal;

[6]IPATIMUP - Institute of Molecular Pathology and Immunology of the University of Porto, 4200-465 Porto, Portugal;

*corresponding author

Dear Editor,

This letter aims to emphasize the importance of proper handling and storage of protein lysates for downstream applications such as Western blot, when analyzing the expression of the protein ALIX (programmed cell death 6-interacting protein).

The increasing interest in extracellular vesicles (EVs) has provided more relevance to the analysis of this protein, since it has been defined as one of the best well known molecular markers of EVs (particularly for exosomes) [1]. ALIX is a cytosolic protein that was initially identified due to its association with pro-apoptotic signaling [2]. More recently, ALIX was found to regulate other cellular mechanisms such as endocytic membrane trafficking and cell adhesion [3]. Much of the recent progress in tackling the function of ALIX has been centered on its connection to the endocytic membrane trafficking. This protein interacts with several ESCRT (*endosomal sorting complexes required for transport*) proteins in order to participate in the budding and abscission processes that ultimately can lead to the formation of exosomes [2,4].

The predicted expression pattern of ALIX in Western Blot analysis is composed of a single band, with an approximate size of 93 kDa [4]. However, several recent studies show more than one band when presenting Western Blots for ALIX expression. Indeed, several bands have been observed, in Western Blots containing protein lysates from both cell lines or EVs [5-10]. In some of these studies [5,6,8], ALIX is presented as having two (or even more) bands, a major one on the predicted size (approximately 93 kDa) and other(s) with smaller sizes. In other studies, although ALIX is presented as only one band within the expected size [7,9,10], the supplementary information (in which the respective uncropped blots are shown) clearly demonstrates the presence of other band(s) which are not identified. Given the increase interest in ALIX in the last few years [9,11] and our own need to analyse the expression of this protein, we decided to further understand the divergence on the expression pattern of ALIX.

It is known that a proper storage temperature is one of the most important factors in order to maintain protein's integrity over an extended period of time [12]. Therefore, we analyzed total protein cell lysates from a chronic myeloid leukaemia cell line (K562) for ALIX protein expression by Western blot, using two of the most commonly used antibodies (ALIX sc-49268 from *Santa Cruz Biotechnology* and ALIX #2171 from *Cell Signaling Technologies*). The samples were kept at -20 ºC (with or without phosphatase inhibitors) and at -80 ºC for different periods of time (1, 2, 3 or 6 weeks). After performing Western blot analysis, of the frozen samples, we detected at least two bands (using either antibody) (Figure 1): i) one with a molecular weight similar to the predicted one, 93 kDa (93 kDa - ALIX) and ii) another with approximately 75 kDa (75 kDa – ALIX). In order to confirm that the antibody was specifically detecting ALIX in both bands, we performed a mass spectrometry analysis. We detected 20 peptides related to ALIX in the 93 kDa protein band corresponding to the N-terminus peptide 24-41 and the C-terminus peptide 716-745. In the 75kDa band, we still detected the N-terminus peptide but the C-terminus 716-745 peptide was absent. This led us to conclude that the 75 kDa protein band corresponds to a degraded form of ALIX in which the C-terminal is missing.

When analyzing the samples kept at -20 ºC over time (1, 2, 3 or 6 weeks), both in the presence or absence of phosphatase inhibitors, we noticed that the C-terminal specific degradation of ALIX depended on the duration of the samples storage at -20 ºC (Fig. 1). In fact, over time and at -20 ºC, the expression levels of the 93 kDa – ALIX band decreased while the levels of the degraded form (75 kDa – ALIX) increased. In addition, under the same conditions (- 20ºC storage), the presence of a phosphatase inhibitor had no effect on the level of degradation of this protein (Figure 1).

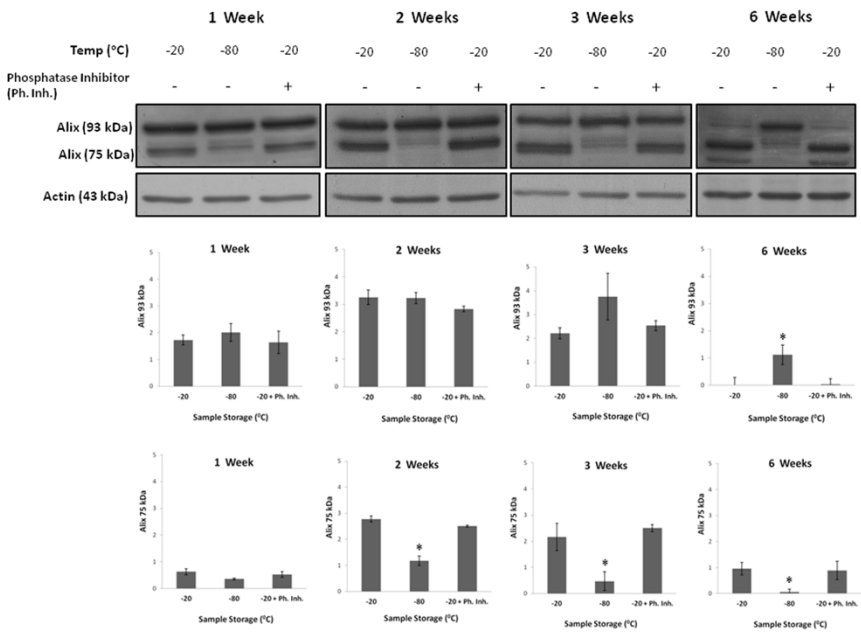

Figure 1 – Expression of ALIX in K562 cells following several storage conditions. Fresh total cell protein lysates were immediately stored at: -20 ºC, -20 ºC with a phosphatase inhibitor cocktail (+ Ph. Inh) or at -80 ºC. Samples were kept frozen for 1, 2, 3 or 6 weeks. (A) Representative Western blot images; (B) Densitometry analysis of the Western blots, represented as mean ± SEM from three independent experiments. Actin was used as a loading control. * $p \leq 0.05$ when comparing protein levels in samples stored at -20 ºC (- Ph. Inh.) vs. other storage conditions (- 80ºC or – 20ºC + Ph. Inh.).

Nevertheless, when analyzing the samples stored at -80 ºC for the same period of time (1, 2, 3 or 6 weeks), no major degradation of ALIX was observed. In fact, the expression level of the 93 kDa – ALIX remained unaltered during the 6 weeks' period and no increase of the degraded form of ALIX (75 kDa – ALIX) was observed (Figure 1).

Storage of protein lysates for long term periods at -80 ºC was previously advised [12], but -20 ºC is commonly used for shorter storage periods. Therefore, the degradation observed in ALIX after a short storage (1 or 2 weeks) at -20 ºC was rather unexpected.

In summary, the obtained results demonstrate that analysis of ALIX protein expression should be only carried out when using samples which are either fresh or have been properly stored at -80ºC, even for a short time storage period. This would avoid misleading information resulting from the analysis of ALIX expression in protein lysates which have not been properly frozen to avoid its degradation.

Yours sincerely,
Vanessa Lopes-Rodrigues
Cristina P. R. Xavier
Diana Sousa
Hugo Osório
Raquel T. Lima
M. Helena Vasconcelos

Acknowledgments

This letter is a result of the project NORTE-01-0145-FEDER-000029, supported by Norte Portugal Regional Programme (NORTE 2020), under the PORTUGAL 2020 Partnership Agreement, through the European Regional Development Fund (ERDF). This work was partially financed by FEDER - Fundo Europeu de Desenvolvimento Regional funds through the COMPETE 2020 - Operacional Programme for Competitiveness and Internationalisation (POCI), Portugal 2020, and by Portuguese funds through FCT - Fundação para a Ciência e a Tecnologia/ Ministério da Ciência, Tecnologia e Inovação in the framework of the project "Institute for Research and Innovation in Health Sciences" (POCI-01-0145-FEDER-007274). The authors thank the Portuguese Foundation for Science and Technology (FCT) for the PhD grants of VLR and DS (SFRH/BD/87646/2012 and SFRH/BD/98054/2013 respectively) and for the post-doc grant of RTL (SFRH/BPD/68787/2010).

References

1 S, E. L. A., Mager, I., Breakefield, X. O. & Wood, M. J. Extracellular vesicles: biology and emerging therapeutic opportunities. *Nature reviews. Drug discovery* **12**, 347-357, doi:10.1038/nrd3978 (2013).

2 Odorizzi, G. The multiple personalities of Alix. *J Cell Sci* **119**, 3025-3032, doi:10.1242/jcs.03072 (2006).

3 Matsuo, H. *et al.* Role of LBPA and Alix in multivesicular liposome formation and endosome organization. *Science* **303**, 531-534, doi:10.1126/science.1092425 (2004).

4 Fujii, K., Hurley, J. H. & Freed, E. O. Beyond Tsg101: the role of Alix in 'ESCRTing' HIV-1. *Nat Rev Microbiol* **5**, 912-916, doi:10.1038/nrmicro1790 (2007).

5 Zhao, C. *et al.* The role of Alix in the proliferation of human glioma cells. *Hum Pathol* **52**, 110-118, doi:10.1016/j.humpath.2015.09.046 (2016).

6 Christ, L. *et al.* ALIX and ESCRT-I/II function as parallel ESCRT-III recruiters in cytokinetic abscission. *J Cell Biol* **212**, 499-513, doi:10.1083/jcb.201507009 (2016).

7 Baietti, M. F. *et al.* Syndecan-syntenin-ALIX regulates the biogenesis of exosomes. *Nat Cell Biol* **14**, 677-685, doi:10.1038/ncb2502 (2012).

8 Mi, S. *et al.* Budding of Tiger Frog Virus (an Iridovirus) from HepG2 Cells via Three Ways Recruits the ESCRT Pathway. *Sci Rep* **6**, 26581, doi:10.1038/srep26581 (2016).

9 Ghossoub, R. *et al.* Syntenin-ALIX exosome biogenesis and budding into multivesicular bodies are controlled by ARF6 and PLD2. *Nat Commun* **5**, 3477, doi:10.1038/ncomms4477 (2014).

10 Campos, Y. *et al.* Alix-mediated assembly of the actomyosin-tight junction polarity complex preserves epithelial polarity and epithelial barrier. *Nat Commun* **7**, 11876, doi:10.1038/ncomms11876 (2016).

11 Iavello, A. *et al.* Role of Alix in miRNA packaging during extracellular vesicle biogenesis. *Int J Mol Med* **37**, 958-966, doi:10.3892/ijmm.2016.2488 (2016).

12 Simpson, R. J. Stabilization of proteins for storage. *Cold Spring Harb Protoc* **2010**, pdb top79, doi:10.1101/pdb.top79 (2010).

5. RESEARCH ARTICLE

A novel curcumin derivative which inhibits P-glycoprotein, arrests cell cycle and induces apoptosis in multidrug resistant cells

Vanessa Lopes-Rodrigues, Ana Oliveira**,** Marta Correia-da-Silva, Madalena Pinto, Raquel T. Lima, Emília Sousa, M. Helena Vasconcelos

Accepted for publication pending revisions (in Bioorganic & Medicinal Chemistry)

A novel curcumin derivative which inhibits P-glycoprotein, arrests cell cycle and induces apoptosis in multidrug resistant cells

Vanessa Lopes-Rodrigues [1,2,3#], Ana Oliveira [4#], Marta Correia-da-Silva [4,5], Madalena Pinto [4,5], Raquel T. Lima,[1,2,6] Emília Sousa [4,5*], M. Helena Vasconcelos [1,2,7*]

[1] i3S - Instituto de Investigação e Inovação em Saúde, Universidade do Porto, Portugal;

[2] Cancer Drug Resistance Group, IPATIMUP - Institute of Molecular Pathology and Immunology of the University of Porto, IPATIMUP, 4200-465 Porto, Portugal;

[3] ICBAS-UP - Institute of Biomedical Sciences Abel Salazar, University of Porto, ICBAS-UP, 4099-003 Porto, Portugal;

[4] Laboratory of Organic and Pharmaceutical Chemistry, Department of Chemical Sciences, Faculty of Pharmacy, University of Porto, Rua Jorge Viterbo Ferreira, 228, 4050-313 Porto, Portugal;

[5] CIIMAR/CIMAR - Interdisciplinary Centre of Marine and Environmental Research, University of Porto, Portugal;

[6] Department of Pathology and Oncology, FMUP - Faculty of Medicine of the University of Porto, Porto, Portugal, Alameda Prof. Hernâni Monteiro, 4200-319 Porto, Portugal;

[7] Department of Biological Sciences, FFUP - Faculty of Pharmacy, University of Porto, 4050-313 Porto, Portugal.

# These authors equally contributed to this work

* Corresponding authors; E-Mail: esousa@ff.up.pt; hvasconcelos@ipatimup.pt

Abstract

Cancer multidrug resistance (MDR) is a major limitation to the success of cancer treatment and is highly associated with the overexpression of drug efflux pumps such as P-glycoprotein (P-gp). In order to achieve more effective chemotherapeutic treatments, it is important to develop P-gp inhibitors to block/decrease its activity.

Curcumin (**1**) is a secondary metabolite isolated from the turmeric of *Curcuma longa* L.. Diverse biological activities have been identified for this compound, particularly, MDR modulation in various cancer cell models. However, curcumin (**1**) has low chemical stability, which severely limits its application. In order to improve stability and P-gp inhibitory effect, two potential more stable curcumin derivatives were synthesized as building blocks, followed by several curcumin derivatives. These compounds were then analyzed in terms of antitumor and anti-P-gp activity, in two MDR and sensitive tumour lines (from chronic myeloid leukaemia and non-small cell lung cancer). We identified from a series of curcumin derivatives a novel curcumin derivative (1,7-*bis*(3-methoxy-4-(prop-2-yn-1-yloxy)phenyl)hepta-1,6-diene-3,5-dione, **10**) with more potent antitumor and anti-P-gp activity than curcumin (**1**). This compound (**10**) was shown to promote cell cycle arrest (at the G2/M phase) and induce apoptosis in the MDR chronic myeloid leukaemia cell line. Therefore, it is a really interesting P-gp inhibitor due to its ability to inhibit both P-gp function and expression.

Keywords: curcumin; curcumin derivatives; multidrug resistance; P-glycoprotein inhibition; antitumor.

1. Introduction

One of the main causes for the failure of cancer therapy is multidrug resistance (MDR) [1]. MDR occurs when cells resist to the treatment with several structurally and functionally different compounds, and may either be intrinsic (occurring from the beginning of the treatment) or acquired (during treatment) [2, 3]. Multiple mechanisms have been identified as being responsible for MDR [4], but although these mechanisms have been intensively studied, not all of them have been completely elucidated. One of those mechanisms is the increasing activity and/or overexpression of drug efflux pumps, such as P-glycoprotein (P-gp).

P-gp is one of the ATP-binding cassette (ABC) transporters whose (over)expression frequently confers chemoresistance in cancer [5, 6] [7, 8]. ABC transporters are active transporter proteins that use the energy derived from the hydrolysis of ATP to ADP to transport their substrates across the cellular membrane, maintaining cellular homeostasis and detoxifying the cells from potentially toxic substances [9, 10]. Consequently, these proteins, and mainly P-gp, have been targets of several studies to identify novel compounds to counteract MDR.

Although most of the compounds that were designed and used as MDR inhibitors did not reach the clinical purpose for which they were developed; the three generations of MDR inhibitors identified so far helped to set ground knowledge for the development of novel inhibitors [11]. In the last decade, several studies have reported natural compounds (such curcumin, **1** or marine compounds) and compounds that were not originally used or approved for MDR cancers (e.g. tyrosine kinase inhibitors) as promising drug candidates to overcome MDR, mostly due to their intrinsic antitumor activity [5, 12]. In particular, great interest has been given to curcumin (**1**) [13, 14] since this major component of turmeric obtained from *Curcuma longa* L. has been shown to overcome MDR in various cancer cell models, also by downregulating *MDR1* gene expression [15].

Curcumin (**1**) has been used in Ayurvedic medicine for thousands of years, for its anti-inflammatory properties and wound healing properties (**Figure 1**) [16-18]. Nowadays, curcumin (**1**) is being extensively studied for its many biological activities and molecular targets. Regarding its anticancer potential, curcumin (**1**) has been described as being responsible for the inhibition of STAT3 and NF-kB signaling pathways [19], associated with cancer development and progression, and as an inducer of apoptosis and cell cycle arrest in tumours/human tumour cell lines [20].

Curcumin (**1**) has low toxicity level, which increases the interest in its possible use as an anticancer agent to overcome MDR. However, due to its low bioavailability and poor solubility [21, 22], it is necessary to obtain derivatives and analogues with similar anticancer

potential but without these disadvantages. Several curcumin (**1**) derivatives have been synthesized since the interest in this natural product and antitumor properties were disclosed [23]. In the present study, we aimed to synthetize new derivatives that could concomitantly reveal tumour cell growth inhibition and P-gp inhibitory activity and to analyze the hit compounds in terms of stability. A new curcumin derivative (1,7-*bis*(3-methoxy-4-(prop-2-yn-1-yloxy)phenyl)hepta-1,6-diene-3,5-dione, **10**) which is more potent than curcumin (**1**) in inhibiting P-gp and decreasing tumour cell growth via cell cycle arrest and induction of apoptosis is described.

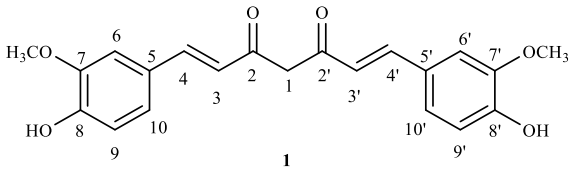

Figure 1 – Chemical structure of curcumin (**1**).

2. Materials and methods

2.1. General Methods

All reagents and solvents were purchased from Sigma-Aldrich, except 2-azidoethyl 2-acetamido-3,4,6-tri-*O*-acetyl-2-deoxy-*β*-D-galactopyranoside which was purchased from LC scientific Inc, Canada (AL356), and had no further purification process, except for 2-bromo-*N*,*N*-diethylethan-1-amine hydrobromide that was submitted to liquid extraction (NaOH, CH_2Cl_2) to be in the non-ionized form. Solvents were evaporated using rotary evaporator under reduced pressure, Buchi Waterchath B-480. All reactions were monitored by thin layer chromatography carried out on precoated plates with 0.2 mm of thickness using Merck silica gel 60 (GF254). MW reactions were performed in glassware open vessel reactors in a MicroSYNTH 1600 Microwave Labstation from Millestone (ThermoUnicam, Portugal). The internal reaction temperature was controlled by a fiber-optic probe sensor. Purification of the synthesized compounds was performed by chromatography flash and semi-flash columns using Merck silica gel 60 (0.040-0.063 mm and 0.063-0.200 mm, respectively), chromatography flash cartridge (GraceResolv®, Grace Company, Deerfield, IL, USA), Discovery® DSC-SAX SPE anionic exchange cartridge, and preparative thin layer chromatography using Merck silica gel HPLC60 RP-18 (GF254) plates (Merck, Germany).

Melting points (mp) were measured in a Köfler microscope and are uncorrected. Infrared (IR) spectra were obtained in KBr microplates in a Fourier transform infrared spectroscopy spectrometer Nicolet iS10 from Thermo Scientific with Smart OMNI-Transmisson accessory (Software OMNIC 8.3) (cm^{-1}). NMR spectra were performed in University of Aveiro, Department of Chemistry, and were taken in $CDCl_3$ (Deutero GmbH) at room temperature (r.t.) on Bruker Avance 300 spectrometer (300.13 MHz for ^{1}H an 75.47 for ^{13}C). ^{13}C NMR assignments were made by 2D (HSQC and HMBC) NMR experiments (long-range ^{13}C-^{1}H coupling constants were optimized to 7 Hz).

Analytical HPLC-DAD (high-performance liquid chromatography-diode array detector) analyses were performed on a SpectraSYSTEM (Thermo Fisher Scientific, Inc, USA) equipped with a P4000 pump, a AS3000 autosampler and a diode array detector UV8000. The separation was carried out on a 250 × 4.6 mm i.d. FortisBIO C18 (5 µm) (Fortis™ Technologies Ltd, Cheshire, UK). ChromQuest 5.0 (version 3.2.1) software (Thermo Fisher Scientific Inc.) managed chromatographic data. Methanol (HPLC grade) was obtained from Carlo Erba Reagents, (Val de Reuil, Italy), acetic acid (HPLC grade) was obtained from Romil Pure Chemistry (Cambridge, UK) and HPLC grade water (Simplicity® UV Ultrapure Water System, Millipore Corporation, USA). Prior to use, mobile phase solvents were degassed in an ultrasonic bath for 15 min. All samples were dissolved and filtered through a PTFE syringe filter of 0.2 µm pore size and 4 mm diameter (Thermo Fisher Scientific) before injection. To determine the purity of compounds **2**, **4**, **5** and **11**, HPLC analysis was performed by isocratic elution using a mixture of MeOH:H_2O:acetic acid (50:50:1), for compound **8** a mixture of MeOH:H_2O:TEA (50:50:1), and for compounds **3** and **10** a mixture of MeOH:H_2O:TEA (70:30:1) as mobile phase. The flow rate was set at 1 mL/ min. The injected volume was 10 µL and the eluent was monitored at 254 nm for every compound except compound **3** which was monitored at 399 nm. The final concentration of the tested compounds was 100 µg/mL. The detector was set at a wavelength range of 220–500 nm with a spectral resolution of 1 nm. The purity parameters included a 95% active peak region and a scan threshold of 5 mAU. With these general conditions compounds **6** and **7** could not be detected (with different mobile phases, with and without ionic suppressors).

Qualitative GC-MS analyses were performed on a Trace GC 2000 Series ThermoQuest gas chromatography equipped with ion-trap GCQ Plus ThermoQuest Finnigan mass detector. Chromatographic separation was achieved using a capillary columm (30 m × 0.25 mm × 0.25 µm, cross-linked 5% diphenyl and 95% dimethyl polysiloxane) from Thermo Scientific™ and high-purity helium C-60 as carrier gas. An initial temperature of 80 ºC was maintained for 1 min, increased to 310 ºC at 10 ºC/min, and held for 5 min giving a total run time of 33 min. The flow of the carrier gas was maintained at 1.5

mL/min. The injector port was set at 280 ºC. Analyses were performed with splitless injection in the full-scan mode in the scan range of m/z 50-700. For derivatized samples 30 µL of *N*-methyl-*N*-(trimethylsilyl)trifluoroacetamide were added and samples heated at 80ºC for 30 min to accomplish silylation. An aliquot of 1 µL of the derivatized extract was injected into the GC-MS system. HRMS (high resolution mass spectrometry) results were obtained in the services of C.A.C.T.I. (Vigo, Spain).

2.2. Synthesis

2.2.1. Synthesis of 4-(4-hydroxy-3-methoxyphenyl)but-3-en-2-one (2)

Compound **2** was synthesized and isolated according to a previously described protocol [24].

Yield: 64%. mp 127-129^{o}C (EtOH) (lit. 127-128 ^{o}C *n*-hexane: ethyl acetate (EtOAc) [24]). Purity: 96%. ^{1}H NMR ($CDCl_3$, 300 MHz) δ: 7.45 (1H, *d*, *J*= 16.2 Hz, H-3), 7.09 (1H, *dd*, *J*= 8.1 and 1.9, H-6'), 7.05 (1H, *d*, *J*= 1.9, H-2'), 6.93 (1H, *d*, *J*= 8.1 Hz, H-5'), 6.59 (1H, *d, J*= 16.2 Hz, H-2), 6.00 (1H, *s*, H-4'), 3.92 (3H, *s*, 3'-OCH_3), 2.37 (3H, *s*, H-1''); ^{13}C NMR (75.47 MHz, $CDCl_3$) δ: 198.7 (C-1), 148.4 (C-4'), 147.0 (C-3'), 144.0 (C-3), 126.8 (C-1'), 124.9 (C-2), 123.6 (C-6'), 114.9 (C-5'), 109.4 (C-2'), 56.0 (3'-OCH_3), 27.3 (C-1'').

2.2.2. Synthesis of 1,5-bis(4-hydroxy-3-methoxyphenyl)penta-1,4-dien-3-one (3)

Compound **3** was synthesized and isolated according to a previously described protocol [25].

Yield: 5%. mp 74-79^{o}C (*n*-hexane:EtOAc) (lit. mp 68-70^{o}C MeOH [25]). Purity 72%. ^{1}H NMR ($CDCl_3$, 300 MHz) δ: 7.68 (2H, *d*, *J*= 15.5 Hz, H-3), 7.18 (2H, *dd*, *J*= 8.2 and 1.8 Hz, H-6'), 7.11 (2H, *d*, *J*= 1.8 Hz, H-2'), 6.92 (2H, *d*, *J*= 8.2 Hz, H-5'), 6.94 (2H, *d*, *J*= 15.5 Hz), 5.99 (2H, *brs*, H-4'), 3.95 (6H, *s*, 3'-OCH_3); ^{13}C NMR (75.47 MHz, $CDCl_3$) δ: 188.9 (C-1), 148.2 (C-4'), 147.2 (C-3'), 143.3 (C-3), 127.5 (C-1'), 123.4 (C-2), 123.3 (C-6'), 114.9 (C-5'), 109.8 (C-2'), 56.0 (3'-OCH_3). HRMS- Electrospray ionization (ESI) (+) *m/z*: Anal. Calc. for $C_{19}H_{19}O_5$ $[M-H]^+$ 327.123250, found: 327.12265.

2.2.3. Synthesis of 4-(4-(allyloxy)-3-methoxyphenyl)but-3-en-2-one (4)

To a solution of 4-(4-hydroxy-3-methoxyphenyl)but-3-en-2-one (**2**, 102.9 mg, 0.315 mmol) and allyl bromide (60 µL, 0.693 mmol) in acetone (20 mL), Cs_2CO_3 (121.2 mg, 0.37 mmol) was added and placed in a opened microwave reactor. The mixture under stirring was irradiated at 200 W for 2 h, at a final temperature of 65°C. The solid was then removed by filtration with a sintered glass Buchner funnel under reduced pressure. The yellow-orange solution was evaporated and the product purified by semi-flash chromatography (SiO_2; petroleum ether: diethyl ether: several proportions). The fractions that eluted with petroleum ether: diethyl ether 8:2 were gathered and concentrated furnishing a yellow solid of 4-(4-(allyloxy)-3-methoxyphenyl)but-3-en-2-one (**4**, 70 mg, 56%).

mp 52-55°C (petroleum ether: diethyl ether). Purity 98%. IR (KBr) u_{max} cm^{-1} 2960, 2924, 1664, 1639, 1624, 1593, 1511, 1418, 1362, 1252, 1164, 1134, 997, 969, 800. ^1H NMR ($CDCl_3$, 300 MHz) δ: 7.46 (1H, *d*, *J*= 16.2 Hz, H-3), 7.11 (1H, *d*, *J*= 2.0 Hz, H-6'), 7.08 (1H, *s*, H-2'), 6.88 (1H, *d*, *J*= 8.1 Hz, H-5'), 6.61 (1H, *d*, *J*= 16.2 Hz, H-2), 6.15-6.02 (1H, *m*, -*H*C=CH_2), 5.46-5.39 (1H, *m*, -HC=CH_2), 5.35-5.30 (1H, *m*, -HC=CH_2), 4.67-4.65 (2H, *dt*, *J*= 5.4 and 1.4 Hz, 4'-OCH_2-), 3.92 (3H, *s*, 3'-OCH_3), 2.38 (3H, *s*, H-1''); ^{13}C NMR (75.47 MHz, $CDCl_3$) δ: 198.4 (C-1), 150.3 (C-4'), 149.6 (C-3'), 143.6 (C-3), 132.7 (-H*C*=CH_2), 127.5 (C-1'), 125.3 (C-2), 122.8 (C-6'), 118.5 (-HC=*C*H_2), 112.8 (C-5'), 110.0 (C-2'), 69.7 (4'-O*C*H_2-), 55.9 (3'-O*C*H_3), 27.4 (C-1''). EI-MS (70 eV) *m/z* (rel. Intensity, %): 233 (M^{+1}, 18), 232 (M^+, 100), 191 (95), 163 (28), 135 (22). HRMS- ESI (+) *m/z*: Anal. Calc. for $C_{14}H_{16}O_3$ $[M-H]^+$ 233.11777, found 233.11722.

2.2.4. Synthesis of 4-(3-methoxy-4-(prop-2-yn-1-yloxy)phenyl)but-3-en-2-one (5)

4-(4-Hydroxy-3-methoxyphenyl)but-3-en-2-one (**2**, 1.00 g, 3.07 mmol) and propargyl bromide (1 mL, 11.22 mmol) were dissolved in acetone (180 mL), Cs_2CO_3 (680.03 mg, 2.08 mmol) was added and placed in an open vessel microwave reactor. The mixture under stirring was irradiated at 200 W for 1h 30 min, at a final temperature of 65°C. The solid was then removed by filtration with a sintered glass Buchner funnel under reduced pressure. The yellow solution was concentrated and the product submitted to a semi-flash chromatography (SiO_2; petroleum ether: diethyl ether: several proportions). The fractions that eluted with petroleum ether: diethyl ether 8:2 were gathered and after solvent evaporation a recrystallization from diethyl ether: petroleum ether (4:1) was performed providing a white solid of 4-(3-methoxy-4-(prop-2-yn-1-yloxy)phenyl)but-3-en-2-one (**5**, 101 mg, 8%).

mp 110-111°C (diethyl ether: petroleum ether). Purity 96%. IR (KBr) u_{max} cm^{-1} 3258, 2922, 2851, 1673, 1597, 1515, 1424, 1372, 1272, 1247, 1225, 1168, 1145, 1034, 1006, 984, 805, 723, 682. ^{1}H NMR ($CDCl_3$, 300 MHz) δ: 7.46 (1H, *d*, *J*= 16.2 Hz, H-3), 7.13 (1H, *d*, *J*= 8.2 Hz, H-6'), 7.09 (1H, *s*, H-2'), 7.04 (1H, *d*, *J*= 8.2 Hz, H-5'), 6.62 (1H, *d*, *J*= 16.2 Hz, H-2), 4.81 (2H, *s*, 4'-OCH_2-), 3.91 (3H, *s*, 3'-OCH_3), 2.53 (1H, *s*, -C≡C*H*), 2.37 (3H, *s*, H-1''); ^{13}C NMR (75.47 MHz, $CDCl_3$) δ: 198.4 (C-1), 149.8 (C-4'), 149.0 (C-3'), 143.3 (C-3), 128.5 (C-1')125.7 (C-2), 122.5 (C-6'), 113.6 (C-5'), 110.2 (C-2'), 77.9 (-*C*≡CH), 76.3 (-C≡*C*H), 56.6 (4'-O*C*H_2-), 55.9 (3'-O*C*H_3), 27.4 (C-1''). EI-MS (70 eV) *m/z* (rel. intensity, %): 231 (M^{+1}, 25), 230 (M^+, 88), 191 (100), 163 (22). HRMS- ESI (+) *m/z*: Anal. Calc. for $C_{14}H_{14}O_3$ $[M-H]^+$ 231.10212, found 231.10157.

2.2.5. Synthesis of 4-(4-(2-(diethylamino)ethoxy)-3-methoxyphenyl)but-3-en-2-one (6)

To a solution of 4-(4-hydroxy-3-methoxyphenyl)but-3-en-2-one (**2**, 106.1 mg, 0.325 mmol) and 2-bromo-*N*,*N*-diethylethan-1-amine (175.1 mg, 0.972 mmol) in acetone (20 mL), K_2CO_3 (174.7 mg, 1.26 mmol) was added and placed in a opened microwave reactor. The mixture under stirring was irradiated at 200 W for 3h, at a final temperature of 65°C. When the reaction was finished, the solid was removed by filtration with a sintered glass Buchner funnel under reduced pressure. After removal of acetone under reduced pressure the crude product was dissolved in dichloromethane, acidified with an aqueous solution of HCl 5N and extracted with H_2O. The aqueous phase was basified with a 20% NaOH aqueous solution and extracted with CH_2Cl_2 (3 × 100 mL). The organic phase was dried with anhydrous sodium sulfate, filtrated, and concentrated under reduced pressure to furnish a yellow solid of 4-(4-(2-(diethylamino)ethoxy)-3-methoxyphenyl)but-3-en-2-one (**6**, 5.0 mg, 3%).

mp 207-209 °C (CH_2Cl_2). IR (KBr) u_{max} cm^{-1} 2959, 2925, 2855, 1729, 1629, 1425, 1384, 1273, 1124, 669 . ^{1}H NMR ($CDCl_3$, 300 MHz) δ: 7.46 (1H, *d*, *J*= 16.2 Hz, H-3), 7.11 (1H, *dd*, *J*= 8.3 and 1.9 Hz, H-6'), 7.07 (1H, *d*, *J*= 1.9 Hz, H-2'), 6.91 (1H, *d*, *J*= 8.3 Hz, H-5'), 6.61 (1H, *d*, *J*= 16 Hz, H-2), 4.24 (2H, *t*, *J*= 6.2 Hz, H-7'), 3.89 (3H, *s*, 3'-OCH_3), 3.08 (2H, t, *J*= 6.2 Hz, H-8'), 2.81 (4H, *q*, *J*= 7.2 Hz, H-9'), 2.38 (3H, s, H-1''). 1.17 (6H, *t*, *J*= 7.2 Hz, H-10'); ^{13}C NMR ($CDCl_3$, 75.47 MHz) δ: 198.4 (C-1), 150.3 (C-4'), 149.6 (C-3'), 143.5 (C-3), 127.8 (C-1'), 125.4 (C-2), 122.9 (C-6'), 112.7 (C-5'), 110.0 (C-2'), 66.4 (C-7'), 55.9 (3'-O*C*H_3), 51.2 (C-8'), 47.7 (C-9'), 27.4 (C-1''), 11.0 (C-10'). HRMS- ESI (+) *m/z*: Anal. Calc. for $C_{17}H_{25}NO_3$ $[M-H]^+$ 292.19127, found 292.19072.

2.2.6. Synthesis of tert-butyl (2-(2-methoxy-4-(3-oxobut-1-en-1-yl)phenoxy)ethyl)carbamate (7)

4-(4-Hydroxy-3-methoxyphenyl)but-3-en-2-one (**2**, 202.5 mg, 0.621 mmol), 2-(boc-amino) and ethyl bromide (274 mg, 1.22 mmol) were dissolved in acetone (40 mL), K_2CO_3 (204.5 mg, 1.48 mmol) was added and placed in a opened microwave reactor. The mixture under stirring was irradiated at 200 W for 3 h, at a final temperature of 65 ^oC. The solid was removed by filtration with a sintered glass Buchner funnel under reduced pressure. The yellow solution was purified by semi-flash chromatography (SiO_2; petroleum ether: diethyl ether: several proportions). The fractions that eluted with petroleum ether: diethyl ether 7:3 were gathered and the product purified by preparative chromatography with $CHCl_3$: acetone: trielthylamine (9:1:0.1) affording an yellow solid of *tert*-butyl (2-(2-methoxy-4-(3-oxobut-1-en-1-yl)phenoxy)ethyl)carbamate (**7**, 4 mg, 1.1%).

mp 89-92 ^oC ($CHCl_3$: acetone). IR (KBr) u_{max} cm^{-1} 3447, 2920, 2852, 1636, 1385, 1099, 668. ^1H NMR ($CDCl_3$, 300 MHz) δ: 7.45 (1H, *d*, *J*= 16.2 Hz, H-3), 7.10 (1H, *dd*, *J*= 8.1 and 1.8 Hz, H-6'), 7.06 (1H, *d*, *J*= 1.8 Hz, H-2'), 6.94 (1H, *d*, *J*=8.1 Hz, H-5'), 6.59 (1H, *d*, *J*= 16.2 Hz, H-2), 4.91 (2H, *m*, H-7'), 3.94 (3H, *s*, 3'-OCH_3), 3.23-3.18 (2H, *m*, H-7'), 2.37 (3H, *s*, H-1''), 2.17 (9H, *s*, H-10'); ^{13}C NMR (75.47 MHz, $CDCl_3$) δ: 198.5 (C-1), 160.5 (C-9'), 148.2 (C-4'), 146.9 (C-3'), 143.8 (C-3), 127.0 (C-1'), 125.0 (C-2), 123.6 (C-6'), 114.8 (C-5'), 109.3 (C-2'), 68.2 (C-7'), 56.0 (3'-OCH_3), 29.7 (C-11'), 27.3 (C-1''). EI-MS (70e V) *m/z* (rel. intensity, %): 335 (M^+, 26), 281 (100), 234 (63), 74 (82). HRMS- ESI (+) *m/z*: Anal. Calc. for $C_{18}H_{25}NO_5$ $[M-H+Na]^+$ 358.18109, found 358.16249.

2.2.7. Synthesis of tert-butyl (3-(2-methoxy-4-(3-oxobut-1-en-1-yl)phenoxy)propyl)carbamate (8)

A mixture of 4-(4-hydroxy-3-methoxyphenyl)but-3-en-2-one (**2**) (101.6 mg, 0.311 mmol), 3-(boc-amino) propyl bromide (137 mg, 0.575 mmol), K_2CO_3 (105.2 mg, 0.76 mmol), and acetone (30 mL), was placed in an opened microwave reactor. The mixture under stirring was irradiated at 200 W for 3 h, at a final temperature of 65 ^oC. The solid was removed by filtration with a sintered glass Buchner funnel under reduced pressure. The yellow solution was purified by semi-flash chromatography (SiO_2; *n*-hexane: diethyl ether: several proportions). The fractions that eluted with *n*-hexane: diethyl ether 7.5:2.5 were gathered and after solvent evaporation a recrystallization from diethyl ether: petroleum ether (4:1) was performed providing a yellow solid of *tert*-butyl (3-(2-methoxy-4-(3-oxobut-1-en-1-yl)phenoxy)propyl)carbamate (**8**,16.6 mg, 9%).

mp 108-110°C (diethyl ether: petroleum ether). Purity 96%. IR (KBr) u_{max} cm^{-1} 3377, 1686, 1669, 1644, 1621, 1595, 1518, 1273, 1260, 1225, 1167, 1138, 1033, 975. ^1H NMR ($CDCl_3$, 300 MHz) δ: 7.46 (1H, *d*, *J*= 16.2 Hz, H-3), 7.11 (1H, *d*, *J*= 8.2 Hz, H-6'), 7.07 (1H, *s*, H-2'), 6.86 (1H, *d*, *J*= 8.2 Hz, H-5'), 6.61 (1H, *d*, *J*= 16.2 Hz, H-2), 5.50 (1H, *brs*, H-10') 4.14 (2H, *t*, *J*= 5 Hz, H-7'), 3.92 (3H, *s*, 3'-OCH_3), 3.38 (2H, *d*, *J*= 5 Hz, H-9'), 2.38 (3H, *s*, H-1''), 2.04 (2H, *t*, *J*= 5 Hz, H-8'), 1.46 (9H, *s*, H-11'); ^{13}C NMR (75.47 MHz, $CDCl_3$) δ: 198.4 (C-1), 156.1 (C-10'), 150.5 (C-4'), 149.5 (C-3'), 143.5 (C-3), 127.6 (C-1'), 125.3 (C-2), 122.9 (C-6'), 112.2 (C-5'), 109.7 (C-2'), 79.0 (C-11'), 68.2 (C-7'), 55.8 (3'-OCH_3), 38.9 (C-9'), 30.9 (C-8'), 28.5 (C-12'), 27.4 (C-1''). EI-MS (70e V) *m/z* (rel. Intensity, %): 349 (M^+, 96), 308 (32), 261 (38), 253 (52). HRMS- ESI (+) *m/z*: Anal. Calc. for $C_{19}H_{27}NO_5$ $[M-H]^+$ 350.19675, found 350.19620.

2.2.8. Synthesis of methyl 2-(2-methoxy-4-(3-oxobut-1-en-1-yl)phenoxy)acetate (9)

4-(4-Hydroxy-3-methoxyphenyl)but-3-en-2-one (**2**, 150 mg, 0.78 mmol) and methyl 2-bromoacetate (80 µL; 0.78 mmol) were dissolved in acetone (20 mL) and K_2CO_3 (261 mg; 1.89 mmol) was added. The mixture was placed in an opened microwave reactor where it was irradiated at 200 W for 3 h, at a final temperature of 65 °C with stirring. The solid was removed by filtration with a sintered glass Buchner funnel under reduced pressure. After acetone evaporation, the crude product was dissolved in a basified aqueous solution with 20% NaOH and extracted with CH_2Cl_2 (3 × 100 mL). The organic phase was dried by anhydrous sodium sulfate, filtrated, and concentrated under reduced pressure to furnish a yellow solid of methyl 2-(2-methoxy-4-(3-oxobut-1-en-1-yl)phenoxy)acetate (**9**, 7.9 mg, 4%).

mp 79-81°C (CH_2Cl_2). IR (KBr) u_{max} cm^{-1} 2918, 2849, 1733, 1634, 1515, 1463, 1262, 1111, 668. ^1H NMR ($CDCl_3$, 300 MHz) δ:7.45 (1H, *d*, *J*= 16.2 Hz, H-3), 7.09 (2H, *dd*, *J*= 6.7 and 1.9 Hz, H-6' and H-2'), 6.80 (1H, *d*, *J*= 6.7 Hz, H-5'), 6.61 (1H, *d*, *J*= 16.2 Hz, H-2), 4.76 (2h, *s*, H-7'), 3.93 (3H, *s*, 3'-OCH_3), 3.81 (3H, *s*, H-8'), 2.38 (3H, *s*, H-1''); ^{13}C NMR (75.47 MHz, $CDCl_3$) δ: 198.4 (C-1), 169. (C-8'), 149.7 (C-4'), 149.3 (C-3'), 143.2 (C-3), 128.8 (C-1'), 125.5 (C-2), 122.5 (C-6'), 113.4 (C-5'), 110.5 (C-2'), 66.0 (C-7'), 56.0 (3'-OCH_3), 52.4 (C-9'), 27.4 (C-1''). HRMS- ESI (+) *m/z*: Anal. Calc. for $C_{14}H_{16}O_5$ $[M-H]^+$ 265.10760, found 265.10705.

2.2.9. Synthesis of 1,7-bis(3-methoxy-4-(prop-2-yn-1-yloxy)phenyl)hepta-1,6-diene-3,5-dione (10)

Curcumin (**1**) (500 mg, 1.35 mmol), anhydrous Cs_2CO_3 (4.40 g, 13.5 mmol; 5 equiv/OH) and Bu_4NBr (4.35 g, 13.5 mmol; 5 equiv/OH), were mixed in acetone (10 mL), then propargyl bromide solution (80% wt % in toluene, 2 mL; 5 equiv/OH) was added. The mixture was refluxed at 60°C during 4 h and filtered. After concentration under reduced pressure, the residue was dissolved in $CHCl_3$ and extracted twice with aqueous NaOH 20%. The combined organic layers were dried over anhydrous sodium sulfate, filtered, concentrated under reduced pressure, and then purified by crystallization with $CHCl_3$/EtOH to give a orange solid of 1,7-bis(3-methoxy-4-(prop-2-yn-1-yloxy)phenyl)hepta-1,6-diene-3,5-dione (**10**, 86.30 mg, 14%).

mp: 149-151 °C ($CHCl_3$/EtOH). Purity 94%. IR (KBr) υ_{max} cm^{-1} 3287, 2920, 2850, 1671, 1592, 1507, 1464, 1423, 1375, 1265, 1221, 1167, 1139, 1080, 1020, 807, 669. ^1H NMR ($CDCl_3$, 300 MHz) δ: 7.74 (2H, *d*, *J*=15.0 Hz, H-4, H-4'), 7.15 (2H, *dd*, *J*=8.4 and 2.0 Hz, H-10, H10'), 7.03 (2H, *d*, *J*=2.0 Hz, H-9, H-9'), 6.99 (2H, *s*, H-6, H-6'), 6.67 (2H, *d*, *J*=15.0 Hz, H-3, H-3'), 4.81-4.79 (4H, *s*, 8-OCH_2-, 8'-OCH_2-), 3.91 (6H, *s*, 7-OCH_3, 7'-OCH_3), 3.17 (2H, d, *J*=2.0 Hz, H-1), 2.52 (2H, *s*, -C≡C*H*, -C≡C*H*'). ^{13}C NMR (75.47 MHz, $CDCl_3$) δ: 193.5 (C-2), 149.7 (C-8), 149.5 (C-7), 145.6 (C-4), 127.9 (C-5), 123.5 (C-3), 118.4 (C-10), 113.4 (C-9), 110.7 (C-6), 78.9 (-<u>C</u>≡C*H*), 72.1 (-C≡<u>C</u>*H*), 56.5 (8-O<u>C</u>H_2-), 56.1 (7'-OCH_3), 21.2 (C-1). HRMS (ESI+) *m/z* Anal. Calc. for $C_{27}H_{25}O_6$ $[M-H]^+$ 445.16456, found 445.16442.

2.2.10. Synthesis of (2R,4S,5R)-5-acetamido-2-(acetoxymethyl)-6-(2-(4-((2-methoxy-4-((E)-3-oxobut-1-en-1-yl)phenoxy)methyl)-1H-1,2,3-triazol-1-yl)ethoxy)tetrahydro-2H-pyran-3,4-diyl diacetate (11)

A mixture of 4-(3-methoxy-4-(prop-2-yn-1-yloxy)phenyl)but-3-en-2-one (**5**, 60.0 mg, 0.149 mmol), 2-azidoethyl 2-acetamido-3,4,6-tri-*O*-acetyl-2-deoxy-*β*-D-galactopyranoside (123.6 mg, 0.297 mmol), $CuSO_4.5H_2O$ (80.1 mg, 0.32 mmol), sodium ascorbate (131.1 mg, 0.66 mmol) and tetrahydrofuran/ H_2O solvent mixture (2:1; 7 mL), were placed in a opened microwave reactor. The non-homogeneous mixture under stirring was irradiated at 200 W for 10 min, at a final temperature of 70°C. After filtration, THF was evaporated under reduced pressure and the aqueous solution was extracted with $CHCl_3$ (3 x 100 mL). The organic phase was dried with anhydrous sodium sulfate, filtrated and concentrated under reduced pressure to furnish a light-brown solid of (2*R*,4*S*,5*R*)-5-acetamido-2-

(acetoxymethyl)-6-(2-(4-((2-methoxy-4-((*E*)-3-oxobut-1-en-1-yl)phenoxy)methyl)-1*H*-1,2,3-triazol-1-yl)ethoxy)tetrahydro-2*H*-pyran-3,4-diyl diacetate (**11**, 63.4 mg, 38%).

mp 84-86°C ($CHCl_3$). Purity 97%. IR (KBr) υ_{max} cm^{-1} 1748, 1667, 1596, 1513, 1424, 1371, 1251, 1165, 1140, 1083, 1047. ^1H NMR ($CDCl_3$, 300 MHz) δ: 7.83 (1H, *s*, -C=C*H*-N), 7.45 (1H, *d*, *J*= 16.2 Hz, H-3), 7.12-7.08 (3H, *m*, H-6', H-2' and H-5'), 6.61 (1H, *d*, *J*= 16.2 Hz, H-2), 5.54 (1H, *d*, *J*= 8.8 Hz, 7''-N*H*), 5.32 (2H, *dd*, *J*= 13.1 Hz, -N-CH_2-CH_2-O-), 5.30 (1H, *s*, -O-CH_2-triazole), 5.15 (1H, *dd*, *J*= 13.1 and 3.2 Hz, N-CH_2-CH_2-O-), 4.65-4.55 (3H, *m*, H-6''', H-7''', and H-8'''), 4.30-4.25 (1H, *m*, H-9'''), 4.13 (1H, *d*, *J*= 1.68 Hz, -CH_2-OAc), 4.07-4.00 (1H, *d*, -CH_2-OAc), 4.07-4.00 (1H, *m*, H-10'''), 3.89 (3H, *s*, 3'-OCH_3), 2.37 (3H, *s*, H-1''), 2.15, 2.04, 1.99 (9H, *s*, -COCH_3), 1.85 (3H, *s*, -COCH_3); ^{13}C NMR (75.47 MHz, $CDCl_3$) δ: 198.2 (C-1), 170.7 (7''-NH-*C*=O), 170.4 (O=*C*-CH_3 and O=*C*-CH_3), 170.1 (O=*C*-CH_3), 149.9 (C-4'), 149.6 (C-3'), 143.2 (C-3), 143.2 (-*C*=CH-N), 128.2 (C-1'), 125.7 (C-2), 125.7 (-C=*C*H-N), 122.9 (C-6'), 113.6 (C-5'), 110.3 (C-2'), 101.0 (C-6'''), 70.9 (C-10'''), 69.8 (C-8'''), 67.4 (-N-CH_2-*C*H_2-O-), 66.1 (C-9'''), 62.8 (-O-*C*H_2-triazole), 61.4 (-*C*H_2-OAc), 55.9 (3'-O*C*H_3), 51.2 (C-7'''), 50.2 (-N-*C*H_2-CH_2-O), 27.4 (C-1''), 23.2 (O=C-*C*H_3), 20.7 (O=C-*C*H_3 and O=C-*C*H_3), 20.6 (O=C-*C*H_3). HRMS- ESI (+) *m/z*: Anal. Calc. for $C_{30}H_{38}N_4O_{12}$ $[M-H]^+$ 647.25645, found 647.25590.

2.2.11. Synthesis of (2S,4R,5S)-5-acetamido-6-(2-(4-((4-((1E,6E)-7-(4-((1-(2-(((3R,4S,6R)-3-acetamido-4,5-diacetoxy-6-(acetoxymethyl)tetrahydro-2H-pyran-2-yl)oxy)ethyl)-1H-1,2,3-triazol-4-yl)methoxy)-3-methoxyphenyl)-3,5-dioxohepta-1,6-dien-1-yl)-2-methoxyphenoxy)methyl)-1H-1,2,3-triazol-1-yl)ethoxy)-2-(acetoxymethyl)tetrahydro-2H-pyran-3,4-diyl diacetate (12)

A mixture of 1,7-bis(3-methoxy-4-(prop-2-yn-1-yloxy)phenyl)hepta-1,6-diene-3,5-dione (**10**, 60.0 mg, 0.13 mmol), 2-azidoethyl 2-acetamido-3,4,6-tri-*O*-acetyl-2-deoxy-*β*-D-galactopyranoside (123.6 mg, 0.297 mmol), $CuSO_4.5H_2O$ (80.1 mg, 0.32 mmol), sodium ascorbate 131.1 mg, 0.66 mmol) and tetrahydrofuran/H_2O solvent mixture (2:1; 10 mL), were placed in a opened microwave reactor. The non-homogeneous mixture under stirring was irradiated at 200 W for 15 min, at a final temperature of 70°C. After filtration, THF was evaporated under reduced pressure. Insolubilization of the product was verified during liquid-liquid extraction with EtOAc (3 x 100 mL) furnishing a brown solid of (2S,4R,5S)-5-acetamido-6-(2-(4-((4-((1E,6E)-7-(4-((1-(2-(((3R,4S,6R)-3-acetamido-4,5-diacetoxy-6-(acetoxymethyl)tetrahydro-2*H*-pyran-2-yl)oxy)ethyl)-1*H*-1,2,3-triazol-4-yl)methoxy)-3-methoxyphenyl)-3,5-dioxohepta-1,6-dien-1-yl)-2-methoxyphenoxy)methyl)-1*H*-1,2,3-

triazol-1-yl)ethoxy)-2-(acetoxymethyl)tetrahydro-2*H*-pyran-3,4-diyl diacetate (**12**, 66 mg, 40 %).

mp: 167-170 ^{o}C (MeOH). IR (KBr) υ_{max} cm^{-1} 2921, 2851, 1744, 1659, 1578, 1510, 1466, 1375, 1260, 1139, 1049. ^{1}H NMR ($CDCl_3$, 300 MHz) δ: 8.07 (1H, *s*, -C=C*H*-N), 7.80-6.98 (5H, *m*, H-4, H-10, H-6, H-9, H-3), 5.22-5.14 (2H, -N-CH_2-CH_2-O-, 7''-N*H*), 4.96-4.93 (2H, *m*, -O-CH_2-triazole, N-CH_2-CH_2-O-), 4.57-4.50 (4H, *m*, H-6''', H-7''', H-8''', H-9'''), 4.05-3.78 (8H, *s*, 7-OCH_3, -CH_2-OAc, H-10''', H-1a, H-1b), 2.10, 1.99, 1.89, 1.70 (12H, *s*, COCH_3).

2.3. Stability studies

Standard solutions of curcumin (**1**), compound **2**, **3**, and **10** were prepared and injected in the HPLC equipment with a final concentration of 1 mg/mL in DMSO, at r.t. and immediately after being prepared. Regarding pH stability assay, five pH values were selected and obtained with following buffers: HCl pH 1.0, sodium acetate pH 5.0, potassium phosphate pH 6.7, PBS pH 7.4, and sodium boric acid pH 9.1. A stock solution of each compound was prepared with the initial concentration of 10^{-2} M in DMSO. Then the compounds were dissolved in each buffer in a final concentration of 10^{-4} M. The solutions were allowed to incubate overnight at r.t., except in HCl buffer that incubated only for 75 min, protected from light exposure. After overnight or 75 min of incubation, certain compounds precipitated. In such cases, the precipitate was filtrated and dissolved in 4 mL of MeOH before being also injected.

The biological buffer assay was performed with cell culture medium. Cell culture medium composition was: 87.5 % RPMI medium, 2.5% *N*-2-hydroxyethylpiperazine-*N*'-2-ethanesulfonic acid (HEPES) supplemented with10% fetal bovine serum (FBS). The compounds were incubated for 5, 10, 20, and 30 min at 37 ^{o}C in biological buffer, protected from light exposure, at a final concentration of 1.5 × 10^{-3} M. Before being injected the samples were filtrated.

Solutions at 10^{-4} M in DMSO of each compound were prepared and store at -20 ^{o}C, 4 ^{o}C and r.t. for 6, 15, and 21 days for the temperature/storage time assay. After the indicated storage time, where the samples were protected from light exposure, the solutions were filtrated and injected. All samples were filtrated using 0.80 µm Minisort ® filters (Sartorius Stedim Biotech).

2.4. Cell culture

The chronic myeloid leukaemia cell line, K562, was from *European Collection of Cell Cultures* (ECACC) and its P-gp overexpressing counterpart cell line K562Dox cells was a kind gift of Dr. J.P. Marie (Paris, France) [26, 27]. The non-small cell lung cancer cell line, NCI-H460, and its drug-resistant P-gp overexpressing counterpart cell line RH460 were a kind gift of Dr. M. Pešić (Belgrade, Serbia) [28, 29]. All cell lines were genotyped and routinely monitored for mycoplasma contamination by PCR (VenorGeM® Advance Mycoplasma Detection Kit, Minerva). All cells were routinely grown in RPMI-1640 (with Ultraglutamine I and 25mM HEPES) medium (Lonza) supplemented with 10% FBS (PAA) at 37 ºC in a humidified incubator with 5 % CO_2 in air. Cell number and viability were analyzed with trypan blue exclusion assay. All experiments were carried out with exponentially growing cells having over 90 % viability.

2.5. Sulforhodamine B assay

The Sulforhodamine B (SRB) assay is an assay that measures cell growth indirectly by measuring the total protein of the cells. Was performed in NCI-H460 and RH460 cell lines according to procedure used by the NCI's Developmental Therapeutics Program [30-33]. Briefly cells were seeded in 96-well plates (5000 cells / well) and incubated for 24 h at 37 ºC. Cells were then treated in duplicate with 5 serial dilutions of each compound (at a maximum of 150 µM) for 48 h. Cells were fixed with 10% (w /v) trichloroacetic acid (TCA) and then washed with distilled water. After staining the proteins with 0.4% (w /v) SRB, cells were washed with 1% (v /v) acetic acid, the bound SRB was solubilized with 10 mM Tris base and absorbance was measured at 510 nm in a multi plate reader (Synergy Mx, Biotek Instruments Inc.). For each compound analyzed, the GI_{50} (the concentration that inhibits 50% of cell growth) was determined by interpolation of the dose-response curve graphic obtained using a NCI datasheet.

2.6. Tumour cell growth inhibition analysis using presto blue assay

Presto blue assay measures cell growth indirectly by measuring the metabolism of the cells. Analysis of K562 and K562Dox cell growth inhibition was carried out using Presto Blue assay (Bio Source, Invitrogen, UK). Briefly, cells were seeded in 96 plates (5000 cells / well) and incubated for 24 h at 37 ºC. Cells were then treated in duplicate with 5 serial dilutions of each compound (at a maximum of 150 µM) at 37 ºC and 5% CO2. After 48 h incubation, Presto Blue (10%) was added to the cells and further incubated for

2 h. Fluorescence was measured in multiplate reader (Synergy Mx, Biotek Instruments Inc., excitation at 560 and emission at 590 nm). For each compound analyzed, the GI_{50} (the concentration that inhibits 50% of cell growth) was determined by interpolation of the dose-response curve graphic obtained.

2.7. Rhodamine-123 efflux assay

K562 and K562Dox (5×10^6 cells) were incubated for 1 h at 37 ºC with 10 μM of the synthesized compounds and 1 mM rh123. Verapamil (10 μM), a known P-gp inhibitor [34], as well as curcumin (**1**, 10 μM), were used as controls. After incubation, cells were washed twice, resuspended in ice cold PBS and kept at 4 ºC in the dark until analysis in a BD AccuriTM C6 Flow cytometer (BD Biosciences). Cells shown in forward scatter and side scatter were electronically gated and acquired through the FL1 channel. For simple interpretation, the ratio of rh123 accumulation was calculated as $(Mean\ FL1_{K562Dox+compound} - Mean\ FL1_{K562Dox}) / Mean\ FL1_{K562Dox}$. At least 20,000 events? were analyzed per sample.

2.8. Cell treatments with curcumin (1) and compound 12

K562Dox cells (2×10^6 cells/well) were plated in 6-well plates and treated with compound 12 (2.7 μM, 4.1 μM, or 5.4 μM) and curcumin (20 μM, 30 μM, or 40 μM) for 48 h. Cells were also treated with complete medium (Blank) or with the maximum corresponding concentration of the extract solvent (DMSO). Following treatment, cells were processed according to different protocols, as follows.

2.8.1. Analysis of cell cycle profile by flow cytometry

Following 48 h treatment, cell pellets were fixed in ice-cold 70% EtOH for at least 12 h. Cells were then resuspended in 5 μg/mL propidium iodide and 0.1 mg/mL RNase A in PBS. Cellular DNA content was analyzed using a BD AccuriTM C6 Flow cytometer after cell debris and aggregates exclusion and plotting at least 20,000 events per sample [35]. FlowJo 7.6.5 software (Tree Star, Inc., Ashland, OR, USA) was used to determine the percentage of cells in the different phases of cell cycle (G0/G1, S, and G2/M) and in the sub-G1 peak.

2.8.2. Analysis of apoptosis by flow cytometry

Analysis of apoptotic cell death was performed using Annexin V-FITC Apoptosis Detection kit (Bender MedSystems, Vienna, Austria) as previously described [36]. Cells were analyzed by flow cytometry using the BD AccuriTM C6 Flow cytometer. Data analysis was carried it using FlowJo 7.6.5 software (Tree Star, Inc., Ashland, OR, USA) evaluating at least 20,000 events per sample.

2.8.3. Analysis of protein expression by Western blot

Total protein extracts were obtained by lysing cell pellets. After treatment of 48 hours, in Winman's Buffer (1% NP-40, 0.1 M Tris-HCl pH 8.0, 0.15 M NaCl, and 5 mM EDTA) with EDTA-free protease inhibitor cocktail (Roche). The "DC Protein assay kit" (Bio-Rad) was used to quantify the total protein content and 20 µg of protein were subjected to SDS-PAGE (12% Bis-Tris gel). Following electrophoretic transfer of the proteins into nitrocellulose membranes (GE Healthcare), membranes were incubated with the following primary antibodies: goat anti-Actin (1:2000; Santa Cruz Biotechnology), mouse anti-P-gp (P7965) (1:2000; Sigma), rabbit anti-PARP-1 (1:2000; Santa Cruz Biotechnology), anti-caspase-3 (1:2000; Upstate), mouse anti-p53 (1:5000; Santa Cruz Biotechnology) and rabbit anti-cyclin B1 (1:1000; Cell Signaling). The following secondary antibodies were then used: anti-mouse IgG-HRP; anti-rabbit IgG-HRP or anti-goat IgG-HRP (all diluted 1:2000; Santa Cruz Biotechnology). Signal was detected using the ECL Western blot Detection Reagents (GE Healthcare), the Amersham Hyperfilm ECL (GE Healthcare), and the Kodak GBX developer and fixer (Sigma) [37]. The intensity of the bands obtained in each film was further analysed using the software Quantity One – 1D Analysis (Bio-Rad, USA).

2.9. Statistical analysis

All presented data resulted from at least three independent experiments. All data was statistically analyzed with the two-tailed paired Student's *t*-test. Results were considered statistically significant when $p \leq 0.05$.

3. Results

3.1. *Synthesis of curcumin mono-carbonyl analogues and analogues synthesized directly from curcumin*

Curcumin (**1**) has shown to be a promising compound in therapeutics; however, the chemical stability and extensive metabolism are substantial limitations to its potential use [38, 39]. Therefore, we aimed to synthesize two mono-carbonyl building blocks chemically more stable, eliminating the unstable portion of the molecule, namely, the methylene portion of the β-diketone moiety. In order to improve the P-gp modulatory activity different derivatives of the phenolic groups were obtained (alkyl, glucosamines, amines, carbamates, and esters).

Claisen-Schmidt condensation reactions were used for the synthesis of the building blocks **2** and **3**, according to previously described protocols [24, 25]. Subsequently, stability studies were performed for compounds **1** and **2-3** (see section 3.9) and following, several enone **2** derivatives (**4-9**, **11**) were synthetized (Figure 2, Scheme 1) along with the new curcumin derivatives **10** and **12** (Scheme 2 and 3). The synthesis approach used to obtain derivatives **4**-**9** followed a microwave (MW) assisted synthesis [40].

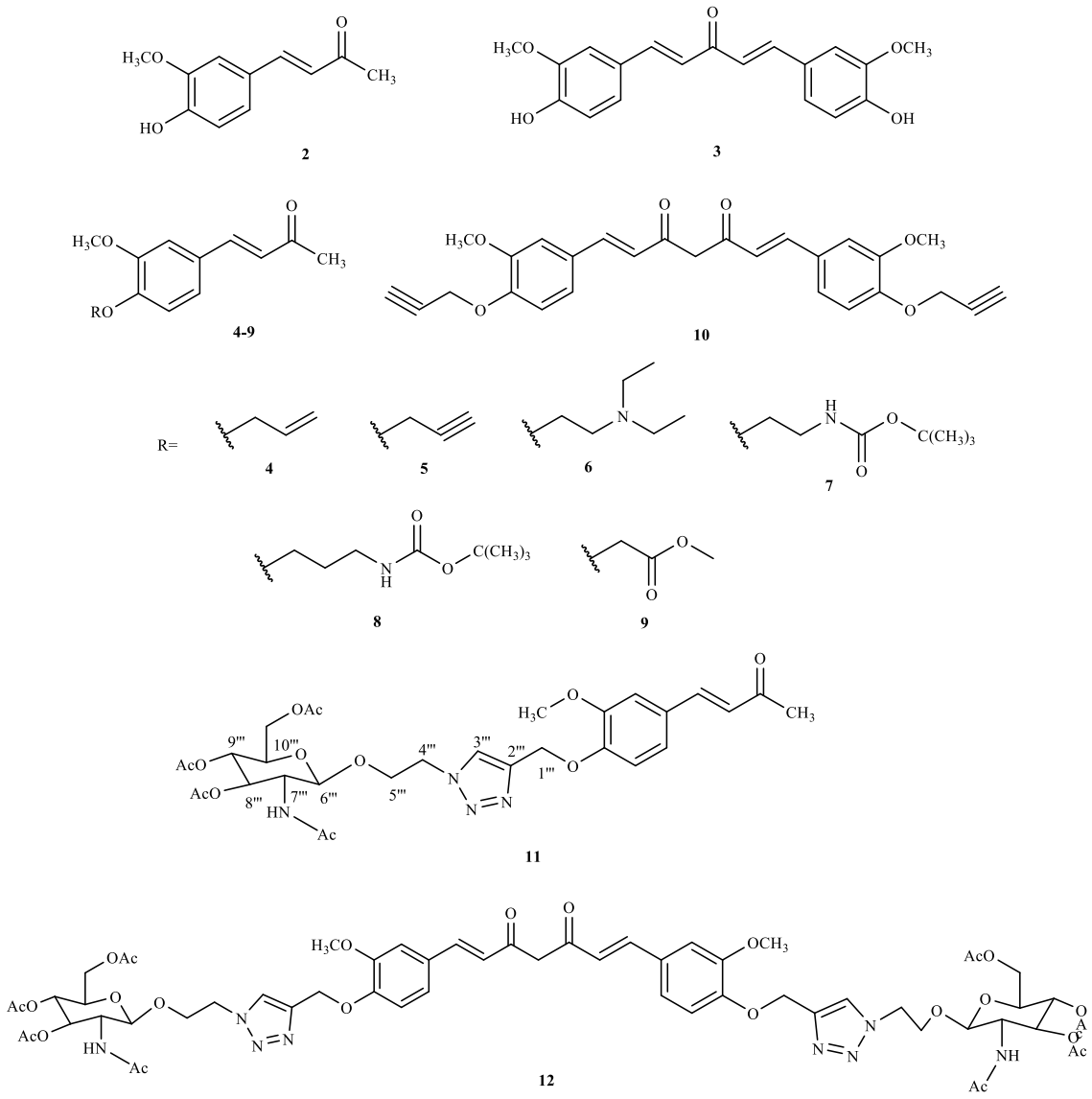

Figure 2 - Structure of compounds **2**-**12**.

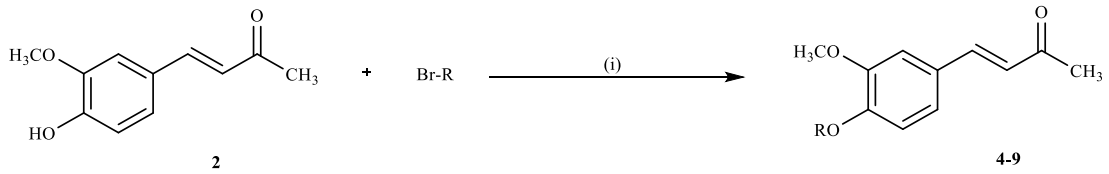

Scheme 1 – Reaction conditions for the synthesis of compounds **4**-**9**, (i): K_2CO_3 or Cs_2CO_3, acetone, MW, 200 W, 65 ^oC, 2 h or 3 h.

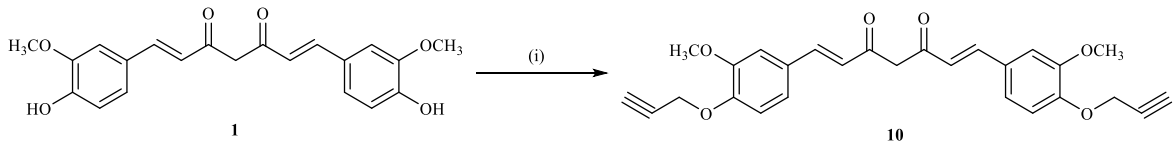

Scheme 2 - Reaction conditions for the synthesis of compound **10**, (i): Cs_2CO_3, Bu_4NBr, acetone, propargyl bromide, 60 °C, 4 h.

The synthesis of the glycosylated derivatives **11** and **12** was accomplished using click chemistry, more precisely, the Huisgen 1,3-dipolar cycloaddition [41, 42] herein used for the first time, to our state of knowledge, to obtain potential bioactive derivatives of curcumin (**1**). To synthesize compound **11**, the derivative **5** was added to 2-azidoethyl 2-acetamido-3,4,6-tri-*O*-acetyl-2-deoxy-β-D-galactopyranoside using a copper (II) salt ($CuSO_4.5H_2O$) as a catalyst in the presence of sodium ascorbate, the reducing agent (

Scheme 3) [42]. Although the structure of compound **4** is protected in a patent application for the treatment of hypertension [43], the synthesis and structure elucidation of derivatives **4-12** is herein described for the first time.

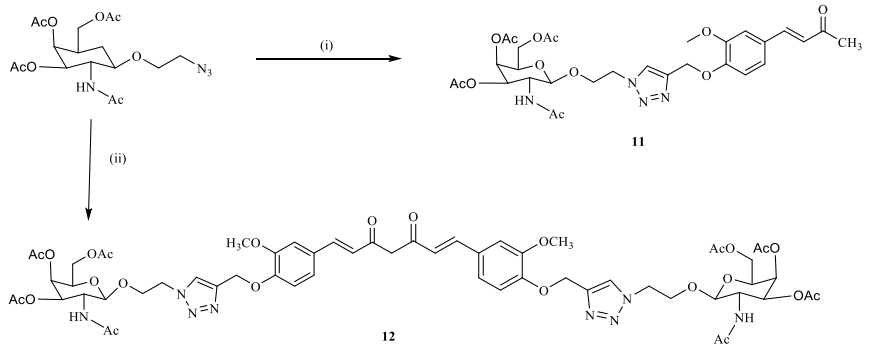

Scheme 3 - Reaction conditions for the synthesis of compound **11** and **12**, (i): compound **4**, $CuSO_4.5H_2O$, sodium ascorbate, H_2O: THF (1:2), MW, 200 W, 70°C, 10 min; (ii): compound **10**, $CuSO_4.5H_2O$, sodium ascorbate, H_2O: THF (1:2), MW, 200 W, 70 °C, 10 min.

3.2. Most of the synthesized compounds inhibited the growth of human tumour cell lines

To evaluate the effect of the synthesized compounds (**2-5, 8-12**) in human tumour cells, two MDR and sensitive tumour lines were used. One cell line was from chronic myeloid leukaemia (CML) consisting of a sensitive cell line (K562) and its MDR counterpart overexpressing P-gp (K562Dox). The other cell line was from non-small cell lung cancer

(NSCLC) consisting of a sensitive cell line (NCI-H460) and its MDR counterpart overexpressing P-gp (RH460). The effect of the compounds was first analyzed to study the growth of human tumour cell lines with the Sulforhodamine B assay (for the solid tumour cells) or with the Presto Blue assay (suspension cell lines). The GI_{50} concentrations determined for most of the compounds were similar for both the MDR and the drug-sensitive counterpart cells (Tables 1 and 2). When comparing our series of synthesized compounds with curcumin (**1**), , compounds **3** and **10** presented more potent antitumor activity (Tables 1 and 2). Compound **10** was even more potent in the MDR cell lines (mostly in K562Dox) (Table 1 and 2) than in the sensitive cells and its GI_{50} concentration determined for the K562Dox cells (2.73 μM) was lower than the one previously published for doxorubicin treatment (11.62 μM, [44]), used as control. Additionally, compound **3** was significantly more potent in K562 than in K52Dox cells (Table 2), with GI_{50} concentrations of 9.33 ± 1.67 μM and 20.67 ± 2.85 μM, respectively. Also, compounds **5** and **8** were found to be only active in the non-small cell lung cancer model. This could be important for future targeted therapy studies. Regarding acetate **9** or the glucosamine acetate derivatives **11-12,** none of them were found to be active in the two pairs of cell lines studied.

Table 1 – GI_{50} concentrations of the synthesized compounds in the non-small cell lung cancer sensitive and MDR counterpart cell lines

	GI_{50} (μM)	
	NCI-H460	***RH460***
Curcumin (1)	27.3 ± 1.86	26 ± 0.24
2	64.75 ± 6.91	62.67 ± 7.75
3	1.47 ± 0.27	1.8 ± 0.25
4	41.5 ± 3.07	39.3 ± 2.19
5	52.67 ± 6.67	41.67 ± 2.96
8	55.25 ± 4.68	41 ± 5.29
9	> 150	> 150
10	3.4 ± 0.84	2.6 ± 0.25
11	> 150	> 150
12	> 150	> 150

Values were determined with the Sulforhodamine B assay and are the mean ± SEM of at least 3 independent experiments. Doxorubicin was used as a positive control (GI_{50} concentrations were the following: 20 nM ± 5.04 in NCI-H460 cells and >150 nM in RH460 cells).

Table 2 – GI_{50} concentrations of the synthesized compounds in the leukaemia sensitive and MDR counterpart cell lines

	GI_{50} (μM)	
	K562	***K562Dox***
Curcumin (1)	21.67 ± 4.63	19,67 ± 4.18
2	85.33 ± 7.42	92 ± 13.32
3	9.33 * ± 1.67	20.67 ± 2.85
4	68.67 ± 3.06	63.33 ± 11.62
5	> 150	133.33 ± 3.33
8	> 150	> 150
9	> 150	> 150
10	6.3 ± 0.95	2.73 ± 0.61
11	> 150	> 150
12	> 150	> 150

Values were determined with the Presto Blue assay and are the mean ± SEM of at least 3 independent experiments. Doxorubicin was used as positive control (GI_{50}:65 nM ± 13.23 in K562 cells and >150 nM in K562Dox cells). * $p \leq 0.01$, K562 *vs*. K562Dox

From the analysis of the data presented in Tables 1-2, the following general observations can to be made: i) the presence of two aromatic rings seems to improve the inhibitory activity (e.g. curcumin **1** and dienone **3** *vs.* enone **2**; compound **10** *vs.* **5**); ii) the hydroxyl group in scaffolds **1**, **2**, and **3** and the di-carbonyl moiety of curcumin (**1**) are not essential for cell growth inhibition, as previously described in structure-activity relationship studies of curcumin derivatives in several cell lines [23].

3.3. Some of the synthesized compounds inhibited P-gp activity

In order to analyze the effect of the derivatives on P-gp activity, the rhodamine-123 (rh123) efflux assay was performed. This assay relies on the quantification of the relative fluorescence accumulation of rh123 (a P-gp substrate) as an indirect way to study the P-gp inhibitory potency of different compounds [45]. As expected, K562 cells (which do not express P-gp) presented increased rh123 accumulation when compared to K562Dox cells, in which the accumulation of rh123 was represented as zero (Fig. 3). Also, K562Dox cells in the presence of verapamil, a known first-generation P-gp inhibitor [46] used as a positive

control, showed an accumulation of rh123 more similar to the one observed in K562 cells (Fig.3). When analyzing the effect of the studied compounds (at 10 µM concentrations) in the K562Dox cells, differences in rh123 accumulation were observed. Treatment with compounds **8** and **10** resulted in a significant increase in the accumulation ratio of rh123, compatible with a possible P-gp inhibition. In contrast, treatments with curcumin (**1**), compounds **5** and **12** showed a significant decrease in the rh123 accumulation, compatible with a possible P-gp activation.

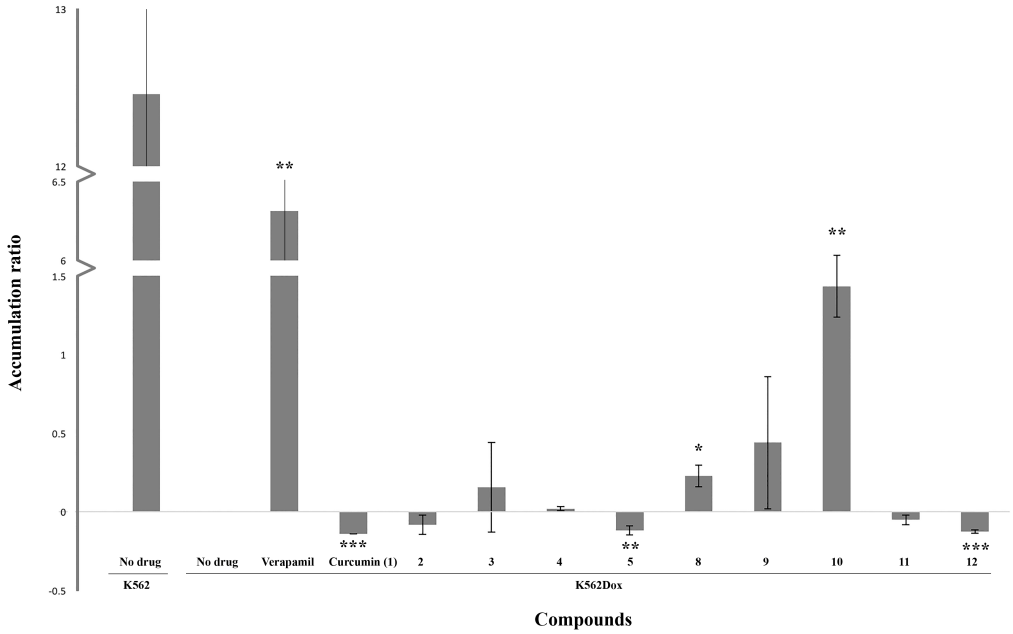

Figure 3 - Relative rh123 accumulation ratios in K562 or K562Dox cells. The accumulation on K562Dox (untreated) cells is represented as zero. Accumulation ratios superior to zero correspond to rh123 accumulation superior to the one obtained in K562Dox cells, (potential P-gp inhibitor). Verapamil (10 µM) was used as a positive control (P-gp inhibitor). Results are the mean ± SEM of 3 independent experiments. * $p \leq 0.05$, ** $p \leq 0.01$ and *** $p \leq 0.001$ K562Dox untreated cells (with no drug) *vs*. K562Dox treated cells.

3.4. Curcumin (1) and compound 10 decreased P-gp expression

Curcumin (**1**) is known to not only inhibit P-gp function but also to inhibit P-gp expression [47, 48]. Since compound **10** presented better anti-P-gp activity than curcumin (**1**), the effect of compound **10** on the inhibition of P-gp expression was also assessed and compared to curcumin (**1**). With this purpose, P-gp levels of MDR K562Dox cells were analysed after 48 h treatement with different concentrations of the two compounds, : compound **10 (**2.7 µM and 4.1 µM) and curcumin (**1**) (20 µM and 30 µM) corresponding to the previously determined GI_{50} and 1.5 x GI_{50}]Results from the Western blot analysis showed a statistically significant decrease in the expression of P-gp protein following treatment with the two compounds (Fig. 4).

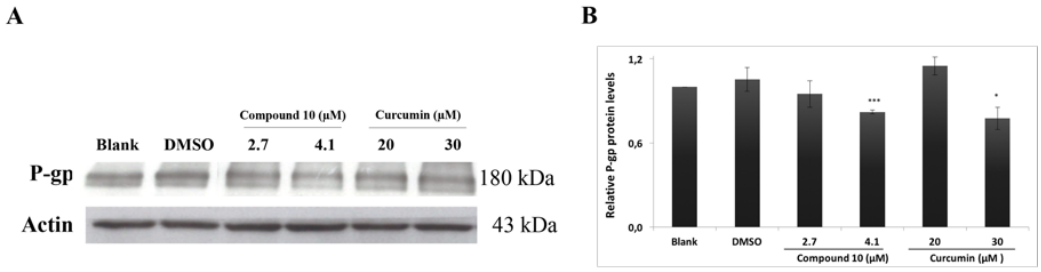

Figure 4 - Expression of P-gp in K562Dox cells treated with compound **10** and curcumin (**1**). Cells were treated with medium (Blank), different concentrations of with the GI_{50} and 1.5 x GI_{50} concentrations of compound **10 (**2.7 μM and 4.1 μM**)** or curcumin (1) (20 μM and 30 μM), or with the highest vehicle/solvent (DMSO) concentration. Actin was used as a loading control. (A) Representative Western blot images of three independent experiments; (B) Densitometry analysis of the Western blots. Results are the mean ± SEM of 3 independent experiments. * $p \leq 0.05$, ** $p \leq 0.01$ and *** $p \leq 0.001$, when comparing DMSO *vs*. treatment.

3.5. Curcumin (1) and compound 10 caused alterations in the cell cycle profile of K562Dox cells

Since compound **10** presented a more potent tumour cell growth inhibitory activity than curcumin (**1**), its mechanism of action was further studied and compared to curcumin (**1**). To analyze the effect of these compounds in the cell cycle profile, K562Dox cells were analyzed by flow cytometry after 48 h treatment with the compounds Increasing concentrations were used in order to evaluate a possible dose dependent effect. Therefore, treatment with compound **10** was carried out with 2.7 μM, 4.1 μM, and 5.4 μM and treatment with curcumin (**1**) was carried out with 20 μM, 30 μM, and 40 μM, corresponding to the previously determined GI_{50}, 1.5xGI_{50}, and 2xGI_{50} concentrations. Results showed clear alterations in the cell cycle profile of K562Dox cells following treatment with the two compounds (Fig. 5). Treatment with the GI_{50} concentration of both compounds [2.7 μM of compound **10** and 20 μM of curcumin (**1**)] caused an increase in the % of cells in G2/M and a decrease in the % of cells in the G0/G1 and S phases of the cell cycle. However, different effects were observed for both compounds when tested at higher concentrations. Cells treated with higher concentrations of compound **10** continued to arrest at the G2/M phase of the cell cycle, while. cells treated with the higher concentrations of curcumin (**1**) showed an arrest in the G0/G1 phase of the cell cycle and a decrease in the % of cells in the G2/M phase.

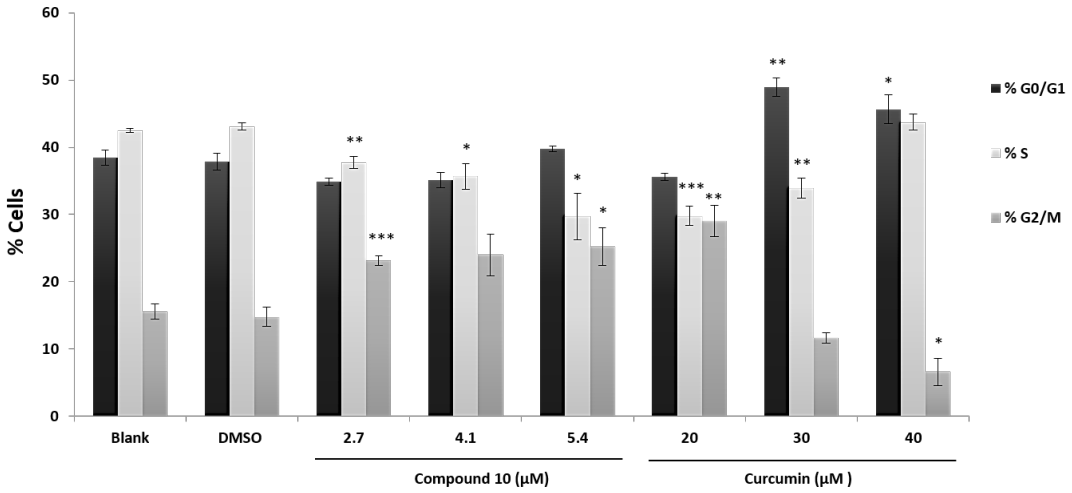

Figure 5 - Cell cycle distribution of K562Dox cells after treatment with compound **10** and curcumin (**1**). Cells were treated with medium (Blank), with the GI_{50}, 1.5xGI_{50}, and 2xGI_{50} concentrations of compound **10** (2.7 μM, 4.1 μM, and 5.4 μM) or curcumin (20, 30 and 40 μM), or with the highest vehicle (DMSO) concentration. Results are the mean ± SEM of 3 independent experiments. * $p \leq 0.05$, ** $p \leq 0.01$ and *** $p \leq 0.001$, DMSO *vs*. treatment.

3.6. Curcumin (1) and compound 10 induced apoptosis in the K562Dox cells

To understand if the cell growth inhibition observed in the K562Dox cells following treatment with curcumin (**1**) and compound **10** could also be due to an induction of apoptosis, an analysis of apoptosis was carried out. Results showed that both compounds induced apoptosis (Table 3). The levels of cellular apoptosis increased from 6.3% in the DMSO treatment to 11.8%, 26.9%and 32.0% following treatment with curcumin (**1**, 20 μM, 30 μM, and 40 μM respectively) and to 9.3%, 11.3%and 14.8% following treatment with compound **10** (2.7 μM, 4.1 μM, and 5.4 μM, respectively).

Table 3. Apoptosis levels in K562Dox cells treated with curcumin (1) or compound 10.

		% Apoptosis
Blank		3.9 ± 1.2
DMSO		6.3 ± 2.0
Curcumin (1)	20 μM	11.8 ± 2.3
	30 μM	26.9 ± 0.9 *
	40 μM	32.0 ± 3.7 **
Compound 10	2.7 μM	9.3 ± 1.1
	4.1 μM	11.3 ± 1.4 ***
	5.4 μM	14.8 ± 2.4 **

Results are the mean ± SEM of 3 independent experiments. * $p \leq 0.05$, ** $p \leq 0.01$ and *** $p \leq 0.001$, DMSO *vs.* treatment

3.7. Curcumin (1) and compound 10 caused alterations in P53 and cyclin B1 protein levels in K562Dox cells

To further examine the mechanism of the above mentioned arrest of the cell cycle at the G2/M phase (with all the tested concentrations of compound **10** and with the GI_{50} concentration of curcumin) and at the G0/G1 phase (only with the two highest concentrations of curcumin), the expression levels of the p53 and cyclin B1 proteins were analyzed. The results from the Western blot analysis showed an increase in p53 levels in the K562Dox cells following the 48 h treatment with either of the compounds (Fig. 6, panels A and B). In addition, the levels of cyclin B1 were found decreased in K562Dox cells following treatment with either of the compounds (Fig. 6, panels C and D).

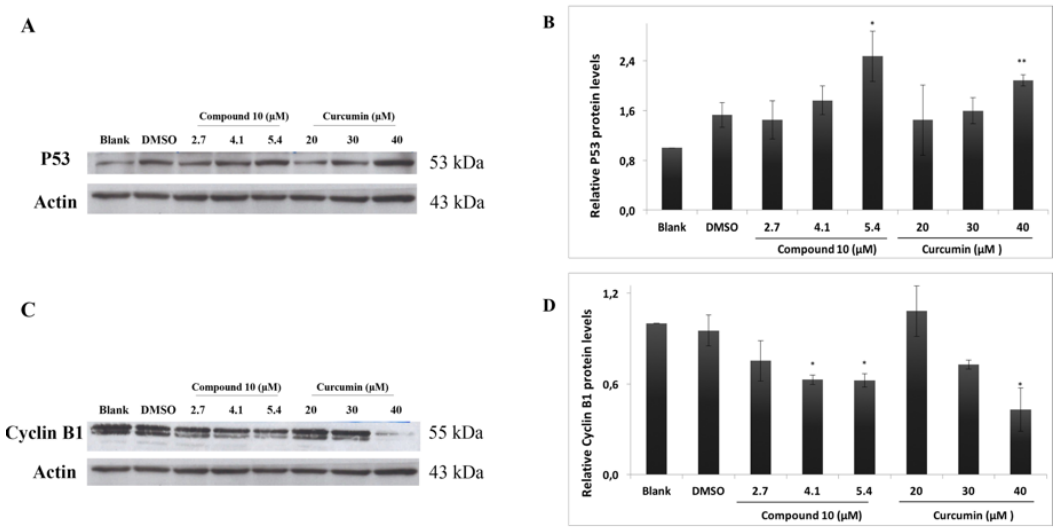

Figure 6 - Expression of p53 and cyclin B1 in K562Dox cells following treatment with compound **10** or curcumin (**1**). Cells were treated with medium (Blank), with the GI_{50}, 1.5xGI_{50}, and 2xGI_{50} concentrations of compound **10** (2.7 μM, 4.1 μM, and 5.4 μM) or curcumin (20, 30 and 40 μM),, or with the highest vehicle (DMSO) concentration. Actin was used as a loading control. (A and C) Representative Western blot images of three independent experiments; (B and D) Densitometry analysis of the Western blots. Results are the mean ± SEM of 3 independent experiments. * $p \leq 0.05$, ** $p \leq 0.01$, and *** $p \leq 0.001$, when comparing DMSO *vs*. treatment.

3.8. *Curcumin (1) and compound 10 caused alterations in PARP-1 and caspase 3 protein levels in K562Dox cells*

To further confirm the involvement of apoptosis in the mechanism of action of compound 10 and curcumin (**1**), the levels of PARP-1 cleavage and pro-caspase 3 protein expression were analysed. Results showed an increase in PARP cleavage and a decrease in pro-caspase 3 levels in K562 Dox cells following treatment of cells with both compounds (Fig. 7).

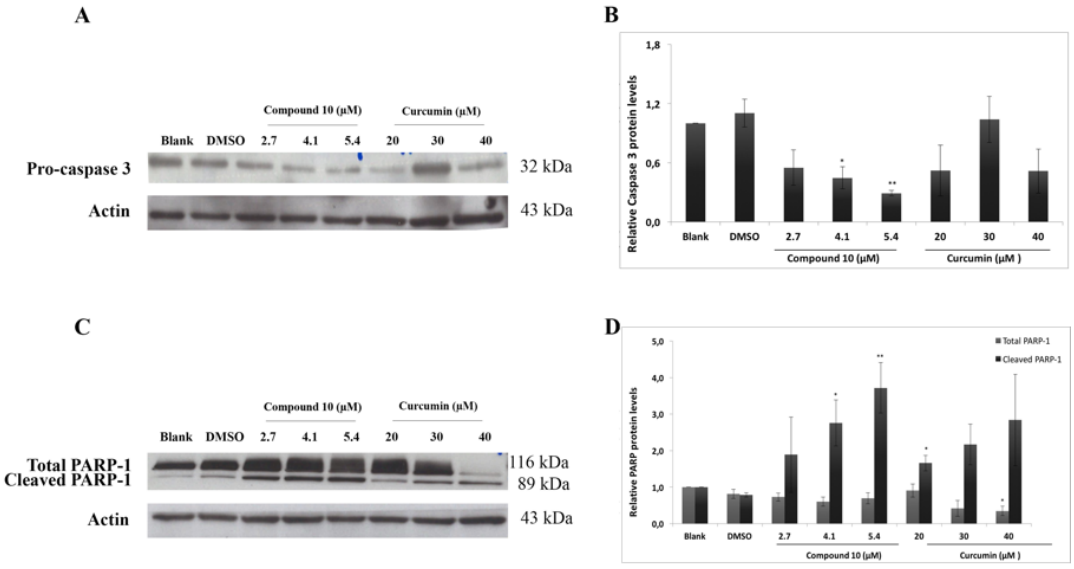

Figure 7 - Expression of PARP-1 and pro-caspase 3 in K562Dox cells following treatment with compound **10** or curcumin (**1**). Cells were treated with medium (Blank), with the GI_{50}, 1.5xGI_{50}, and 2xGI_{50} concentrations of compound **10** (2.7 μM, 4.1 μM, and 5.4 μM) or curcumin (20, 30 and 40 μM), or with the highest vehicle (DMSO) concentration. Actin was used as a loading control. (A and C) Representative Western blot images of three independent experiments; (B and D) Densitometry analysis of the Western blots. Results are the mean ± SEM of 3 independent experiments. * $p \leq 0.05$, ** $p \leq 0.01$, and *** $p \leq 0.001$, when comparing DMSO vs. treatment.

3.9. Among the studied compounds curcumin (1) showed to be the most unstable

Under neutral and basic pH conditions, curcumin (**1**) is very unstable, and eventually is degraded to ferulic acid and feruloylmethane [38, 39]. Besides being prone to hydrolysis under alkaline conditions, curcumin (**1**) is also very susceptible to photochemical degradation [39]. Given these curcumin (**1**) characteristics, the building blocks enone **2** and dienone **3** were initially investigated for stability and the hit compound **10** was also investigated following the *in vitro* studies and compared with curcumin (**1**).

Stability studies with different pH, solvents, temperature, and storage time were performed by high-performance liquid chromatography (HPLC). Overall results showed that regarding the pH buffers assay, dienone **3** is the most stable compound, followed by enone **2** and compound **10.** Among the studied compounds curcumin (**1**) showed to be the most unstable.

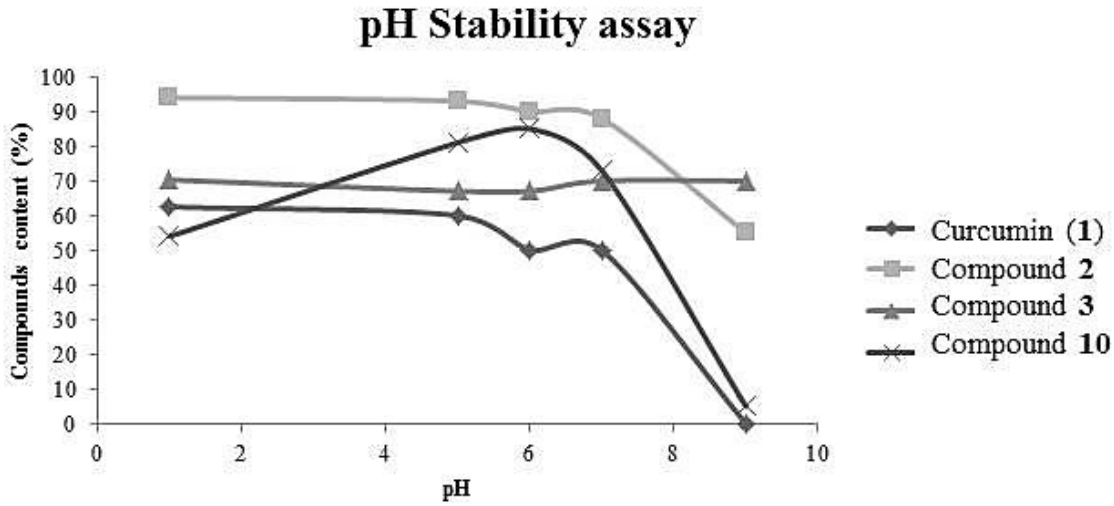

Figure 8 - Compounds content rate after incubation with five buffers with different pH values at r.t. overnight (except for pH 1, which incubated for 75 min).

The biological buffer assay has shown that compounds **1**, **2**, and **3** did not degrade in this medium. Although the cell medium showed a higher interference in the chromatograms of compound **10** than in the other compounds chromatograms, compound **10** is still present.

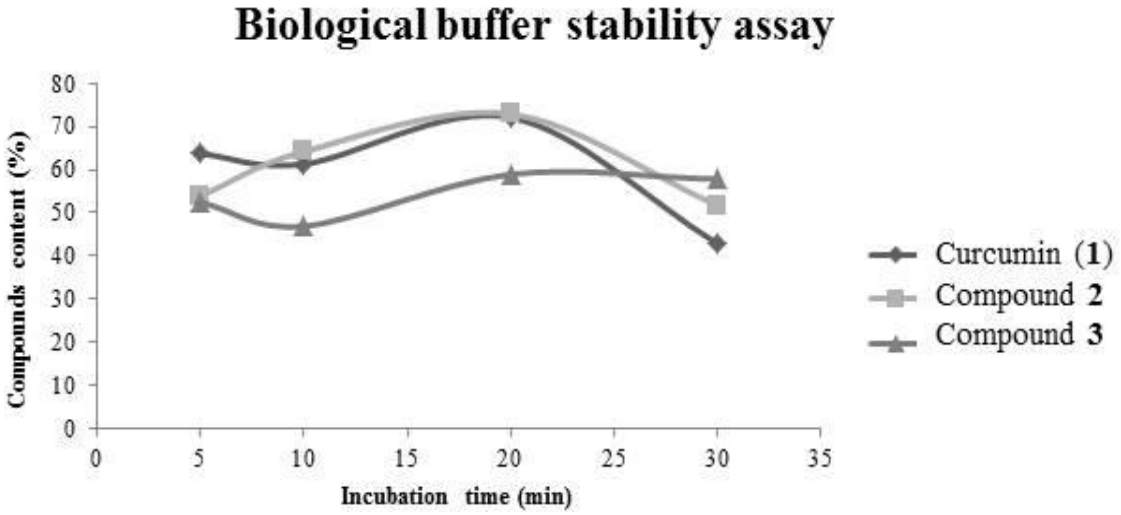

Figure 9 - Compounds content rate after incubation with cell culture medium at 37 °C for different time intervals.

The temperature/storage time assay showed that all of the tested compounds are unstable along the temperature and storage times tested. Curcumin (**1**) and compound **2** and **10** exhibited similar stability; and compound **3** has proven to be the most unstable in the described conditions.

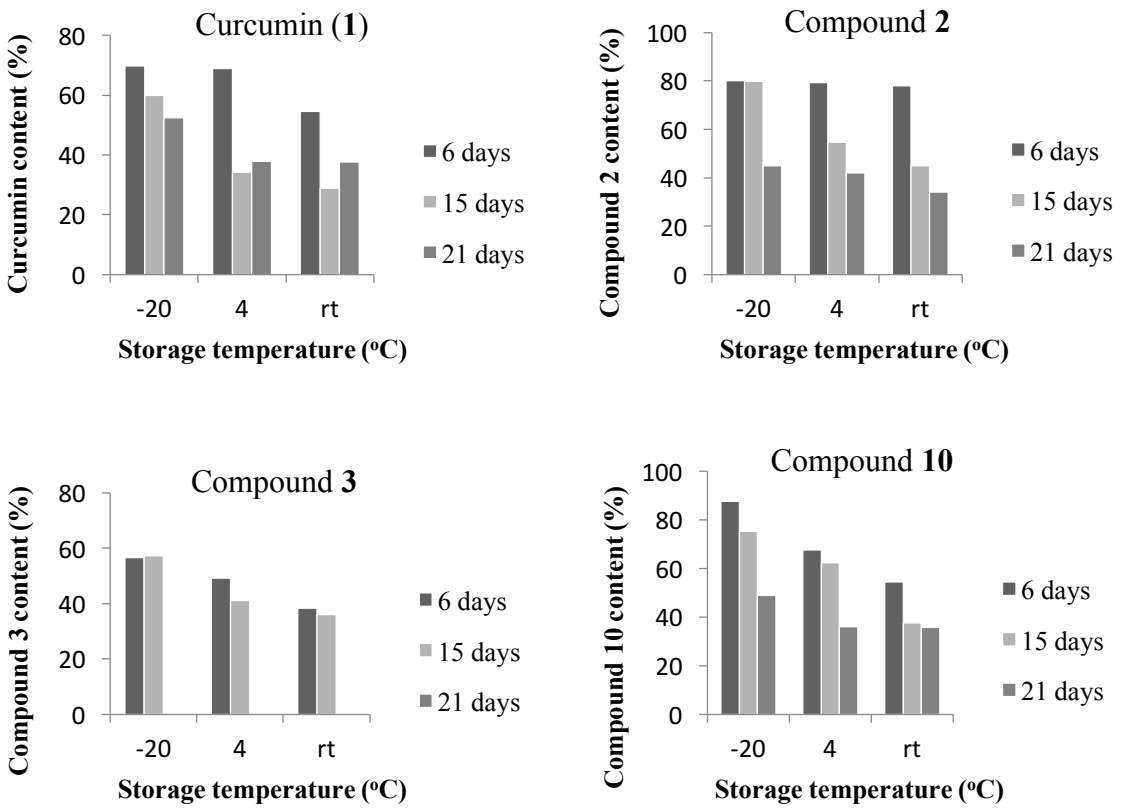

Figure 10 - Compounds content rate after incubation in DMSO for 6, 15, and 21 days at -20 °C, 4 °C and r.t..

4. Discussion

Drug resistance is one of main causes for chemotherapy failure. P-gp activity and expression have been the most investigated mechanisms by which MDR occurs. Since the discovery of P-gp, several studies and clinical trials have attempted to circumvent MDR using well known P-gp inhibitors, such as verapamil and cyclosporine. However, none of these compounds have been successful, due to undesirable side effects as well as low effectiveness [4, 49, 50].

Nature provides a large variety of molecules, with different degrees of complexity and many biological activities. Curcumin (**1**) is an example of such molecules, which has been associated with several interesting biological activities. However, extensive metabolism and instability have prevented curcumin (**1**) from being used at its full potential. In this study, we present a small library of new curcumin derivatives and tested their antitumor and P-gp modulatory activities.

The study of the cell growth inhibitory effect of the synthesized compounds revealed that the GI_{50} concentrations determined for most of the compounds were similar between the MDR and the drug-sensitive counterpart cells (Tables 1 and 2), probably indicating that these compounds were not P-gp substrates. Interestingly, previous studies using other curcumin derivatives and analogues have also described their growth inhibitory effect to be similar in drug-sensitive and drug resistant cells [51, 52]. From the studied compounds, compound **10** was even more potent in the MDR cell lines than in the sensitive cells, possibly due to an ability of the compound to affect MDR cells selectively over the sensitive cells from which they were derived, named collateral sensitivity [53].

Regarding the capacity of MDR reversal of the P-gp overexpressing cell line K562Dox (by inhibiting function and expression of P-gp), results showed that compounds **10** and **12** presented P-gp inhibitory function (Fig. 3). Previous studies had described curcumin (**1**) as a P-gp inhibitor [15, 47], but the concentrations (e.g. 50 μM) and time of treatment (e.g. 2 hours) used in those studies were higher than the concentration (10 μM) and treatment duration (1 hour) used in the present work. From all the studied compounds, compound **10** showed the strongest effect on rh123 accumulation, indicating that it was the most potent P-gp inhibitor. Interestingly, this compound was also one of the compounds which presented the most potent antitumor effect (Tables 1 and 2). The corresponding enone analogue **5,** even though having the same pattern of substitution in the aromatic ring as compound **10**, was also shown to interfere with the accumulation of rh123, but eliciting an opposite effect.

In terms of inhibition of P-gp expression, results from the Western blot analysis showed a statistically significant decrease in the expression of P-gp protein following treatment with compound **10** (and also curcumin) (Fig. 4). However, since the concentrations used for compound **10** (GI_{50} and 1.5 times GI_{50}) were much lower than the concentrations used for curcumin, it can be concluded that compound **10** was a stronger inhibitor of P-gp expression. The inhibition of P-gp expression by curcumin (**1**) has been previously described [54, 55] but, to our knowledge, this activity had not been explored for synthetic curcumin derivatives and analogues. Therefore, compound **10** is a very interesting P-gp inhibitor since it simultaneously inhibits the function and the expression of P-gp. Inhibitors of P-gp expression are very important chemical tools because they can be used as controls of P-gp expression in several pharmacological studies, including inhibition of P-gp expressed in [56] and transferred by extracellular vesicles.

The study of the mechanism of action of compound **10** (and curcumin) in the MDR chronic myeloid leukaemia model (K562Dox) showed that cells treated with GI_{50} concentrations of curcumin presented an arrest at the G2/M phase of the cell cycle but when treated with higher concentrations presented an arrest in the G0/G1 phase. Compound **10**,

independently of the concentration, arrested cells at G2/M phase (Fig. 5). Interestingly, previous studies using other synthesized curcumin analogues and derivatives had shown similar effects (arrest at G2/M) in different cell lines (particularly in another resistant chronic myeloid leukaemia cell line) [51, 52, 57, 58]. Also, the effect in the cell cycle profile observed for the curcumin (**1**) treatment (i.e. increase in the % of cells in G2/M with the lowest concentrations and decrease in the % of cells in G2/M with the higher concentrations) has also been previously described in non-small cell lung cancer cells [20]. Our results suggest that compound **10** is associated a different mechanism of action when compared to curcumin (**1**).

Regarding induction of apoptosis, our results showed that both compounds (**10** and curcumin) induced apoptosis (Table 3). Even though the levels of apoptosis were lower for compound **10** than for curcumin (**1**), the concentrations tested for compound **10** were also considerably lower (since the GI_{50} concentration of this compound was much lower). Therefore, it can be concluded that both compounds induced apoptosis in the K562Dox cells. Several studies have previously described the apoptotic activity of curcumin (**1**) and of other synthesized curcumin derivatives and analogues, in other human tumour cell lines such as in other non-small cell lung cancer cell lines [20, 51, 57, 58].

In addition to the above mentioned arrest of the cell cycle (at G2/M phase) (Fig. 5) and induction of apoptosis (Table 3), treatments with compound **10** (or curcumin) increased cellular p53 levels and cyclin B1 levels (Fig. 6), which is in agreement with the fact that p53 activation (being the guardian of the genome) usually results in a cell cycle arrest and a consequent induction of apoptosis [59]. Also, cell cycle is controlled by a serious of actions performed by cyclin dependent kinases in association with cyclin proteins. Cyclin B1 (establishing a complex with CDK1) regulates progression of G2 and mitosis [60] and therefore its downregulation promotes cell cycle arrest at the G2/M phase, which is in agreement with the above mentioned observed results. Other published studies have also shown similar alterations in the expression levels of these proteins (increased p53 and decreased cyclin B1) in tumour cells following treatment with curcumin (**1**) and other curcumin derivatives [20, 57, 58].

The mitochondrial pathway of apoptosis functions in response to several types of stress. Following a trigger of apoptosis, a serious of events leads to caspase 3 activation (with a decrease in pro-caspase 3 levels). Once activated, caspase 3 cleaves cytoskeletal and nuclear proteins such as PARP-1 (with a decrease in total PARP-1 levels) [61]. By treating cells with compound **10** (or curcumin) a decrease in total PARP-1 and pro-caspase 3 levels and an increase in the expression levels of cleaved PARP-1 were observed (Fig. 7). This is in agreement with an activation of the mitochondrial apoptotic pathway. Several studies have previously described such alterations in different cancer models following

treatment with curcumin (**1**) [20, 52]. Moreover, some synthesized curcumin derivatives and analogues have previously been described to induce apoptosis through caspase 3 activation and PARP-1 cleavage [51, 52, 57, 58].

Given the fact that curcumin (**1**) is an unstable compound, three stability assays were performed in order to evaluate the stability of curcumin (**1**), the building blocks enone **2**, and dienone **3** and the hit compound **10**. Considering the stability results, it was very similar for the tested compounds; however, compound **3** was shown to be very stable in most of the assays, which indicates that this is the most stable of the four compounds. Compound **2, 10** and curcumin (**1**) are subsequently less stable. Overall, the results obtained are consistent with the chemical structure of these compounds: compounds **2** and **3** lack the β-diketone moiety responsible for the chemical instability associated to curcumin (**1**) and compound **10**.

None of the investigated derivatives was found to be very stable in the range of conditions assessed, which highlights the difficulty in investigating both chemical and biological properties of curcumin (**1**); nevertheless, this work shows the potential of synthesizing new curcumin derivatives to improve curcumin (**1**) stability and characterized the promising dual activity (antitumor and anti-P-gp) of a curcumin derivative (**10**). These results could be useful in future pharmacological studies whenever an inhibitor of P-gp expression and function is needed. Also, the use compound **10** as an inhibitor of P-gp expression in tumour cells shedding extracellular vesicles (carrying P-gp on their cargo) could help the inhibition of the non-genetic transfer of P-gp from MDR to drug-sensitive cancer cells.

5. Conclusions

From the series of synthesized curcumin derivatives and analogues, a newly synthesized curcumin derivative (compound **10**) that presented more potent antitumor and anti-P-gp activity than curcumin (**1**) itself was identified. In addition, the study of its mechanism of action in a MDR chronic myeloid leukaemia cell line showed that it caused cell cycle arrest at the G2/M phase and increased cell death by apoptosis.

6. Abbreviations

ABC = ATP-binding cassette; DMSO = Dimethyl sulfoxide; EtOAc = Ethyl acetate; EtOH = Ethanol; FBS = Fetal bovine serum; h = Hours; HPLC = High-performance liquid

chromatography; HRMS-ESI = High resolution mass spectrometry-Electrospray ionization; MDR = Multidrug resistance; MeOH = Methanol; min = Minutes; mp = Melting point; MW = Microwave; PBS = Phosphate buffered saline; P-gp = P-glycoprotein; r.t. = Room temperature; SRB = Sulforhodamine B; THF = Tetrahydrofuran.

Aknowledgments

This work was partially financed by FEDER - Fundo Europeu de Desenvolvimento Regional funds through the COMPETE 2020 - Operacional Programme for Competitiveness and Internationalisation (POCI), Portugal 2020, and by Portuguese funds through FCT - Fundação para a Ciência e a Tecnologia/ Ministério da Ciência, Tecnologia e Inovação in the framework of the project "Institute for Research and Innovation in Health Sciences" (POCI-01-0145-FEDER-007274). This research was also partially supported by the Strategic Funding UID/Multi/04423/2013 through national funds provided by FCT – Foundation for Science and Technology and European Regional Development Fund (ERDF), in the framework of the *programme PT2020* and INNOVMAR - Innovation and Sustainability in the Management and Exploitation of Marine Resources, reference NORTE-01-0145-FEDER-000035, Research Line NOVELMAR. The authors thank the Portuguese Foundation for Science and Technology (FCT) for the PhD grant of VLR (SFRH/BD/87646/2012) and for the post-doc grant of RTL (SFRH/BPD/68787/2010).

The authors also thank Dr. Sara Cravo, Department of Chemistry, Laboratory of Organic and Pharmaceutical Chemistry, Faculty of Pharmacy, University of Porto, for technical assistance. The authors have no conflict of interests to declare.

7. References

[1] A. Persidis, Cancer multidrug resistance, Nature biotechnology. 1999, 17 (1), 94-95.

[2] V.R. Fonseca, C. Freitas, M. Palmeira, C. Ferreira, R. Victorino, Cardiac noradrenergic denervation in a patient with multiple symmetric lipomatosis, Cardiology. 2012, 121 (3), 160-163.

[3] K.M. Pluchino, M.D. Hall, A.S. Goldsborough, R. Callaghan, M.M. Gottesman, Collateral sensitivity as a strategy against cancer multidrug resistance, Drug Resistance Updates. 2012, 15 (1), 98-105.

[4] G. Szakacs, J.K. Paterson, J.A. Ludwig, C. Booth-Genthe, M.M. Gottesman, Targeting multidrug resistance in cancer, Nature reviews. Drug discovery. 2006, 5 (3), 219-34.

[5] R.J. Kathawala, P. Gupta, C.R. Ashby, Z.-S. Chen, The modulation of ABC transporter-mediated multidrug resistance in cancer: A review of the past decade, Drug Resistance Updates. 2015, 18 1-17.

[6] V. Lopes-Rodrigues, H. Seca, D. Sousa, E. Sousa, R.T. Lima, M.H. Vasconcelos, The network of P-glycoprotein and microRNAs interactions, International journal of cancer. Journal international du cancer. 2014, 135 (2), 253-63.

[7] M.M. Gottesman, T. Fojo, S.E. Bates, Multidrug resistance in cancer: role of ATP–dependent transporters, Nature Reviews Cancer. 2002, 2 (1), 48-58.

[8] H. Dinsa, G. Melesie, A Literature Review on Cancer Multi Drug Resistance and Its Therapy, International Journal of Pharma Sciences. 2014, 4 (1), 417-423.

[9] R. Silva, V. Vilas-Boas, H. Carmo, R.J. Dinis-Oliveira, F. Carvalho, M. de Lourdes Bastos, F. Remião, Modulation of P-glycoprotein efflux pump: induction and activation as a therapeutic strategy, Pharmacology & therapeutics. 2015, 149 1-123.

[10] A.K. Tiwari, K. Sodani, C.L. Dai, C.R. Ashby Jr, Z.S. Che, Revisiting the ABCs of multidrug resistance in cancer chemotherapy, Current Pharmaceutical Biotechnology. 2011, 12 (4), 570-594.

[11] A. Palmeira, E. Sousa, M.H. Vasconcelos, M. Pinto, M.X. Fernandes, Structure and ligand-based design of P-glycoprotein inhibitors: a historical perspective, Curr Pharm Des. 2012, 18 (27), 4197-214.

[12] A. Palmeira, E. Sousa, M.X. Fernandes, M.M. Pinto, M.H. Vasconcelos, Multidrug resistance reversal effects of aminated thioxanthones and interaction with cytochrome P450 3A4, Journal of pharmacy & pharmaceutical sciences : a publication of the Canadian Society for Pharmaceutical Sciences, Societe canadienne des sciences pharmaceutiques. 2012, 15 (1), 31-45.

[13] A.C. Huang, S.Y. Lin, C.C. Su, S.S. Lin, C.C. Ho, T.C. Hsia, T.H. Chiu, C.S. Yu, S.W. Ip, T.P. Lin, J.G. Chung, Effects of curcumin on N-bis(2-hydroxypropyl) nitrosamine

(DHPN)-induced lung and liver tumourigenesis in BALB/c mice in vivo, In Vivo. 2008, 22 (6), 781-5.
[14] S. Prasad, S.C. Gupta, A.K. Tyagi, B.B. Aggarwal, Curcumin, a component of golden spice: From bedside to bench and back, Biotechnology advances. 2014,
[15] T. Nabekura, Overcoming multidrug resistance in human cancer cells by natural compounds, Toxins (Basel). 2010, 2 (6), 1207-24.
[16] M. Akram, A.A. Shahab-Uddin, K. Usmanghani, A. Hannan, E. Mohiuddin, M. Asif, Curcuma longa and curcumin: a review article, Res J Biol Plant Biol. 2010, 55 (2), 65-70.
[17] G. Grynkiewicz, P. Slifirski, Curcumin and curcuminoids in quest for medicinal status, Acta Biochimica Polonica. 2012, 59 (2), 201.
[18] R. Sreedhar, S. Arumugam, R.A. Thandavarayan, V. Karuppagounder, K. Watanabe, Curcumin as a therapeutic agent in the chemoprevention of inflammatory bowel disease, Drug discovery today. 2016, 21 (5), 843-849.
[19] M. Kasdagly, S. Radhakrishnan, L. Reddivari, D.N. Veeramachaneni, J. Vanamala, Colon carcinogenesis: influence of Western diet-induced obesity and targeting stem cells using dietary bioactive compounds, Nutrition. 2014, 30 (11-12), 1242-56.
[20] S.S. Lin, H.P. Huang, J.S. Yang, J.Y. Wu, T.C. Hsia, C.C. Lin, C.W. Lin, C.L. Kuo, W. Gibson Wood, J.G. Chung, DNA damage and endoplasmic reticulum stress mediated curcumin-induced cell cycle arrest and apoptosis in human lung carcinoma A-549 cells through the activation caspases cascade- and mitochondrial-dependent pathway, Cancer letters. 2008, 272 (1), 77-90.
[21] N. Dhillon, B.B. Aggarwal, R.A. Newman, R.A. Wolff, A.B. Kunnumakkara, J.L. Abbruzzese, C.S. Ng, V. Badmaev, R. Kurzrock, Phase II trial of curcumin in patients with advanced pancreatic cancer, Clinical cancer research : an official journal of the American Association for Cancer Research. 2008, 14 (14), 4491-9.
[22] B.K. Adams, E.M. Ferstl, M.C. Davis, M. Herold, S. Kurtkaya, R.F. Camalier, M.G. Hollingshead, G. Kaur, E.A. Sausville, F.R. Rickles, Synthesis and biological evaluation of novel curcumin analogs as anti-cancer and anti-angiogenesis agents, Bioorganic & medicinal chemistry. 2004, 12 (14), 3871-3883.
[23] A.S. Oliveira, E. Sousa, M. Helena Vasconcelos, M. Pinto, Curcumin: A Natural Lead for Potential New Drug Candidates, Current medicinal chemistry. 2015, 22 (36), 4196-4232.
[24] P.-Y. Chen, Y.-H. Wu, M.-H. Hsu, T.-P. Wang, E.-C. Wang, Cerium ammonium nitrate-mediated the oxidative dimerization of p-alkenylphenols: a new synthesis of substituted (±)-trans-dihydrobenzofurans, Tetrahedron. 2013, 69 (2), 653-657.
[25] H. Ohori, H. Yamakoshi, M. Tomizawa, M. Shibuya, Y. Kakudo, A. Takahashi, S. Takahashi, S. Kato, T. Suzuki, C. Ishioka, Synthesis and biological analysis of new

curcumin analogues bearing an enhanced potential for the medicinal treatment of cancer, Molecular cancer therapeutics. 2006, 5 (10), 2563-2571.

[26] J.P. Marie, A.M. Faussat-Suberville, D. Zhou, R. Zittoun, Daunorubicin uptake by leukemic cells: correlations with treatment outcome and mdr1 expression, Leukaemia. 1993, 7 (6), 825-31.

[27] H. Seca, R.T. Lima, J.E. Guimaraes, M. Helena Vasconcelos, Simultaneous targeting of P-gp and XIAP with siRNAs increases sensitivity of P-gp overexpressing CML cells to imatinib, Hematology. 2011, 16 (2), 100-8.

[28] M. Pesic, J.Z. Markovic, D. Jankovic, S. Kanazir, I.D. Markovic, L. Rakic, S. Ruzdijic, Induced resistance in the human non small cell lung carcinoma (NCI-H460) cell line in vitro by anticancer drugs, Journal of chemotherapy. 2006, 18 (1), 66-73.

[29] A. Podolski-Renic, M. Jadranin, T. Stankovic, J. Bankovic, S. Stojkovic, M. Chiourea, I. Aljancic, V. Vajs, V. Tesevic, S. Ruzdijic, S. Gagos, N. Tanic, M. Pesic, Molecular and cytogenetic changes in multi-drug resistant cancer cells and their influence on new compounds testing, Cancer chemotherapy and pharmacology. 2013, 72 (3), 683-97.

[30] V. Vichai, K. Kirtikara, Sulforhodamine B colorimetric assay for cytotoxicity screening, Nat Protoc. 2006, 1 (3), 1112-6.

[31] P. Skehan, R. Storeng, D. Scudiero, A. Monks, J. McMahon, D. Vistica, J.T. Warren, H. Bokesch, S. Kenney, M.R. Boyd, New colorimetric cytotoxicity assay for anticancer-drug screening, J Natl Cancer Inst. 1990, 82 (13), 1107-12.

[32] M.P. Neves, H. Cidade, M. Pinto, A.M. Silva, L. Gales, A.M. Damas, R.T. Lima, M.H. Vasconcelos, M. de Sao Jose Nascimento, Prenylated derivatives of baicalein and 3,7-dihydroxyflavone: synthesis and study of their effects on tumour cell lines growth, cell cycle and apoptosis, Eur J Med Chem. 2011, 46 (6), 2562-74.

[33] M.P. Neves, S. Cravo, R.T. Lima, M.H. Vasconcelos, M.S. Nascimento, A.M. Silva, M. Pinto, H. Cidade, A.G. Correa, Solid-phase synthesis of 2'-hydroxychalcones. Effects on cell growth inhibition, cell cycle and apoptosis of human tumour cell lines, Bioorg Med Chem. 2012, 20 (1), 25-33.

[34] A. Palmeira, F. Rodrigues, E. Sousa, M. Pinto, M.H. Vasconcelos, M.X. Fernandes, New uses for old drugs: pharmacophore-based screening for the discovery of P-glycoprotein inhibitors, Chemical biology & drug design. 2011, 78 (1), 57-72.

[35] R.M. Abreu, I.C. Ferreira, R.C. Calhelha, R.T. Lima, M.H. Vasconcelos, F. Adega, R. Chaves, M.J. Queiroz, Anti-hepatocellular carcinoma activity using human HepG2 cells and hepatotoxicity of 6-substituted methyl 3-aminothieno[3,2-b]pyridine-2-carboxylate derivatives: in vitro evaluation, cell cycle analysis and QSAR studies, Eur J Med Chem. 2011, 46 (12), 5800-6.

[36] M.J. Queiroz, D. Peixoto, R.C. Calhelha, P. Soares, T. Dos Santos, R.T. Lima, J.F. Campos, R.M. Abreu, I.C. Ferreira, M.H. Vasconcelos, New di(hetero)arylethers and di(hetero)arylamines in the thieno[3,2-b]pyridine series: synthesis, growth inhibitory activity on human tumour cell lines and non-tumour cells, effects on cell cycle and on programmed cell death, Eur J Med Chem. 2013, 69 855-62.

[37] R.T. Lima, L.M. Martins, J.E. Guimaraes, C. Sambade, M.H. Vasconcelos, Chemosensitization effects of XIAP downregulation in K562 leukaemia cells, J Chemother. 2006, 18 (1), 98-102.

[38] A. Goel, A.B. Kunnumakkara, B.B. Aggarwal, Curcumin as “Curecumin”: From kitchen to clinic, Biochemical pharmacology. 2008, 75 (4), 787-809.

[39] M. Tomren, M. Masson, T. Loftsson, H.H. Tønnesen, Studies on curcumin and curcuminoids: XXXI. Symmetric and asymmetric curcuminoids: stability, activity and complexation with cyclodextrin, International journal of pharmaceutics. 2007, 338 (1), 27-34.

[40] R.A. Castanheiro, M.M. Pinto, A.M. Silva, S.M. Cravo, L. Gales, A.M. Damas, N. Nazareth, M.S. Nascimento, G. Eaton, Dihydroxyxanthones prenylated derivatives: synthesis, structure elucidation, and growth inhibitory activity on human tumour cell lines with improvement of selectivity for MCF-7, Bioorganic & medicinal chemistry. 2007, 15 (18), 6080-6088.

[41] H.C. Kolb, M. Finn, K.B. Sharpless, Click chemistry: diverse chemical function from a few good reactions, Angewandte Chemie International Edition. 2001, 40 (11), 2004-2021.

[42] G.C. Tron, T. Pirali, R.A. Billington, P.L. Canonico, G. Sorba, A.A. Genazzani, Click chemistry reactions in medicinal chemistry: Applications of the 1, 3-dipolar cycloaddition between azides and alkynes, Medicinal research reviews. 2008, 28 (2), 278-308.

[43] A.M. Barrett, J. Carter, R. Hull, D.J.L. Count, C.J. Squire, Alkanolamine derivatives for treating hypertension, US 3934032 A, 1976.

[44] A. Palmeira, M.H. Vasconcelos, A. Paiva, M.X. Fernandes, M. Pinto, E. Sousa, Dual inhibitors of P-glycoprotein and tumour cell growth: (re)discovering thioxanthones, Biochemical pharmacology. 2012, 83 (1), 57-68.

[45] C. Coburger, J. Wollmann, C. Baumert, M. Krug, J. Molnar, H. Lage, A. Hilgeroth, Novel insight in structure-activity relationship and bioanalysis of P-glycoprotein targeting highly potent tetrakishydroxymethyl substituted 3,9-diazatetraasteranes, Journal of medicinal chemistry. 2008, 51 (18), 5871-4.

[46] R.B. Kim, Drugs as P-glycoprotein substrates, inhibitors, and inducers, Drug Metab Rev. 2002, 34 (1-2), 47-54.

[47] S. Anuchapreeda, P. Leechanachai, M.M. Smith, S.V. Ambudkar, P.N. Limtrakul, Modulation of P-glycoprotein expression and function by curcumin in multidrug-resistant human KB cells, Biochemical pharmacology. 2002, 64 (4), 573-82.
[48] W. Chearwae, S. Anuchapreeda, K. Nandigama, S.V. Ambudkar, P. Limtrakul, Biochemical mechanism of modulation of human P-glycoprotein (ABCB1) by curcumin I, II, and III purified from Turmeric powder, Biochemical pharmacology. 2004, 68 (10), 2043-52.
[49] S.V. Ambudkar, S. Dey, C.A. Hrycyna, M. Ramachandra, I. Pastan, M.M. Gottesman, Biochemical, cellular, and pharmacological aspects of the multidrug transporter, Annu Rev Pharmacol Toxicol. 1999, 39 361-98.
[50] P.D. Eckford, F.J. Sharom, ABC efflux pump-based resistance to chemotherapy drugs, Chem Rev. 2009, 109 (7), 2989-3011.
[51] L.X. Wu, Y. Wu, R.J. Chen, Y. Liu, L.S. Huang, L.G. Lou, Z.H. Zheng, Y.Z. Chen, J.H. Xu, Curcumin derivative C817 inhibits proliferation of imatinib-resistant chronic myeloid leukaemia cells with wild-type or mutant Bcr-Abl in vitro, Acta Pharmacol Sin. 2014, 35 (3), 401-9.
[52] P. Poma, M. Notarbartolo, M. Labbozzetta, A. Maurici, V. Carina, A. Alaimo, M. Rizzi, D. Simoni, N. D'Alessandro, The antitumor activities of curcumin and of its isoxazole analogue are not affected by multiple gene expression changes in an MDR model of the MCF-7 breast cancer cell line: analysis of the possible molecular basis, Int J Mol Med. 2007, 20 (3), 329-35.
[53] K.M. Pluchino, M.D. Hall, A.S. Goldsborough, R. Callaghan, M.M. Gottesman, Collateral sensitivity as a strategy against cancer multidrug resistance, Drug Resist Updat. 2012, 15 (1-2), 98-105.
[54] S. Sreenivasan, S. Ravichandran, U. Vetrivel, S. Krishnakumar, Modulation of multidrug resistance 1 expression and function in retinoblastoma cells by curcumin, Journal of pharmacology & pharmacotherapeutics. 2013, 4 (2), 103-9.
[55] W.-D. Lu, Y. Qin, C. Yang, L. Li, Effect of curcumin on human colon cancer multidrug resistance in vitro and in vivo, Clinics. 2013, 68 (5), 694-701.
[56] V. Lopes-Rodrigues, A. Di Luca, D. Sousa, H. Seca, P. Meleady, M. Henry, R.T. Lima, R. O'Connor, M.H. Vasconcelos, Multidrug resistant tumour cells shed more microvesicle-like EVs and less exosomes than their drug-sensitive counterpart cells, Biochimica et biophysica acta. 2016, 1860 (3), 618-27.
[57] K. Selvendiran, L. Tong, S. Vishwanath, A. Bratasz, N.J. Trigg, V.K. Kutala, K. Hideg, P. Kuppusamy, EF24 induces G2/M arrest and apoptosis in cisplatin-resistant human ovarian cancer cells by increasing PTEN expression, The Journal of biological chemistry. 2007, 282 (39), 28609-18.

[58] Y.Q. Xia, X.Y. Wei, W.L. Li, K. Kanchana, C.C. Xu, D.H. Chen, P.H. Chou, R. Jin, J.Z. Wu, G. Liang, Curcumin analogue A501 induces G2/M arrest and apoptosis in non-small cell lung cancer cells, Asian Pac J Cancer Prev. 2014, 15 (16), 6893-8.
[59] S.A. Amundson, T.G. Myers, A.J. Fornace, Jr., Roles for p53 in growth arrest and apoptosis: putting on the brakes after genotoxic stress, Oncogene. 1998, 17 (25), 3287-99.
[60] E.A. Nigg, Mitotic kinases as regulators of cell division and its checkpoints, Nat Rev Mol Cell Biol. 2001, 2 (1), 21-32.
[61] Z. Tian, J. Shen, A.P. Moseman, Q. Yang, J. Yang, P. Xiao, E. Wu, I.S. Kohane, Dulxanthone A induces cell cycle arrest and apoptosis via up-regulation of p53 through mitochondrial pathway in HepG2 cells, International journal of cancer. Journal international du cancer. 2008, 122 (1), 31-8.

CHAPTER III – GENERAL DISCUSSION AND FUTURE PERSPECTIVES

The development of multidrug resistance (MDR) in cancer is a serious impediment to treatment success. MDR is defined as a phenotype in which cells are resistant to multiple structurally different drugs. Such resistance is multifactorial and could be due to various mechanisms [39,190]. Some of the most important mechanisms of MDR are: the overexpression of ABC transporters [such as P-glycoprotein (P-gp)] [39], alterations in apoptosis, increase drug detoxification and metabolic phenotype alterations [191]. Interestingly, the release of extracellular vesicles (EVs) by MDR cells and their transfer to drug-sensitive cells may confer a MDR phenotype in the recipient cells [187]. The identification and the study of MDR mechanisms and of potential molecular targets and biomarkers is important, in order to generate valuable information and tools to circumvent this phenotype and further improve cancer chemotherapy treatment.

Thus, driven by the need to circumvent P-gp mediated MDR , we aimed to: i) identify new targets for overcoming P-gp mediated MDR in cancer, by identifying metabolic alterations associated with P-gp mediated MDR in cancer and by verifying if those alterations are transferred by EVs from MDR cells to drug-sensitive cells; ii) identify potential biomarkers of MDR in EVs shed by cancer cells; and iii) find novel molecules to overcome MDR, by identifying curcumin derivatives with improved P-gp inhibitory effect.

In this work we used two different cancer cell models, a chronic myeloid leukaemia model (CML) and a non-small cell lung cancer model (NSCLC), in order to identify possible mechanisms and molecular targets of MDR that were not specific of a particular cancer. Thus, the K562/K562Dox (CML) and the NCI-H460/RH460 (NSCLC) cell lines were used as models of P-gp mediated MDR cancer cells and their respective drug-sensitive counterparts. These two pairs of cells were established and kindly provided to our group by Dr. J. P. Marie (Paris, France) [192] and by Dr. M. Pesic (Belgrade, Serbia) [193,194] respectively. They have the remarkable feature of being two pairs of counterpart cell lines, in which the parental cell lines (K562 and NCI-H460) are drug-sensitive and the counterpart cell lines (K562Dox and RH460) are MDR and have overexpression of P-gp.

The results presented in this thesis clearly identified a complex network of metabolic alterations that are associated with the MDR phenotype. Furthermore, we have shown that comparative proteomic approaches are powerful tools to investigate MDR mechanisms in cancer cells. Indeed, by performing a label-free LC-MS quantitative profiling we showed that, in terms of biological processes, most of the identified DEPs (differentially expressed proteins between MDR and drug-sensitive cells) (e.g. G6PD, IDH1 and PGD) were involved in metabolic processes and the most active pathways that were found enriched were the ones involved in cellular metabolism, namely GSH, PPP and glycolysis.

Interestingly, most of the DEPs involved in the PPP (including the rate limiting enzyme, G6PD) were found downregulated in the MDR cells. Data presented in this thesis also shows that GSH levels were increased in MDR cells (from both tumour models), as previously published by other authors. [195,196] Since GSH is a detoxification agent [118], the levels of ROS in the MDR cells, as expected, were decreased. Evidence suggests that elevated levels of NADPH and GSH, together with an active PPP, play a critical role in MDR [104,197]. However, the results here presented together with other recent studies [110,111] contradict those reports, showing that PPP enzymes may be downregulated in MDR cells. **Therefore, this work shows that MDR cells are capable of maintaining high levels of GSH in order to decrease ROS, even when PPP is downregulated.** This suggests that MDR cells must have upregulation of another source of GSH.

The present work also showed clear differences between MDR and drug-sensitive cells, in the amount of several metabolites of the methionine/S-adenosylmethionine pathway and an increase in the methylation index of both MDR (K562Dox and RH460) cell lines. Methionine levels were significantly increased in the MDR cells, which could be involved in the GSH increase observed in those cells. Indeed, the methionine cycle leads to cysteine production, a rate-limiting factor in cellular GSH biosynthesis [198]. Also, the fact that the methylation capacity of the cells (methylation index) was increased in the MDR cells could be due to the metabolic alterations that MDR cells suffer when developing the resistance phenotype. In agreement with these results, other authors have described that cell treatment with a methylation inhibitor reversed drug resistance, which indicates that the development of drug resistance in some cases could be methylation-dependent [136].

Importantly, this study raised the possibility that MDR cells, when acquiring the resistant phenotype, switch their main energy supply from OXPHOS to glycolysis in order to fulfill the high demand for energy and biomass of these cells. Indeed, the results here presented showed a statistically significant increase in glycolysis (and in the glycolytic capacity) of MDR cells (RH460), together with a decrease in the mitochondrial basal respiration and in the maximal capacity of these cells to perform OXPHOS, when compared to the drug-sensitive counterpart cells (NCI-H460). In agreement with these results, several studies in different cancer models have demonstrated an efficient suppression of MDR by glycolytic inhibitors [23,45,81,91,199]. This altered metabolic activity of MDR cells could be crucial for: i) supporting uncontrolled proliferation, since glycolysis provides cells with intermediates needed for biosynthetic pathways and ii) allowing the use of the most abundant extracellular nutrient (glucose) to produce abundant ATP. Even though the yield of ATP per glucose molecule consumed is low, if the glycolytic flux is high enough, the percentage of cellular ATP produced by glycolysis can exceed the one

produced by OXPHOS [63,200]. Also, it was reported that an association between drug resistance and glycolysis may partially be due to the radical scavenging potential of the glycolytic intermediates, and the link between them and the cellular redox status [201]. Indeed, the results here presented are in agreement with this report, since the MDR cell models studied showed a decrease in ROS levels and an increase in glycolysis, when compared to their drug-sensitive counterpart cells.

The present work also demonstrates that following PPP pathway inhibition (with DCA [202]) the drug-sensitive cells (NCI-H460) acquire a metabolic phenotype more similar to the one of the MDR cells, by increasing glycolysis and decreasing OXPHOS. These results support a direct interaction between glycolysis and PPP activity in the MDR phenotype. Since some of the intermediates from glycolysis and PPP are the same, it is possible that MDR cells may be directing these intermediates mostly to glycolysis, in order to sustain the energy and the production of intermediates to the cellular biosynthetic pathways request.

We found that following P-gp inhibition (with verapamil [203]) in P-gp overexpressing MDR cells (RH460), those cells acquire a metabolic phenotype more similar to the one of drug-sensitive cells, with a decrease in glycolysis and an increase in OXPHOS. In agreement with these results, it has been reported that, in multicellular tumour spheroids and in doxorubicin-resistant human breast adenocarcinoma cells, the inhibition of glycolysis raised intracellular ROS, downregulated P-gp and reverted the MDR phenotype [23,45]. Since inhibition of glycolysis could induce a dramatic reduction in the cellular levels of ATP, the mechanism involved may be related to the function of the drug-efflux pumps, since the activity of transmembrane transporters is ATPase dependent. Further studies, such as through the silencing and/or the overexpression of some of the DEPs (e.g. G6PD, IDH1 and PGD) will be essential to verify the hypothesis that these proteins may be potential targets to overcome MDR.

Interestingly, this work also showed that EVs released by MDR cells are capable of causing a metabolic switch in the receiving drug-sensitive cancer cells (towards a similar phenotype to the one observed in the donor MDR cells). In fact, when the drug-sensitive cells (NCI-H460) were co-incubated with EVs from MDR cells (RH460 or K562Dox), they acquired a metabolic phenotype more similar to the one of MDR cells (*i.e*, an increase in glycolysis). The importance of EVs in the transfer of the MDR phenotype between cells has been recently described [178,180,186]. Therefore, it is possible that the acquisition of an altered metabolic phenotype (by MDR cells) could be associated with alterations in the type of EVs that are released by those cells, in their cargo and in the capacity to transfer phenotypes to receiving cells. Thus, it would be interesting to verify if

there is EVs-mediated transfer of some of the proteins involved in glycolysis, from MDR cells to drug-sensitive cells.

In addition to verifying that EVs (released by MDR cells) are capable of causing metabolic alterations in receiving drug-sensitive cells, in this thesis we have raised the possibility that MDR cells produce more microvesicles whereas drug-sensitive cells produce more exosomes. Indeed, regarding size, EVs released by the drug-sensitive cells presented mostly a size range between 10 and 80 nm, which is closer to the "exosomes size range" (30 to 100 nm) [143]. On the other hand, EVs released by the MDR cells presented sizes ranging mostly between 40 and 200 nm, closer to the microvesicles size range described in the literature (50 to 2000 nm) [143]. Moreover, proteins described to be mainly involved in the biogenesis of exosomes, such as TSG101 [147,155,204-206], CHMP4 [147], CD63 [143], Syntenin-1 [147] and Clathrin [206], were here found to have increased levels in the EVs shed by drug-sensitive cells (when compared to the ones shed by the MDR cells). This was true for both the MDR models used in this thesis (CML and NSCLC), which suggests that MDR cells decrease the amount of released exosomes and increase the amount of released microvesicles.

Another highly relevant observed difference was that the MDR cells produced more EVs than the sensitive counterpart cells. This fact has been previously described in other studies [174,207,208]. According to those reports, and the results presented on this thesis, P-gp (or drug-efflux pumps in general) may be involved in the regulation of the EVs release (though a still unidentified mechanism), since both MDR models used in this study had P-gp overexpression. Thus, it would be interesting to confirm this and to further study how P-gp could be involved in the release as well as in the definition of the cargo of EVs.

Interestingly, a recent study observed that glutamine metabolism was altered in cancer cells following incubation with large EVs (microvesicles) released by prostate cancer cells, an effect that was not observed upon incubation with exosomes released by the same cells [184]. With these results in mind, we propose that it is possible that the specific type of EVs that are responsible for the transfer of the metabolic phenotype in our cell models may be microvesicles, rather than exosomes. This highlights the importance of verifying the type of EVs that donor cells release, since different EVs may transfer different phenotypes to receiving cells. **Additionally, the protein cargo that was found different in the EVs released by the two pairs of MDR and drug-sensitive cell lines, was detected with similar expression levels in the cell lines that released those EVs, which suggests that there is selective packaging of those proteins into the EVs.** In fact, the selective packaging of EVs has been previously described in several other studies [150,209]. However, this work adds knowledge and impact to the previous studies, since we have shown

selective packaging of proteins involved in the biogenesis of the EVs themselves, which are associated with different sizes/types of EVs.

Additionally, we proposed in this thesis that the specific size and protein content that we have here identified in the EVs released by the MDR cells may have diagnostic significance in cancer, as biomarkers to identify the MDR phenotype. **Further studies are needed to validate this hypothesis,** such as by monitoring these biomarkers in the plasma of nude mice xenografted with MDR human tumours and, more importantly, in the plasma of patients with MDR tumours.

In addition, during this thesis we came across the need to understand if there was degradation of the (EV marker) ALIX protein, when freezing samples for Western blots analysis. The obtained conclusions regarding the need to freeze these samples at – 80ºC will in the future allow to avoid misleading information resulting from the analysis of ALIX expression in protein lysates.

As was previously shown on this thesis, treating MDR cells with a P-gp inhibitor significantly altered the metabolic phenotype of these cells, towards a phenotype more similar to the one of drug-sensitive cells. This highlights the importance of identifying novel P-gp inhibitors. **The present study identifies a novel curcumin derivative (compound 10) that presented more potent antitumor and anti-P-gp activity than curcumin itself.** In terms of cell growth inhibitory effect, from the eleven studied compounds (curcumin derivatives synthesized by our collaborators of FFUP/CIIMAR), compound **10** was the most potent, being even more potent than curcumin. Interestingly, this compound was even more potent in the MDR cell lines than in the sensitive cells, possibly due to its ability to affect MDR cells more selectively than the sensitive cells, a process named collateral sensitivity [210].

Regarding the capacity of MDR reversal in the P-gp overexpressing cell line K562Dox (by inhibiting the function or expression of P-gp), our results showed that compound 10 was also the most potent P-gp inhibitor. Indeed, compound **10** presented the strongest effect on rh123 intracellular accumulation and on the inhibition of P-gp expression. Since the concentrations tested for compound **10** were much lower than the concentrations tested for curcumin, it can be concluded that compound **10** is a stronger inhibitor of P-gp expression. The inhibition of P-gp expression by curcumin had already been described [211,212] but, to our knowledge, this activity had not been explored for synthetic curcumin derivatives and analogues.

In addition, the study of the mechanism of action of compound 10 indicated that it caused a cell cycle arrest at the G2/M phase and an increase in cell death by apoptosis. Indeed, treatments with compound **10** (or curcumin) increased cellular levels of p53 and cyclin B1, which is in agreement with the fact that p53 activation (being the guardian

of the genome) usually results in a cell cycle arrest and a consequent induction of apoptosis [213]. Also, since cyclin B1 (establishing a complex with CDK1) regulates progression of G2 and mitosis [214], its downregulation promotes cell cycle arrest at the G2/M phase, which is in agreement with the observed results. By treating K562Dox cells with compound **10** (or curcumin) a decrease in total PARP-1 and pro-caspase 3 levels and an increase in the expression levels of cleaved PARP-1 were observed, which is in agreement with an activation of apoptosis.

Unfortunately, none of the investigated derivatives was found to be particularly stable in the range of conditions assessed, which supports the difficulty observed by other authors in obtaining more stable curcumin derivatives.

In conclusion, this work allowed to further identify new targets for overcoming P-gp mediated MDR in cancer. In addition, these results contributed to clarify the complex metabolic network between the various metabolic alterations that are associated with P-gp mediated MDR in cancer cells. Moreover, this work demonstrated that a EV-mediated transfer of metabolic information related with the production of energy by the cell may occur, from MDR cells to drug-sensitive cancer cells. Importantly, this work also proved that MDR cells release more microvesicle-like EVs than exosomes. These microvesicles, shed in higher amounts by MDR cells, could potentially be the source of biomarkers of MDR in cancer [215]. Finally, in this work a novel P-gp inhibitor (derived from curcumin) was described, which simultaneously inhibits the function and the expression of P-gp. Inhibitors of P-gp expression in particular are very important chemical tools, since they can be used to control P-gp expression in several pharmacological studies, not only by inhibiting cellular P-gp expression but also by inhibiting its production and therefore its intercellular transfer by EVs.

REFERENCES

1 Szakacs, G., Paterson, J. K., Ludwig, J. A., Booth-Genthe, C. & Gottesman, M. M. Targeting multidrug resistance in cancer. *Nature reviews. Drug discovery* **5**, 219-234, doi:10.1038/nrd1984 (2006).

2 Shaffer, B. C. *et al.* Drug resistance: still a daunting challenge to the successful treatment of AML. *Drug Resist Updat* **15**, 62-69, doi:10.1016/j.drup.2012.02.001 (2012).

3 Shapira, A., Livney, Y. D., Broxterman, H. J. & Assaraf, Y. G. Nanomedicine for targeted cancer therapy: towards the overcoming of drug resistance. *Drug Resist Updat* **14**, 150-163, doi:10.1016/j.drup.2011.01.003 (2011).

4 Saraswathy, M. & Gong, S. Different strategies to overcome multidrug resistance in cancer. *Biotechnol Adv* **31**, 1397-1407, doi:10.1016/j.biotechadv.2013.06.004 (2013).

5 Lage, H. An overview of cancer multidrug resistance: a still unsolved problem. *Cell Mol Life Sci* **65**, 3145-3167, doi:10.1007/s00018-008-8111-5 (2008).

6 Baguley, B. C. Multidrug resistance in cancer. *Methods Mol Biol* **596**, 1-14, doi:10.1007/978-1-60761-416-6_1 (2010).

7 Rich, J. N. & Bao, S. Chemotherapy and cancer stem cells. *Cell Stem Cell* **1**, 353-355, doi:10.1016/j.stem.2007.09.011 (2007).

8 Shackleton, M. Normal stem cells and cancer stem cells: similar and different. *Semin Cancer Biol* **20**, 85-92, doi:10.1016/j.semcancer.2010.04.002 (2010).

9 Yap, T. A., Gerlinger, M., Futreal, P. A., Pusztai, L. & Swanton, C. Intratumor heterogeneity: seeing the wood for the trees. *Sci Transl Med* **4**, 127ps110, doi:10.1126/scitranslmed.3003854 (2012).

10 McGranahan, N. & Swanton, C. Biological and therapeutic impact of intratumor heterogeneity in cancer evolution. *Cancer Cell* **27**, 15-26, doi:10.1016/j.ccell.2014.12.001 (2015).

11 Swanton, C. Intratumor heterogeneity: evolution through space and time. *Cancer research* **72**, 4875-4882, doi:10.1158/0008-5472.CAN-12-2217 (2012).

12 Venkatesan, S. & Swanton, C. Tumor Evolutionary Principles: How Intratumor Heterogeneity Influences Cancer Treatment and Outcome. *Am Soc Clin Oncol Educ Book* **35**, e141-149, doi:10.14694/EDBK_158930 (2016).

13 Gottesman, M. M. Mechanisms of cancer drug resistance. *Annu Rev Med* **53**, 615-627, doi:10.1146/annurev.med.53.082901.103929 (2002).

14 Fletcher, J. I., Haber, M., Henderson, M. J. & Norris, M. D. ABC transporters in cancer: more than just drug efflux pumps. *Nature reviews. Cancer* **10**, 147-156, doi:10.1038/nrc2789 (2010).

15 Hamada, S., Kamada, M., Furumoto, H., Hirao, T. & Aono, T. Expression of glutathione S-transferase-pi in human ovarian cancer as an indicator of resistance to chemotherapy. *Gynecol Oncol* **52**, 313-319 (1994).

16 Uozaki, H. *et al.* Overexpression of resistance-related proteins (metallothioneins, glutathione-S-transferase pi, heat shock protein 27, and lung resistance-related protein) in osteosarcoma. Relationship with poor prognosis. *Cancer* **79**, 2336-2344 (1997).

17 Mackay, H. J. *et al.* Reduced MLH1 expression in breast tumors after primary chemotherapy predicts disease-free survival. *J Clin Oncol* **18**, 87-93 (2000).

18 Bottini, A. *et al.* p53 but not bcl-2 immunostaining is predictive of poor clinical complete response to primary chemotherapy in breast cancer patients. *Clinical cancer research : an official journal of the American Association for Cancer Research* **6**, 2751-2758 (2000).

19 Swisher, E. M. *et al.* Secondary BRCA1 mutations in BRCA1-mutated ovarian carcinomas with platinum resistance. *Cancer research* **68**, 2581-2586, doi:10.1158/0008-5472.CAN-08-0088 (2008).

20 Wilson, W. H. *et al.* Relationship of p53, bcl-2, and tumor proliferation to clinical drug resistance in non-Hodgkin's lymphomas. *Blood* **89**, 601-609 (1997).

21 Abdel-Fatah, T. M. *et al.* Bcl2 is an independent prognostic marker of triple negative breast cancer (TNBC) and predicts response to anthracycline combination (ATC) chemotherapy (CT) in adjuvant and neoadjuvant settings. *Ann Oncol* **24**, 2801-2807, doi:10.1093/annonc/mdt277 (2013).

22 Chen, Y., Tsai, Y. H., Fang, Y. & Tseng, S. H. Micro-RNA-21 regulates the sensitivity to cisplatin in human neuroblastoma cells. *J Pediatr Surg* **47**, 1797-1805, doi:10.1016/j.jpedsurg.2012.05.013 (2012).

23 Ma, S., Jia, R., Li, D. & Shen, B. Targeting Cellular Metabolism Chemosensitizes the Doxorubicin-Resistant Human Breast Adenocarcinoma Cells. *Biomed Res Int* **2015**, 453986, doi:10.1155/2015/453986 (2015).

24 Gottesman, M. M., Fojo, T. & Bates, S. E. Multidrug resistance in cancer: role of ATP-dependent transporters. *Nature reviews. Cancer* **2**, 48-58, doi:10.1038/nrc706 (2002).

25 International Transporter, C. *et al.* Membrane transporters in drug development. *Nature reviews. Drug discovery* **9**, 215-236, doi:10.1038/nrd3028 (2010).

26 Kivisto, K. T., Kroemer, H. K. & Eichelbaum, M. The role of human cytochrome P450 enzymes in the metabolism of anticancer agents: implications for drug interactions. *Br J Clin Pharmacol* **40**, 523-530 (1995).

27 Ang, W. H., Khalaila, I., Allardyce, C. S., Juillerat-Jeanneret, L. & Dyson, P. J. Rational design of platinum(IV) compounds to overcome glutathione-S-transferase mediated drug resistance. *J Am Chem Soc* **127**, 1382-1383, doi:10.1021/ja0432618 (2005).

28 Bouwman, P. & Jonkers, J. The effects of deregulated DNA damage signalling on cancer chemotherapy response and resistance. *Nature reviews. Cancer* **12**, 587-598, doi:10.1038/nrc3342 (2012).

29 Curtin, N. J. DNA repair dysregulation from cancer driver to therapeutic target. *Nature reviews. Cancer* **12**, 801-817, doi:10.1038/nrc3399 (2012).

30 Khamisipour, G., Jadidi-Niaragh, F., Jahromi, A. S., Zandi, K. & Hojjat-Farsangi, M. Mechanisms of tumor cell resistance to the current targeted-therapy agents. *Tumour Biol* **37**, 10021-10039, doi:10.1007/s13277-016-5059-1 (2016).

31 Lowe, S. W., Cepero, E. & Evan, G. Intrinsic tumour suppression. *Nature* **432**, 307-315, doi:10.1038/nature03098 (2004).

32 Zuckerman, V., Wolyniec, K., Sionov, R. V., Haupt, S. & Haupt, Y. Tumour suppression by p53: the importance of apoptosis and cellular senescence. *J Pathol* **219**, 3-15, doi:10.1002/path.2584 (2009).

33 Bossi, G. *et al.* Mutant p53 gain of function: reduction of tumor malignancy of human cancer cell lines through abrogation of mutant p53 expression. *Oncogene* **25**, 304-309, doi:10.1038/sj.onc.1209026 (2006).

34 Gemba, K., Ueoka, H., Kiura, K., Tabata, M. & Harada, M. Immunohistochemical detection of mutant p53 protein in small-cell lung cancer: relationship to treatment outcome. *Lung Cancer* **29**, 23-31 (2000).

35 Brown, J. M. & Attardi, L. D. The role of apoptosis in cancer development and treatment response. *Nature reviews. Cancer* **5**, 231-237, doi:10.1038/nrc1560 (2005).

36 Hanahan, D. & Weinberg, R. A. Hallmarks of cancer: the next generation. *Cell* **144**, 646-674, doi:10.1016/j.cell.2011.02.013 (2011).

37 Miyashita, T. & Reed, J. C. bcl-2 gene transfer increases relative resistance of S49.1 and WEHI7.2 lymphoid cells to cell death and DNA fragmentation induced by glucocorticoids and multiple chemotherapeutic drugs. *Cancer research* **52**, 5407-5411 (1992).

38 Konopleva, M. *et al.* Mechanisms of apoptosis sensitivity and resistance to the BH3 mimetic ABT-737 in acute myeloid leukemia. *Cancer Cell* **10**, 375-388, doi:10.1016/j.ccr.2006.10.006 (2006).

39 Lopes-Rodrigues, V. *et al.* The network of P-glycoprotein and microRNAs interactions. *International journal of cancer. Journal international du cancer* **135**, 253-263, doi:10.1002/ijc.28500 (2014).

40 Tekiner, T. A. & Basaga, H. Role of microRNA deregulation in breast cancer cell chemoresistance and stemness. *Current medicinal chemistry* **20**, 3358-3369 (2013).

41 Croce, C. M. Causes and consequences of microRNA dysregulation in cancer. *Nature reviews. Genetics* **10**, 704-714, doi:10.1038/nrg2634 (2009).

42 Semenza, G. L. HIF-1 mediates metabolic responses to intratumoral hypoxia and oncogenic mutations. *J Clin Invest* **123**, 3664-3671, doi:10.1172/JCI67230 (2013).

43 Koczula, K. M. *et al.* Metabolic plasticity in CLL: adaptation to the hypoxic niche. *Leukemia : official journal of the Leukemia Society of America, Leukemia Research Fund, U.K* **30**, 65-73, doi:10.1038/leu.2015.187 (2016).

44 Zub, K. A. *et al.* Modulation of cell metabolic pathways and oxidative stress signaling contribute to acquired melphalan resistance in multiple myeloma cells. *PloS one* **10**, e0119857, doi:10.1371/journal.pone.0119857 (2015).

45 Wartenberg, M. *et al.* Glycolytic pyruvate regulates P-Glycoprotein expression in multicellular tumor spheroids via modulation of the intracellular redox state. *J Cell Biochem* **109**, 434-446, doi:10.1002/jcb.22422 (2010).

46 Milane, L., Duan, Z. & Amiji, M. Role of hypoxia and glycolysis in the development of multi-drug resistance in human tumor cells and the establishment of an orthotopic multi-drug resistant tumor model in nude mice using hypoxic pre-conditioning. *Cancer Cell Int* **11**, 3, doi:10.1186/1475-2867-11-3 (2011).

47 Juliano, R. L. & Ling, V. A surface glycoprotein modulating drug permeability in Chinese hamster ovary cell mutants. *Biochimica et biophysica acta* **455**, 152-162 (1976).

48 Omote, H. & Al-Shawi, M. K. Interaction of transported drugs with the lipid bilayer and P-glycoprotein through a solvation exchange mechanism. *Biophys J* **90**, 4046-4059, doi:10.1529/biophysj.105.077743 (2006).

49 Fu, D., Bebawy, M., Kable, E. P. & Roufogalis, B. D. Dynamic and intracellular trafficking of P-glycoprotein-EGFP fusion protein: Implications in multidrug resistance in cancer. *International journal of cancer. Journal international du cancer* **109**, 174-181, doi:10.1002/ijc.11659 (2004).

50 Molinari, A. *et al.* Subcellular detection and localization of the drug transporter P-glycoprotein in cultured tumor cells. *Curr Protein Pept Sci* **3**, 653-670 (2002).

51 Fu, D. & Roufogalis, B. D. Actin disruption inhibits endosomal traffic of P-glycoprotein-EGFP and resistance to daunorubicin accumulation. *Am J Physiol Cell Physiol* **292**, C1543-1552, doi:10.1152/ajpcell.00068.2006 (2007).

52 Palmeira, A., Sousa, E., Vasconcelos, M. H. & Pinto, M. M. Three decades of P-gp inhibitors: skimming through several generations and scaffolds. *Current medicinal chemistry* **19**, 1946-2025 (2012).

53 Krishna, R. & Mayer, L. D. Multidrug resistance (MDR) in cancer. Mechanisms, reversal using modulators of MDR and the role of MDR modulators in influencing the pharmacokinetics of anticancer drugs. *European journal of pharmaceutical sciences : official journal of the European Federation for Pharmaceutical Sciences* **11**, 265-283 (2000).

54 Newman, D. J. & Cragg, G. M. Natural products as sources of new drugs over the last 25 years. *J Nat Prod* **70**, 461-477, doi:10.1021/np068054v (2007).

55 Oliveira, A. P., Jewett, M.C., & Nielsen, J. in *Introduction to Systems Biology* (ed S. Choi) (The Human Press Inc, 2007).

56 Cairns, R. A., Harris, I. S. & Mak, T. W. Regulation of cancer cell metabolism. *Nature reviews. Cancer* **11**, 85-95, doi:10.1038/nrc2981 (2011).

57 Ward, P. S. & Thompson, C. B. Metabolic reprogramming: a cancer hallmark even warburg did not anticipate. *Cancer Cell* **21**, 297-308, doi:10.1016/j.ccr.2012.02.014 (2012).

58 Hsu, P. P. & Sabatini, D. M. Cancer cell metabolism: Warburg and beyond. *Cell* **134**, 703-707, doi:10.1016/j.cell.2008.08.021 (2008).

59 DeBerardinis, R. J., Lum, J. J., Hatzivassiliou, G. & Thompson, C. B. The biology of cancer: metabolic reprogramming fuels cell growth and proliferation. *Cell metabolism* **7**, 11-20, doi:10.1016/j.cmet.2007.10.002 (2008).

60 Scatena, R., Bottoni, P., Pontoglio, A., Mastrototaro, L. & Giardina, B. Glycolytic enzyme inhibitors in cancer treatment. *Expert Opin Investig Drugs* **17**, 1533-1545, doi:10.1517/13543784.17.10.1533 (2008).

61 Shoshan, M. C. Potentiation of anti-cancer treatment by modulators of energy metabolism. *Curr Pharm Biotechnol* **14**, 313-330 (2013).

62 Warburg, O. On respiratory impairment in cancer cells. *Science* **124**, 269-270 (1956).

63 Warburg, O. On the origin of cancer cells. *Science* **123**, 309-314 (1956).

64 Cox, D. L. N. a. M. M. *Principles of Biochemestry*. (W. H. Freeman and Company, 2012).

65 Christofk, H. R. *et al.* The M2 splice isoform of pyruvate kinase is important for cancer metabolism and tumour growth. *Nature* **452**, 230-233, doi:10.1038/nature06734 (2008).

66 Locasale, J. W. & Cantley, L. C. Altered metabolism in cancer. *BMC Biol* **8**, 88, doi:10.1186/1741-7007-8-88 (2010).

67 Gatenby, R. A. & Gillies, R. J. Why do cancers have high aerobic glycolysis? *Nature reviews. Cancer* **4**, 891-899, doi:10.1038/nrc1478 (2004).

68 Lunt, S. Y. & Vander Heiden, M. G. Aerobic glycolysis: meeting the metabolic requirements of cell proliferation. *Annu Rev Cell Dev Biol* **27**, 441-464, doi:10.1146/annurev-cellbio-092910-154237 (2011).

69 Lopez-Lazaro, M. The warburg effect: why and how do cancer cells activate glycolysis in the presence of oxygen? *Anticancer Agents Med Chem* **8**, 305-312 (2008).

70 Vander Heiden, M. G., Cantley, L. C. & Thompson, C. B. Understanding the Warburg effect: the metabolic requirements of cell proliferation. *Science* **324**, 1029-1033, doi:10.1126/science.1160809 (2009).

71 Hamanaka, R. B. & Chandel, N. S. Targeting glucose metabolism for cancer therapy. *J Exp Med* **209**, 211-215, doi:10.1084/jem.20120162 (2012).

72 Deberardinis, R. J., Sayed, N., Ditsworth, D. & Thompson, C. B. Brick by brick: metabolism and tumor cell growth. *Curr Opin Genet Dev* **18**, 54-61, doi:10.1016/j.gde.2008.02.003 (2008).

73 Gottschalk, S., Anderson, N., Hainz, C., Eckhardt, S. G. & Serkova, N. J. Imatinib (STI571)-mediated changes in glucose metabolism in human leukemia BCR-ABL-positive cells. *Clinical cancer research : an official journal of the American Association for Cancer Research* **10**, 6661-6668, doi:10.1158/1078-0432.CCR-04-0039 (2004).

74 Elstrom, R. L. *et al.* Akt stimulates aerobic glycolysis in cancer cells. *Cancer research* **64**, 3892-3899, doi:10.1158/0008-5472.CAN-03-2904 (2004).

75 Kondoh, H. *et al.* A high glycolytic flux supports the proliferative potential of murine embryonic stem cells. *Antioxid Redox Signal* **9**, 293-299, doi:10.1089/ars.2006.1467 (2007).

76 Cascorbi, I. Role of pharmacogenetics of ATP-binding cassette transporters in the pharmacokinetics of drugs. *Pharmacol Ther* **112**, 457-473, doi:10.1016/j.pharmthera.2006.04.009 (2006).

77 GM, C. in *The Cell: A Molecular Approach. 2nd edition.* (ed Cooper GM) (Sinauer Associates, 2000).

78 Warburg, O., Wind, F. & Negelein, E. The Metabolism of Tumors in the Body. *J Gen Physiol* **8**, 519-530 (1927).

79 Lyon, R. C., Cohen, J. S., Faustino, P. J., Megnin, F. & Myers, C. E. Glucose metabolism in drug-sensitive and drug-resistant human breast cancer cells monitored by magnetic resonance spectroscopy. *Cancer research* **48**, 870-877 (1988).

80 Broxterman, H. J., Pinedo, H. M., Kuiper, C. M., Schuurhuis, G. J. & Lankelma, J. Glycolysis in P-glycoprotein-overexpressing human tumor cell lines. Effects of resistance-modifying agents. *FEBS Lett* **247**, 405-410 (1989).

81 Tavares-Valente, D., Baltazar, F., Moreira, R. & Queiros, O. Cancer cell bioenergetics and pH regulation influence breast cancer cell resistance to paclitaxel and doxorubicin. *Journal of bioenergetics and biomembranes* **45**, 467-475, doi:10.1007/s10863-013-9519-7 (2013).

82 Zheng, J. Energy metabolism of cancer: Glycolysis versus oxidative phosphorylation (Review). *Oncol Lett* **4**, 1151-1157, doi:10.3892/ol.2012.928 (2012).

83 Haq, R. *et al.* Oncogenic BRAF regulates oxidative metabolism via PGC1alpha and MITF. *Cancer Cell* **23**, 302-315, doi:10.1016/j.ccr.2013.02.003 (2013).

84 Vazquez, F. *et al.* PGC1alpha expression defines a subset of human melanoma tumors with increased mitochondrial capacity and resistance to oxidative stress. *Cancer Cell* **23**, 287-301, doi:10.1016/j.ccr.2012.11.020 (2013).

85 LeBleu, V. S. *et al.* PGC-1alpha mediates mitochondrial biogenesis and oxidative phosphorylation in cancer cells to promote metastasis. *Nat Cell Biol* **16**, 992-1003, 1001-1015, doi:10.1038/ncb3039 (2014).

86 Tan, A. S. *et al.* Mitochondrial genome acquisition restores respiratory function and tumorigenic potential of cancer cells without mitochondrial DNA. *Cell metabolism* **21**, 81-94, doi:10.1016/j.cmet.2014.12.003 (2015).

87 Yang, L. *et al.* Metabolic shifts toward glutamine regulate tumor growth, invasion and bioenergetics in ovarian cancer. *Mol Syst Biol* **10**, 728, doi:10.1002/msb.20134892 (2014).

88 Pasto, A. *et al.* Cancer stem cells from epithelial ovarian cancer patients privilege oxidative phosphorylation, and resist glucose deprivation. *Oncotarget* **5**, 4305-4319, doi:10.18632/oncotarget.2010 (2014).

89 Matassa, D. S. *et al.* Oxidative metabolism drives inflammation-induced platinum resistance in human ovarian cancer. *Cell death and differentiation*, doi:10.1038/cdd.2016.39 (2016).

90 Vellinga, T. T. *et al.* SIRT1/PGC1alpha-Dependent Increase in Oxidative Phosphorylation Supports Chemotherapy Resistance of Colon Cancer. *Clinical cancer research : an official journal of the American Association for Cancer Research* **21**, 2870-2879, doi:10.1158/1078-0432.CCR-14-2290 (2015).

91 Koshkin, V., Ailles, L. E., Liu, G. & Krylov, S. N. Metabolic Suppression of a Drug-Resistant Subpopulation in Cancer Spheroid Cells. *J Cell Biochem* **117**, 59-65, doi:10.1002/jcb.25247 (2016).

92 Cordes, W. A death in a case of malarial fever undergoing treatment with plasmochin compound. *Annual report, United Fruit Company, Medical Department* **15**, 72-73 (1926).

93 Kruger, N. J. & von Schaewen, A. The oxidative pentose phosphate pathway: structure and organisation. *Curr Opin Plant Biol* **6**, 236-246 (2003).

94 De Angioletti, M. *et al.* Glucose 6-phosphate dehydrogenase expression is less prone to variegation when driven by its own promoter. *Gene* **267**, 221-231 (2001).

95 Cabezas, H., Raposo, R. R. & Melendez-Hevia, E. Activity and metabolic roles of the pentose phosphate cycle in several rat tissues. *Mol Cell Biochem* **201**, 57-63 (1999).

96 Riganti, C., Gazzano, E., Polimeni, M., Aldieri, E. & Ghigo, D. The pentose phosphate pathway: an antioxidant defense and a crossroad in tumor cell fate. *Free radical biology & medicine* **53**, 421-436, doi:10.1016/j.freeradbiomed.2012.05.006 (2012).

97 Jonas, S. K. *et al.* Increased activity of 6-phosphogluconate dehydrogenase and glucose-6-phosphate dehydrogenase in purified cell suspensions and single cells from the uterine cervix in cervical intraepithelial neoplasia. *Br J Cancer* **66**, 185-191 (1992).

98 Langbein, S. *et al.* Expression of transketolase TKTL1 predicts colon and urothelial cancer patient survival: Warburg effect reinterpreted. *Br J Cancer* **94**, 578-585, doi:10.1038/sj.bjc.6602962 (2006).

99 Boros, L. G. *et al.* Transforming growth factor beta2 promotes glucose carbon incorporation into nucleic acid ribose through the nonoxidative pentose cycle in lung epithelial carcinoma cells. *Cancer research* **60**, 1183-1185 (2000).

100 Cascante, M., Centelles, J. J., Veech, R. L., Lee, W. N. & Boros, L. G. Role of thiamin (vitamin B-1) and transketolase in tumor cell proliferation. *Nutr Cancer* **36**, 150-154, doi:10.1207/S15327914NC3602_2 (2000).

101 Salvioli, S. *et al.* Apoptosis-resistant phenotype in HL-60-derived cells HCW-2 is related to changes in expression of stress-induced proteins that impact on redox status and mitochondrial metabolism. *Cell death and differentiation* **10**, 163-174, doi:10.1038/sj.cdd.4401124 (2003).

102 Langbein, S. *et al.* Metastasis is promoted by a bioenergetic switch: new targets for progressive renal cell cancer. *International journal of cancer. Journal international du cancer* **122**, 2422-2428, doi:10.1002/ijc.23403 (2008).

103 Kruh, G. D. *et al.* MRP subfamily transporters and resistance to anticancer agents. *Journal of bioenergetics and biomembranes* **33**, 493-501 (2001).

104 Meijerman, I., Beijnen, J. H. & Schellens, J. H. Combined action and regulation of phase II enzymes and multidrug resistance proteins in multidrug resistance in cancer. *Cancer treatment reviews* **34**, 505-520, doi:10.1016/j.ctrv.2008.03.002 (2008).

105 Gessner, T., Vaughan, L. A., Beehler, B. C., Bartels, C. J. & Baker, R. M. Elevated pentose cycle and glucuronyltransferase in daunorubicin-resistant P388 cells. *Cancer research* **50**, 3921-3927 (1990).

106 Polimeni, M. *et al.* Modulation of doxorubicin resistance by the glucose-6-phosphate dehydrogenase activity. *Biochem J* **439**, 141-149, doi:10.1042/BJ20102016 (2011).

107 Catanzaro, D. *et al.* Inhibition of glucose-6-phosphate dehydrogenase sensitizes cisplatin-resistant cells to death. *Oncotarget* **6**, 30102-30114, doi:10.18632/oncotarget.4945 (2015).

108 Lutzky, J. *et al.* Role of glutathione and dependent enzymes in anthracycline-resistant HL60/AR cells. *Cancer research* **49**, 4120-4125 (1989).

109 Post, J. F., Baum, E. & Ezell, E. L. 13C NMR studies of glucose metabolism in human leukemic CEM-C7 and CEM-C1 cells. *Magn Reson Med* **23**, 356-366 (1992).

110 Wang, Z. *et al.* Identification of proteins responsible for adriamycin resistance in breast cancer cells using proteomics analysis. *Sci Rep* **5**, 9301, doi:10.1038/srep09301 (2015).

111 Gehrmann, M. L., Fenselau, C. & Hathout, Y. Highly altered protein expression profile in the adriamycin resistant MCF-7 cell line. *J Proteome Res* **3**, 403-409 (2004).

112 Kostrzewa-Nowak, D., Paine, M. J., Wolf, C. R. & Tarasiuk, J. The role of bioreductive activation of doxorubicin in cytotoxic activity against leukaemia HL60-sensitive cell line and its multidrug-resistant sublines. *Br J Cancer* **93**, 89-97, doi:10.1038/sj.bjc.6602639 (2005).

113 Kostrzewa-Nowak, D. *et al.* Bioreductive activation of mitoxantrone by NADPH cytochrome P450 reductase. Implications for increasing its ability to inhibit the growth of sensitive and multidrug resistant leukaemia HL60 cells. *Cancer letters* **245**, 252-262, doi:10.1016/j.canlet.2006.01.012 (2007).

114 Day, R. M. & Suzuki, Y. J. Cell proliferation, reactive oxygen and cellular glutathione. *Dose Response* **3**, 425-442, doi:10.2203/dose-response.003.03.010 (2005).

115 Fojo, T. & Bates, S. Strategies for reversing drug resistance. *Oncogene* **22**, 7512-7523, doi:10.1038/sj.onc.1206951 (2003).

116 Trachootham, D., Alexandre, J. & Huang, P. Targeting cancer cells by ROS-mediated mechanisms: a radical therapeutic approach? *Nature reviews. Drug discovery* **8**, 579-591, doi:10.1038/nrd2803 (2009).

117 Wu, G., Fang, Y. Z., Yang, S., Lupton, J. R. & Turner, N. D. Glutathione metabolism and its implications for health. *J Nutr* **134**, 489-492 (2004).

118 Dirven, H. A., van Ommen, B. & van Bladeren, P. J. Glutathione conjugation of alkylating cytostatic drugs with a nitrogen mustard group and the role of glutathione S-transferases. *Chem Res Toxicol* **9**, 351-360, doi:10.1021/tx950066l (1996).

119 Townsend, D. M. & Tew, K. D. The role of glutathione-S-transferase in anti-cancer drug resistance. *Oncogene* **22**, 7369-7375, doi:10.1038/sj.onc.1206940 (2003).

120 Volm, M., Kastel, M., Mattern, J. & Efferth, T. Expression of resistance factors (P-glycoprotein, glutathione S-transferase-pi, and topoisomerase II) and their interrelationship to proto-oncogene products in renal cell carcinomas. *Cancer* **71**, 3981-3987 (1993).

121 Sau, A., Pellizzari Tregno, F., Valentino, F., Federici, G. & Caccuri, A. M. Glutathione transferases and development of new principles to overcome drug resistance. *Arch Biochem Biophys* **500**, 116-122, doi:10.1016/j.abb.2010.05.012 (2010).

122 Versantvoort, C. H., Broxterman, H. J., Bagrij, T., Scheper, R. J. & Twentyman, P. R. Regulation by glutathione of drug transport in multidrug-resistant human lung tumour cell lines overexpressing multidrug resistance-associated protein. *Br J Cancer* **72**, 82-89 (1995).

123 Avila, M. A., Garcia-Trevijano, E. R., Lu, S. C., Corrales, F. J. & Mato, J. M. Methylthioadenosine. *Int J Biochem Cell Biol* **36**, 2125-2130, doi:10.1016/j.biocel.2003.11.016 (2004).

124 Anderson, M. E. Glutathione: an overview of biosynthesis and modulation. *Chem Biol Interact* **111-112**, 1-14 (1998).

125 Thomas, T. & Thomas, T. J. Polyamines in cell growth and cell death: molecular mechanisms and therapeutic applications. *Cell Mol Life Sci* **58**, 244-258, doi:10.1007/PL00000852 (2001).

126 Leach, R. A. & Tuck, M. T. Methionine depletion induces transcription of the mRNA (N6-adenosine)methyltransferase. *Int J Biochem Cell Biol* **33**, 1116-1128 (2001).

127 Mato, J. M., Alvarez, L., Ortiz, P. & Pajares, M. A. S-adenosylmethionine synthesis: molecular mechanisms and clinical implications. *Pharmacol Ther* **73**, 265-280 (1997).

128 Chiang, P. K. *et al.* S-Adenosylmethionine and methylation. *FASEB J* **10**, 471-480 (1996).

129 Thomas, D., Becker, A. & Surdin-Kerjan, Y. Reverse methionine biosynthesis from S-adenosylmethionine in eukaryotic cells. *The Journal of biological chemistry* **275**, 40718-40724, doi:10.1074/jbc.M005967200 (2000).

130 Cellarier, E. *et al.* Methionine dependency and cancer treatment. *Cancer treatment reviews* **29**, 489-499 (2003).

131 Johnson, C., Warmoes, M. O., Shen, X. & Locasale, J. W. Epigenetics and cancer metabolism. *Cancer letters* **356**, 309-314, doi:10.1016/j.canlet.2013.09.043 (2015).

132 Wagner, C., Luka, Z. & Mato, J. M. Hepatocellular carcinoma in GNMT-/- mice. *Toxicol Appl Pharmacol* **237**, 246; author reply 247, doi:10.1016/j.taap.2009.03.017 (2009).

133 Locasale, J. W. Serine, glycine and one-carbon units: cancer metabolism in full circle. *Nature reviews. Cancer* **13**, 572-583, doi:10.1038/nrc3557 (2013).

134 Limm, K. *et al.* Deregulation of protein methylation in melanoma. *Eur J Cancer* **49**, 1305-1313, doi:10.1016/j.ejca.2012.11.026 (2013).

135 Ushijima, T. & Okochi-Takada, E. Aberrant methylations in cancer cells: where do they come from? *Cancer Sci* **96**, 206-211, doi:10.1111/j.1349-7006.2005.00035.x (2005).

136 Onda, K. *et al.* Decitabine, a DNA methyltransferase inhibitor, reduces P-glycoprotein mRNA and protein expressions and increases drug sensitivity in drug-resistant MOLT4 and Jurkat cell lines. *Anticancer Res* **32**, 4439-4444 (2012).

137 Marguerite, V., Gkikopoulou, E., Alberto, J. M., Gueant, J. L. & Merten, M. Phospholipase D activation mediates cobalamin-induced downregulation of Multidrug Resistance-1 gene and increase in sensitivity to vinblastine in HepG2 cells. *Int J Biochem Cell Biol* **45**, 213-220, doi:10.1016/j.biocel.2012.09.018 (2013).

138 Harding, C., Heuser, J. & Stahl, P. Receptor-mediated endocytosis of transferrin and recycling of the transferrin receptor in rat reticulocytes. *J Cell Biol* **97**, 329-339 (1983).

139 Pan, B. T. & Johnstone, R. M. Fate of the transferrin receptor during maturation of sheep reticulocytes in vitro: selective externalization of the receptor. *Cell* **33**, 967-978 (1983).

140 Colombo, M., Raposo, G. & Thery, C. Biogenesis, secretion, and intercellular interactions of exosomes and other extracellular vesicles. *Annu Rev Cell Dev Biol* **30**, 255-289, doi:10.1146/annurev-cellbio-101512-122326 (2014).

141 Gould, S. J. & Raposo, G. As we wait: coping with an imperfect nomenclature for extracellular vesicles. *J Extracell Vesicles* **2**, doi:10.3402/jev.v2i0.20389 (2013).

142 Johnstone, R. M., Adam, M., Hammond, J. R., Orr, L. & Turbide, C. Vesicle formation during reticulocyte maturation. Association of plasma membrane activities with released vesicles (exosomes). *The Journal of biological chemistry* **262**, 9412-9420 (1987).

143 Akers, J. C., Gonda, D., Kim, R., Carter, B. S. & Chen, C. C. Biogenesis of extracellular vesicles (EV): exosomes, microvesicles, retrovirus-like vesicles, and apoptotic bodies. *J Neurooncol* **113**, 1-11, doi:10.1007/s11060-013-1084-8 (2013).

144 S, E. L. A., Mager, I., Breakefield, X. O. & Wood, M. J. Extracellular vesicles: biology and emerging therapeutic opportunities. *Nature reviews. Drug discovery* **12**, 347-357, doi:10.1038/nrd3978 (2013).

145 Zhao, C. *et al.* The role of Alix in the proliferation of human glioma cells. *Hum Pathol* **52**, 110-118, doi:10.1016/j.humpath.2015.09.046 (2016).

146 Christ, L. *et al.* ALIX and ESCRT-I/II function as parallel ESCRT-III recruiters in cytokinetic abscission. *J Cell Biol* **212**, 499-513, doi:10.1083/jcb.201507009 (2016).

147 Baietti, M. F. *et al.* Syndecan-syntenin-ALIX regulates the biogenesis of exosomes. *Nat Cell Biol* **14**, 677-685, doi:10.1038/ncb2502 (2012).

148 Aatonen, M. T. *et al.* Isolation and characterization of platelet-derived extracellular vesicles. *J Extracell Vesicles* **3**, doi:10.3402/jev.v3.24692 (2014).

149 Graham, T. R. & Kozlov, M. M. Interplay of proteins and lipids in generating membrane curvature. *Current opinion in cell biology* **22**, 430-436, doi:10.1016/j.ceb.2010.05.002 (2010).

150 Valadi, H. *et al.* Exosome-mediated transfer of mRNAs and microRNAs is a novel mechanism of genetic exchange between cells. *Nat Cell Biol* **9**, 654-659, doi:10.1038/ncb1596 (2007).

151 Minciacchi, V. R., Freeman, M. R. & Di Vizio, D. Extracellular vesicles in cancer: exosomes, microvesicles and the emerging role of large oncosomes. *Semin Cell Dev Biol* **40**, 41-51, doi:10.1016/j.semcdb.2015.02.010 (2015).

152 Kalra, H. *et al.* Vesiclepedia: a compendium for extracellular vesicles with continuous community annotation. *PLoS Biol* **10**, e1001450, doi:10.1371/journal.pbio.1001450 (2012).

153 Kim, D. K. *et al.* EVpedia: an integrated database of high-throughput data for systemic analyses of extracellular vesicles. *J Extracell Vesicles* **2**, doi:10.3402/jev.v2i0.20384 (2013).

154 *EVpedia*, <evpedia.info> (2012).

155 Trajkovic, K. *et al.* Ceramide triggers budding of exosome vesicles into multivesicular endosomes. *Science* **319**, 1244-1247, doi:10.1126/science.1153124 (2008).

156 Zhang, W. *et al.* Annexin A2 promotes the migration and invasion of human hepatocellular carcinoma cells in vitro by regulating the shedding of CD147-harboring microvesicles from tumor cells. *PloS one* **8**, e67268, doi:10.1371/journal.pone.0067268 (2013).

157 Liao, C. F. *et al.* CSE1L, a novel microvesicle membrane protein, mediates Ras-triggered microvesicle generation and metastasis of tumor cells. *Mol Med* **18**, 1269-1280, doi:10.2119/molmed.2012.00205 (2012).

158 Rilla, K. *et al.* Hyaluronan production enhances shedding of plasma membrane-derived microvesicles. *Experimental cell research* **319**, 2006-2018, doi:10.1016/j.yexcr.2013.05.021 (2013).

159 Yang, J. M. & Gould, S. J. The cis-acting signals that target proteins to exosomes and microvesicles. *Biochem Soc Trans* **41**, 277-282, doi:10.1042/BST20120275 (2013).

160 Yoon, Y. J., Kim, O. Y. & Gho, Y. S. Extracellular vesicles as emerging intercellular communicasomes. *BMB Rep* **47**, 531-539 (2014).

161 Losche, W., Scholz, T., Temmler, U., Oberle, V. & Claus, R. A. Platelet-derived microvesicles transfer tissue factor to monocytes but not to neutrophils. *Platelets* **15**, 109-115, doi:10.1080/09537100310001649885 (2004).

162 Aguilar, P. S. *et al.* Genetic basis of cell-cell fusion mechanisms. *Trends Genet* **29**, 427-437, doi:10.1016/j.tig.2013.01.011 (2013).

163 Huang, Q. *et al.* Epigenetic and non-epigenetic regulation of syncytin-1 expression in human placenta and cancer tissues. *Cell Signal* **26**, 648-656, doi:10.1016/j.cellsig.2013.11.002 (2014).

164 Bissig, C. & Gruenberg, J. ALIX and the multivesicular endosome: ALIX in Wonderland. *Trends Cell Biol* **24**, 19-25, doi:10.1016/j.tcb.2013.10.009 (2014).

165 Yanez-Mo, M. *et al.* Biological properties of extracellular vesicles and their physiological functions. *J Extracell Vesicles* **4**, 27066, doi:10.3402/jev.v4.27066 (2015).

166 Ratajczak, J. *et al.* Embryonic stem cell-derived microvesicles reprogram hematopoietic progenitors: evidence for horizontal transfer of mRNA and protein delivery. *Leukemia : official journal of the Leukemia Society of America, Leukemia Research Fund, U.K* **20**, 847-856, doi:10.1038/sj.leu.2404132 (2006).

167 Gatti, S. *et al.* Microvesicles derived from human adult mesenchymal stem cells protect against ischaemia-reperfusion-induced acute and chronic kidney injury. *Nephrol Dial Transplant* **26**, 1474-1483, doi:10.1093/ndt/gfr015 (2011).

168 Raposo, G. *et al.* B lymphocytes secrete antigen-presenting vesicles. *J Exp Med* **183**, 1161-1172 (1996).

169 Del Conde, I., Shrimpton, C. N., Thiagarajan, P. & Lopez, J. A. Tissue-factor-bearing microvesicles arise from lipid rafts and fuse with activated platelets to initiate coagulation. *Blood* **106**, 1604-1611, doi:10.1182/blood-2004-03-1095 (2005).

170 Reiners, K. S., Dassler, J., Coch, C. & Pogge von Strandmann, E. Role of Exosomes Released by Dendritic Cells and/or by Tumor Targets: Regulation of NK Cell Plasticity. *Front Immunol* **5**, 91, doi:10.3389/fimmu.2014.00091 (2014).

171 Bobrie, A., Colombo, M., Raposo, G. & Thery, C. Exosome secretion: molecular mechanisms and roles in immune responses. *Traffic* **12**, 1659-1668, doi:10.1111/j.1600-0854.2011.01225.x (2011).

172 Lv, M. M. *et al.* Exosomes mediate drug resistance transfer in MCF-7 breast cancer cells and a probable mechanism is delivery of P-glycoprotein. *Tumour Biol* **35**, 10773-10779, doi:10.1007/s13277-014-2377-z (2014).

173 Jaiswal, R., Luk, F., Dalla, P. V., Grau, G. E. & Bebawy, M. Breast cancer-derived microparticles display tissue selectivity in the transfer of resistance proteins to cells. *PloS one* **8**, e61515, doi:10.1371/journal.pone.0061515 (2013).

174 Goler-Baron, V., Sladkevich, I. & Assaraf, Y. G. Inhibition of the PI3K-Akt signaling pathway disrupts ABCG2-rich extracellular vesicles and overcomes multidrug resistance in breast cancer cells. *Biochemical pharmacology* **83**, 1340-1348, doi:10.1016/j.bcp.2012.01.033 (2012).

175 Kharaziha, P. *et al.* Molecular profiling of prostate cancer derived exosomes may reveal a predictive signature for response to docetaxel. *Oncotarget* **6**, 21740-21754, doi:10.18632/oncotarget.3226 (2015).

176 Beloribi-Djefaflia, S., Siret, C. & Lombardo, D. Exosomal lipids induce human pancreatic tumoral MiaPaCa-2 cells resistance through the CXCR4-SDF-1alpha signaling axis. *Oncoscience* **2**, 15-30, doi:10.18632/oncoscience.96 (2015).

177 Gong, J. *et al.* Microparticle drug sequestration provides a parallel pathway in the acquisition of cancer drug resistance. *Eur J Pharmacol* **721**, 116-125, doi:10.1016/j.ejphar.2013.09.044 (2013).

178 Sousa, D., Lima, R. T. & Vasconcelos, M. H. Intercellular Transfer of Cancer Drug Resistance Traits by Extracellular Vesicles. *Trends Mol Med* **21**, 595-608, doi:10.1016/j.molmed.2015.08.002 (2015).

179 Levchenko, A. *et al.* Intercellular transfer of P-glycoprotein mediates acquired multidrug resistance in tumor cells. *Proceedings of the National Academy of Sciences of the United States of America* **102**, 1933-1938, doi:10.1073/pnas.0401851102 (2005).

180 Bebawy, M. *et al.* Membrane microparticles mediate transfer of P-glycoprotein to drug sensitive cancer cells. *Leukemia : official journal of the Leukemia Society of America, Leukemia Research Fund, U.K* **23**, 1643-1649, doi:10.1038/leu.2009.76 (2009).

181 Zhang, F. F. *et al.* Microvesicles mediate transfer of P-glycoprotein to paclitaxel-sensitive A2780 human ovarian cancer cells, conferring paclitaxel-resistance. *Eur J Pharmacol* **738**, 83-90, doi:10.1016/j.ejphar.2014.05.026 (2014).

182 Fruhbeis, C., Helmig, S., Tug, S., Simon, P. & Kramer-Albers, E. M. Physical exercise induces rapid release of small extracellular vesicles into the circulation. *J Extracell Vesicles* **4**, 28239, doi:10.3402/jev.v4.28239 (2015).

183 Santana, S. M., Antonyak, M. A., Cerione, R. A. & Kirby, B. J. Cancerous epithelial cell lines shed extracellular vesicles with a bimodal size distribution that is sensitive to glutamine inhibition. *Phys Biol* **11**, 065001, doi:10.1088/1478-3975/11/6/065001 (2014).

184 Minciacchi, V. R. *et al.* Large oncosomes contain distinct protein cargo and represent a separate functional class of tumor-derived extracellular vesicles. *Oncotarget* **6**, 11327-11341, doi:10.18632/oncotarget.3598 (2015).

185 Looze, C. *et al.* Proteomic profiling of human plasma exosomes identifies PPARgamma as an exosome-associated protein. *Biochem Biophys Res Commun* **378**, 433-438, doi:10.1016/j.bbrc.2008.11.050 (2009).

186 Corcoran, C. *et al.* Docetaxel-resistance in prostate cancer: evaluating associated phenotypic changes and potential for resistance transfer via exosomes. *PloS one* **7**, e50999, doi:10.1371/journal.pone.0050999 (2012).

187 Pasquier, J. *et al.* Different modalities of intercellular membrane exchanges mediate cell-to-cell p-glycoprotein transfers in MCF-7 breast cancer cells. *The Journal of biological chemistry* **287**, 7374-7387, doi:10.1074/jbc.M111.312157 (2012).

188 Boukouris, S. & Mathivanan, S. Exosomes in bodily fluids are a highly stable resource of disease biomarkers. *Proteomics Clin Appl* **9**, 358-367, doi:10.1002/prca.201400114 (2015).

189 Wind, N. S. & Holen, I. Multidrug resistance in breast cancer: from in vitro models to clinical studies. *Int J Breast Cancer* **2011**, 967419, doi:10.4061/2011/967419 (2011).

190 Larsen, A. K., Escargueil, A. E. & Skladanowski, A. Resistance mechanisms associated with altered intracellular distribution of anticancer agents. *Pharmacol Ther* **85**, 217-229 (2000).

191 Rahman, M. & Hasan, M. R. Cancer Metabolism and Drug Resistance. *Metabolites* **5**, 571-600, doi:10.3390/metabo5040571 (2015).

192 Marie, J. P., Faussat-Suberville, A. M., Zhou, D. & Zittoun, R. Daunorubicin uptake by leukemic cells: correlations with treatment outcome and mdr1 expression. *Leukemia : official journal of the Leukemia Society of America, Leukemia Research Fund, U.K* **7**, 825-831 (1993).

193 Pesic, M. *et al.* Induced resistance in the human non small cell lung carcinoma (NCI-H460) cell line in vitro by anticancer drugs. *J Chemother* **18**, 66-73, doi:10.1179/joc.2006.18.1.66 (2006).

194 Podolski-Renic, A. *et al.* Molecular and cytogenetic changes in multi-drug resistant cancer cells and their influence on new compounds testing. *Cancer Chemother Pharmacol* **72**, 683-697, doi:10.1007/s00280-013-2247-1 (2013).

195 Krzyzanowski, D., Bartosz, G. & Grzelak, A. Collateral sensitivity: ABCG2-overexpressing cells are more vulnerable to oxidative stress. *Free radical biology & medicine* **76**, 47-52, doi:10.1016/j.freeradbiomed.2014.07.020 (2014).

196 Tai, D. J. *et al.* Changes in intracellular redox status influence multidrug resistance in gastric adenocarcinoma cells. *Exp Ther Med* **4**, 291-296, doi:10.3892/etm.2012.591 (2012).

197 Estrela, J. M., Ortega, A. & Obrador, E. Glutathione in cancer biology and therapy. *Crit Rev Clin Lab Sci* **43**, 143-181, doi:10.1080/10408360500523878 (2006).

198 Wang, S. T., Chen, H. W., Sheen, L. Y. & Lii, C. K. Methionine and cysteine affect glutathione level, glutathione-related enzyme activities and the expression of glutathione S-transferase isozymes in rat hepatocytes. *J Nutr* **127**, 2135-2141 (1997).

199 Xu, R. H. *et al.* Inhibition of glycolysis in cancer cells: a novel strategy to overcome drug resistance associated with mitochondrial respiratory defect and hypoxia. *Cancer research* **65**, 613-621 (2005).

200 Guppy, M., Greiner, E. & Brand, K. The role of the Crabtree effect and an endogenous fuel in the energy metabolism of resting and proliferating thymocytes. *Eur J Biochem* **212**, 95-99 (1993).

201 Sattler, U. G., Walenta, S. & Mueller-Klieser, W. [Lactate and redox status in malignant tumors]. *Anaesthesist* **56**, 466-469, doi:10.1007/s00101-007-1164-2 (2007).

202 De Preter, G. *et al.* Inhibition of the pentose phosphate pathway by dichloroacetate unravels a missing link between aerobic glycolysis and cancer cell proliferation. *Oncotarget* **7**, 2910-2920, doi:10.18632/oncotarget.6272 (2016).

203 Palmeira, A. *et al.* Dual inhibitors of P-glycoprotein and tumor cell growth: (re)discovering thioxanthones. *Biochemical pharmacology* **83**, 57-68, doi:10.1016/j.bcp.2011.10.004 (2012).

204 Colombo, M. *et al.* Analysis of ESCRT functions in exosome biogenesis, composition and secretion highlights the heterogeneity of extracellular vesicles. *J Cell Sci* **126**, 5553-5565, doi:10.1242/jcs.128868 (2013).

205 Abrami, L. *et al.* Hijacking multivesicular bodies enables long-term and exosome-mediated long-distance action of anthrax toxin. *Cell Rep* **5**, 986-996, doi:10.1016/j.celrep.2013.10.019 (2013).

206 Escrevente, C., Keller, S., Altevogt, P. & Costa, J. Interaction and uptake of exosomes by ovarian cancer cells. *BMC Cancer* **11**, 108, doi:10.1186/1471-2407-11-108 (2011).

207 Yin, J. *et al.* Secretion of annexin A3 from ovarian cancer cells and its association with platinum resistance in ovarian cancer patients. *J Cell Mol Med* **16**, 337-348, doi:10.1111/j.1582-4934.2011.01316.x (2012).

208 Aung, T. *et al.* Exosomal evasion of humoral immunotherapy in aggressive B-cell lymphoma modulated by ATP-binding cassette transporter A3. *Proceedings of the National Academy of Sciences of the United States of America* **108**, 15336-15341, doi:10.1073/pnas.1102855108 (2011).

209 Jaiswal, R. *et al.* Microparticle conferred microRNA profiles--implications in the transfer and dominance of cancer traits. *Molecular cancer* **11**, 37, doi:10.1186/1476-4598-11-37 (2012).

210 Pluchino, K. M., Hall, M. D., Goldsborough, A. S., Callaghan, R. & Gottesman, M. M. Collateral sensitivity as a strategy against cancer multidrug resistance. *Drug Resist Updat* **15**, 98-105, doi:10.1016/j.drup.2012.03.002 (2012).

211 Sreenivasan, S., Ravichandran, S., Vetrivel, U. & Krishnakumar, S. Modulation of multidrug resistance 1 expression and function in retinoblastoma cells by curcumin. *J Pharmacol Pharmacother* **4**, 103-109, doi:10.4103/0976-500X.110882 (2013).

212 Lu, W.-D., Qin, Y., Yang, C. & Li, L. Effect of curcumin on human colon cancer multidrug resistance in vitro and in vivo. *Clinics* **68**, 694-701 (2013).

213 Amundson, S. A., Myers, T. G. & Fornace, A. J., Jr. Roles for p53 in growth arrest and apoptosis: putting on the brakes after genotoxic stress. *Oncogene* **17**, 3287-3299, doi:10.1038/sj.onc.1202576 (1998).

214 Nigg, E. A. Mitotic kinases as regulators of cell division and its checkpoints. *Nat Rev Mol Cell Biol* **2**, 21-32, doi:10.1038/35048096 (2001).

215 Lopes-Rodrigues, V. *et al.* Multidrug resistant tumour cells shed more microvesicle-like EVs and less exosomes than their drug-sensitive counterpart cells. *Biochimica et biophysica acta* **1860**, 618-627, doi:10.1016/j.bbagen.2015.12.011 (2016).